The Role of Subterminal Hydroxyeicosatetraenoic Acids in the Pathogenesis of Cardiac Hypertrophy

by

Sherif Mohamed Ali Mohamed Shoieb

A thesis submitted in partial fulfillment of the requirements for the degree of

Doctor of Philosophy
in
Pharmaceutical Sciences

Faculty of Pharmacy and Pharmaceutical Sciences
University of Alberta

ABSTRACT

Cardiac hypertrophy is a complex condition which is characterized by increased mass of the heart muscle. If untreated, cardiac hypertrophy can ultimately lead to heart failure (HF), arrhythmia and sudden death. Accumulating evidence suggest that pathological cardiac hypertrophy is strongly correlated with aberrations in cytochrome P450 (CYP)-mediated arachidonic acid (AA) metabolism in the cardiac tissue. In the heart, AA is metabolized by the recently recognized CYP pathway, forming several biologically-active epoxyeicosatrienoic acids (EETs) and hydroxyeicosatetraenoic acids (HETEs). HETEs could be further classified as mid-chain, subterminal and terminal HETEs. Subterminal HETEs are group of lipid mediators that are implicated in a spacious array of physiological and pathophysiological processes. However, their role in the heart has yet to be investigated. Another important group of AA metabolites in the heart are mid-chain HETEs. Several experimental studies have demonstrated a role of CYP1B1 and its associated mid-chain HETEs metabolites in the development of cardiovascular diseases. Characterization of the role of subterminal HETEs in the heart and modulating the CYP1B1/mid-chain HETEs pathway will help to identify novel points of intervention that could help in the development of new therapeutic agents for cardiac hypertrophy and heart failure. Therefore, the objectives of the current work were to test whether R- and S-enantiomers of 19-HETE have differential role in the cardioprotective mechanism against cardiac hypertrophy, examine the inhibitory effect of both enantiomers of 19-HETE on human recombinant CYP1B1 enzyme, test the capability of synthetic analogues of 19-HETE to exert an inhibitory effect on some human recombinant CYP enzymes and test the cardioprotective effects of CYP modulators such as resveratrol and fluconazole on experimental models of cardiac hypertrophy and HF. The results demonstrated that both

enantiomers of 19-HETE protected against angiotensin II (Ang II)-induced cardiac hypertrophy via decreasing the level of cardiotoxic mid-chain HETEs, inhibiting the catalytic activity of CYP1B1 and decreasing the protein expression level of LOX and COX-2 enzymes, with the S-enantiomer having more protection than the R-enantiomer. In addition, both enantiomers of 19-HETE noncompetitively inhibited human recombinant CYP1B1 enzymatic activity with higher potency of the S-enantiomer. Also, we have tested the potential inhibitory effect of synthetic 19-HETE analogs on different CYP enzymes. We showed that the synthetic analogues of 19(R)-HETE and 19(S)-HETE noncompetitively inhibited CYP1A1 and CYP1B1 enzymatic activity with preferential selectivity of the S-analogue. Interestingly, we demonstrated that resveratrol attenuated Ang II-induced cardiac hypertrophy and caused a significant decrease of CYP1B1 protein expression and mid-chain HETEs. Furthermore, in vivo studies showed that low dose resveratrol reduces the severity of myocardial infarction (MI)-induced HF, at least in part, through the inhibition of CYP1B1 and cardiotoxic mid-chain HETE metabolites. Lastly, the results showed that the protective role of fluconazole against pressure overload-induced cardiac hypertrophy is associated with a significant inhibition of CYP1B1 at the gene and protein levels and a reduction in the formation rate of mid-chain HETEs. In conclusion, the findings of the current work highlight the role of subterminal HETEs in the development of cardiac hypertrophy and indicate that their synthetic analogues could serve as a novel target for the treatment of heart diseases. Also, the findings of this work point out the potential repurposing of available clinically-approved drugs including resveratrol and fluconazole as a CYP1B1 inhibitors for the treatment of cardiovascular diseases.

PREFACE

This thesis is an original work done by Mr. Sherif Shoieb. All experimental animal procedures were approved by the University of Alberta Health Sciences Animal Policy and Welfare Committee. Section 1.5 of this thesis has been published as a review article: Shoieb SM, El-Sherbeni A, El-Kadi AOS. (2019). Subterminal hydroxyeicosatetraenoic acids: Crucial lipid mediators in normal physiology and disease states. Chemico Biological Interactions. 299:140–150. I was responsible for collecting and summarizing data from the literature and writing the manuscript. El-Kadi AOS was the supervisory author and was involved with concept formation and manuscript composition. Sections 3.1 and 4.1 of this thesis have been published as Shoieb SM, El-Kadi AOS. (2018). S-enantiomer of 19-hydroxyeicosatetraenoic acid preferentially protects against angiotensin II-induced cardiac hypertrophy. Drug Metabolism and Disposition. 46: 1157–1168. I was responsible for designing the research, conducting experiments and data analysis as well as the manuscript writing. El-Kadi AOS was the supervisory author and was involved with concept formation and manuscript composition. Sections 3.2 and 4.2 of this thesis have been published as Shoieb SM, El-Sherbeni A, El-Kadi AOS. (2019). Identification of 19-(S/R) hydroxyeicosatetraenoic acid as the first endogenous noncompetitive inhibitor of cytochrome P450 1B1 with enantioselective activity. Drug Metabolism and Disposition. 47: 67–70. I was responsible for designing the research, conducting experiments, and analysis as well as the manuscript composition. El-Sherbeni A assisted with the data analysis and contributed to the manuscript revision. El-Kadi AOS was the supervisory author and was involved with concept formation and manuscript composition. Section 3.3

and 4.3 of this thesis have been published as Shoieb SM, Dakarapu R, Falck JR, El-Kadi AOS. (2021). Novel Synthetic Analogues of 19(S/R)-Hydroxyeicosatetraenoic Acid Exhibit Noncompetitive Inhibitory Effect on the Activity of Cytochrome P450 1A1 and 1B1. European Journal of Drug Metabolism and Pharmacokinetics. *In Press.* I was responsible for designing the research, conducting experiments and data analysis as well as the manuscript composition. Dakarapu R, Department of Biochemistry, UT Southwestern Medical Center, Dallas, TX, USA, synthesized and provided the synthetic compounds. Falck JR, Department of Biochemistry, UT Southwestern Medical Center, Dallas, TX, USA, contributed to the manuscript writing and revision. El-Kadi AOS was the supervisory author and was involved with concept formation and manuscript composition. Section 3.4 and 4.4 of this thesis have been published as Shoieb SM, El-Kadi AOS. (2020). Resveratrol attenuates angiotensin II-induced cellular hypertrophy through the inhibition of CYP1B1 and the cardiotoxic mid-chain HETE metabolites. Molecular and Cellular Biochemistry. 471: 165–176. I was responsible for designing the research, conducting experiments and data analysis as well as the manuscript composition. El-Kadi AOS was the supervisory author and was involved with concept formation and manuscript composition. Section 3.5 of this thesis has been published as a part of the following study: Matsumura N, Takahara S, Maayah Z, Parajuli N, Byrne N, Shoieb S, Soltys C-LM, Beker D, Masson G, El-Kadi A, Dyck J. (2018). Resveratrol improves cardiac function and exercise performance in MI-induced heart failure through the inhibition of cardiotoxic HETE metabolites. Journal of Molecular and Cellular Cardiology. 125: 162–173. I was responsible for conducting the experiments related to the assessment of CYP1B1 and mid-chain HETEs metabolites in the heart, data analysis as well as the manuscript composition.

Section 3.6 and 4.5 of this thesis have been submitted as Shoieb SM, Levasseur J, Silver H, Dyck JRB, El-Kadi AOS (2021). Ameliorative Role of Fluconazole against Abdominal Aortic Constriction-Induced Cardiac Hypertrophy in rats. British Journal of Pharmacology. I was responsible for designing the research, conducting experiments and data analysis, as well as the manuscript composition. Levasseur J and Silver H, Faculty of Medicine and Dentistry, University of Alberta, Edmonton, Alberta, Canada, carried out the AAC surgery and performed the echocardiography assessment. Dyck JRB, Faculty of Medicine and Dentistry, University of Alberta, Edmonton, Alberta, Canada, assisted with the analysis and contributed to manuscript edits. El-Kadi AOS was the supervisory author and was involved with concept formation and manuscript composition.

This dissertation is dedicated to my parents, wife, daughter;

Alia, sisters and many of my friends.

Thank you for your unconditional love and support

ACKNOWLEDGEMENTS

I would like to express my deepest gratitude and appreciation to my supervisor and mentor Dr. Ayman El-Kadi for suggesting the original line of research presented in this thesis and for his trust, guidance, encouragement and time during my doctoral program.

I sincerely acknowledge the members of my supervisory committee, Dr. Arno Siraki and Dr. John Ussher for their endless advice and valuable suggestions.

I would like to thank my former lab members, Drs. Zaid Maayah, Osama Elshenawy, Ahmed El-Sherbeni, and Ahmed Alammari whose enthusiasm gave me to keep working on this research project. My special appreciation is extended to my present lab colleagues, especially Mahmoud Elghiaty, Mohammed Alqahtani and Rahmat Hidayat. Special thanks to Jody Levasseur and Heidi Silver for their help with echocardiography and aortic constriction surgery.

I would like thank the Dean of the Faculty of Pharmacy and Pharmaceutical sciences, Dr. Neal Davies and the faculty administrative and support staff for their kind advice and financial support throughout my program. Special thanks go out to Diseray Schamehorn, the Graduate Studies Coordinator in the faculty.

I am also grateful for the generous financial support provided by the University of Alberta for supporting me with the University of Alberta Doctoral Recruitment Scholarship, the Alberta Innovates Graduate Student Scholarship, the Alberta Graduate Excellence Scholarship, the Andrew Stewart Memorial Graduate Prize and others. In addition, this work was supported by a grant from the Canadian Institutes of Health Research [CIHR PS 168846] to Ayman O. S. El-Kadi

Finally, I would like to express my sincere gratitude to my wife, Sahar Konbor. This work would not have been completed without the support and encouragement I receive from her. Thank you for your unwavering love, tremendous understanding and belief in me.

TABLE OF CONTENTS

LIST OF TABLES

LIST OF FIGURES

LIST OF ABBREVIATIONS

7-ER	7-ethoxyresorufin
AA	arachidonic acid
AAC	Abdominal aortic constriction
AC	Adenylyl cyclase
ACS	Acute coronary syndrome
ACS	Acute coronary syndrome;
ALT	Alanine aminotransferase
AMPK	AMP-activated protein kinase
Ang II	Angiotensin II
ANP	Atrial natriuretic peptide
AST	Aspartate aminotransferase
ATCC	American Type Culture Collection
ATR	Angiotensin II receptor
BCAA	Branched-chain amino acid
BNP	B-type natriuretic peptide
CaMKII	Calcium/calmodulin-dependent protein kinase type II
cGMP	Cyclic guanosine monophosphate

COXs	Cyclooxygenases
CVD	Cardiovascular diseases
DAG	Diacylglycerol
DDMS	Dibromo-dodecenyl-methylsulfimide
DHETs	Dihydroxyeicosatrienoic acids
DMEM	Dulbecco's Modified Eagle's Medium
DMSO	Dimethyl sulfoxide
DR	Diabetic retinopathy
EETs	Epoxyeicosatrienoic acids
EF	Ejection fraction
EndoR	Endothelin 1 receptor
EPACs	Exchange proteins directly activated by Camp
EROD	Ethoxyresorufin O-deethylase
GAPDH	Glyceraldehyde-3-phosphate dehydrogenase
GC	Guanylate cyclase
GPCRs	G-protein-coupled receptors
GRKs	G protein-coupled receptor kinases
GSK-3	Glycogen synthase kinase-3

HDAC	Histone deacetylase
HETEs	Hydroxyeicosatetraenoic acids
HF	Heart failure
HFmrEF	Heart failure with mid-range ejection fraction
HFpEF	Heart failure with preserved ejection fraction
HFrEF	Heart failure with reduced ejection fraction
ICP	Intracranial pressure
ICSI	Intracytoplasmic sperm injection
IGF	Insulin-like growth factor
IP3	Inositol 1,4,5-triphosphate
IP3R3	Inositol 1,4,5-triphosphate receptor type 3
IRS1	Insulin receptor substrate 1
JNK	JUN N-terminal kinases
LC-ESI-MS	Liquid chromatographic-electrospray ionization-mass spectrometry
LKB1	Liver kinase B1
LOs	Lipoxygenases
LTs	Leukotrienes
LV	Left ventricle

MACE	Major adverse cardiovascular event
MAPK	Mitogen activated protein kinases
MAPKKK	Mitogen-activated protein kinase kinase kinase
MCIP1	Modulatory calcineurin-interacting protein
MEF2A	Myocyte enhancer factor 2 A
MEK	MAP/ERK kinase
MROD	Methoxyresorufin O-demethylase
mTOR	Mammalian target of rapamycin
NADPH	Nicotinamide adenine dinucleotide phosphate
NAFLD	Non-alcoholic fatty liver disease
NFAT	Nuclear factor of activated T cells
NF-κB	Nuclear factor-κB
NO	Nitric oxide
NPR	Natriuretic peptide receptor
PAHs	Polycyclic aromatic hydrocarbons
PDE	Phosphodiesterase
PGs	Prostaglandins
PHAHs	Polyhalogenated aromatic hydrocarbons

PI3Ks	Phosphoinositide 3-kinases
PIP2	Phosphoinositol bisphosphate
PKB	Protein kinase B
PKC	Protein kinase C
PKG	protein kinase G
PLC	Phospholipase C
PMNL	Polymorphonuclear leukocytes
PPARs	Peroxisome proliferator activated receptors
RAAS	Renin-angiotensin-aldosterone system
sEH	Soluble epoxide hydrolase
SERCA	Sarcoplasmic reticulum Ca^{++} ATPase
SFM	Serum-free medium
SHR	Spontaneously hypertensive rats
SIRT	NAD-dependent protein deacetylase sirtuin
SOCE	Store-operated Ca2+ entry
STIM1	Stromal interaction molecule 1
TCDD	2,3,7,8-tetrachlorodibenzodioxin
TMS	2,3′,4,5′-tetramethoxystilbene

TNF	Tumour necrosis factor
TRPC	Transient receptor protein channel
TXN	Thioredoxin.
β-AR	β-adrenergic receptor
β-MHC	β-myosin heavy chain

CHAPTER 1: INTRODUCTION

Portions of this chapter have been published in:

1- **Shoieb SM,** Dakarapu R, Falck JR, El-Kadi AOS. (2021). Novel Synthetic Analogues of 19(S/R)-Hydroxyeicosatetraenoic Acid Exhibit Noncompetitive Inhibitory Effect on the Activity of Cytochrome P450 1A1 and 1B1. European Journal of Drug Metabolism and Pharmacokinetics. In Press.

2- **Shoieb SM,** El-Kadi A. (2020). Resveratrol attenuates angiotensin II-induced cellular hypertrophy through the inhibition of CYP1B1 and the cardiotoxic mid-chain HETE metabolites.Molecular and Cellular Biochemistry. 471: 165–176.

3- **Shoieb SM,** El-Sherbeni A, El-Kadi A. (2019). Subterminal hydroxyeicosatetraenoic acids: Crucial lipid mediators in normal physiology and disease states. Chemico Biological Interactions. 299:140–150.

4- **Shoieb SM,** El-Sherbeni A, El-Kadi A. (2019). Identification of 19-(s/r) hydroxyeicosatetraenoic acid as the first endogenous noncompetitive inhibitor of cytochrome P450 1B1 with enantioselective activity. Drug Metabolism and Disposition. 47: 67–70.

5- **Shoieb SM,** El-Kadi A. (2018). S-enantiomer of 19-hydroxyeicosatetraenoic acid preferentially protects against angiotensin II-induced cardiac hypertrophy. Drug Metabolism and Disposition. 46: 1157–1168.

6- Matsumura N, Takahara S, Maayah Z, Parajuli N, Byrne N, **Shoieb SM,** Soltys C-LM, Beker D, Masson G, El-Kadi A, Dyck J. (2018). Resveratrol improves cardiac function and exercise performance in MI-induced heart failure through the inhibition of cardiotoxic HETE metabolites. Journal of Molecular and Cellular Cardiology. 125: 162–173.

1.1 Heart failure

HF cases are increasing globally, it remains a leading cause of morbidity and mortality worldwide. Despite advances in the treatment options, there are yet cases where HF patients continue to develop symptoms, posing a huge burden on the health care system (Inamdar and Inamdar, 2016; Metra and Teerlink, 2017). HF is defined as "a complex clinical syndrome that results from any structural or functional impairment of ventricular filling or ejection of blood" (Yancy et al., 2017). Early diagnosis and aggressive medical interventions have been widely available, however HF patients still have a poor prognosis, with a reported annual mortality rate of 33% (Roger, 2013).

1.1.1 Etiology of heart failure

Traditionally, HF has been always classified into either ischemic or non-ischemic idiopathic HF (Fox et al., 2001). While the etiology of HF might differ, there is accumulating consensus that development of HF is closely related to activation of several neurohormonal systems, regardless of the cause. Stimulus injuries such as coronary artery disease, hypertension, valvular heart disease, toxins, or other stimuli cause harm to the cardiac tissue, therefore they activate the neurohormonal systems specially the renin-angiotensin-aldosterone system (RAAS) and boost the sympathetic nervous system (Jackson, 2000). These events will eventually lead to progressive worsening of LV function, cause the remodelling of the cardiac tissue, and result in a continued stimulation of neurohormonal systems. The LV dysfunction starts as asymptomatic, then it develop into the clinical syndrome of heart failure that is characterized by symptoms of breathlessness (dyspnea) at low or normal levels of exertion, fluid and sodium retention,

fatigue, rehospitalisation and high rate of mortality among patients, episodes of arrhythmias, pump failure, and death (Bui et al., 2011; Ziaeian and Fonarow, 2016). Therefore, while the primary mechanism of myocardial insult might be different in patients with ischemic and non-ischemic HF, the pathophysiology of the disease following the myocardial injury is quite comparable (DeFilippis et al., 2019).

1.1.2 Pathophysiology of HF

In order to maintain adequate function, the failing heart depends on several compensatory mechanisms, including enhancing cardiac output, increasing LV volume and wall thickness via the cardiac remodelling process, and preserving tissue perfusion with elevated mean arterial pressure upon the activation of neurohormonal pathways. While these compensatory mechanisms initially provide some benefits in the early stages of HF, they will eventually result in a vicious cycle of worsening HF (French and Kramer, 2007; Abbate et al., 2015). The initial decrease in cardiac output enhances the baroreceptor-mediated adrenergic system activity, therefore increased inotropy will compensate for an acutely reduced cardiac output (Lymperopoulos et al., 2013). On the other hand, high sympathetic output is linked to desensitization of the cardiac β-receptor; and it also enhances the release of renin from the juxtaglomerular apparatus in the renal system. The activation of RAAS is considered as a major player in the pathophysiology of HF (Mann and Bristow, 2005).

As an integral part of RAAS, angiotensin II (Ang II) exerts its action as a vasoconstrictor through Ang II receptors. Ang II is a peptide hormone which is biosynthesized from the precursor molecule angiotensinogen, it is also responsible for the adrenal and posterior

pituitary gland secretion of aldosterone and vasopressin, respectively (Wright et al., 1995). These peptide hormones are responsible for heightened sodium and water retention, edema and increased preload on the cardiac muscle. Therefore, it will cause a hemodynamic injury to the heart and lastly lead to maladaptive hypertrophic remodeling and eventually heart failure (Jacob et al., 2013). It is worth mentioning that the majority of HF patients have a history of hypertension and cardiac hypertrophy (Gradman and Alfayoumi, 2006).

1.1.3 Phenotyping HF

Generally, HF involves impaired cardiac pumping function; the traditional indicator of pump dysfunction is ejection fraction (EF) which is defined as the percent of blood volume ejected with each beat (Sharma and Kass, 2014). For decades, the main focus of basic and clinical research was on HF that involves depressed LV systolic performance (systolic HF), currently known as HF with reduced ejection fraction (HFrEF) (Ponikowski et al., 2016). Nevertheless, up to 50% of patients with HF signs and symptoms have LVEF ≥ 50% and comprise another phenotype of HF known as HF with preserved ejection fraction (HFpEF) (Yancy et al., 2013). In addition to aging, it is noteworthy that HFpEF patients typically have comorbid conditions including atrial fibrillation, hypertension, pulmonary hypertension, metabolic syndrome, and renal dysfunction, however the precise contribution of each condition to the pathophysiology of the disease is still poorly-defined (Desai and Fang, 2008; ter Maaten and Voors, 2016; Altara et al., 2017; Rosenkranz et al., 2019; Sugumar et al., 2019). The third type of HF is heart failure with mid-range EF (HFmrEF) with EF falls between 40% and 49%

according to the Canadian and the United States guidelines (Maddox et al., 2021; McDonald et al., 2021). The following table summarizes the key differences between HFrEF and HFpEF.

Table 1.1. Summary of the major differences between HFrEF and HFpEF.

	HFrEF	**HFpEF**	**References**
Ejection Fraction	≤ 40%	≥ 50%	(Florea et al., 2016)
Primary Contributor	Systolic Dysfunction	Diastolic Dysfunction	(Plitt et al., 2018)
Risk Factors /Comorbidities	- Obesity - Hypertension - Diabetes - Kidney disease - Cardiomyopathy - Myocardial infarction - Male	- Atrial Fibrillation - Hypertension - Pulmonary hypertension - Metabolic syndrome - Renal dysfunction - Age - Female	(Lee et al., 2009; Ho et al., 2013; Jeong and Dudley, 2015; Ergatoudes et al., 2019)
Endothelial dysfunction	- Late stage symptom - Prevalence: low	- Early stage symptom - Prevalence: high	(Paulus and Tschöpe, 2013; Tromp et al., 2019)
Cardiac Hypertrophy	Eccentric	Concentric	(Ooi and Allen, 2008; González et al., 2011; Zile et al., 2011)

1.2 Cardiac hypertrophy

Cardiac hypertrophy is defined as a complex adaptive response to increased biomechanical stress, which is usually associated with acute events, including myocardial infarction, or results from an accompanying chronic CVD such as hypertension (Vakili et al., 2001). As a response, the heart muscle thickens in order that the diastolic and systolic functions would not deteriorate (Lalande and Johnson, 2008). While cardiac hypertrophy represents an adaptive response, extended cardiac hypertrophy could become maladaptive and ultimately progress to dilated cardiomyopathy, HF, serious arrhythmias and even sudden death (Tomaselli and Zipes, 2004).

Pathological cardiac hypertrophy is considered a sign of poor prognosis in several heart diseases and it typically predisposes to most phenotypes of HF (Bernardo et al., 2010). The number of HF patients is continuously increasing in North America. The most up-to-date heart disease statistics showed that the number of the US HF patients (≥20 years of age) has risen from 5.7 million (2009 to 2012) to 6.5 million (2011 to 2014) (Benjamin et al., 2017). In Canada, approximately 600,000 people are living with heart failure and it costs $2.8 billion per year as direct costs (Heart and Stroke Foundation, 2016). In addition to HF, left ventricular hypertrophy is not only associated with myocardial infarction and arrhythmia but also is considered a solid predictor of future cardiovascular mortality (Brown et al., 2000; Elkhatali et al., 2015). Understanding conceptual aspects of pathogenesis of cardiac hypertrophy is considered a research of an important risk factor of HF and will allow for emergence of novel therapeutic targets.

Histologically, the myocardium of is composed of a wide range of cells, approximately 70% non-myocytes and 30% cardiac myocytes, non-myocytes represent fibroblasts, extracellular matrix, endothelial cells and vascular smooth muscle cells (Souders et al., 2009). The functions of these cells are to maintain the electrical, chemical and biomechanical responsive nature of the heart. In addition, these cells contribute to the preservation of the three-dimensional structure of the cardiac tissue via autocrine and paracrine action of their secreted mediators (Manabe et al., 2002). Modifications in these signals or increased biomechanical stress can lead to deleterious, adaptive and/or compensatory changes in the heart including cardiac hypertrophy (Frey et al., 2004).

It is noteworthy that cardiac hypertrophy is defined as a growth of existing cardiac myocytes, this condition is different from hyperplasia, which is defined as an increase in the number of myocardial cells by mitotic division during embryonic and fetal life (Oparil et al., 1984). The most distinct hallmarks of cardiac hypertrophy include an increase in cell volume, induced protein synthesis, and heightened organization of basic contractile units of the heart (Maillet et al., 2013). These events will eventually lead to ventricular remodelling and dilatation, fibrosis, and diminished cardiac output lately (Van Berlo et al., 2013).

1.2.1 Types of cardiac hypertrophy

Cardiac hypertrophy could be classified according to the pathophysiology into either physiological or pathological. It is classified as physiological when the cardiac function is preserved or as pathological when it associated with cardiac dysfunction (Shimizu and Minamino, 2016). Also, it could be categorized into 2 phenotypes known as concentric

hypertrophy and eccentric hypertrophy, indicating that the heart responds differently to stressful stimuli. Both types of cardiac hypertrophy result as a response to different stimuli, and are characterized by different structural and molecular phenotypes (Khouri et al., 2010).

1.2.1.1 Physiological cardiac hypertrophy

Physiological enlargement of the heart as a result of postnatal growth, exercise, and pregnancy is usually accompanied by maintenance of normal cardiac function and is described as "physiological" hypertrophy. In humans, the heart weight is directly proportional to the increase in body weight (Dorn, 2007). The major contributor to the increase in cardiac weight during growth is the enlargement of cardiomyocytes. During development from infants to adults in human, it is estimated that there is an almost 3-fold increase of cardiomyocyte diameter (Bergmann et al., 2015). Importantly, physiological hypertrophy does not develop into dilated cardiomyopathy, is not associated with changes in the pattern of fetal gene expression and is associated with enhanced glucose and fatty acid oxidation capacity (Dyck and Lopaschuk, 2006; Kolwicz and Tian, 2011).

1.2.1.2 Pathological cardiac hypertrophy

The development and progression of pathological cardiac hypertrophy occur as a response to different disease states, including myocardial infarction, hypertension, and valvular heart disease (Drazner, 2011). Pressure overload is one of the major burdens that cause pathological cardiac hypertrophy, it develops as a result of hypertension or aortic stenosis. The adaptation to pressure overload can be classified into three phases: the first phase occurs immediately after the initiation of the defect during which hypertrophy

develops. The second phase is described as the stable hypertrophy phase, and, if untreated, a third phase of decompensation and myocardial failure will follow (Crozatier and Hittinger, 1988; Pitoulis and Terracciano, 2020). Molecularly, pathological hypertrophy is associated with a re-activation of fetal genes such as β-myosin heavy chain (β-MHC), atrial natriuretic peptide (ANP) and B-type natriuretic peptide (BNP). Also, a down-regulation of sarcoplasmic reticulum Ca^{++} ATPase (SERCA) is only reported in pathological hypertrophy (Du, 2007). Metabolically, during decompensated cardiac hypertrophy and HF, the failing heart faces an energy deficit. This deficit is primarily caused by the decrease in mitochondrial oxidative capacity. In this case, the failing heart compensate for this deficit by an increase in ATP production from glycolysis (Lopaschuk et al., 2021).

1.2.1.3 Concentric vs eccentric cardiac hypertrophy

In case of pressure overload such as in hypertensive patients, elevation in blood pressure will lead to a concentric hypertrophic phenotype of pathological cardiac hypertrophy. However, in case of valvular heart diseases, an increase in volume will result in an eccentric pathological hypertrophic phenotype (Müller and Dhalla, 2013). In patients with pressure overload, it was noticed that there was an increase in the measurement of the ratio of left ventricle (LV) wall thickness to LV radius as an adaptive response to the elevated LV peak systolic and end diastolic pressures. Conversely, patients who have volume overload, characterized with consistently increased end-diastolic pressure, showed no change in the ratio of wall thickness to LV radius (Grossman et al., 1975). Physiologic cardiac hypertrophy can morphologically develop into either eccentric or

concentric. Generally, it has been reported that athletes who exercise in more endurance-focused sports, such as running and rowing, develop eccentric cardiac hypertrophy. On the other hand, athletes who are focusing on resistance training, including weight-lifting, develop concentric cardiac hypertrophy without ventricular dysfunction or cavity reduction (Barauna et al., 2007). Figure 1.1 shows the major differences between concentric and eccentric cardiac hypertrophy.

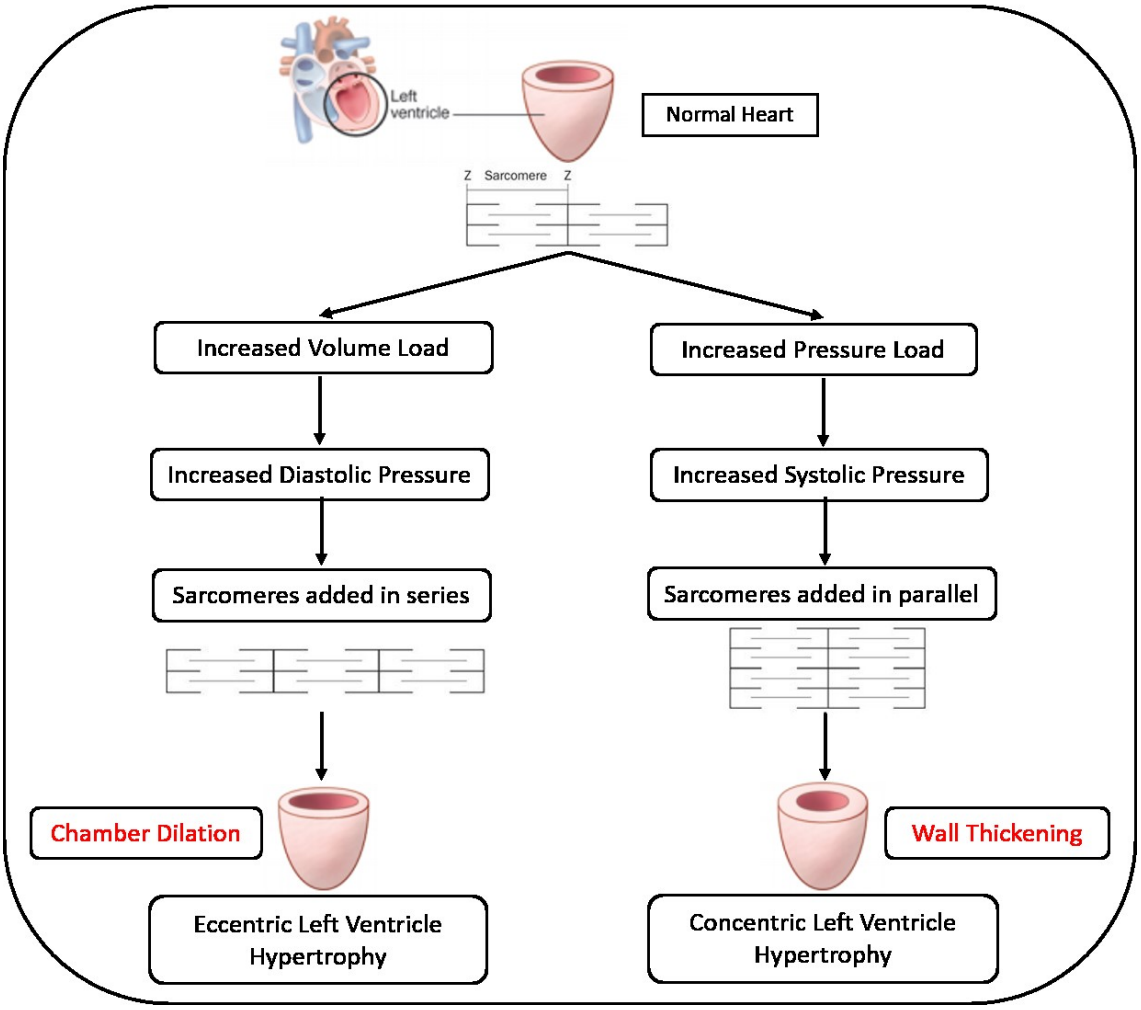

Figure 1.1. Schematic diagram of the development of eccentric and concentric cardiac hypertrophy

In this schematic figure, pressure overload is associated with parallel addition of sarcomeres leading to concentric cardiac hypertrophy while the volume overload results in series addition of sarcomeres in case of eccentric cardiac hypertrophy.

1.2.2 Signaling pathways involved in mediating cardiac hypertrophy

Generally, the causative stimuli for cardiac hypertrophy can be classified into biomechanical and stretch-sensitive mechanisms, or neurohumoral pathways which are responsible for the release of hormones, cytokines, and peptide growth factors. Several ligands exert their actions on cardiac myocytes through a wide range of membrane-bound G-protein-coupled receptors (GPCRs). These receptors possess either intracellular tyrosine kinase domains or intracellular serine/threonine kinase domains (Sala et al., 2012). Biomechanical signals are thought to be mediated through internal stretch-sensitive receptors with molecular mechanisms that have not been fully elucidated, and no distinctive cellular mechanisms have yet been identified. These intracellular signal-transduction pathways are responsible for mediating the cardiac growth response (Heineke and Molkentin, 2006). The main target of these signalling circuits is to coordinate hypertrophic growth by modulating gene expression in the nucleus and also to elevate the rates of protein translation and inhibiting protein degradation in the cytoplasm. These pathways include phosphoinositide 3-kinases (PI3Ks), protein kinase C (PKC), mitogen activated protein kinases (MAPK) and nuclear factor-κB (NF-κB) and others.

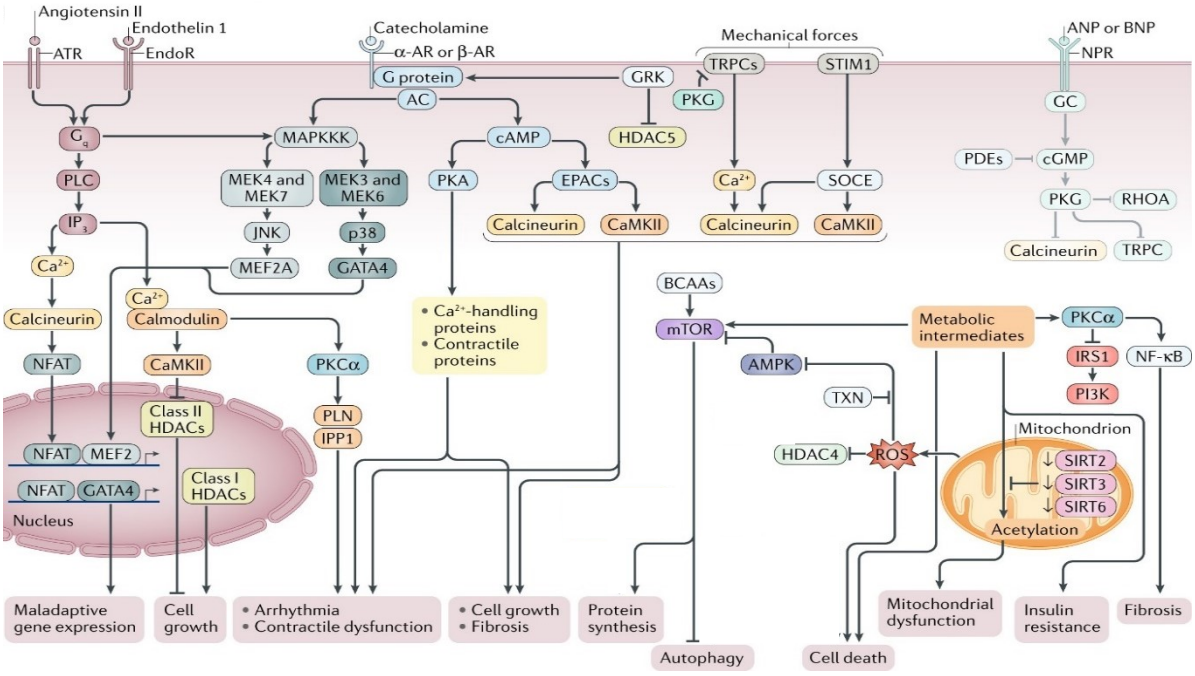

Figure 1.2. Integrated schematic diagram of the most studied intracellular signaling pathways involved in the pathogenesis of cardiac hypertrophy.

Pathological cardiac hypertrophy and consequent HF are triggered by neuroendocrine hormones (including angiotensin II, endothelin 1, and catecholamines) or by mechanical forces including hypertension. The aforementioned triggers lead to increase in reactive oxygen species (ROS) formation in direct or indirect ways. This also results in myocardial accumulation of metabolic intermediates leading to induction of cell death, fibrosis, and mitochondrial dysfunction. Increase in cyclic GMP (cGMP) levels is mediated by natriuretic peptides leading to activation of protein kinase G (PKG) to inhibit cell growth. It is worthy to mention that the natriuretic peptide receptor (NPR) is desensitized in

cardiac hypertrophy. G protein-coupled receptor kinases (GRKs) are reported to mediate β-adrenergic receptor (β-AR) desensitization, cardiomyocyte hypertrophy, insulin resistance, cell death, and mitochondrial dysfunction. Activation of mechanistic target of rapamycin (mTOR) is deleterious because it leads to inhibition of autophagy and subsequent excessive protein synthesis. AC, adenylyl cyclase; AMPK, AMP-activated protein kinase; ANP, natriuretic peptide A; ATR, angiotensin II receptor; BCAA, branched-chain amino acid; cAMP, 3′,5′-cyclic AMP; BNP, natriuretic peptide B; CaMKII, calcium/calmodulin-dependent protein kinase type II; EndoR, endothelin 1 receptor; EPACs, exchange proteins directly activated by cAMP; GATA4, transcription factor GATA4; GC, guanylate cyclase; HDAC, histone deacetylase; IP3, inositol 1,4,5-triphosphate; IP3R3, inositol 1,4,5-triphosphate receptor type 3; IRS1, insulin receptor substrate 1; JNK, JUN N-terminal kinases; MAPKKK, mitogen-activated protein kinase kinase kinase; MEF2A, myocyte enhancer factor 2 A; MEK, MAP/ERK kinase; NF-κB, nuclear factor-κB; NFAT, nuclear factor of activated T cells; p38, mitogen-activated protein kinase 11; PDE, phosphodiesterase; PI3K, phosphoinositide 3-kinase; PKA, protein kinase A; PKCα, protein kinase Cα; PLC, phospholipase C; PLN, phospholamban; RHOA, transforming protein RHOA; SIRT, NAD-dependent protein deacetylase sirtuin; SOCE, store-operated Ca2+ entry; STIM1, stromal interaction molecule 1; TRPC, transient receptor protein channel; TXN, thioredoxin. The figure is reprinted from (Nakamura and Sadoshima, 2018) with permission from Springer Nature.

1.2.2.1 Ca^{2+} Calcineurin/NFAT

Calcineurin is a calmodulin-dependent phosphatase that is activated by calcium, that functions as an effector downstream protein of Gq-protein coupled receptors as well as PKC activation. Once activated, it dephosphorylates the nuclear factor of activated T cells (NFAT) transcription factor (Park et al., 2020). NFAT is activated by multiple mechanical and neurohormonal factors and it translocates to the nucleus where it activates GATA-4 transcription factor, GATA4 is a zinc-finger-containing transcription factor that can regulate hypertrophic gene expression and leads to the development of cardiac hypertrophy (Konhilas and Leinwand, 2006). Accumulating evidence have found that deficiency of calcineurin in mice is linked to prevention against pressure overload-, Ang-II- or isoproterenol-induced cardiac hypertrophy (Wilkins and Molkentin, 2002). In addition, overexpression of modulatory calcineurin-interacting protein (MCIP1) in the heart prevented against hypertrophy induced by isoproterenol, exercise, or pressure overload. These studies speculate that calcineurin/NFAT pathway is directly involved in both physiological and pathological cardiac hypertrophy (Rothermel et al., 2001; Wilkins and Molkentin, 2002).

1.2.2.2 Protein kinase C and Gq-protein coupled receptor

PKC is a family of phospholipid-dependent serine/threonine kinases expressed in a wide range of tissues, they can be further classified into three PKC isozymes subfamilies: conventional, novel, and atypical. This family of isozymes are known to be involved in mediating cell proliferation, survival, invasion, migration, apoptosis, angiogenesis, platelet function and inflammation (Kang, 2014). The protein is named PKC as it is a

protein kinase enzyme that is highly dependent on calcium and phospholipids as second messengers in its activation (Lipp and Reither, 2011). Three isoforms exist for this enzyme, namely α, β and γ; they differ from each other in their composition of the fifty amino acids at the C-terminal. The three isoforms are expressed in different organs of the human body and their physiological functions are closely related to their specificity. Importantly, PKC-alpha isoform is found in nearly all organs, especially in the myocardium. PKC-alpha act as a nodal integrator of cardiac contractility by sensing intracellular Ca^{2+} and signal transduction events, which can profoundly affect propensity toward cardiac hypertrophy and HF (Braz et al., 2004).

A comparative study has investigated the major differences between PKC isoforms. The analysis was carried out using adenovirus-mediated transfection of wild-type or dominant inhibitory forms of PKCα, -β2, -δ, and -ε in neonatal rat cardiomyocytes. The results showed that only PKCα isoform was able to mediate cellular hypertrophy and only inhibition of PKCα protected against agonist-mediated cellular hypertrophy. The results of this study suggest that PKCα isoform is a dominant regulator of cardiomyocyte hypertrophic growth (Braz et al., 2002). PKCα is regulated by Gq-protein coupled receptor, activation of Gq-protein coupled receptor leads to stimulation of the effector enzyme phospholipase C (PLC). Thereafter, PLC interacts with phosphoinositol bisphosphate (PIP2) in the membrane to produce diacylglycerol (DAG) and inositol trisphosphate. DAG is involved the intermediate transduction of signals to activate PKC (Putney and Tomita, 2012).

1.2.2.3 PI3K/Akt/Glycogen Synthase Kinase-3 dependent pathway

The binding of ligands to tyrosine kinase receptors including insulin-like growth factor (IGF), fibroblast growth factor, transforming growth factor, and G protein coupled receptors (GPCRs) leads to the activation of phosphoinositide 3-kinase (PI3K) (Aoyagi and Matsui, 2011). Upon activation of PI3K, the enzyme activates one of its major targets known as Akt, a serine/threonine kinase, also known as protein kinase B (PKB) (Manning and Toker, 2017). Several reports have previously demonstrated that the PI3K-Akt signaling pathway is associated with cardiac hypertrophy. In dominant negative PI3K transgenic (dnPI3K) mice, exercise-induced cardiac hypertrophy was ameliorated in comparison with wild type animals. On the other hand, pathological cardiac hypertrophy induced by pressure overload in wild type and dnPI3K mice showed no significant difference (McMullen et al., 2003). These data suggest that PI3K-Akt signaling pathway plays a critical role for the induction of physiological, but not pathological, cardiac hypertrophy. Of interest, activation of PI3K/Akt to induce experimental cardiac hypertrophy had no significant effect on the cardiac systolic function, suggesting a direct impact of PI3K/Akt pathway on the cardiomyocyte size, and not an adaptation to impaired contractility (Bass-Stringer et al., 2021).

The effect of PI3K/Akt pathway activation to induce cardiac hypertrophy is mediated through two well-defined downstream targets of Akt, the first one is glycogen synthase kinase-3 (GSK-3) and the second target is mammalian target of rapamycin (mTOR) (Shiojima and Walsh, 2006). To study the role of GSK-3α in cardiac hypertrophy, studies on overexpression of GSK-3α in transgenic mice have been carried out. These mice

showed smaller hearts with increases in apoptosis and fibrosis but with preserved cardiac function at baseline. On the other hand, in response to pressure overload, mice demonstrated attenuated cardiac hypertrophy, enhanced apoptosis and fibrosis, suggesting that GSK-3α appears to inhibit physiological cardiac growth (Zhai et al., 2007). PI3K/Akt pathway activation also leads to activation of the second target, mTOR. Upon activation, mTOR was shown to aggravate aging-induced cardiac hypertrophy and worsen myocardial contractile function through inhibition of autophagy (Hua et al., 2011). Also, mTOR is known to be a major promoter of protein synthesis, cell growth and proliferation. mTOR activity is elevated during the cardiomyocyte hypertrophic response to hypertrophic agonists such as isoproterenol, Ang-II and IGF-1 (Sadoshima and Izumo, 1995; Lavandero et al., 1998; Simm et al., 1998). Interestingly, partial and selective pharmacologic and genetic inhibition of mTOR demonstrated significant protection against pathological cardiac hypertrophy and HF caused by pressure overload or genetic cardiomyopathies (Sciarretta et al., 2014).

1.2.2.4 MAPK signalling pathways

MAPK are serine/threonine specific protein kinases, that are responsible for the regulation of diverse cellular responses including gene expression, mitosis, metabolism, differentiation, proliferation and survival/apoptosis (Cargnello and Roux, 2011). This group of kinases regulate the genes that induce protein synthesis and initiate cardiac hypertrophy (Zhang et al., 2003). A wide array of external stimuli are known to activate MAPKs, consequently they are translocated from the cytoplasm to the nucleus through large pores on the nuclear membrane. They exert their action through the regulation of

certain cardiac gene expression by phosphorylating various transcriptional factors (Zehorai et al., 2010). MAPK pathways can be classified into three major subfamilies: extracellularly responsive kinases (ERKs), c-Jun N-terminal Kinases (JNKs), and p38 MAPKs (Roux and Blenis, 2004). Interestingly, activation of p38 resulted in induction of myocyte hypertrophy and apoptosis and promoted fetal gene expression and cytokine production (Zechner et al., 1997). Additionally, Harris et al. showed that inhibition of the ERK pathway successfully prevents hypertrophy and fetal gene induction in response to pressure overload (Harris et al., 2004). Also, constitutive expression of MAP kinase phosphatases (MKP-1), counteracting factor of MAPKs, in cultured primary cardiomyocytes using adenovirus-mediated gene transfer halts the activation of p38, JNK1/2, and ERK1/2 and protects against agonist-induced hypertrophy. Similarly, transgenic mice expressing physiological levels of MKP-1 in the heart showed diminished activity of p38, JNK1/2, or ERK1/2, decreased developmental myocardial growth; and ameliorated cardiac hypertrophy induced by pressure overload and isoproterenol infusion (Bueno et al., 2001).

1.2.2.5 NF-κB

NF-κB is an universally expressed and extremely regulated dimeric transcription factor that is involved in a wide range of physiological and pathophysiological functions, including innate and adaptive immunity, tissue regeneration, stress responses, apoptosis, cell proliferation, carcinogenesis and differentiation (Ghosh et al., 1998; Schoonbroodt et al., 2000; Bui et al., 2001). Based on the canonical view of the regulation of NF-κB activity, NF-κB remains in the cytosol after binding with the inhibitory protein IκBα. This

complex keeps NF-κB in an inactive form, therefore its transcriptional activity is inhibited. External stimuli such as inflammatory mediators or hypertrophic agonists increase IκBα phosphorylation at two conserved serine and one tyrosine residues, leading to induction of its protein ubiquitination and proteosomal degradation (Kopp and Ghosh, 1994; Traenckner and Baeuerle, 1995). It is well established that the main form of NF-κB has two particular polypeptides of 50 and 65 kDa, named as p50 and p65 NF-κB subunits, respectively. Upon degradation of IκB, NF-κB is released and freed in order to form dimers, which most commonly exist as p65/p50 dimers. This dimerization process unmasks a nuclear localization site within the p50 subunit that promotes their translocation to the nucleus. Inside the nucleus, the complex binds to distinctive sequences within promoters or enhancer regions of target genes involved in cardiac hypertrophy (Li et al., 2004; Leychenko et al., 2011; Gaspar-Pereira et al., 2012).

Accumulating evidence demonstrated that NF-κB signaling pathway activation is linked to the pathogenesis of cardiac hypertrophy and its progression to HF. The transgenic Myo-Tg mouse model, a model that achieve overexpression of myotrophin in the myocardium to initiates hypertrophy, develops hypertrophy in the heart and the hypertrophic effect is associated with an elevated level of NF-κB activity (Gupta et al., 2008). Interestingly, pharmacological inhibition of NF-κB by pyrrolidine dithiocarbamate, a pharmacological inhibitor of NF-κB, in the Myo-Tg mice led to a remarkable decrease in cardiac mass, NF-κB activity, and the expression of profibrotic genes as well as enhancement of cardiac function (Kumar et al., 2011). Additionally, inhibition of NF-κB using direct gene delivery of sh-p65 RNA resulted in protection

against cardiac hypertrophy (Gupta et al., 2008). Furthermore, blockade of NF-κB activation attenuated Ang-II-induced cardiac hypertrophy without deteriorating cardiac function, suggesting that NF-κB plays a plausible role in cardiac hypertrophy and remodeling besides promoting inflammation (Kawano et al., 2005).

1.2.2.6 Oxidative stress

Reactive oxygen species (ROS) are considered the metabolic by-products of the consumption of oxygen. Cellular ROS are produced either endogenously as a part of the process of mitochondrial oxidative phosphorylation, or they may result from interactions with exogenous sources such as xenobiotic compounds (Ray et al., 2012). There are naturally occurring antioxidant systems in place keep the ROS levels low in normal situations, however some of these ROS exert physiological actions (Kurutas, 2016). Examples of ROS include hydrogen peroxide, superoxide anion ($O_2^{\bullet -}$), hydrogen peroxide (H_2O_2), hydroxyl radical (HO•), nitric oxide, and peroxynitrite. They consist of radical and non-radical oxygen species. A detrimental event called oxidative stress happens when there is an overproduction of ROS and/or deficiency in antioxidant mechanisms (Nita and Grzybowski, 2016). Reactive oxygen species production in the heart is mainly achieved by the mitochondria, NADPH oxidases, xanthine oxidase, and uncoupled nitric oxide synthase (NOS) (van der Pol et al., 2019). Increased levels of ROS result in inactivation of essential metabolic enzymes and disruption of signal transduction pathways in the heart (Farías et al., 2017).

Growing evidence highlights oxidative stress as an important mechanism for the pathogenesis of cardiac hypertrophy and LV remodelling (McMurray et al., 1993; Sawyer

et al., 2002; Murdoch et al., 2006). Mechanistically, excessive ROS leads to activation of a broad variety of hypertrophy signaling pathways including kinases and transcription factors. For instance, in rat neonatal cardiomyocytes, hydrogen peroxide was found to stimulate the tyrosine kinase Src, GTP-binding protein Ras, PKC, MAPK and JNK leading to hypertrophic growth (Aikawa et al., 2001; Wei et al., 2001). Treatment with some antioxidants demonstrated a protective effect against superoxide-mediated hypertrophic response in cardiomyocytes (Tanaka et al., 2001; Yun and Yang, 2020).

1.2.2.7 Other signaling pathways

Peroxisome proliferator activated receptors (PPARs), the Na+/H+ exchanger and CYP enzymes have been also reported to be involved in the pathogenesis of cardiac hypertrophy.

PPARs are ligand-activated transcription factors that are responsible for the regulation of lipid metabolism, energy production as well as inflammation. It is well established that all of the three isoforms of PPARs, typified by PPARα, PPARβ and PPARγ, are expressed in the cardiomyocytes (Liao et al., 2016). PPARγ ligands such as troglitazone, pioglitazone, and rosiglitazone were able to protect against Ang II-induced upregulation of skeletal alpha-actin and atrial natriuretic peptide genes and an increase in cell surface area in cardiomyocytes. Furthermore, pioglitazone ameliorated pressure overload-induced increases in the heart weight-to-body weight ratio, wall thickness, and myocyte diameter in mice, suggesting that PPARγ-dependent pathway is critically involved in the inhibition of cardiac hypertrophy (Asakawa et al., 2002).

Another pathway to consider is the Na^+/H^+ exchanger, an integral membrane glycoprotein widely expressed in mammalian cells. The main function of the Na^+/H^+ exchanger is to exchange intracellular H^+ for extracellular Na^+ (1:1) in order to regulate intracellular pH (pH_i) and the concentration of $[Na^+]_i$ (Cingolani and Ennis, 2007). Several pieces of evidence suggest that the harmful effect of hyperactivity of the Na^+/H^+ exchanger originates from the increase in $[Na^+]_i$ and its associated Ca^{2+} overload through the $Na^{+/}Ca^{2+}$ exchanger leading to myocardial dysfunction, cardiac hypertrophy and heart failure (Bak and Ingwall, 2003; Aiello et al., 2005; Baartscheer et al., 2005; Chahine et al., 2005). Of particular interest, Camilión de Hurtado *et al* showed that cariporide, a specific Na^+/H^+ exchanger inhibitor, was able to protect against cardiac hypertrophy in spontaneously hypertensive rats (SHR) with no change in arterial pressure (Camilión De Hurtado et al., 2002).

The role of CYP enzymes and their associated arachidonic acid (AA) metabolism in the pathogenesis of cardiac hypertrophy will be discussed in detail in the following section.

1.3 Cytochrome P450 enzymes

CYP is a superfamily of enzymes, comprised of about 500 different CYP isozymes. They are involved in the oxidative metabolism of a broad range of drugs, environmental chemicals in addition to endogenous compounds. Although they represent a small proportion of CYP-mediated reactions, CYP enzymes could catalyze reductive reactions in form of halide elimination in the absence of molecular oxygen (Behrendorff, 2021). CYP enzymes are classified as the major phase I metabolic enzymes (Bak et al., 2011). Additionally, vital processes such as carbon source assimilation and biosynthesis of

hormones, and carcinogenesis are partly mediated by CYP enzymes (Werck-Reichhart and Feyereisen, 2000). Progress made over the past decades upholds an evident role for CYP enzymes and their AA metabolites in human normal physiology and the pathogenesis of several diseases (Liu et al., 2004). Comprehensive understanding of the biological and pathophysiological roles of CYP-mediated AA metabolites allows for the characterization of novel therapeutic targets, hence helping in the designing and developing new therapeutic modalities (Roman, 2002).

1.3.1 Classification of CYPs and their cardiac expression

The CYP enzymes in the mammalian cells are found to be localized to the endoplasmic reticulum, however they have a very limited expression in mitochondria (Myasoedova, 2008). CYP enzymes are primarily expressed in the liver; nevertheless they are also significantly expressed in extrahepatic tissues including lung, kidney, gastrointestinal tract, and heart (Myasoedova, 2008; Pavek and Dvorak, 2008). Importantly, the metabolic capacity and their capability for drug clearance in extrahepatic tissues are low (Zanger and Schwab, 2013).

CYP enzymes are classified into families and subfamilies according to the primary amino acid sequences of the purified CYP isozyme (Sim and Ingelman-Sundberg, 2006; Nebert et al., 2013). CYP enzymes that share more than or equal to 40% identity are assigned to a specific family denoted by an Arabic number. In addition, if there is 55% or more identity sharing between the members of one family, they will make up a particular subfamily designated by a letter (Nelson et al., 1996). The metabolism of xenobiotics including pharmacological agents in mammalian tissues are predominantly mediated by

CYP families 1, 2 and 3. On the other hand, the oxidative metabolism of endogenous compounds such as eicosanoids, fatty acids and steroids is largely carried out through other families of CYP enzymes (Barouki and Morel, 2001). Of interest, CYP enzymes have been previously reported to be expressed in the cardiovascular tissue. Also, the specific isoforms of CYP enzymes have been detected in other species such as rat and mouse heart in addition to various compartments of human heart (Roman, 2002; Imaoka et al., 2005; DeLozier et al., 2007). Accumulating evidence suggests that CYP enzymes and their associated metabolites play a major role in the maintenance of cardiovascular health, including the regulation of vascular tone, extracellular fluid volume, and heart function (El-Kadi and Zordoky, 2008).

1.3.2 CYP1 family

1.3.2.1 CYP1A1

In humans and most mammals, the CYP family 1 represents three well-studied monooxygenases, CYP1A1, CYP1A2, and CYP1B1 (Divanovic et al., 2013). CYP1A1 is a well-known aryl hydrocarbon hydroxylase that is found primarily in extrahepatic tissues (Androutsopoulos et al., 2009). CYP1A1 is mainly involved in the metabolic activation of environmental procarcinogens forming highly reactive conversion products; its substrates include polycyclic aromatic hydrocarbons (PAHs) and polyhalogenated aromatic hydrocarbons (PHAHs) (Walsh et al., 2013). Accumulating evidence has shown that *CYP1A1* genetic variation is significantly correlated with the individual's vulnerability to more than one type of cancer such as lung, breast and prostate cancers (Miller, 1994; Sergentanis and Economopoulos, 2010; Hoidy et al., 2019). Due to its

evident role in human malignancies, modulation of CYP1A1 activity has been proposed as a possible therapeutic modality for cancer chemoprevention (Badal and Delgoda, 2014; Mescher and Haarmann-Stemmann, 2018).

1.3.2.2 CYP1A2

CYP1A2 is another member of CYP family 1 that is involved in the metabolism of a variety of compounds including PAH and heterocyclic aromatic amines/amides, in addition to its role in metabolizing a number of clinically-approved drugs such as clozapine, theophylline, zolmitriptan, melatonin and duloxetine (Rendic, 2002; Chen et al., 2017). CYP1A2 is also involved in the bioactivation process of procarcinogenic compounds. Moreover, genetic polymorphism of CYP1A2 has been positively associated with increased risk of developing myocardial infarction (Cornelis et al., 2004). Taken together these data suggest that CYP1A2 could be considered as a therapeutic target for cancer chemoprevention and prevention of cardiovascular diseases (CVD) (Cornelis et al., 2004; Hong et al., 2004).

1.3.2.3 CYP1B1

The third member of CYP family 1 is CYP1B1, this enzyme has the capacity to metabolize a wide range of endobiotics and xenobiotics (Li et al., 2017). CYP1B1 is mainly found in extrahepatic tissues such as the heart, and its expression is significantly correlated with certain types of cancer as well. In the heart, CYP1B1 is responsible for the biosynthesis of a group of arachidonic acid (AA) metabolites known as mid-chain hydroxyeicosatetraenoic (HETE) namely 5-, 8-, 9-, 11-, 12- and 15-HETE (Choudhary et al., 2004; Nayeem, 2018a). Several reports have demonstrated that there is a positive

correlation between the level of mid-chain HETEs and the development of CVD in different experimental models including hypertension, cardiac hypertrophy, heart failure and myocardial infarction (Huang et al., 2020; Shoieb and El-Kadi, 2020). This emphasizes the need for establishment of therapies that have the ability to modulate the activity of CYP1B1 enzyme (Wang et al., 2016; Li et al., 2017).

1.3.2.3.1 CYP1B1 expression in the cardiovascular system

Several studies reported the constitutive expression of CYP1B1 in adult human heart and in the human fetal ventricular cardiomyocyte cell line, RL-14, at the mRNA and protein levels (Choudhary et al., 2005; Maayah et al., 2015b). In addition, wild type AhR amd AhR-null mice showed a significant expression of Cyp1b1 mRNA in the heart, cyp1b1 expression accounted for about 13% of the total cardiac CYPs (Choudhary et al., 2004). Also, CYP1B1 has been reported to be constitutively expressed in the vascular smooth muscle cells and coronary artery smooth muscle cells (Dubey et al., 2003; Tang et al., 2009).

In the heart, CYP1B1 is constitutively active, however the induction of this enzyme has been proven to play a major role in the pathogenesis of several CVDs including hypertension, cardiac hypertrophy and heart failure (Korashy and El-Kadi, 2006; Malik et al., 2012). Regarding hypertension, the role of CYP1B1 in the induction and development of Ang II – mediated hypertension has been investigated. The rats were administered Ang II for 13 days. The results showed that the elevation in blood pressure and its associated pathophysiological changes including cardiac hypertrophy were alleviated by using specific CYP1B1 inhibitor 2,3′,4,5′-tetramethoxystilbene.

Interestingly, these effects were found to be markedly reduced in Cyp1b1 null mice (Jennings et al., 2010). Several studies have previously shown that CYP1B1 contributes to the pathogenesis of hypertension and cardiac hypertrophy through activation of nicotinamide adenine dinucleotide phosphate oxidase and generation of ROS and inflammatory mediators (Song et al., 2016). However, its role in the pathogenesis of HF is yet to be investigated. The research in this thesis highlights the role of CYP1B1 in the pathogenesis of HF and cardiac hypertrophy through investigating its involvement in the generation of the cardiotoxic metabolites of midchain HETEs.

1.3.2.3.2 CYP1B1 expression in cancer

CYP1B1 expression has been reported to be elevated in some tumors compared to normal tissues (Shimada et al., 1996; Murray et al., 1997). Elevation of CYP1B1 expression has been observed in hormone-dependent cancers such as breast, ovarian, and prostate cancer (McKay et al., 1995; McFadyen et al., 2001; Tokizane et al., 2005b). Recently, it has been postulated that CYP1B1 induces cell proliferation by enhancing cell cycle transition and inhibiting apoptosis in endometrial and breast cancer cells (Saini et al., 2009; Hong et al., 2014). Additionally, polymorphisms in CYP1B1 have been considered as risk factors predisposing to various types of cancers (Saini et al., 2009; Hong et al., 2014). Altogether, these findings propose that CYP1B1 plays a significant role in cancer progression and, consequently, represent a potential target for anti-tumor therapy.

1.3.3 CYP2 family

CYP2 subfamily enzymes are widely expressed in the cardiovascular system, with the main CYP2 isozymes involved in expoxygenase activity in cardiac tissue being CYP2C8,

CYP2C9, CYP2C19 and CYP2J2. It was previously reported that these isoforms are constitutively expressed in the healthy human heart, noting that CYP2J2 is the most highly expressed enzyme (Thum and Borlak, 2002; Bièche et al., 2007). High levels of CYP2J2 expression were reported in healthy hearts, also there was significant level of expression of CYP2C8 and CYP2C9 mRNA and protein after ischemic injury (DeLozier et al., 2007). The cardiac expression of other CYP2 subfamilies has not been fully studied. One study reported that CYP2B6/7 has been detected in the right ventricle and aorta of patients with dilated cardiomyopathy (Thum and Borlak, 2002). The mRNA of CYP2D6 and CYP2E1 was detected in normal hearts as well as individuals with dilated cardiomyopathy. CYP2C23 and CYP2J3 were detected in rat ventricular tissues (Imaoka et al., 2005). Moreover, *in vitro* studies have demonstrated that CYP2J3 was expressed in H9c2 cells at levels similar to those expressed in rat heart tissues (Zordoky and El-Kadi, 2007).

1.3.4 CYP3 family

CYP family 3 subfamily A consists of several isoforms including CYP3A4, CYP3A5, CYP3A7, CYP3A43 and CYP3A47. It has been reported that CYP3A4 is the most primarily expressed and is responsible for the majority, nearly 60%, of the hepatic CYP-mediated metabolism of pharmacological agents in humans (Martínez-Jiménez et al., 2007). Although it has not been reported to have significant role in cardiovascular physiology and diseases, the expression of CYP3A4 in the myocardium has been reported in the endothelium, endocardium and coronary vessels as evidenced by intense binding of CYP3A4 in immunohistochemistry of cardiac tissues (Minamiyama et al., 1999). Also,

one study has reported the presence of CYP3A1 mRNA and protein in isolated adult rat cardiomyocytes (Thum and Borlak, 2000). However, real time-PCR analysis of human heart tissue showed that there was no expression of CYP3A4, 3A5, 3A7, and 3A47 mRNA (Bièche et al., 2007).

1.3.5 CYP4 family

CYP4A and CYP4F subfamilies are considered the most important members of CYP4 family, members of these subfamilies are responsible for the fatty acid omega-hydroxylation (Edson and Rettie, 2013). Regarding the cardiovascular expression of CYP4 enzymes, it has been shown that CYP4 is expressed in freshly isolated cardiomyocytes of control adult rats and adult human cardiomyocytes (Thum and Borlak, 2000). Moreover, it has been demonstrated that cyp4al2 mRNA was detected in cardiac mouse tissue (Theken et al., 2011). CYP4A and CYP4F were reported to be found in the failing human heart. Also, CYP4A protein expression has been demonstrated to be increased in hypertrophied human hearts (Thum and Borlak, 2002; Elbekai and El-Kadi, 2006).

1.4 CYP-mediated arachidonic acid metabolism

AA is an omega-6 long chain fatty acid with 20 carbons and 4 double bonds. It is a polyunsaturated fatty acid present in the phospholipids of cell membranes that can be released by phospholipases (Carlson and Colombo, 2016). For decades, AA was thought to be solely metabolized by cyclooxygenases (COXs) and lipoxygenases (LOs). COX and LO enzymatic families are capable of producing a wide range of eicosanoids through converting AA into prostaglandins (PGs) and leukotrienes (LTs), respectively

(Chandrasekharan et al., 2016). Discovery of the third branch of the arachidonic acid cascade through CYP enzymes has led to the understanding of the pivotal role of these enzymes in the generation of biologically active metabolites (Westphal et al., 2015). The 3 branches together build up complex signaling networks of over 100 chemical mediators involved in crucial biological actions in practically each tissue, organ and cell in human body (Funk, 2001).

1.4.1 Pathways involved in arachidonic acid metabolism

AA is a polyunsaturated fatty acid present in the phospholipids of cell membrane, it is known to be metabolized into various classes of eicosanoids, by COX, LOX, and CYP enzymes. PGs are autocrine and paracrine lipid mediators, synthesized from AA by COX enzymes (Smith et al., 2000); they have a wide distribution throughout the body and exert diversified physiological functions and responses (Ricciotti and FitzGerald, 2011). The role of PGs in inflammation has been extensively studied and the inhibition of their production has a significant impact on treatment of several disease states (Nathan, 2002). LOX enzymes produce mid-chain HETEs, lipoxins (LXs), and LTs, with the proinflammatory LTs being arguably the most significant based on their function in the pathogenesis of different diseases (Liu and Yokomizo, 2015). The biosynthesis, enzymology, and biological roles of the LOX-derived AA metabolites have been vastly reviewed (Haeggström and Funk, 2011).

CYP monooxygenases are a large family of enzymes largely involved in hepatic drug metabolism. While the majority of CYP are extensively expressed in the liver, they are widely distributed throughout the body where they participate in AA metabolism to a

variety of eicosanoids (2005). Structural elucidation of the metabolites indicated that CYP enzymes could metabolize AA, by incorporation of oxygen at different positions in AA, through three pathways (Figure 1.2) (Capdevila et al., 1992).

First, AA can undergo allylic oxidation reaction to form mid-chain HETEs (5-, 8-, 9-, 11-, 12- and 15-HETE) (Roman, 2002). The second pathway involves hydroxylation at or near the terminal methyl group (ω-/(ω-n)-hydroxylase reaction) yielding terminal HETE known as 20-HETE and 4 subterminal HETEs namely 19-, 18-, 17- and 16-HETE respectively (Powell and Rokach, 2015). Olefin epoxidation (epoxygenase reaction) represents the third pathway of CYP-mediated AA metabolism leading to formation of four regioisomeric epoxyeicosatrienoic acids (EETs) exemplified as 5,6-, 8,9-, 11,12- and 14,15-EET, each of which can be produced as either the R,S or the S,R enantiomer (Xu et al., 2011).

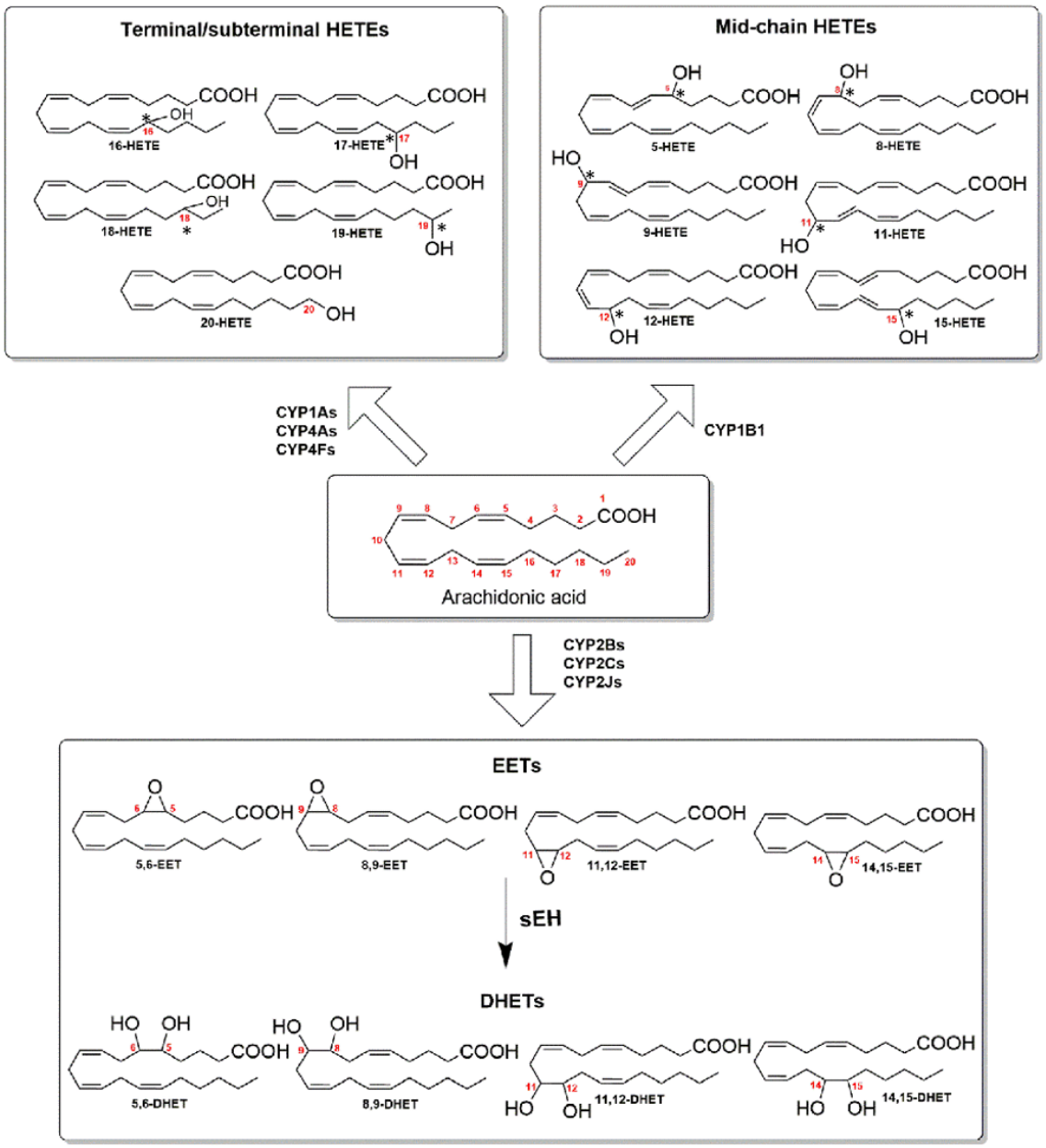

Figure 1.3. Cytochrome CYP-mediated arachidonic acid metabolism.

Arachidonic acid is metabolized by different CYP families into mid-chain HETEs, terminal/subterminal HETEs and EETs. EETs are subsequently metabolized into the less

biologically active dihydroxyeicosatrienoic acids (DHETs) via soluble epoxide hydrolase (sEH). * denotes a chiral center. The figure is reprinted from (Shoieb et al., 2019c).

1.4.2 Mid-chain HETEs

Cardiac CYP1B1 and its associated mid-chain HETEs, typified by 5-, 8-, 9-, 11-, 12- and 15-HETE, have received a particular interest as a potential therapeutic target. Mid-chain HETEs are a group of biologically active eicosanoids that are produced from the metabolism of AA by both lipoxygenase- and CYP-catalyzed bis-allylic oxidation reaction to incorporate a hydroxyl group in the middle of the eicosanoid chain ranging from carbon no. 5 to carbon no. 15 (Jennings et al., 2010; Shoieb et al., 2019a). A growing body of evidence demonstrates that mid-chain HETEs possess cardiotoxic effects and they are involved in the pathogenesis of CVD including atherosclerosis, hypertension, cardiac hypertrophy and HF (Jennings et al., 2014; Song et al., 2016; Anderson and Mazzoccoli, 2019a).

Several reports showed that overexpression of CYP1B1 in cardiac muscle causes an increase in the level of cardiotoxic mid-chain HETEs leading to deterioration of the cardiac histo-architecture and function (Jennings et al., 2014; Maayah et al., 2016; Matsumura et al., 2018). On the contrary, strategies to mitigate CYP1B1 activity either through pharmacological inhibition or genetic deletion have been employed to protect against CVD. 2,3′,4,5′-tetramethoxystilbene (TMS), a well-known CYP1B1 inhibitor, was able to significantly decrease the level of mid-chain HETEs and protect against Ang II-induced cardiac hypertrophy (Elkhatali et al., 2017). In addition, CYP1B1 genetic

disruption resulted in a reduction of cardiac hypertrophy in Ang II–induced model of hypertension in mice (Jennings et al., 2010).

1.4.3 EETs

AA is metabolized by a group of CYP enzymes known as CYP epoxygenases, including CYP2B, CYP2C and CYP2J subfamilies. They produce four regioisomers of cardioprotective EETs namely, 14,15-EET, 11,12-EET, 8,9-EET and 5,6-EET metabolites (Roman, 2002). EETs are defined as being endothelium derived hyperpolarizing factors that act as vasodilators, with this group of metabolites possessing anti-inflammatory and anti-apoptotic effects and they were also reported to reduce vascular smooth muscle cell proliferation (Tacconelli and Patrignani, 2014).

Several *in vivo* and *in vitro* studies demonstrated that EETs can act as protective effectors against cardiac remodeling and amelioration of HF. Transgenic or overexpression of CYP epoxygenase resulted in lowering blood pressure in different animal models of hypertension. For instance, recombinant adeno-associated virus-mediated overexpression of CYP 2J2 protected against the development of hypertension in spontaneously hypertensive rats (Xiao et al., 2010).

In addition, EETs were demonstrated to protect against isoproterenol-induced cardiac hypertrophy and Ang II-induced HF (Wang et al., 2014b; Althurwi et al., 2015). Moreover, CYP2J2 transgenic hearts, with higher levels of EETs, showed less doxorubicin-mediated cardiomyocyte apoptosis in comparison with wild type hearts. Chronic treatment with doxorubicin has resulted in an improved cardiac function in CYP2J2 transgenic mice hearts compared to wild type mice hearts (Zhang et al.,

2009). Furthermore, sEH was highly expressed in the heart of Ang II-induced mice cardiac hypertrophy compared to control mice. However, treatment with a potent sEH inhibitor was able to prevent the pathogenesis of the hypertrophy, suggesting the protective role of EETs against the condition (Ai et al., 2009).

1.4.4 20-HETE

20-HETE is the ω-hydroxylation product of CYP-mediated AA metabolism, with the biosynthesis of this metabolite being catalyzed by a group of CYP enzymes known as monooxygenases, including the CYP4A and 4F gene subfamilies (Hardwick, 2008). The two major 20-HETE-producing CYPs in humans are CYP4A11 and CYP4F2 as well as lower producing capacity of CYP4F11 and CYP4F3 (Bannenberg et al., 2005; Edson and Rettie, 2013). 20-HETE has been reported to exert a potent vasoconstrictor action on coronary, renal, cerebral, mesenteric and skeletal muscle vessels (Dunn et al., 2008; Bubb et al., 2013; Rocic and Schwartzman, 2018).

Several studies have highlighted the possible role of 20-HETE in hypertrophic cardiac remodeling and HF. CYP4A and 4F were found to be upregulated in patients and experimental models of cardiac hypertrophy linked with HF. CYP4A and 4F expression were elevated in isoproterenol-mediated cardiac hypertrophy in rats (Zordoky et al., 2008; Althurwi et al., 2015). Moreover, 20-HETE levels were found to be increased in case of Ang II-induced cardiac hypertrophy (Elkhatali et al., 2015). Interestingly, treatment with HET0016, an inhibitor of 20-HETE synthesis, was demonstrated to protect against benzo(a)pyrene- and doxorubicin-induced cardiotoxicity and cardiac hypertrophy (Aboutabl et al., 2009; Alsaad et al., 2013). Moreover, the correlation between increased

20-HETE levels and myocardial ischemia in humans has been established (Issan et al., 2013). Also, acute inhibition of the formation of 20-HETE using HET0016, as a selective 20-HETE synthesis inhibitor, for half an hour before ischemia/reperfusion injury showed a significant improvement in the recovery of cardiac function in the hearts (Yousif et al., 2009).

1.5 Subterminal HETEs

Subterminal (ω-n)-hydroxylation is an oxidation reaction catalyzed by CYP monooxygenases that turns the methylene groups number 16 to 19 of the hydrophobic aliphatic chain of AA into a more polar alcohol metabolites namely subterminal HETEs (Guengerich, 2018). Subterminal HETEs are group of lipid mediators that are implicated in a spacious array of physiological and pathophysiological processes.

1.5.1 Cytochrome P450 Enzymes Implicated in Subterminal Arachidonic Acid Hydroxylation

CYP monooxygenases can mediate the insertion of the hydroxyl function group to any of the methinyl, methylene or the terminal methyl of AA (Westphal et al., 2015; El-Sherbeni and El-Kadi, 2017b). Accordingly, terminal/subterminal hydroxylation of AA is a function of the proximity of the terminal region of AA to the ferryl oxygen of CYP, which depends on how AA binds to the active site (de Visser et al., 2002). Basically, CYPs with a more lipophilic active site would favour the binding of the most lipophilic part (terminal region) of AA deeper inside the active site and closer to the ferryl oxygen. Also, confining the conformation arrangements that AA can take inside CYP active site - as in case of CYP with smaller active site - will improve the regioselectivity and stereoselectivity of

the subterminal hydroxylation. It is well-known that CYP1 and CYP4 families have very lipophilic active sites, and therefore, they metabolize the most lipophilic substrates of all of the microsomal CYP, i.e. polycyclic aromatic hydrocarbons and polyunsaturated fatty acids, respectively (Aboutabl et al., 2009; Ingelman-Sundberg, 2009). These two CYP families, CYP1 and CYP4, have been also reported to play a significant role in the formation of terminal/subterminal HETEs.

Several previous reports have demonstrated that CYP1As effectively mediate the subterminal hydroxylation of AA. In rats, CYP1A1 and CYP1A2 were reported to metabolize AA to 19-, 18-, 17- and 16-HETE, predominantly producing 19-HETE for CYP1A1 and 16-HETE for CYP1A2 (El-Sherbeni and El-Kadi, 2014b). In human, CYP1A1 was similarly reported to metabolize AA to produce 19-HETE > 18-HETE > 17-HETE = 16-HETE (Schwarz et al., 2004). Human CYP1A2, which shares about 70% homology with rat CYP1A2 (Lewis et al., 2006), was reported to mediate the subterminal hydroxylation; however, EETs formation was also observed by human CYP1A2 along with subterminal HETEs formation, c.f. rat CYP1A2 (El-Sherbeni and El-Kadi, 2016). In a study comparing recombinant human CYP, CYP1A1 was the highest active enzyme amongst tested CYP enzymes in the production of 16-, 17-, and 18-HETE but it stands as the second most active enzyme for formation of 19-HETE after CYP2C19, and the third most active CYP for 19-HETE formation is CYP4A11 (El-Sherbeni and El-Kadi, 2016).

The CYP4 family is believed to be the oldest CYP to be evolved in nature, which highlights its pivotal physiological role (Ingelman-Sundberg, 2009). CYP4 has been reported to mediate the metabolism of fatty acids, including AA, to their

terminal/subterminal hydroxy-analogues (Johnson et al., 2015). Rat CYP4A1/2/3 effectively mediate the formation of 19-HETE, which is six- to nine-fold greater by CYP4A1 than its formation by CYP4A2 and CYP4A3 (Nguyen et al., 1999). For human CYP4 enzymes, considerable amounts of 16-HETE were found to be produced by CYP4F2, CYP4F3A and CYP4F12. In addition to human CYP4A11, which is reported to be one of the top CYP producing 19-HETE, CYP4F2 and CYP4F3B were also found to produce higher amounts of 19-HETE compared with other human CYP (El-Sherbeni and El-Kadi, 2016). CYP4F8 and CYP4F12 metabolize AA by (ω-2)/ (ω-3)-hydroxylation and form 18-HETE as the principal product (Westphal et al., 2015).

CYP2E1 is considered to have the smallest active site among the CYP enzymes of ~250 Å (Miller, 2008), which makes the CYP2E1-mediated metabolism of AA of high regioselectivity and stereoselectivity, albeit with low overall activity. CYP2E1 mediates the formation of two major metabolites 19-HETE and 18-HETE with a higher percentage of 19-HETE from the total products. Stereo analysis showed that the produced 19-HETE was 70% 19(S)-HETE and 30% 19(R)-HETE; whereas, 18-HETE was essentially 100% R isomer (Laethem et al., 1993).

Also, it has been reported that CYP2C isoenzymes are involved in subterminal HETEs production. In recombinant human CYP enzymes, CYP2C19 has shown higher 19-HETE-forming capacity than other CYP members, and, in addition, it mediates the formation of 16-, 17- and 18-HETE (El-Sherbeni and El-Kadi, 2016). In another study in which five murine cyp2c cDNAs were cloned and depicted, including four novel members of this subfamily: CYP2c37, CYP2c38, CYP2c39 and CYP2c40, CYP2c40

primarily produced 16-HETE in addition to 17-, and 18-HETEs (Luo et al., 1998). Moreover, cyp2j9 provides an example of an enzyme that almost metabolizes AA to 19-HETE exclusively, while other CYP2J subfamily members act predominantly as epoxygenases and produce 19-HETE only as a minor product (Qu et al., 2001). In the brain, 19-HETE is primarily produced by CYP2U1, which is one of the so called orphan CYP, including CYP2S1, 2W1 and 4X1, that may have a contribution in subterminal HETE formation (Chuang et al., 2004). Table 1.1 shows the summarized list of CYP isozymes involved in subterminal HETEs production.

Table 1.2. Cytochrome P450 enzymes implicated in subterminal HETEs production.

P450 Enzyme	Species	Subterminal HETEs Produced	References
CYP1A1	Human	19-, 18-, 17- and 16-HETE in a ratio of 5:3:1:1.5	(Schwarz et al. 2004)
CYP2C19	Human	High capacity for 19-HETE, also 16-, 17- and 18-HETE	(El-Sherbeni and El-Kadi, 2016)
cyp2c37, cyp2c38, cyp2c39, and cyp2c40	Mouse	Primarily produced 16-HETE in addition to 17-, and 18-HETEs	(Luo et al. 1998; Tsao et al., 2000)
CYP2E1	Human	19-HETE: 70% 19(S)-HETE and 30% 19(R)-HETE 18-HETE: 100% 18(R)-HETE	(Elkhatali et al. 2015; Laethem et al. 1993)
cyp2j9	Mouse	Exclusively produced 19-HETE	(Qu et al. 2001)
CYP2U1	Human	19-HETE	(Chuang et al. 2004)
CYP4A1, CYP4A2, and CYP4A3	Rat	19-HETE	(Nguyen et al. 1999)
CYP4F2, CYP4F3A and CYP4F12	Human	16-HETE, 19-HETE to lesser extent	(El-Sherbeni and El-Kadi, 2016)
CYP4F8 and CYP4F12	Human	18-HETE	(Westphal et al. 2015)

1.5.2 19-HETE

As previously mentioned, subterminal hydroxylation of AA leads to formation of 4 metabolites known as 16-, 17-, 18- and 19-HETE (El-Sherbeni and El-Kadi, 2014c). Several studies reported that these hydroxyl metabolites are physiologically active in normal states and have significant beneficial effects in different disease states. However, physiological and pathophysiological roles of subterminal HETEs are not fully unraveled to date.

(ω-1)-hydroxylation of AA leads to formation of 19-hydroxy-5(Z),8(Z),11(Z),14(Z)-eicosatetraenoic acid. It is formed through hydroxylation reaction at carbon number 19 of the 20 carbons of AA to form chiral center leading to formation of 19(S)-HETE and 19(R)-HETE enantiomers (Elkhatali et al., 2015). Among the members of subterminal HETEs, 19-HETE has received the highest attention. It has been reported that this lipid mediator could modulate several physiological functions and possesses protective mechanisms in specific disease states, summarized in (Figure 1.3). For instance, it antagonizes 20-HETE vasoconstrictive effects in the kidney, it enhances nitric oxide production in the renal arteries and it has a vasoprotective role in retinal vasculature.

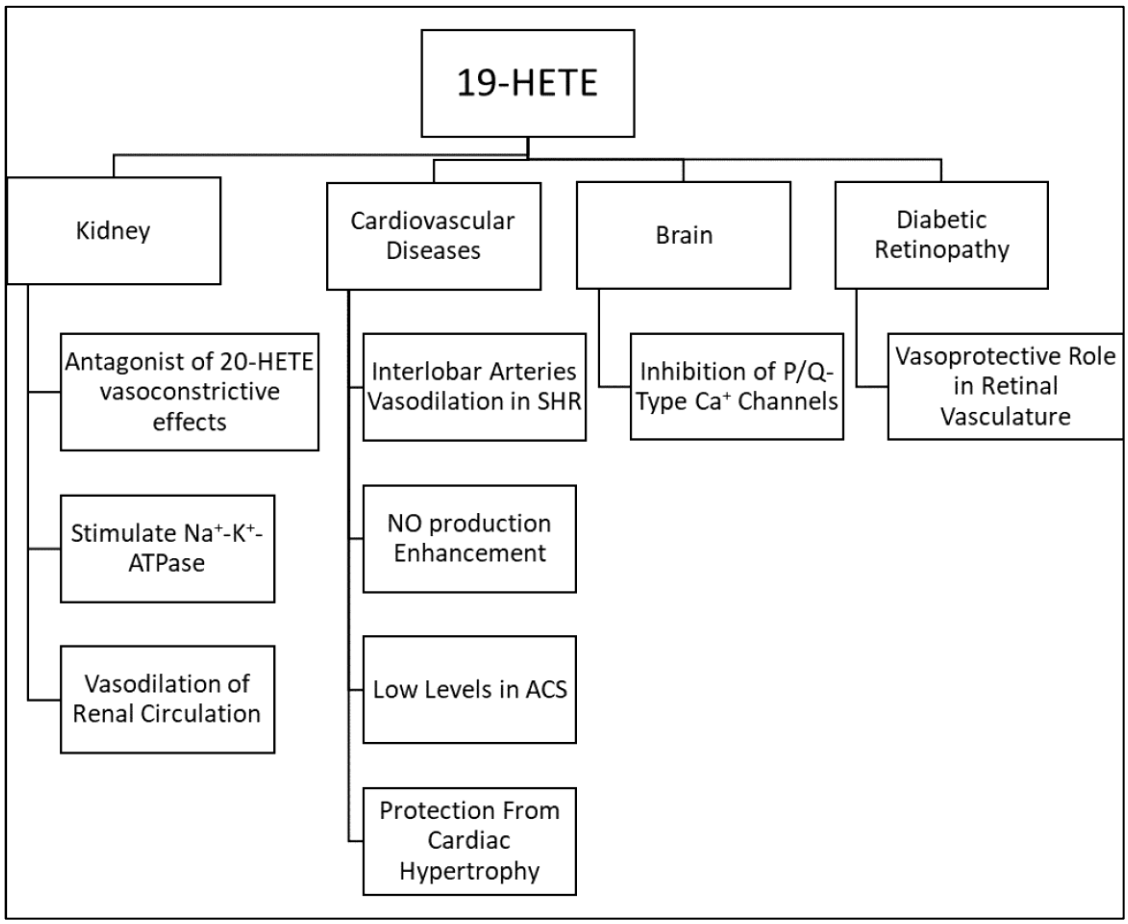

Figure 1.4. Role of 19-HETE in normal physiology and disease states. ACS, acute coronary syndrome; NO, nitric oxide; SHR, spontaneously hypertensive rats.

1.5.2.1 The role of 19-HETE in normal physiology

In the kidney, considerable variation was shown in the quantity of individual HETEs liberated from the perfused rabbit kidney under basal conditions. 19-HETE has shown to be the highest concentration in the perfusate, more than fivefold higher than that of 16-HETE (Carroll et al., 1996). The reno-vascular effects of 19-HETE synthesized by kidneys were studied in the rabbit isolated kidney under conditions of constant flow. It has been reported that 19-HETE acts as an endogenous antagonist of 20-HETE-mediated renal vasoconstrictor effects (Elshenawy et al., 2017a). 20-HETE was reported to be the highest CYP metabolite of AA in different parts of the renal histoarchitecture (Oliw, 1990; Wang et al., 2004). 20-HETE has a major role in the modulation of renal microvasculature and it was found to be responsible for the sensitization of renal microvessels to vasoconstrictors such as phenylephrine (Kaide et al., 2003; Zhao et al., 2004). Moreover, 20-HETE is involved in the increase of intracellular calcium in renal microvascular smooth muscle cells augmenting its role in the vasoconstriction of the kidney microvasculature (Zhao et al., 2004). On the contrary, the pressure–natriuretic response has been reported to be regulated by 20-HETE. It suppresses Na^+-K^+-ATPase activity through protein kinase C (PKC)–mediated phosphorylation of the pump α subunit at serine 23 residue. Therefore, its effect as a natriuretic contributes to the antihypertensive mechanisms in the kidney (Wu et al., 2014).

Interestingly, blocking the action of 20-HETE leads to the activation of potassium channels and the switching on the vasodilator effects of nitric oxide in the renal

microvasculature (Sun et al., 1998). Pre-treatment with 19(S)-HETE completely blocked the vasoconstrictor response to 20-HETE in renal arterioles (Alonso-Galicia et al., 1999).

Moreover, 19(S)-HETE was shown to directly stimulate the activity of Na^+-K^+-ATPase of the kidney proximal tubules leading to stimulation of proximal tubule transport. This action is not dependent on any effect due to 20-HETE production as 19(S)-HETE is capable of stimulating volume transport in the presence and absence of dibromo-dodecenyl-methylsulfimide (DDMS), a selective inhibitor of endogenous 20-HETE production. Renal function is highly dependent on the activity of Na+-K+-ATPase, stimulation of this pump by 19(S)-HETE could be considered as an endogenous regulatory mechanism of salt and water excretion by the kidney. Therefore, 19(S)-HETE contributes to the maintenance of body fluid and circulatory homeostasis (Kaide et al., 2003; Wang et al., 2004).

In the brain, it has been reported that the cDNA cloning and heterologous expression of a new mouse CYP that is abundantly expressed in the brain, CYP2j9, showed ω-1 hydroxylation activity of AA to 19-HETE. CYP2j9 mRNA and protein are focused to Purkinje cells in the cerebellum. Of importance, activity of recombinant P/Q-type Ca2+channels, voltage-gated ion channels are significantly inhibited by 19-HETE. These ion channels are primarily expressed in Purkinje cells and are responsible for triggering the release of brain neurotransmitters. According to the effects of 19-HETE on voltage-gated Ca2+ channel activity, and the reported role of intracellular Ca2+ mediated by the influx through these channels on neurotransmitter release rates, it has been proposed that 19-HETE play a substantial functional role in the brain (Qu et al., 2001).

1.5.2.2 The role of 19-HETE in disease states

There is mounting evidence that abnormality of CYP-mediated subterminal HETEs is evident in specific cardiovascular disease states. In SHR, there was increased sensitivity of renal interlobar arteries to phenylephrine and this effect is attributable to an imbalance in the vaso-regulatory mechanisms produced by a decrease in vascular CYP2E1-derived products, most likely 19(R)-HETE. This effect leads to amplification of the sensitizing action of 20-HETE toward the vasoconstrictive agent (Zhang et al., 2005). In addition, 20-HETE inhibits vasodilatory nitric oxide production in renal arteries and this effect was negated by 19(R)-HETE, a functional antagonist of 20-HETE (Cheng et al., 2008). On the contrary, two studies have reported that 19-HETE favors hypertension via causing vasoconstriction and sodium retention in SHR (Sun et al., 1998; Alonso-Galicia et al., 1999). Therefore, a further comprehensive understanding of the role of 19-HETE in hypertension is needed. In patients with acute coronary syndrome (ACS), plasma level of 19-HETE in patients with major adverse cardiovascular event (MACE) during follow-up was significantly lower than those without MACE. ACS patients with 19-HETE levels higher than 0.13 ng/ml show better prognosis than those lower than 0.13 ng/ml. Therefore, CYP-mediated 19-HETE may act as prognostic marker for ACS patients (Zu et al., 2016).

In the heart, it has been reported that 19-HETE represents the major subterminal HETE formed in the rat cardiac tissue, and its formation was decreased in a descending aortic constriction model of cardiac hypertrophy (El-Sherbeni and El-Kadi, 2014c). A 19-HETE cardioprotective role was evidenced in vitro in human ventricular cardiomyocyte RL-14

cells and in vivo in angiotensin II-induced cardiac hypertrophy. 19-HETE protects RL-14 cells cardiomyocytes from hypertrophy as evidenced by a decrease in β/α-myosin heavy chain hypertrophic markers. Moreover, isoniazid, a well-known inducer of hepatic CYP2E1, gave rise to significant alterations in CYP-mediated AA metabolism in the heart, most importantly an increase in the cardioprotective 19-HETE. These alterations were associated with protection against angiotensin II-induced cardiac hypertrophy, proposing a probable therapeutic effect of isoniazid and other pharmacological inducers of cardiac 19-HETE on cardiac hypertrophy (Elkhatali et al., 2015).

In the kidney, CYP-mediated eicosanoids, including 19-HETE, may play a role in the pathogenesis of chronic kidney disease. In addition, they could be used as biomarker for this disease as a significant correlation between estimated glomerular filtration rate and 19-HETE/ creatinine levels in African-Americans were observed (Dreisbach et al., 2014).

It has been reported that 19-HETE plays a role in diabetic retinopathy (DR), 19-HETE is biosynthesized in human endothelial cells by CYP2C19 and has a vasoprotective role in retinal vasculature. To study the association between CYP2C19 polymorphisms and an increased risk of diabetic retinopathy, a clinic-based retrospective longitudinal study was performed. The study has highlighted that female intermediate metabolizers and poor metabolizers were at a significantly higher risk of developing DR in comparison with male extensive metabolizers. Therefore, 19-HETE could be a novel therapeutic target in type 2 diabetes mellitus patients with DR (Kajiwara et al., 2013).

1.5.3 16-HETE

16-Hydroxyeicosa-5(Z),8(Z),11(Z),14(Z)-tetraenoic acid is a member of the metabolites of the CYP branch of the arachidonate cascade (Reddy et al., 2003). It is formed through introduction of a hydroxyl group to carbon number 16 of the 20 carbons of AA to form chiral center leading to 16(S)-HETE and 16(R)-HETE enantiomers (Powell and Rokach, 2015). It has been previously reported that 16-HETE possesses several physiological roles and is involved in different disease states, summarized in (Figure 1.4).

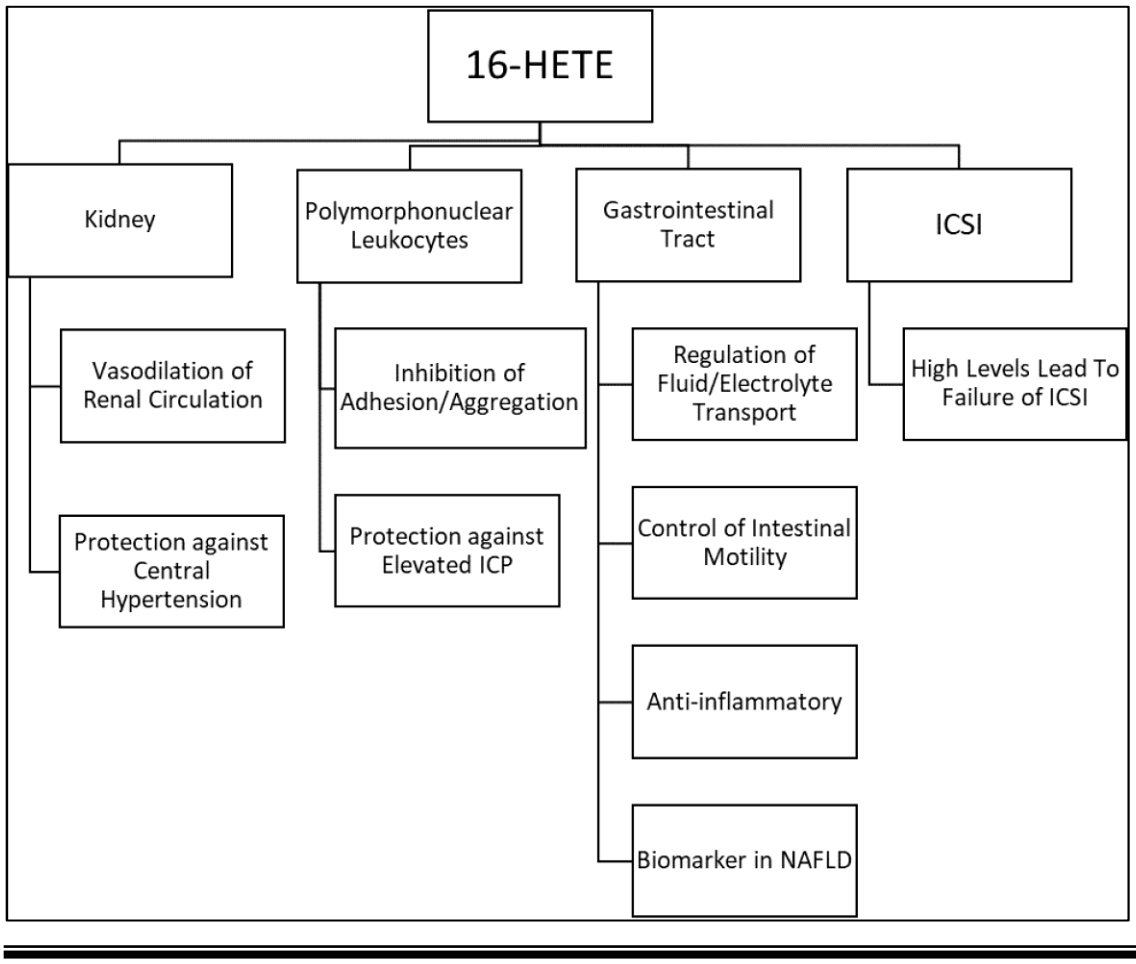

Figure 1.5. Role of 16-HETE in different organs and disease states.

ICP, intracranial pressure; ICSI, intracytoplasmic sperm injection; NAFLD, non-alcoholic fatty liver disease.

1.5.3.1 The role of 16-HETE in normal physiology

The perfusion of rabbit kidneys in vitro in the presence or absence of different hormones (angiotensin II, bradykinin, and vasopressin) resulted in considerable amounts of different subterminal HETEs including 16-HETE. These metabolites have been involved in vasodilation, regulation of renal perfusion and in mechanisms of tubular transport (Ivanov et al., 2004).

In intact human polymorphonuclear leukocytes (PMNL), incubation with sub-stimulatory amounts of arachidonic acid produced 16(R)-HETE which is likely to play a role in the unstimulated neutrophil. PMNL may be inhibited by 16(R)-HETE in a hormone-like reaction, hence aggregation and adhesion are inhibited. Interestingly, esterified 16(R)-HETE could have a potential effect on the affinity of PMNL adhesion receptors for endothelial cells as they modify the composition and physical characteristics of the PMNL cell membrane (Bednar et al., 2000a). Therefore, the CYP pathway is able to activate an endogenous neutrophil inhibitor (16-HETE) in addition to simultaneously inhibiting the formation of a neutrophil proaggregant/chemoattractant, leukotriene B4, which is formed by the lipoxygenase pathway of AA metabolism. This anti-neutrophil effect could be a novel anti-inflammatory strategy in case of acute ischemic stroke in which neutrophil activation deteriorates brain injury (Bednar et al., 1997).

Several reports have addressed the role of 16-HETE in the murine intestinal tract. It is postulated that CYPcyp2c40 is the first enzyme to produce 16(R)-HETE as a major product of AA. This hydroxyl AA metabolite and the presence of CYP2cypc40 in the intestinal tract propose that CYPcyp2c40, which is highly expressed in the cecum, could

have significant biological functions in murine intestine via the production of 16(R)-HETE. 16(R)-HETE has physiological functions such as intestinal fluid/electrolyte transport, control of intestinal motility, and anti-inflammatory effects (Tsao et al., 2000a).

In a study performed to investigate the impact of AA derivatives on oocyte intracytoplasmic sperm injection (ICSI), increased activity of secreted phospholipase A2 and significantly higher 16-HETE levels were found in the follicular fluid of oocytes that have not shown two pronuclei or have undergone degeneration after ICSI in comparison to oocytes with the appearance of two pronuclei (Ciepiela et al., 2015). In the light of the aforementioned findings, much more attention should be paid for the investigation of 16-HETE biological effects in other organs.

1.5.3.2 The role of 16-HETE in disease states

16- HETE could be a promising therapeutic target in cardiovascular diseases in the light of its previously mentioned vasodilatory effects. It has been proposed that 16-HETE may be a reliable diagnostic marker or therapeutic target for central blood pressure as its upregulation could be a protective mechanism in patients with central hypertension (Caligiuri et al., 2016).

Moreover, in agreement with the previous reports, 16(R)-HETE has shown to be a potent and specific inhibitor of PMN function in vitro and is able to suppress elevated intracranial pressure (ICP) in a rabbit model of thromboembolic stroke. Therefore, 16(R)-HETE could be used as a therapeutic strategy as elevated ICP results in cerebral ischemia and trauma which are the reason for a considerable proportion of death and disability. It is noteworthy that there are very limited pharmacological strategies currently available

for treatment of these pathophysiological processes (Bednar et al., 2000b). 16-HETE has also been characterized as a prime AA metabolite in the phospholipid bilayer of platelet membranes, but the function of this membrane component is yet elusive (Zhu et al., 1995). Furthermore, it seems that the lipid profile of AA-mediated metabolites is a helpful biomarker to assess the development of non-alcoholic fatty liver disease. In a pilot study, Maciejewska *et al.* showed that 16-HETE profile can help to differentiate the early stages of non-alcoholic fatty liver disease (Maciejewska et al., 2015).

1.5.4 The role of 17- and 18- HETE in different organs

Introduction of hydroxyl group to carbon number 17 and carbon number 18 of the 20 carbons of AA leads to formation of (±)17-hydroxy-5Z,8Z,11Z,14Z-eicosatetraenoic acid and (±)18-hydroxy-5Z,8Z,11Z,14Z-eicosatetraenoic acid, respectively. Carroll *et al.* assessed HETEs exiting isolated perfused rabbit kidney in response to angiotensin II stimulation. 17-HETE was the principal urinary HETE, and is confined foremost to neutral lipids and phosphatidylethanolamine of renal cortical and medullary lipids while 18-HETE was found almost wholly in the neutral lipid portion of the cortex (Carroll et al., 1997). 17-HETE potently inhibits proximal tubule ATPase activity while it had no significant effects on 70-pS K^+ channel in the thick ascending limb of the rat kidney (Wang and Lu, 1995). In the brain, 17-HETE levels were significantly elevated in response to acute arsenite (As(III)) treatment in C57Bl/6 mice proposing that 17-HETE could have significant role in case of acute arsenite toxicity (Anwar-Mohamed et al., 2014).

There is a direct correlation between elevated level of 18-HETE and microvascular insulin resistance. Moreover, it has been reported that increased 18-HETE levels are linked to abnormal skeletal muscle vascular recruitment. Consequently, 18-HETE could play a role in insulin resistance (Chadderdon et al., 2016). In renal interlobar arteries of spontaneously hypertensive rats, augmented vasoconstrictive activity of phenylephrine has been attributed to vasoregulatory imbalance resulting from a decrease in vascular CYP2E1-derived R-enantiomer of 18-HETE (Zhang et al., 2005). On grounds of the aforementioned roles, further studies are needed to be performed on 17- and 18-HETE since only scarce data are available on their impact on health and disease status.

1.5.5 Stereoselectivity of subterminal HETEs

During the past 4 decades, correlation of drug actions and drug disposition with stereochemical aspects of the drug molecule has become a matter of interest (Bhateria et al., 2016). Formerly, the majority of chiral drugs in the market have been used as a racemic mixture. In some cases, chiral switch approaches have shown pharmacokinetic and pharmacodynamics benefits in drug discovery (Patrick and Straughn, 2016). Different enantiomers of a chiral drug could vary in their properties such as drug absorption, metabolism, CYP induction or inhibition and excretion. Moreover, they could differ in their action at the receptor site or toxicity (Campo et al., 2009). Consequently, there is a trend toward design of stereochemically refined molecules aiming to decrease the administered drug dose, make dose response relationships simpler and ameliorate inactive isomer toxicity (Caldwell, 1996).

Incorporation of hydroxyl group in the carbon skeleton of AA generates a chiral center, hence there are 2 enantiomers from each HETE metabolite; R/S enantiomers (El-Sherbeni and El-Kadi, 2017a). They have been proven to be produced in a stereoselective manner and could have differential effects in case of normal physiological or pathophysiological states. As previously mentioned, 19-HETE formed with CYP2E1 was 70% 19(S)-HETE and 30% 19(R)-HETE (Figure 1.5), while 18-HETE was wholly 100% R isomer (Laethem et al., 1993). Recently, we demonstrated that the S-enantiomer of 19-HETE has preferential protection against Ang II-induced cellular hypertrophy, compared to the R-enantiomer, through decreasing the level of cardiotoxic mid-chain HETEs, inhibiting the catalytic activity of CYP1B1 and reducing the protein expression of LOX and COX-2 enzymes as well as decreasing the mRNA expression of interleukin-6 and interleukin-8 (Shoieb and El-Kadi, 2018c).

Direct stimulation of the activity of Na^+-K^+-ATPase renal proximal tubules has been mediated by 19(S)-HETE leading to stimulation of proximal tubule transport, while 19(R)-HETE negated 20-HETE-mediated inhibition of vasodilatory nitric oxide production in renal arteries (Cheng et al., 2008). In a dose dependent manner, 16(R)-HETE has stimulated vasodilation of the rabbit kidney, while 16(S)-HETE has not affected perfusion pressure. The (S)-enantiomer of 16-HETE has shown proximal tubule ATPase activity by as much as 60%, whereas the (R)-isomer has not affected ATPase activity (Carroll et al., 1996).

The aforementioned effects have shown the relevance of chirality in different subterminal HETEs in regard to their production and biological roles. Chirality issues should be taken

in consideration in case of testing the role of subterminal HETEs in normal physiology and disease states as they may have differential effects. Moreover, designing and developing subterminal HETEs analogs require special techniques to ensure the enantiomeric purity, and their enantioselective assay in pharmacokinetics is an issue to be considered (Brocks, 2006).

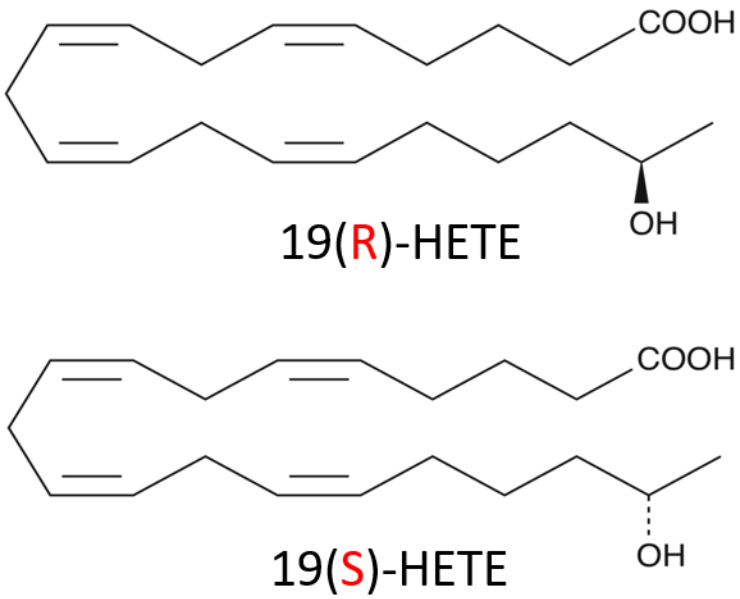

Figure 1.6. R- and S-enantiomers of 19-HETE as an example of stereoisomerism of CYP-mediated arachidonic acid metabolites.

Incorporation of hydroxyl group in the carbon skeleton of arachidonic acid generates a chiral center, hence there are 2 enantiomers from each HETE metabolite.

1.5.6 Modulating subterminal HETEs as a promising therapeutic direction

Subterminal HETEs are biologically active, and their biological activity seems to be more pronounced in some body's organs, such as kidneys and heart. While the degradation of subterminal HETEs is mainly through non-specific pathways, such as fatty-acid β-oxidation, passive diffusion and esterification to cellular membranes, the formation of subterminal HETEs is mediated by limited number of enzymes, notably CYP1As and CYP4s (Roman, 2002; Imig, 2012). The fatty-acid β-oxidation occurs in the peroxisomes, with each β-oxidation cycle, an acetyl-CoA and an acyl-CoA which is two carbons shorter are formed. The products of β-oxidation are largely excreted from the cells or incorporated into endothelial phospholipids (Mathur et al., 1990; Gordon et al., 1994). Therefore, modulating subterminal HETEs by altering their formation could provide a feasible and promising modality for the treatments of several cardiovascular and kidney diseases. This conclusion was substantiated by several animal and clinical studies investigating the genetic variations in levels and activity of CYP1As and CYP4s. For animal studies, a high blood pressure was reported in *cyp1a1*-knockout mice (Agbor et al., 2012), as well as in *aryl hydrocarbon-receptor*-knockout mice, which show that decreased levels of cyp1a1 and cyp1a2 (Lund et al., 2003). In addition, systolic blood pressure was reported to be higher in cyp4a14-knockout mice, which surprisingly was associated with an increase in 20-HETE formation (Fidelis et al., 2010). The authors also reported an impairment of renal excretion of salt load, and an enhanced sensitivity of renal vasculatures toward vasoconstrictors, such as Ang II; the opposite was true for vasodilators, such as bradykinin. Also, cyp4a10/14-knockout mice showed less bacterial-infection-induced inflammation compared to wild-type mice (Nyagode et al., 2014).

Clinical studies investigating the association between genetic polymorphisms causing alterations in the activity or levels of CYP1As or CYP4s and cardiovascular and kidney diseases are sparse. However, in a study by Tsatsakis et al a significant association was found between *CYP1A1*2A* allele, which leads to higher CYP1A1 inducibility, and protection against peripheral circulatory problems (Tsatsakis et al., 2009). Another study by Cornelis et al found that homozygous individuals carrying the *CYP1A2*1F* allele, which leads to lower CYP1A2 inducibility, have a higher risk to myocardial infarction that is not dependent on the level of smoking (Cornelis et al., 2004). With respect to CYP4A polymorphism, the loss of function *CYP4A11* allele (*CYP4A11* 8590C) has been reported to be associated with higher blood pressure in several studies (Mayer et al., 2006; Gainer et al., 2008; Williams et al., 2011), of which a renal malfunction was observed in homozygous individuals of *CYP4A11* 8590C. In these individual the renal plasma flow surprisingly decreased by increasing salt intake, which is the reverse of the normal physiology of the kidneys (Williams et al., 2011).

Chemical inhibition of key steps in the formation cascade of subterminal HETEs has been experimentally used in animals. The inhibition of the starting points of the cascade, i.e. inhibition of the phospholipase A2, by mepacrine (Adeagbo, 1997), or inhibition of AA metabolism by eicosatetraynoic acid (ETYA) (Vazquez et al., 1995), is effective in decreasing subterminal HETE formation, but also non-selective method, and will lead to altering all other polyunsaturated fatty acids/AA metabolites. The same is seen with general CYP inhibitors, such as 17-octadecynoic acid (17-ODYA) and ketoconazole, which are selective toward CYP enzymes, but also affect EET and midchain HETE

formation and can alter drug metabolism (Yoshida et al., 1990; Adeagbo, 1997). Therefore, CYP1As and CYP4s selective inhibitors/inducers, as well as structural analogues of subterminal HETEs acting as antagonists or agonists at receptor level, are the most promising venues to selectively and effectively alter subterminal HETEs levels, especially for 16-HETE (Morgan D' et al., 2003). There is a recently proposed strategy, which is to use the already established knowledge on CYP inhibitors and inducers gained from drug metabolism observations to reposition one of the CYP inhibitor/inducers approved for clinical use. This would facilitate finding subterminal HETE modulators that can be tested clinically for treatment of heart and kidney diseases (El-Sherbeni and El-Kadi, 2017a).

Another critical aspect that should be considered throughout the process of drug design and development is sexual dimorphism. Differences in the levels of HETEs due to sexually dimorphic patterns of their biosynthesis have been previously reported, however the mechanisms for these variations are still under investigation (Grant et al., 2017). CYP enzymes, in different species, have been reported to be differentially expressed in a sexually dimorphic manner. Therefore, CYP-associated metabolites are preferentially synthesized in either males or females (Lin and Lu, 1997). For instance, 5-HETE was synthesized at lower levels in male blood compared to female counterparts when the male and female subjects were stimulated with substance that induce inflammatory response (Pergola et al., 2008). Moreover, 20-HETE-related increase in blood pressure was positively correlated with testosterone-mediated induction of CYP4A enzymes that are responsible for its biosynthesis (Wu and Schwartzman, 2011). Another study has shown

that male rats have higher ratio of 20-HETE to EETs, in renal interlobar arteries, in comparison with female rats. Negation of this sexually dimorphic differences was achieved through treatment of female rats with testosterone, confirming the role of sex hormones in the observed variations. Therefore, the reduced levels of vasodilatory EETs and the increased formation of vasoconstrictive 20-HETE in male rats might represent key factors in testosterone-induced hypertension (Singh and Schwartzman).

Here, we have shown that one of the most studied subterminal HETEs, 19-HETE, is largely biosynthesized by CYP2C19 and CYP2E1. Both enzymes have been reported to show gender differences in their catalytic activity (Xie et al., 1997). For example, castration caused a significant decrease in the CYP2C19 mRNA in males to a level comparable to its level in female rats (Löfgren et al., 2009). Consequently, any suggested method for modulating subterminal HETEs should take in consideration that there is a potential sexual dimorphic pattern in the metabolism of these compounds. However, further studies are needed with respect to the effect of sexual dimorphism on CYP expression/activity and eventually on the subterminal HETEs production.

1.6 Repurposing FDA-approved drugs to new indications

Drug repurposing has been recently observed as a lower-cost and shorter-time practicability than de novo development of novel drugs. Adding a new therapeutic indication of an already FDA-approved drug has the advantage of presence of enhancing information about pharmacokinetic, pharmacodynamic and toxicological properties of that drug (Sleire et al., 2017). For decades, the focus was on the discovery of new

molecules which act upon novel targets. However, big companies in the pharmaceutical field consider this process tedious and highly expensive.

Of importance, metabolism of AA leads to biosynthesis of plethora of biologically active lipid mediators such as prostaglandins, leukotrienes and HETEs. Modulation of AA metabolic pathways led to phenomenal effects in multiple diseases and conditions (Serrano-Mollar and Closa, 2005). For example, aspirin, a non-steroidal anti-inflammatory (NSAID), is vastly used for its analgesic and antipyretic effects (Siegel et al., 1979). It is an example of a drug that modulates AA metabolic pathways through irreversible inhibition of the COX-1 enzyme and modification of the catalytic activity of COX-2 enzyme with much higher selectivity towards COX-1 (Patrono et al., 2017). Aspirin is considered one of the top drugs employed in repurposing. After being discovered to irreversibly acetylate COX-1 enzyme in the platelets leading to inhibition of formation of thromboxane A_2 for the platelet lifetime, aspirin has been widely used as an antiplatelet agent in prevention against cardiovascular diseases (Hennekens, 2002).

Similarly, research of FDA-approved drugs that could modulate AA metabolic pathways, most importantly the CYP pathway, and alter the levels of subterminal HETEs would possess significant benefit in different disease states in which subterminal HETEs play a crucial role. As previously mentioned, subterminal HETEs are produced through different CYP isozymes that could be pharmacologically modulated by wide array of FDA-approved drugs. For instance, cardiac hypertrophic growth predisposes to, and accompanies, a number of serious cardiovascular diseases (Katare et al., 2017). 19-HETE has been approved to protect against Ang-II-induced cardiac hypertrophy (Elkhatali et

al., 2015). One component of the standard therapy used for the treatment of tuberculosis is isoniazid (Hassan et al., 2016). Isoniazid is a well-known CYP2E1 inducer (Valencia-Olvera et al., 2014). Since CYP2E1 is one of the enzymes involved in production of 19-HETE, repositioning of isoniazid to be used as a cardioprotective agent has been suggested in case of cardiac hypertrophy (Elkhatali et al., 2015). Applying the same concept of modulation of CYP enzymes to alter the levels of subterminal HETEs would open the door for novel indications of clinically-approved drugs that are already present in the market.

Initial determination of CYP isozymes implicated in the production of subterminal HETEs is the primary step in the process of searching for modulators of these isozymes. For example, it has been previously reported that 16-, 17-, 18-, and 19-HETE formation is partly mediated by CYP2C19 at a particular activity of 0.46, 0.31, 0.62, and 11.34 pmol/pmol P450/min, respectively (El-Sherbeni and El-Kadi, 2016). 16-HETE previously showed potent and specific inhibition of PMN *in vitro* and could be considered as a potential therapeutic target in case of elevated ICP based on its role in reduction of ICP in a rabbit model of thromboembolic stroke (Ivanov et al., 2004; Zu et al., 2016). Moreover, the protective role of 19-HETE has been previously reported in case of cardiac hypertrophy.

Based on the aforementioned roles of subterminal HETEs in different disease, we propose testing of some FDA-approved drugs in different models of these diseases. One candidate drug that could be tested is aspirin. It has been clinically reported that low-dose aspirin (50 mg daily) given to healthy male volunteers could induce the activity of CYP2C19 in

both 7-day and 14-day time course (Chen et al., 2003). There are several studies that show a protective role of aspirin against cardiac hypertrophy, and it has been proven to possess anti-hypertrophic effect when used as an anti-thrombotic agent at a concentration that is clinically relevant (low-dose). It is claimed that this anti-hypertrophic property is mediated through prevention from elevation of β-catenin and p-Akt expression and reversal of downregulation of glycogen synthase kinase 3 beta (GSK-3β) (Gitau et al., 2015). In another study, Yin *et al.* showed that aspirin could protect against ang II-induced cardiac hypertrophy *in vitro* and *in vivo* through inhibition of the Ca^{2+}/calcineurin-NFAT signaling pathway (Yin et al., 2016). We suggest that further *in vitro* and *in vivo* studies could be performed in order to investigate the potential role of low-dose aspirin in protection against and treatment of cardiac hypertrophy through induction of CYP2C19 and increasing the levels of subterminal HETEs specially 19-HETE. The proposed mechanism of action could be, at least partly, a contributing factor in the hypertrophic effect exerted by aspirin upon cardiac muscle.

1.6.1 Resveratrol

Resveratrol is a naturally occurring polyphenol that is found in many food sources and beverages including black grapes, peanuts, blueberries and red wine and as a commercially available dietary supplement (Cione et al., 2019). Resveratrol possesses anti-oxidant, anti-inflammatory, anti-apoptotic and anti-fibrotic effects. Of interest, resveratrol has been shown to improve myocardial energetics and is experimentally used for prevention and treatment of multiple CVD (Bonnefont-Rousselot, 2016; Abdelgawad et al., 2019). In a mice model of pressure overload-induced HF, resveratrol has been

reported to restore the levels of mitochondrial oxidative phosphorylation complexes, restore cardiac AMP-activated protein kinase activation, and enhance myocardial insulin sensitivity to induce glucose metabolism and remarkably improve myocardial energetic status (Sung et al., 2015). Resveratrol has been shown to exert an inhibitory effect on recombinant CYP1B1 supersomes with IC_{50}= 11.2 μM (Mikstacka et al., 2008). In addition, it inhibited 2,3,7,8-tetrachlorodibenzodioxin (TCDD)-mediated induction of CYP1B1 in cultured human mammary epithelial cells and human breast cancer cell line MCF-7 (Chen, 2004; Beedanagari et al., 2009). Several reports have demonstrated that resveratrol protects against cardiac hypertrophy through modulation of various pathways (Chen et al., 2019; Guan et al., 2019; Zou et al., 2019). However, none of these studies investigated the effects of resveratrol on CYP1B1.

1.6.2 Fluconazole

Fluconazole is a member of the azole antifungal family of medications, that is an FDA-approved drug that is broadly used in the prevention and treatment of a wide range of fungal and yeast infections (Shoham et al., 2017). Intriguingly, fluconazole is a renowned moderate inhibitor of several CYP enzymes in humans, including CYP2Cs and CYP3A4 (Lu et al., 2008). To study drug-drug interactions, the FDA advises that fluconazole could be considered to investigate the moderate-case scenarios of CYP3A4 and CYP2C9 inhibition (FDA, 2020). Previously, we have reported that fluconazole possesses the ability to attenuate angiotensin–II–induced cellular hypertrophy. Additionally, when administered to Sprague Dawley rats in a dose at 20 mg/kg, fluconazole was able to significantly decrease CYP1B1 enzyme expression and the level of mid-chain HETEs in

the heart (Alammari et al., 2020). Based on the aforementioned findings, we have proposed that fluconazole could be a potential therapeutic agent in case of cardiac hypertrophy, and if proved successful, it could be repurposed as a suitable pharmacological inhibitor of cardiac CYP1B1.

In order to have a clearer image about the expected inhibition in CYP-mediated AA metabolism in humans after safe oral doses of fluconazole, the inhibition patterns were predicted based upon Monte Carlo simulation method. The method was carried out to simulate 10,000 human subjects orally administered 50, 150, or 400 mg of fluconazole. The results showed that fluconazole in doses of 50, 150, and 400 mg led to an inhibition of 13–23%, 23–41%, and 45–57% for 11-HETE, 16–27%, 34–49%, and 54–68% for 12-HETE, and 9–17%, 20–31%, and 36–46% for 15-HETE, respectively, in 90% of the simulated human population. The simulation results of this study demonstrated that pharmacological modulation of CYP-derived AA metabolites, similar to COX and LOX-derived metabolites, might possess a major potential for future clinical uses (El-Sherbeni and El-Kadi, 2016).

It is noteworthy to mention that using resveratrol and fluconazole as examples for drug repurposing is only as a proof of concept. Indeed, these drugs has some limitations that might hinder them from being clinically approved for the treatment of HF. For instance, Resveratrol possesses poor oral bioavailability in humans (<1%) due to rapid and extensive metabolism in the intestine and liver to glucuronides and sulphates (Almeida et al., 2009; Cottart et al., 2010). Also, the results of clinical studies on resveratrol in various cardiovascular conditions have been inconclusive or conflicting (Berman et al., 2017). In

addition, fluconazole has a number of reported side effects, including hepatotoxicity, which may limit its future use in case of CVD (Khoza et al., 2017). Also, it has multiple drug-drug interactions that lead to slowing down of the metabolism of other drugs due to its inhibitory effect on CYP enzymes (Malhotra et al., 2011). Therefore, development of novel therapeutic agents or searching for clinically-approved drugs that have the same pharmacological actions with higher selectivity and fewer side effects would be a plausible approach for the treatment of CVD.

1.7 Rationale, hypotheses and objectives

1.7.1 Rationale

Cardiac hypertrophy is a complex condition which is characterized by increased mass of the cardiac muscle. Pathological cardiac hypertrophy is associated with disruption in cardiac morphology. It develops as a pathophysiologic condition in response to stimuli such as pressure overload accompanying hypertension; and it represents a key risk factor for developing heart failure and other heart conditions (Kahan and Bergfeldt, 2005; Bernardo et al., 2010). HF remains a global pandemic that represents a leading cause of morbidity and mortality worldwide (Inamdar and Inamdar, 2016; Metra and Teerlink, 2017). According to the Heart and Stroke Foundation of Canada, HF is affecting more than 600,000 Canadians with 50,000 new cases being diagnosed with the disease annually and it is responsible for an estimated health expenditure of around $2.8 billion per year as a direct cost (Heart and Stroke Foundation, 2016). Searching for possible treatments that halt the development and progression of cardiac hypertrophy is regarded as a vital

step in the prevention of a major risk factor of heart failure and will allow for designing improved drug therapies (Olson and Molkentin, 1999).

Accumulating evidence suggest that pathological cardiac hypertrophy is strongly correlated with aberrations in CYP-mediated AA metabolism in cardiac tissue (Roman, 2002; El-Sherbeni and El-Kadi, 2014c). Many AA metabolic products are known to be involved in the pathogenesis of cardiac hypertrophy, especially mid-chain HETEs, including 5-, 8-, 9-, 11-, 12- and 15-HETE. Mid-chain HETEs represent a group of eicosanoids that possess evident biological activity in the heart, these lipid molecules are the products of AA metabolism either by LOX- or CYP-mediated bis-allylic oxidation reaction (Nayeem, 2018b).

In the heart, CYP1B1 is constitutively active and is reported to contribute to the pathogenesis of several cardiovascular diseases including atherosclerosis, hypertension and cardiac hypertrophy (Song et al., 2016; Anderson and Mazzoccoli, 2019b). The major metabolites of CYP1B1-mediated AA biotransformation are mid-chain HETEs. Alongside CYP1B1, they have drawn a distinct attention, as they could serve as a potential target for developing drugs to treat CVD (Choudhary et al., 2004; Li et al., 2017). Overexpression of CYP1B1 has been previously reported in the heart in several experimental models of cardiac hypertrophy (Elkhatali et al., 2017; Maayah et al., 2017). For instance, abdominal aortic constriction-induced cardiac hypertrophy in rats was associated with a significant induction of CYP1B1 protein expression and elevated levels of its associated mid-chain HETEs metabolites (Maayah et al., 2018). On the other hand, approaches such as CYP1B1 pharmacological inhibition or knockout have been taken to

protect against experimentally-induced cardiac hypertrophy (Jennings et al., 2010; Zhang et al., 2020b).

Amongst subterminal HETEs, 19-HETE grabbed the highest consideration as it represents the major cardiac subterminal HETE (El-Sherbeni and El-Kadi, 2014c). 19-HETE acts as an endogenous antagonist of 20-HETE and inhibits its mediated vasoconstrictor effects (Elshenawy et al., 2017b). Additionally, acute coronary syndrome patients with higher plasma levels of 19-HETE have significantly better prognosis than those who have lower plasma levels (Zu et al., 2016). In pressure overload-induced cardiac hypertrophy, there was a significant decrease in the level of 19-HETE in hypertrophied hearts compared to control hearts (El-Sherbeni and El-Kadi, 2014c). Furthermore, racemic mixture of (±)19-HETE provides cardioprotection against Ang II-induced cardiac hypertrophy (Elkhatali et al., 2015).

19(R)-HETE and 19(S)-HETE have been proven to be produced in a stereoselective manner and could have differential effects in case of normal physiological or pathophysiological states. 19(S)-HETE causes direct stimulation of the activity of Na^+-K^+-ATPase renal proximal tubules leading to stimulation of proximal tubule transport, while 19(R)-HETE negated 20-HETE-mediated inhibition of vasodilatory nitric oxide production in renal arteries (Cheng et al., 2008). Therefore, we hypothesized that R- and S- enantiomers of 19-HETE might protect against cardiac hypertrophy in an enantioselective manner

1.7.2 Hypotheses

1- Subterminal-HETEs (19(R)-HETE and 19(S)-HETE) prevent cardiac hypertrophy in an enantioselective manner

2- Synthetic 19-HETE analogs (R- and S-analogues) could be considered as a novel therapeutic approach in the treatment of CVD

3- Repurposing clinically-approved drugs to prevent the development of cardiac hypertrophy, through inhibition of CYP1B1 and its associated mid-chain HETEs, is a possible approach for the treatment of cardiac hypertrophy and subsequent HF.

1.7.3 Objectives

1- To test whether 19(R)-HETE and 19(S)-HETE have a differential role in their protective effect against Ang II-induced cellular hypertrophy.

2- To examine the inhibitory effect of both enantiomers of 19-HETE on the human recombinant CYP1B1 enzyme.

3- To test the capability of synthetic analogues of 19-HETE to exert an inhibitory effect on human recombinant CYP1A1, CYP1B1, CYP1A2 and CYP3A4 enzymes.

4- To investigate whether resveratrol, a CYP modulator, protects against Ang II-induced cellular hypertrophy through inhibition of CYP1B1/mid-chain HETEs mechanism.

5- To investigate the potential ameliorative role of fluconazole against abdominal aortic constriction (AAC)-induced cardiac hypertrophy in rats and to elucidate the underlying molecular mechanisms involved.

CHAPTER 2: MATERIALS AND METHODS

Portions of this chapter have been published in:

1- **Shoieb SM,** Dakarapu R, Falck JR, El-Kadi AOS. (2021). Novel Synthetic Analogues of 19(S/R)-Hydroxyeicosatetraenoic Acid Exhibit Noncompetitive Inhibitory Effect on the Activity of Cytochrome P450 1A1 and 1B1. European Journal of Drug Metabolism and Pharmacokinetics. In Press.

2- **Shoieb SM,** El-Kadi A. (2020). Resveratrol attenuates angiotensin II-induced cellular hypertrophy through the inhibition of CYP1B1 and the cardiotoxic mid-chain HETE metabolites.Molecular and Cellular Biochemistry. 471: 165–176.

3- **Shoieb SM,** El-Sherbeni A, El-Kadi A. (2019). Identification of 19-(s/r) hydroxyeicosatetraenoic acid as the first endogenous noncompetitive inhibitor of cytochrome P450 1B1 with enantioselective activity. Drug Metabolism and Disposition. 47: 67–70.

4- **Shoieb SM,** El-Kadi A. (2018). S-enantiomer of 19-hydroxyeicosatetraenoic acid preferentially protects against angiotensin II-induced cardiac hypertrophy. Drug Metabolism and Disposition. 46: 1157–1168.

2.1 Chemicals and Materials

19(R)-, 19(S)-HETEs, 15-HETE-D8 and 14, 15-EET-D11 were purchased from Cayman Chemical (Ann Arbor, MI, USA). 7-ethoxyresorufin (7-ER), 7-methoxyresorufin (7-MR) and nicotinamide adenine dinucleotide phosphate (NADPH) tetrasodium salt were purchased from Sigma Chemical Co. (St. Louis, MO). 19(R)-HETE synthetic analogue [sodium 19(R)-hydroxyeicosa-5(Z),14(Z)-dienoyl glycinate] and 19(S)-HETE synthetic analogue [sodium 19(S)-hydroxyeicosa-5(Z),14(Z)-dienoate] (Figure 2.1) were synthesized in Dr. J. Falck laboratory (University of Texas, Southwestern Medical Center, Texas, USA). Resveratrol was purchased from Sigma-Aldrich Co. (St. Louis, MO, USA). Fluconazole injection (2mg/ml) was purchased from McKesson Medical-Surgical (Auburn, WA, USA). Human recombinant CYP1A1, CYP1A2, CYP1B1 and CYP3A4 microsomes supplemented with NADPH–cytochrome P450-oxidoreductase (Corning-Supersomes™) were obtained from Fisher Scientific (Hampton, NH). InVitroCYP ™ human liver microsomes were purchased from BioIVT (Hicksville, NY, USA). P450-Glo™ CYP3A4 Assay V9001 (Luciferin-IPA) kit was purchased from Promega (Madison, WI, USA). Dulbecco's Modified Eagle's Medium/F-12 (DMEM/F-12) and DMEM were purchased from Gibco, Life Technologies (Grand Island, NY, USA). Fetal bovine serum was purchased from Sigma-Aldrich Co. (St. Louis, MO, USA). TRIzol reagent was purchased from Invitrogen Co. (Carlsbad, CA, USA). High Capacity cDNA Reverse Transcription kit and SYBR® Green PCR Master Mix were purchased from Applied Biosystems (Foster City, CA, USA). Real-time PCR primers were formulated by Integrated DNA Technologies (Coralville, IA, USA). Immun-Blot® PVDF membrane was purchased from Bio-Rad Laboratories (Hercules, CA, USA).

Glyceraldehyde-3-phosphate dehydrogenase (GAPDH) mouse monoclonal, 5-LOX mouse monoclonal, 12-LOX rabbit polyclonal, 15-LOX mouse monoclonal, COX-2 mouse monoclonal primary antibodies were purchased from Santa Cruz Biotechnology, Inc. (Santa Cruz, CA, USA), while recombinant monoclonal anti-CYP1B1 antibody, CYP2B6, CYP2C8, and CYP4F2 rabbit polyclonal primary antibodies and CYP2J2 mouse monoclonal primary antibody were purchased from Abcam (Toronto, ON). CYP4F11 mouse monoclonal primary antibodies were purchased from Sigma Chemical Co. (St. Louis, MO, USA). Chemiluminescence Western blotting detection reagents were obtained from GE Healthcare Life Sciences (Pittsburgh, PA, USA). The Alanine Aminotransferase (ALT) Activity Assay Kit (MAK052), Aspartate Aminotransferase (AST) Activity Assay Kit (MAK055) and Bromocresol Green Albumin Assay Kit (MAK124) were purchased from Sigma Aldrich Canada Co. (Oakville, ON, Canada). Reagents used for liquid chromatographic-electrospray ionization-mass spectrometry (LC-ESI-MS) were at HPLC-grade. Acetonitrile and water (HPLC grade) were purchased from Sigma Chemical Co. (St. Louis, MO, USA). All of the other chemicals used were obtained from Fisher Scientific Co. (Toronto, ON, Canada).

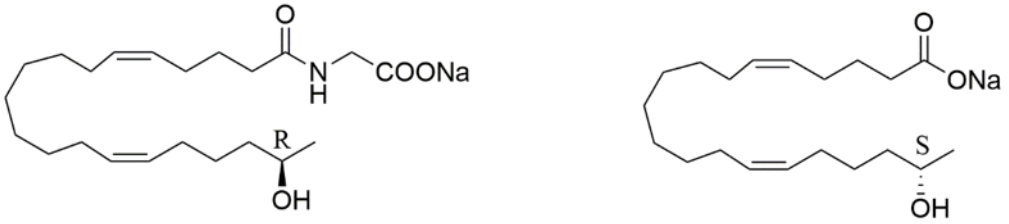

19(R)-HETE analogue
[sodium 19(R)-hydroxyeicosa-5(Z), 14(Z)-dienoyl glycinate]

19(S)-HETE analogue
[sodium 19(S)-hydroxyeicosa-5(Z),14(Z)-dienoate]

Figure 2.1. 19-HETE R- and S-enantiomers novel synthetic analogues

Chemical structures of the synthetic analogues of 19(R)-HETE [sodium 19(R)-hydroxyeicosa-5(Z),14(Z)-dienoyl glycinate] and 19(S)-HETE [sodium 19(S)-hydroxyeicosa-5(Z),14(Z)-dienoate].

2.2 Cell culture

Rat cardiomyoblast (H9c2) cell line and human cardiomyocyte (RL-14) cells were obtained from American Type Culture Collection (ATCC) (Manassas, VA, USA). H9c2 cells were maintained in DMEM containing 10% heat-inactivated fetal bovine serum, and 1% penicillin–streptomycin. RL-14 cells were maintained in DMEM/F-12, with phenol red supplemented with 12.5% fetal bovine serum, 20µM l-glutamine, 1% penicillin–streptomycin. Cells were grown in 75 cm^2 cell culture flasks at 37 °C in a 5% CO2 humidified enviroment. Each 75 cm^2 flask had an average of 7.5 x 10^6 cells. Seeding of cells in the plates was based upon the following parameters: each well in the 6-well plate would contain an average of 9.5 x 10^5 cells, each well in the 12-well plate would contain an average of 3.8 x 10^5 cells and each well in the 24-well plate would contain an average of 1.9 x 10^5 cells.

2.3 Chemical treatment

For determination of the effects of both enantiomers of 19-HETE, cells were treated with vehicle (serum-free DMEM/F12 containing 0.05% DMSO) or 20μM of 19(R)-HETE or 19(S)-HETE in serum-free medium (SFM) for the time indicated for each experiment, as described in the figure legends. 19(R)-HETE or 19(S)-HETE were supplied as a stock solution in dimethyl sulfoxide (DMSO) and maintained in DMSO at −20 °C until use. The treatment of cells was carried out in the corresponding culture media in 12- well cell culture plates for RNA assay and 6-well cell culture plates for protein and determination of AA metabolites assays. To investigate the effect of 19(R)-HETE or 19(S)-HETE on cardiac hypertrophic and inflammatory markers, cells were treated with 10 μM Ang II in the absence or presence of 20 μM 19(R)-HETE or 19(S)-HETE for 24 h as described in the figure legends. Ang II stock solution was prepared in saline and maintained at −20 °C until use. Diluted solutions of Ang II, 19(R)-HETE or 19(S)-HETE were freshly prepared in serum free medium (SFM) before each experiment. In all experiments, the DMSO concentration did not exceed 0.05% (v/v).

For determination of the effects of resveratrol, cells were treated with vehicle (serum-free DMEM/F12 containing 0.05% DMSO), 10 μM Ang II, 10 μM Ang II in combination with (2, 10 or 50 μM resveratrol) or (2, 10 or 50 μM resveratrol alone) in SFM for the time indicated for each experiment as described in the figure legends. Resveratrol was prepared as a stock solution in DMSO and maintained in DMSO at −20 °C until use. The treatment of cells was performed in the corresponding culture media in 12- well cell culture plates for RNA assay and 6-well cell culture plates for protein and determination

of AA metabolites assays. Diluted solutions of Ang II and resveratrol were freshly prepared in SFM before each experiment.

2.4 Measurement of cell viability

The viability of H9c2 and RL-14 cells was measured by the MTT assay. The assay depends on the ability of viable cells to reduce tetrazolium dye MTT 3-(4,5-dimethylthiazol-2-yl)-2,5-diphenyltetrazolium bromide to its insoluble colored formazan crystals. In brief, cells were seeded in 96-well plates, treated as indicated, incubated for 24 h at 37 °C in a 5% CO2 humidified incubator, incubated with 20 µl/well MTT (1.2 mM) dissolved in phosphate-buffered saline (PBS; pH 7.4) for 3 h at 37 °C, and then 150 µl/well isopropyl alcohol to dissolve the formazan for 10 min at room temperature. The optical density was assessed at a wavelength of 550 nm using the Bio-Tek Synergy H1Hybrid Multi-Mode Microplate Readers (Bio-Tek Instruments, Winooski, VT, USA). The cell viability was presented as a percentage of the control mean absorbance value.

2.5 Metabolism of AA by H9c2 and RL-14 cells

In order to investigate the effect of both enantiomers of 19-HETE on the AA metabolites, H9c2 and RL-14 cells were treated with vehicle or 20 µM of 19(R)-HETE or 19(S)-HETE in SFM for 24 h and then the cells were incubated with 50 µM AA for 3 h. Extraction of AA metabolites was performed using ethyl acetate and dried using speed vacuum (Savant, Farmingdale, NY, USA). The resultant extracted AA and its metabolites were analyzed using LC–ESI–MS (Waters Micromass ZQ 4000 spectrometer) method.

2.6 Assessment of CYP1B1 enzymatic activity

Enzymatic activity of CYP1B1 was determined by methoxyresorufin O-demethylase (MROD) assay which was performed on intact living RL-14 and H9c2 cells. Briefly, the cells were seeded in 24-well plates and test compounds and methoxyresorufin (5 μM) in assay buffer (0.05 M Tris, 0.1 M NaCl, pH 7.8) were added. Instantly, an initial fluorescence measurement (t = 0) at excitation/emission wavelengths (535/585 nm), respectively, was carried out. Fluorescence of the samples was recorded every 5 min interval for 40 min using the Bio-Tek Synergy H1 Hybrid Multi-Mode Microplate Readers (Bio-Tek Instruments, Winooski, VT, USA). The content of each sample of resorufin formed was assessed by comparison with a standard curve of known concentrations. The CYP1B1 enzymatic activity was normalized to protein content in the cells which was assessed using a fluorescence-based protein assay (Lorenzen and Kennedy, 1993). The assay steps were as the following: the cells were rinsed with PBS, and 50 μL of double de-ionized water was added to each well, and cell plates were placed at −80°C for 30 min to lyse the cells. Thereafter, the cell lysates were allowed to thaw, then, 100 μL of 0.1 M potassium phosphate buffer was added to each well followed by 50 μL of 1.08 mM fluorescamine and plates were shaken for five min. The florescence was measured using Synergy H1 Hybrid Multi-Mode Microplate Reader (BioTek Instruments, Winooski, VT, USA) using excitation and emission wavelengths of 365 and 470 nm, respectively. The formation rate of resorufin was represented as pmol/min/mg protein.

2.7 Determination of CYP1B1-inhibition kinetics by 19-HETE enantiomers

The O-dealkylation rate of 7-ER by recombinant human CYP1B1 was measured in the absence or presence of 19(R)-HETE or 19(S)-HETE. Briefly, 96-well solid black polystyrene microplates were used to carry out the florescent assay. The reaction mixture containing 100 mM potassium phosphate (pH 7.4) buffer supplemented with 5 mM magnesium chloride hexahydrate and 1 pmol of human CYP1B1, was incubated with 10-100 nM of 7-ER. In addition, 0, 5, 10, 20, or 40 nM of either 19(R)-HETE or 19(S)-HETE was added to the reaction mixture. The volume of the reaction mixture was 100 µL. The reaction was initiated by the addition of 100 µL of 2 mM NADPH, the fluorescent signal related to the formation of resorufin was measured every min (excitation and emission wavelengths of 550 and 585 nm, respectively) for 30 min at 37°C using a BioTek Synergy H1 Hybrid Reader (BioTek Instruments, Inc.). The quantity of formed resorufin was measured by the construction of standard curve of 0-200 nM of resorufin dissolved in the same incubation buffer. The formation rate of resorufin in each well was determined over the first 9 min period using linear regression. The formation rates of resorufin at different 7-ER concentrations were fitted to Michaelis-Menten equation; while, 19(R)-HETE-CYP1B1 and 19(S)-HETE-CYP1B1 inhibition rates were fitted to competitive, noncompetitive, uncompetitive, and mixed models of enzyme inhibition. The most probable enzyme inhibition model was selected according to Akaike information criteria (AIC). The fitting was carried out using GraphPad Prism (version 5.01; GraphPad Software, Inc., La Jolla, CA).

2.8 Determination of 19(R)-HETE and 19(S)-HETE in-vitro stability

In order to assess the stability of 19-HETE enantiomers in solution under the same experimental conditions of the kinetic study, the stability experiment has been performed using 7-ER concentration corresponding to the K_m of the reaction. 19(R)-HETE and 19(S)-HETE were added to the reaction mixture at their Ki concentrations of 89.1 and 37.3 nM, respectively. After initiation of the reaction using 2 mM NADPH, 200 µL was taken from the mixture at the start of the reaction (T0), after 10, 20 and 30 min at 37°C. The reaction was stopped using 400 µL ice-cold acetonitrile and the extraction of 19-HETE enantiomers was performed using ethyl acetate and dried using speed vacuum (Savant, Farmingdale, NY, USA). The analysis of 19-HETE enantiomers was performed using LC–ESI–MS as described later in this chapter.

2.9 Determination of CYP1A1-, CYP1A2- and CYP1B1-inhibition kinetics by 19-HETE synthetic analogues

The O-dealkylation rate of 7-ER (EROD) by recombinant human CYP1A1 and CYP1B1 as well as MROD by recombinant human CYP1A2, were determined in the absence and presence of 19(R)-HETE or 19(S)-HETE synthetic analogues. Briefly, 96-well solid black polystyrene microplates were used to perform the fluorescent assay. The reaction mixture containing 100 mM potassium phosphate (pH 7.4) buffer supplemented with 5 mM magnesium chloride hexahydrate and 1 pmol of human recombinant CYP1A1, CYP1A2 or CYP1B1, was incubated with 10-200 nM of 7-ER, 10-200 nM of 7-MR or with 10-100 nM of 7-ER, respectively. In addition, 0, 5, 10, 20, or 40 nM of either 19(R)-HETE or 19(S)-HETE synthetic analogues were added to the reaction mixture. The

volume of the reaction mixture was 100 µL. The reaction was initiated by the addition of 100 µL of 2 mM NADPH, the fluorescent signal related to the formation of resorufin was measured every min (excitation and emission wavelengths of 550 and 585 nm, respectively) for 20 min at 37°C using a BioTek Synergy H1 Hybrid Reader (BioTek Instruments, Inc.). The quantity of formed resorufin was determined by the construction of a standard curve of 0-200 nM of resorufin dissolved in the same incubation buffer. The formation rate of resorufin in each well was determined using linear regression. The formation rates of resorufin at different 7-ER or 7-MR concentrations were fitted to Michaelis-Menten equation; while, 19(R)-HETE analogue-CYP1A1, 19(S)-HETE analogue-CYP1A1, 19(R)-HETE analogue-CYP1B1 and 19(S)-HETE analogue-CYP1B1 inhibition rates were fitted to competitive, noncompetitive, uncompetitive, and mixed models of enzyme inhibition. The calculation of enzyme kinetics parameters and the fitting of data were carried out using GraphPad Prism (version 5.01; GraphPad Software, Inc., La Jolla, CA). The most probable enzyme inhibition model was selected according to Akaike information criteria (AIC).

2.10 Assessment of CYP1A1 and CYP1B1 enzymatic activity in human microsomes

Enzymatic activity of CYP1A1 and CYP1B1 was determined by EROD and MROD assays, respectively, using human microsomes separated from the liver, in the absence and presence of 19(R)-HETE or 19(S)-HETE synthetic analogues. Briefly, 96-well solid black polystyrene microplates were used to perform the fluorescent assay. The reaction mixture containing 100 mM potassium phosphate (pH 7.4) buffer supplemented with 5 mM magnesium chloride hexahydrate and 0.2mg/ml human liver microsomes, was

incubated with 2 μM of 7-ER for EROD assay or 5 μM of 7-MR for MROD assay. In addition, 0, 20, 40, 80, or 100 nM of either 19(R)-HETE or 19(S)-HETE synthetic analogues were added to the reaction mixture. The volume of the reaction mixture was 100 μL. The reaction was initiated by the addition of 100 μL of 2 mM NADPH. The fluorescent signal related to the formation of resorufin was measured every min (excitation and emission wavelengths of 550 and 585 nm, respectively) for 20 min at 37°C using a BioTek Synergy H1 Hybrid Reader (BioTek Instruments, Inc.). The calculation of IC_{50} and the fitting of data were carried out using GraphPad Prism (version 5.01; GraphPad Software, Inc., La Jolla, CA) using the dose-response inhibition module.

2.11 Assessment of CYP3A4 enzymatic activity using human recombinant enzyme

The assay was carried out according to the manufacturer's instructions. P450-Glo™ Assays provide a luminescent method to measure CYP activity. The assay measures the activities of CYP enzymes from recombinant source and test the effects of inhibitors on CYP activities. The P450-Glo™ Substrates are CYP enzyme substrates that are proluciferins, derivatives of beetle luciferin [(4S)-4,5-dihydro-2-(6′-hydroxy-2′-benzothiazolyl)-4- thiazolecarboxylic acid]. The derivatives are converted by CYP enzymes to luciferin products. D-luciferin is formed and detected in a second reaction with the Luciferin Detection Reagent. The amount of light produced in the second reaction is proportional to CYP activity. Briefly, 12.5μl of either 19(R)-HETE or 19(S)-HETE synthetic analogues (4X) were added per well of a 96-well plate. Thereafter, 12.5μl of the 4X CYP reaction mixture (containing CYP3A4 0.1 pmol per reaction and the P450-Glo™ substrate) were added to each well and mixed gently. The plate was pre-incubated

at room temperature for 10 min. The reaction was initiated by the addition of 25 µL of 2X concentration of NADPH (200µM). Then, the plate was incubated for another 10 min at room temperature. 50µl of reconstituted Luciferin Detection Reagent were added to the wells. The plate was mixed for 10 sec on an orbital shaker, and it was then incubated at room temperature for 20 min to stabilize the luminescent signal. The luminescence signal was recorded using a luminometer (Bio-Tek Synergy H1 Hybrid Multi-Mode Microplate Readers, Winooski, VT, USA).

2.12 Animals

The protocol of the current study has been approved by the University Animal Policy and Welfare Committee (UAPWC) in University of Alberta. Animal studies are reported in compliance with the ARRIVE guidelines (Percie du Sert et al., 2020) and the Canadian Council on Animal Care. Male Sprague-Dawley rats, weighing 180-200g, were purchased from Charles River Canada (Senneville, QC, Canada). All animals were housed in cages under standard animal housing conditions, exposed to a 12-hour light/dark cycle, and had free access to food and water available *ad libitum*.

2.13 Experimental design and treatment protocol

Male Sprague-Dawley rats were randomly assigned into four groups and were subjected to sham (n = 12) or AAC surgery (n = 12) to experimentally induce cardiac hypertrophy. The first group (n = 6) consisted of sham control rats that received intraperitoneal (IP) normal saline. The second group (n = 6) consisted of sham rats that received IP fluconazole (20 mg/kg) daily for 4 weeks. The third group (n = 6) consisted of AAC rats

that received IP normal saline. The fourth group (n = 6) represents AAC rats that were treated with IP fluconazole (20 mg/kg) daily for 4 weeks.

Rats underwent baseline echocardiography before the commencement of experimental protocols. Afterwards, rats were anaesthetized using isoflurane anesthesia (3% for induction and 1–1.5% for maintenance), disinfected with chlorohexidine soap and swab with betadine solution on the abdomen. The abdomen hair was removed using hair removal cream, then a small incision was made through the skin beginning at the xyphoid sternum approximately 3–4 cm. The intestinal tissues were carefully displaced to the side using cotton balls to expose the inferior vena cava. The abdominal aorta was surgically dissected from the inferior vena cava at a site slightly above the renal arteries. A double-blunt needle was then placed side by side with the isolated aorta segment. The ligation of the abdominal aorta was carried out using a double-blunt needle sized 21 G together by the silk suture sized 0. Afterwards, the needle was removed, thus causing severe aortic constriction above the renal arteries. Viscera was carefully returned to its position, abdominal wall was sutured and the abdominal skin was closed with wound clips. The Sham procedure was carried out as above with no ligation. One week after surgery, rats started to receive daily IP saline or fluconazole according to the treatment protocol for 4 consecutive weeks.

Five weeks post-surgery, rats were echoed then euthanized under isoflurane anesthesia (3% induction and 1–1.5% maintenance). Blood collection from the abdominal aorta was slowly carried out after removal of connective tissue and application of finger pressure to dilate the vessel. Then, hearts were rapidly excised, washed with saline, blotted with filter

paper, and then the left ventricle was fragmented and homogenized to evaluate the mRNA, protein and metabolites level using a Branson homogenizer (VWR Scientific, Danbury, Conn., USA).

2.14 Echocardiographic evaluation of cardiac function

The echocardiographic evaluations were carried out at baseline before the AAC procedure and 5 w post AAC procedure. All rats were anesthetized with isoflurane, then transthoracic M-mode echocardiography (Vevo 770, Visualsonics, Toronto) was carried out using a small animal imaging ultrasound system to measure cardiac function and wall thickness. Images were retained and analyzed using VisualSonics software version: 3.0.0. Systolic and wall measurements (LVID: left ventricular internal diameter; LVPW: left ventricular posterior wall thickness; and IVS: inter-ventricular septum), left ventricular mass (LV mass), diastolic function, heart rate and tissue Doppler parameters in addition to ejection fraction (%EF) and fractional shortening (%FS) were assessed using M-mode measurements taken from parasternal long and short axis views at the mid-papillary level. Left ventricular dimensions were recorded at both systolic and diastolic levels. The pressure gradient (mmHg) was determined from the mitral flow using the velocity time integral measurement. Measurements were averaged from 3 to 6 cardiac cycles according to the American Society of Echocardiography (Byrd et al., 2015), and digitally transferred online to a computer, and subsequently analyzed by an analyst blinded to the treatment groups.

2.15 Assessment of serum biomarkers of hepatotoxicity

Serum activities of alanine aminotransferase (ALT), aspartate aminotransferase (AST), and albumin level were assessed using colorimetric assays according to the kit instructions purchased from Sigma Aldrich Canada Co. (Oakville, ON, Canada). ALT was measured based on a pyridoxalphosphate-dependent enzyme that catalyzes the reversible transfer of an amino group from alanine to α-ketoglutarate, generating a colorimetric (570 nm) product, proportional to the pyruvate generated. AST was measured based on a pyridoxal phosphate (PLP)-dependent enzyme that catalyzes the conversion of aspartate and α-ketoglutarate to oxaloacetate and glutamate, generating a colorimetric (450 nm) product. Albumin level was measured based on bromocresol green, which forms a colored complex specifically with albumin. The intensity of the color, measured at 620 nm, is directly proportional to the albumin concentration in the sample.

2.16 RNA extraction and cDNA synthesis

TRIzol reagent (Invitrogen®) was used according to the manufacturer's instructions for total isolation of RNA from cells or frozen tissues, and quantified by measuring the absorbance at 260 nm, while the purity was determined by measuring the 260/280 ratio (>1.8). Afterwards, first-strand cDNA synthesis was carried out using the High-Capacity cDNA reverse transcription kit (Applied Biosystems) according to the manufacturer's instructions. In brief, 1.5 µg of total RNA from each sample was added to a mix of 2.0 µl 10× RT buffer, 0.8 µl 25× dNTP mix (100 mM), 2.0 µl 10× reverse transcriptase random primers, 1.0 µl MultiScribe™ reverse transcriptase enzyme and 4.2 µl nuclease-free

water. The final reaction mixture was kept at 25 °C for 10 min, heated to 37 °C for 120 min, heated for 85 °C for 5 min and finally cooled to 4 °C.

2.17 Real-time polymerase chain reaction (real-time PCR) for quantification of mRNA expression

Real-time PCR was utilized to quantitatively determine specific mRNA expression of different targets by subjecting the resultant cDNA to PCR amplification using 96-well optical reaction plates in the Applied Biosystems™ QuantStudio 5 Real-Time PCR System. The reaction mixture (20 µl) contained 0.04 µl of 10 µM forward primer and 0.04 µl of 10 µM reverse, 10 µl of SYBR Green Universal Master mix, 8.92 µl of RNAse/DNAse-free water, and 1 µl of cDNA sample. Human primer sequences for CYP1B1, CYP2B6, CYP2C8, CYP2J2, CYP4F2, CYP4F11, ANP, α-MHC, β-MHC, 5-LOX, 12-LOX, 15-LOX, COX-2,IL-6, IL-8 and β-actin as well as rat primer sequences for CYP1A1, CYP1A2, CYP1B1, CYP2B2, CYP2C11, CYP2C23, CYP2E1, CYP2J3, CYP3A2, CYP4A1, CYP4F4, CYP4F6, ANP, BNP, α-MHC, β-MHC, 5-LOX, 12-LOX, 15-LOX, COX-2, IL-6, IL-8 and β-actin are listed in (Table 2.1). Primers were purchased from Integrated DNA technologies IDT (Coralville, IA, USA). Analysis of the real-time PCR data was carried out using the relative gene expression (i.e., ΔΔ CT) method. In brief, the fold change in the level of target genes between treated and untreated cells, corrected for the level of housekeeping gene (β-actin), was determined using the following equation: fold change = $2^{-\Delta(\Delta Ct)}$, where ΔCt = Ct(target) − Ct(β-actin) and Δ(ΔCt) = ΔCt(treated) − ΔCt(untreated). The thermal cycle parameters were as follow:

initiation of the reaction at 95°C for 10 min and 40 cycles of denaturation (95°C, 15s) and combined annealing/extension (60°C, 60s).

Table 2.1. Primer sequences used for RT- PCR reactions.

Gene	Forward primer	Reverse primer
Human		
CYP1B1	5′-TTCGGCCACTACTCGGAGC-3′	5′-AAGAAGTTGCGCATCATGCTG-3′
CYP2B6	5′-TTAGGGAAGCGGATTTGTCTTG-3′	5′-GGAGGATGGTGAAGAAGAG-3′
CYP2C8	5′-CACCCAGAGGTCACAGCTAAAGT-3′	5′-CATGTGGCTCCTATCCTGCAT-3′
CYP2J2	5′-GAGCTTAGAGGAACGCATTCAG-3′	5′-GAAATGAGGGTCAAAAGGCTGT-3′
CYP4F2	5′-GAGGGTAGTGCCTGTTTGGAT-3′	5′-CAGGAGGATCTCATGGTGTCTT-3′
CYP4F11	5′-CATCTCCCGATGTTGCACG-3′	5′-TCTCTTGGTCGAAACGGAAGG-3′
ANP	5′-CAACGCAGACCTGATGGATTT-3′	5′-AGCCCCCGCTTCTTCATTC-3′
α-MHC	5′-GCCCTTTGACATTCGCACTG-3′	5′-GGTTTCAGCAATGACCTTGCC-3′
β-MHC	5′-TCACCAACAACCCCTACGATT-3′	5′-CTCCTCAGCGTCATCAATGGA-3′
5-LOX	5′-ACAAGCCCTTCTACAACGACT-3′	5′-AGCTGGATCTCGCCCAGTT-3′
12-LOX	5′-CTTCCCGTGCTACCGCTG-3′	5′-TGGGGTTGGCACCATTGAG-3′
15-LOX	5′-TGGAAGGACGGGTTAATTCTGA-3′	5′-GCGAAACCTCAAAGTCAACTCT-3′
COX-2	5′-CTGGCGCTCAGCCATACAG-3′	5′-CGCACTTATACTGGTCAAATCCC-3′
IL-6	5′-GGTACATCCTCGACGGCATCT-3′	5′-GTGCCTCTTTGCTGCTTTCAC-3′
IL-8	5′-CTCTTGGCAGCCTTCCTGATT-3′	5′-TATGCACTGACATCTAAGTTCTTTAGCA-3′
β-actin	5′-CTGGCACCCAGCACAATG-3′	5′-GCCGATCCACACGGAGTACT-3′
Rat		
CYP1A1	5′-CCAAACGAGTTCCGGCCT-3′	5′-TGCCCAAACCAAAGAGAATGA-3′
CYP1A2	5′-GAATGGCTTCTAGTCCCA-3′	5′-TCATCTTCTCACTAAGGGCT-3′
CYP1B1	5′-AATCCATGCGATTCACCAGC-3′	5′-TGTTTGAGGGCTCGTTTTGG-3′
CYP2B2	5′-CCATCCCTTGATGATCGTACCA-3′	5′-AATTGGGGCAAGATCTGCAAA-3′
CYP2C11	5′-CACCAGCTATCAGTGGATTTGG-3′	5′-GTCTGCCCTTTGCACAGGAA-3′
CYP2C23	5′-TTCGGGCTCCTGCTCCTTA-3′	5′-CGTCCAATCACACGGTCAAG-3′
CYP2E1	5′-AAAGCGTGTGTGTGTTGGAGAA-3′	5′-AGAGACTTCAGGTTAAAATGCTGCA-3′
CYP2J3	5′-CATTGAGCTCACAAGTGGCTTT-3′	5′-CAATTCCTAGGCTGTGATGTCG-3′
CYP3A2	5′-CCATCCCTTGATGATCGTACCA-3′	5′-AATTGGGGCAAGATCTGCAAA-3′
CYP4A1	5′-TTGAGCTACTGCCAGATCCCAC-3′	5′-CCCATTTTTGGACTTCAGCACA-3′
CYP4F4	5′-CAGGTCTGAAGCAGGTAACTAAGC-3′	5′-CCGTCAGGGTGGCACAGAGT-3′
CYP4F6	5′-CAGCTCAACTTCCCGCACA-3′	5′-AGGGTCATTTCCTTGGGTGC-3′

ANP	5′-GGAGCCTGCGAAGGTCAA-3′	5′-TATCTTCGGTACCGGAAGGTGT-3′
BNP	5′-CAGAAGCTGCTGGAGCTGATAAG-3′	5′-TGTAGGGCCTTGGTCCTTTG-3′
α-MHC	5′-TATGCTGGCACCGTGGACTA-3′	5′- GAGTTTGAGGGAGGACTTCTGG-3′
β-MHC	5′-AGCTCCTAAGTAATCTGTTTGCCAA-3′	5′-AAAGGATGAGCCTTTCTTTGCT-3′
5-LOX	5′-ACCAGTTCCTGAATGGCTGC-3′	5′-GGCTGCACTCCACCATTTCT-3′
12-LOX	5′-CCTGGTTCTGCAACCTCATCA-3′	5′-CTCAACATGACAAGAGGGGCA-3′
15-LOX	5′-GCTAACCCCATGGTGCTGAA-3′	5′-GGTGCAGGGTGCATTAGGAA-3′
COX-2	5′-CCAAACCAGCAGGCTCATACT-3′	5′-ATTCAGAGGCAATGCGGTTCT-3′
IL-6	5′-ATATGTTCTCAGGGAGATCTTGGAA-3′	5′-GTGCATCATCGCTGTTCATACA-3′
IL-8	5′-TGCCAAGGAGTGCTAAAGAAC-3′	5′-TCTCCACAACCCTCTGCACC-3′
β-actin	5′-CCAGATCATGTTTGAGACCTTCAA-3′	5′-GTGGTACGACCAGAGGCATACA-3′

2.18 Protein extraction from cells

Cells were grown in 6-well plates and incubated with the test compounds for 24 h. Afterwards, lysis buffer containing 50 mM HEPES, 0.5 M sodium chloride, 1.5 mM magnesium chloride, 1 mM EDTA, 10% (v/v) glycerol, 1% Triton X-100, and 5 µl/mL protease inhibitor cocktail was used to collect the cells. The cell homogenates were prepared by incubating the cell lysates on ice for 1 h, with sporadic vortex every 10 min, followed by centrifugation at 12,000 × g for 10 min at 4°C. Supernatant of total cellular lysate was collected and stored at −80 °C. Afterwards, the Lowry method was used to determine concentration of protein by using bovine serum albumin as a standard (Lowry et al., 1951).

2.19 Microsomal protein preparation from the heart

Differential ultra-centrifugation was utilized to prepare microsomal fractions from homogenized cardiac tissues, as described previously (Elkhatali et al., 2017). In brief, organs were washed in ice-cold potassium chloride (1.15%, w/v). Successively cut into pieces, and homogenized in ice-cold 0.25 M sucrose solution (17%, w/v). After

homogenization, the tissues were separated by differential ultra-centrifugation. The final pellet was re-suspended in cold sucrose and stored at −80 °C. The microsomal protein concentration was determined by the Lowry method using bovine serum albumin (BSA) as a standard (LOWRY et al., 1951).

2.20 Western blot analysis

Western blot analysis was performed according to previously detailed assay (Shoieb and El-Kadi, 2018b). Briefly, proteins from each group were separated by 10% sodium dodecyl sulfate–polyacrylamide gel electrophoresis (SDS–PAGE), samples underwent electrophoresis at 120 V for 2 h and separated proteins were transferred onto Immun-Blot® PVDF membranes. Afterwards, protein membranes were blocked overnight at 4 °C using blocking solution containing 0.15 M sodium chloride, 3 mM potassium chloride, 25 mM Tris-base, 5% skim milk, 2% bovine serum albumin, and 0.5% Tween 20. Following blocking, the blots were subjected to washing cycles 3 times for 30 min with Tris-buffered saline (TBS)–Tween-20. The blots were subsequently incubated for 2 h at 4 °C with primary antibodies in TBS solution (0.05% (v/v) Tween-20, 0.02% sodium azide). Incubation with secondary antibodies (peroxidase-conjugated IgG) in blocking solution was performed for 30-45 min at room temperature. Visualization of the bands was carried out using the enhanced chemiluminescence method according to the manufacturer's guide (GE Healthcare Life Sciences). ImageJ software (National Institutes of Health, Bethesda, MD, USA; http://rsb.info.nih.gov/ij) was used to quantify the intensity of the protein bands in relation to the signals acquired from GAPDH loading

control. Data, given in the figures, are represented as relative protein intensity (%) + SEM, as compared to the control group.

2.21 Separation of AA Metabolites by Liquid Chromatography–Electrospray Ionization–Mass Spectrometry

The incubation buffer (5 mM magnesium chloride hexahydrate dissolved in 0.1 M potassium phosphate buffer, pH 7.4) was utilized to incubate heart tissue microsomes (1 mg protein/ml) at 37 °C in a shaking water bath (50 rpm) for 5 min as a pre-equilibration period. 1 μM NADPH was then added to initiate the reaction and a final concentration of 50 μM AA was incubated for 30 min. The reaction was terminated by the addition of 600 μl of ice-cold acetonitrile followed by the internal standard, 15-HETE-D8. Mid-chain HETEs metabolite were extracted with ethyl acetate, dried using speed vacuum (Savant, Farmingdale, NY) and analyzed using liquid chromatography–electrospray ionization mass spectrometry (LC–ESI–MS) (Waters Micromass ZQ 4000 spectrometer) method, as described previously (El-Sherbeni and El-Kadi, 2014b).

2.22 Apparatus and chromatographic conditions

The assessment of mid-chain HETE and other AA metabolites was carried out using LC–ESI-MS as previously described (Shoieb and El-Kadi, 2020). In brief, the mode of the mass spectrometer was negative ionization mode with single ion monitoring: m/z = 319 for AA metabolites, and m/z = 327 and 330 for internal standards, 15-HETE-D8 and 14,15-EET-D11, respectively. The nebulizer gas was supplied from an in house nitrogen source with high purity. The source temperature was set to of 150 °C, and voltage of the capillary and cone were 3.51 kV and 25 V, respectively. A gradient separation was

performed on a reverse phase C18 column (Alltima HP, 150 × 2.1 mm) at 35 °C. The mobile phase (A) was composed of water with 0.01% formic acid and 0.005% triethylamine (v/v), whereas mobile phase (B) consisted of 8% methanol, 8% isopropanol, and 84% acetonitrile with 0.01% formic acid and 0.005% triethylamine (v/v). Samples were subjected to linear gradient elution at a flow rate of 200 µL/min, as follows: 60 to 48% in 4 min, held isocratically at 48% for 24 min, 48 to 35% in 11 min, 35 to 0% in 11 min, and finally held isocratically at 0% for 7 min of mobile phase A.

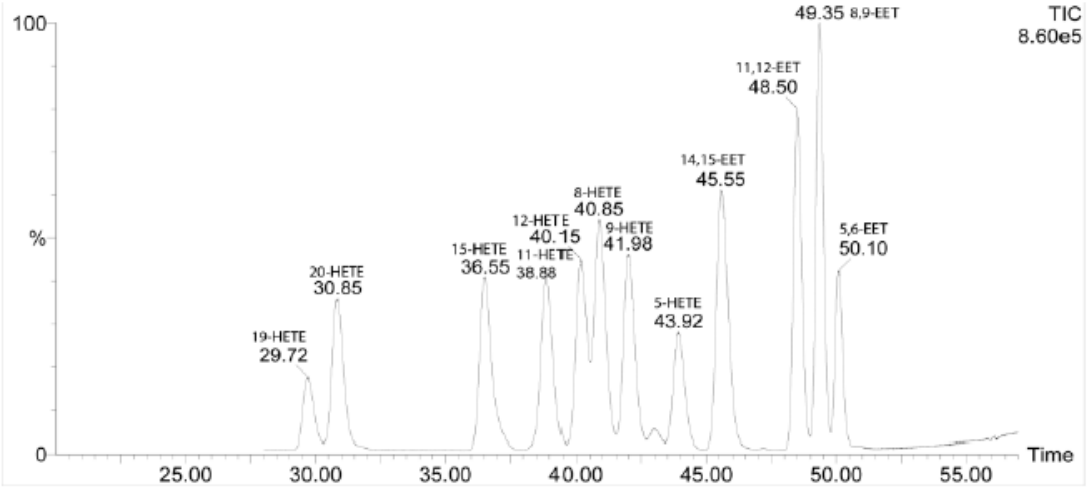

Figure 2.2. Separation of AA metabolites by LC-ESI-MS

Peaks and retention time for 20-, 19-, 15-, 12-, 11-, 9-, 8- and 5-HETE in addition to 14,15, 11,12-, 8,9- and 5,6-EET standards (min).

2.23 Data and statistical analysis

All results are presented as the mean ± SEM. Multiple group comparisons was performed using one-way analysis of variance (ANOVA) followed by the Student–Newman–Keuls as a post hoc test. Western blot data were analyzed using Kruskal-Wallis One Way Analysis of Variance on Ranks followed by the Student–Newman–Keuls as a *post hoc* test. Differences between means were considered significant at $p < .05$. All analyses were performed using SigmaPlot® for Windows (Systat Software, San Jose, CA, USA). K_m, Vmax and Ki values were determined using Enzyme Kinetics module from GraphPad Prism, version 5.01 and Microsoft Excel Solver. Nonlinear regression analysis and fitting to simple or sigmoid Michaelis-Menten equations were applied, the most probable mode of binding was selected based on the measures of goodness of fit including r^2 between the observed and fitted values as well as the sum of squares of the differences. The fitting was applied to the following equations:

$$v_{resorufin} = \frac{V_{max} \times C_{ethoxyresorufin}}{k_m + C_{ethoxyresorufin}}$$ Simple Michaelis-Menten model

$$v_{resorufin} = \frac{V_{max} \times C^n_{ethoxyresorufin}}{k^n_m + C^n_{ethoxyresorufin}}$$ Sigmoid Michaelis-Menten model

where V_{max} is the maximum velocity rate of resurofin formation, km is the affinity constant, C is the substrate concentration, n is the Hill coefficient.

CHAPTER 3: RESULTS

Portions of this chapter have been published in:

1- **Shoieb SM,** Dakarapu R, Falck JR, El-Kadi AOS. (2021). Novel Synthetic Analogues of 19(S/R)-Hydroxyeicosatetraenoic Acid Exhibit Noncompetitive Inhibitory Effect on the Activity of Cytochrome P450 1A1 and 1B1. European Journal of Drug Metabolism and Pharmacokinetics. In Press.

2- **Shoieb SM,** El-Kadi A. (2020). Resveratrol attenuates angiotensin II-induced cellular hypertrophy through the inhibition of CYP1B1 and the cardiotoxic mid-chain HETE metabolites.Molecular and Cellular Biochemistry. 471: 165–176.

3- **Shoieb SM,** El-Sherbeni A, El-Kadi A. (2019). Identification of 19-(s/r) hydroxyeicosatetraenoic acid as the first endogenous noncompetitive inhibitor of cytochrome P450 1B1 with enantioselective activity. Drug Metabolism and Disposition. 47: 67–70.

4- **Shoieb SM,** El-Kadi A. (2018). S-enantiomer of 19-hydroxyeicosatetraenoic acid preferentially protects against angiotensin II-induced cardiac hypertrophy. Drug Metabolism and Disposition. 46: 1157–1168.

5- Matsumura N, Takahara S, Maayah Z, Parajuli N, Byrne N, **Shoieb SM,** Soltys C-LM, Beker D, Masson G, El-Kadi A, Dyck J. (2018). Resveratrol improves cardiac function and exercise performance in MI-induced heart failure through the inhibition of cardiotoxic HETE metabolites. Journal of Molecular and Cellular Cardiology. 125: 162–173.

3.1 S-Enantiomer of 19-Hydroxyeicosatetraenoic Acid Preferentially Protects Against Angiotensin II-Induced Cardiac Hypertrophy

3.1.1 Effect of 19(R)-HETE and 19(S)-HETE on cell viability

In order to determine the maximum concentrations of both enantiomers of 19-HETE that do not possess a toxic effect on cells, human RL-14 and rat H9c2 cells were treated for 24 h with concentrations ranging from 5 to 40 μM of 19(R)-HETE or 19(S)-HETE. Thereafter, cell viability was assessed using the MTT assay. Figure 3.1A and B showed that both enantiomers, over the concentration range used, did not significantly affect the cell viability of the two cell lines (cell viability was above 90%). Consequently, 20 μM was selected to perform all subsequent experiments in this study based on the MTT assay results.

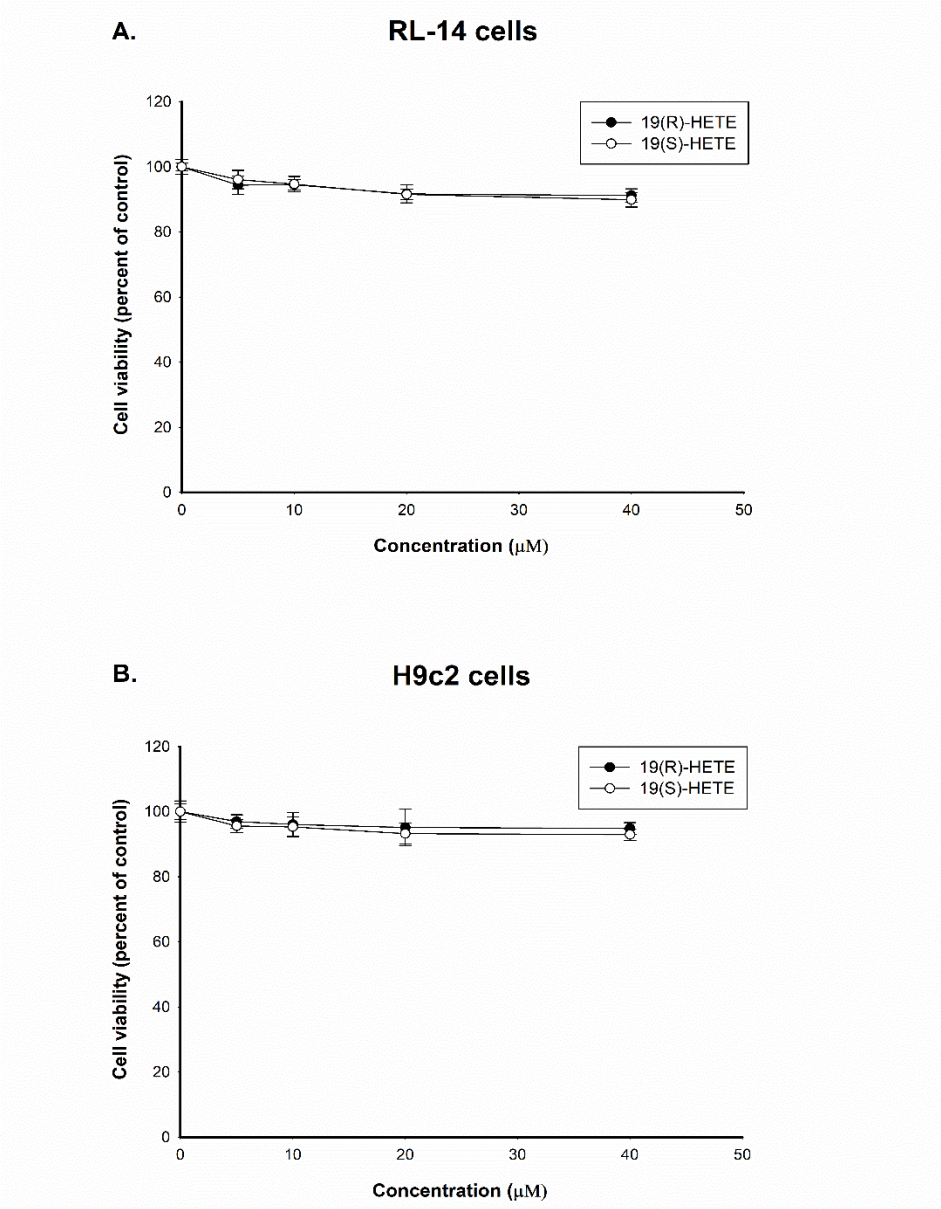

Figure 3.1. Effect of 19(R)-HETE and 19(S)-HETE on cell viability in RL-14 and H9c2 cells

RL-14 (A) and H9c2 (B) cells were treated for 24 h with 5–40 μM of 19(R)-HETE or 19(S)-HETE. Cell cytotoxicity was assessed using the MTT assay. Data are presented as the percentage of control (set at 100%) ± SEM (n = 3). Data were analyzed using one-way ANOVA followed by Student–Newman–Keuls as a post hoc test. T-test was used to compare 19(R)-HETE vs 19(S)-HETE at each concentration.

3.1.2 Effect of 19(R)-HETE and 19(S)-HETE on the formation of mid-chain HETEs

In order to investigate the effect of both enantiomers of 19-HETE on the formation of AA metabolites, RL-14 cells were treated for 24 h with vehicle or 20 μM of 19(R)-HETE or 19(S)-HETE. Thereafter, the cells were incubated with 50 μM AA for 3 h and AA metabolites (mid-chain HETEs, EETs and subterminal/terminal HETEs) were analyzed using LC–ESI–MS. Figure 3.2A showed that treatment of RL-14 cells with 19(R)-HETE significantly decreased the level of 15-HETE, 11-HETE, 12-HETE, 8-HETE and 9-HETE by approximately 21%, 28%, 25%, 22% and 25%, respectively, compared to the control group with no significant effect on the level of 5-HETE. On the other hand, the S enantiomer was able to significantly decrease the level of all mid-chain HETEs namely 15-HETE, 11-HETE, 12-HETE, 8-HETE, 9-HETE and 5-HETE by approximately 19%, 29%, 24%, 25%, 29% and 31%, respectively, compared to control. In order to confirm the results in another species, we used rat H9c2 cells. The results showed that both 19(R)-HETE and 19(S)-HETE significantly decreased the level of mid-chain HETEs namely 15-HETE, 12-HETE, 8-HETE and 5-HETE by approximately 42%, 35%, 37%, 33% and 44%, 39%, 39%, 35%, respectively (Figure 3.2B).

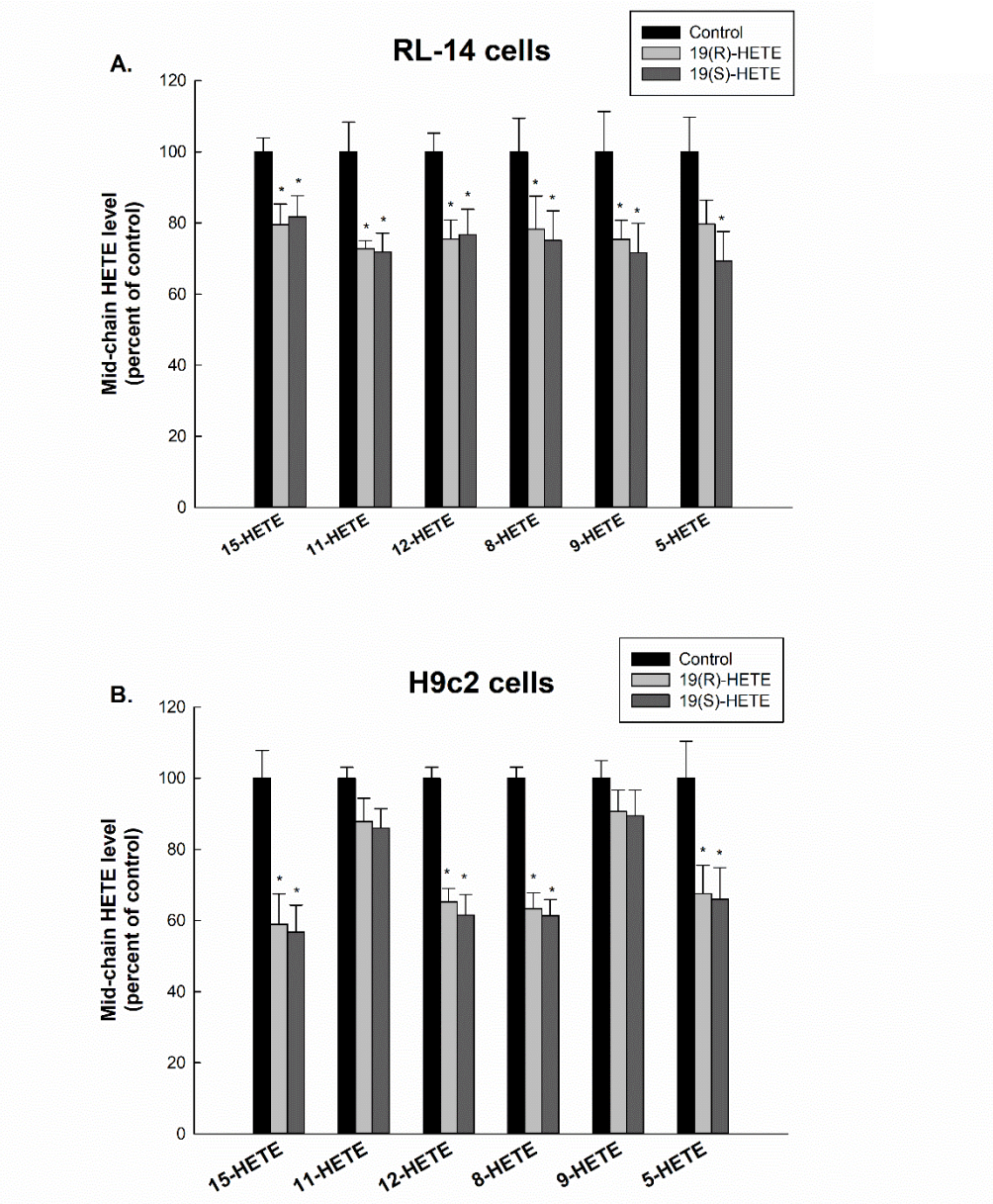

Figure 3.2. Effect of 19(R)-HETE and 19(S)-HETE on mid-chain HETE level in RL-14 and H9c2 cells

RL-14 (A) and H9c2 (B) cells were treated for 24 h with 20 μM of 19(R)-HETE or 19(S)-HETE. 5-, 8-, 9-, 11-, 12-, and 15-HETE metabolites were measured using LC–ESI–MS. The results are presented as the mean and SEM (n=3). Data were analyzed using one-way ANOVA followed by Student–Newman–Keuls as post hoc test. *$p < 0.05$ significantly different from the control group.

3.1.3 Effect of 19(R)-HETE and 19(S)-HETE on the formation of EETs and subterminal/terminal HETEs

The decrease in the formation of mid-chain HETEs prompted us to examine the effect of both enantiomers of 19-HETE on other AA metabolites such as EETs and subterminal/terminal HETEs. Our results showed that treatment of RL-14 cells with vehicle or 20 μM of 19(R)-HETE or 19(S)-HETE for 24 h did not significantly alter the formation rate of EETs (Figure 3.3A), namely 14,15-EET, 11,12-EET, 8,9-EET and 5,6-EET or subterminal/terminal HETEs (Figure 3.3B), specifically 16-HETE, 17-HETE, 18-HETE and 20-HETE compared to the control group.

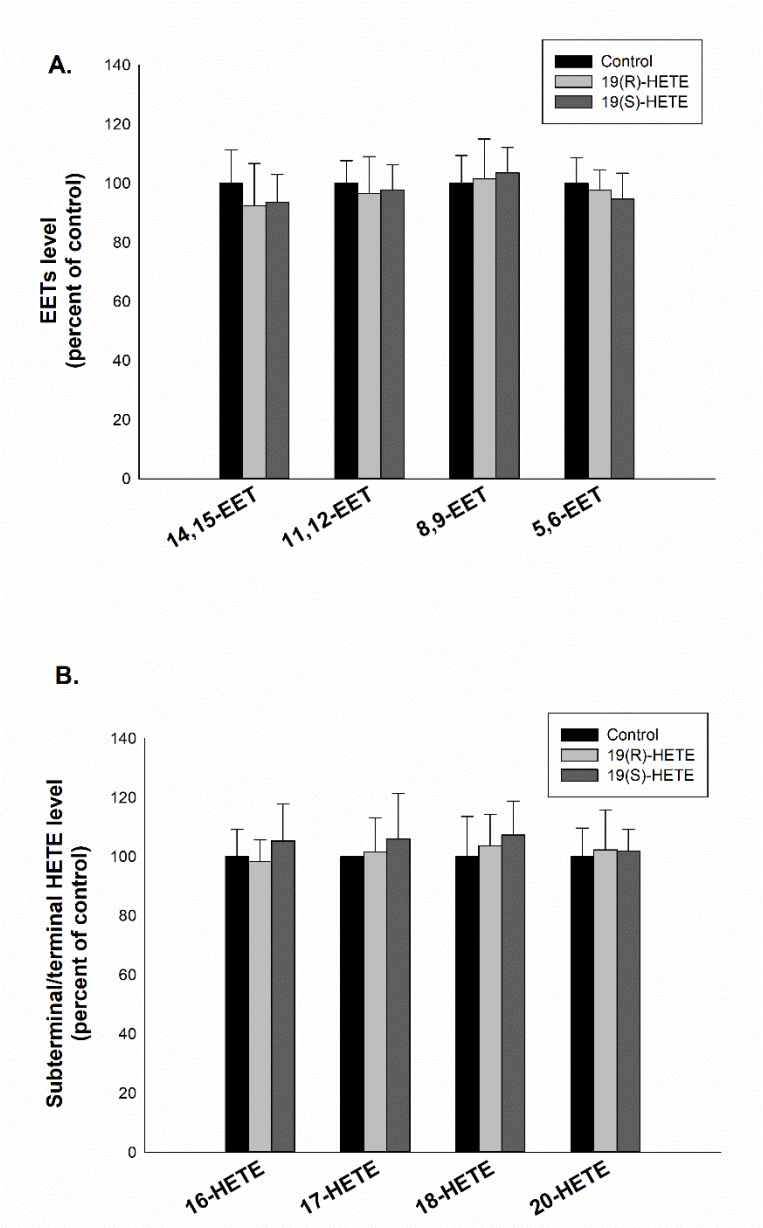

Figure 3.3. Effect of 19(R)-HETE and 19(S)-HETE on EETs and subterminal/terminal HETEs levels in RL-14 cells

RL-14 cells were treated for 24 h with 20 μM of 19(R)-HETE or 19(S)-HETE. (A) 5,6-, 8,9-, 11,12- and 14,15-EET and (B) 20-, 18-, 17- and 16-HETE metabolites were measured using LC–ESI–MS. The results are presented as the mean and SEM (n=3). Data were analyzed using one-way ANOVA followed by Student–Newman–Keuls as a post hoc test.

3.1.4 Effect of 19(R)-HETE and 19(S)-HETE on the mRNA and protein expression of cytochrome P450 epoxygenases and hydroxylases

To elucidate the mechanism by which both enantiomers of 19-HETE decrease the formation of mid-chain HETEs, the three pathways involved in mid-chain HETEs formation were further investigated. The first pathway is the CYP enzymes such as epoxygenases, hydroxylases and CYP1B1. The effect of 19(R)-HETE and 19(S)-HETE on CYP epoxygenases (CYP2B6, CYP2C8 and CYP2J2) and CYP hydroxylases (CYP4F2 and CYP4F11) was assessed (in RL-14 cells) on mRNA expression level using real-time PCR and protein expression level using Western blot analysis. Regarding CYP epoxygenases, the results showed that both enantiomers of 19-HETE have no significant effect on CYP2B6, CYP2C8 or CYP2J2 on mRNA (Figure 3.4A) or protein expression (Figure 3.4B) level compared to the control group. On the other hand, the S-enantiomer of 19-HETE significantly increased CYP4F2 and CYP4F11 mRNA expression level by 81% and 82%, respectively (Figure 3.5A). In agreement with mRNA expression results, Western blot analysis showed that the protein expression levels of CYP4F2 and CYP4F11 were also increased by 19(S)-HETE by 110% and 93%, respectively (Figure 3.5B).

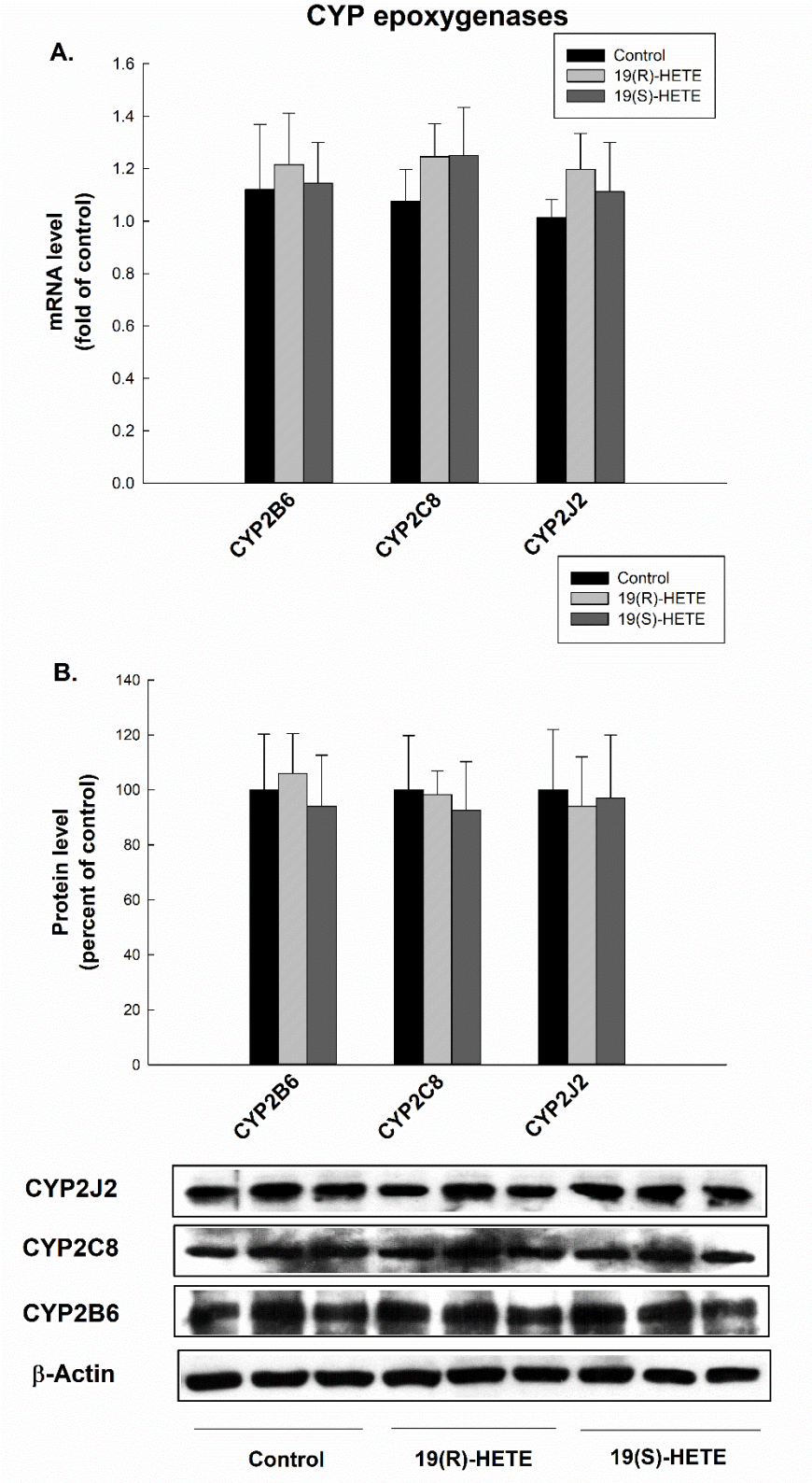
CYP epoxygenases
A.
Control
19(R)-HETE
19(S)-HETE
mRNA level
(fold of control)
1.6
1.4
1.2
1.0
0.8
0.6
0.4
0.2
0.0
CYP2B6
CYP2C8
CYP2J2
Control
19(R)-HETE
19(S)-HETE
B.
Protein level
(percent of control)
140
120
100
80
60
40
20
0
CYP2B6
CYP2C8
CYP2J2
CYP2J2
CYP2C8
CYP2B6
β-Actin
Control
19(R)-HETE
19(S)-HETE

Figure 3.4. Effect of 19(R)-HETE and 19(S)-HETE on mRNA and protein expression of CYP2B6, CYP2C8 and CYP2J2 in RL-14 cells

RL-14 cells were treated for 24 h with 20 μM of 19(R)-HETE or 19(S)-HETE. CYP2B6, CYP2C8 and CYP2J2 mRNA (A) and protein (B) expression levels were determined using real-time PCR and Western blot analysis, respectively. For real-time PCR, total RNA was isolated using TRIzol reagent, the mRNA level was quantified and its level was normalized to β-actin housekeeping gene. For Western blot analysis, protein levels were detected using the enhanced chemiluminescence method. The intensity of protein band was normalized to the signals obtained for β-actin protein and quantified using ImageJ®. The results are presented as the mean and SEM on at least 3 individual experiments. Data were analyzed using one-way ANOVA followed by Student–Newman–Keuls as a post hoc test.

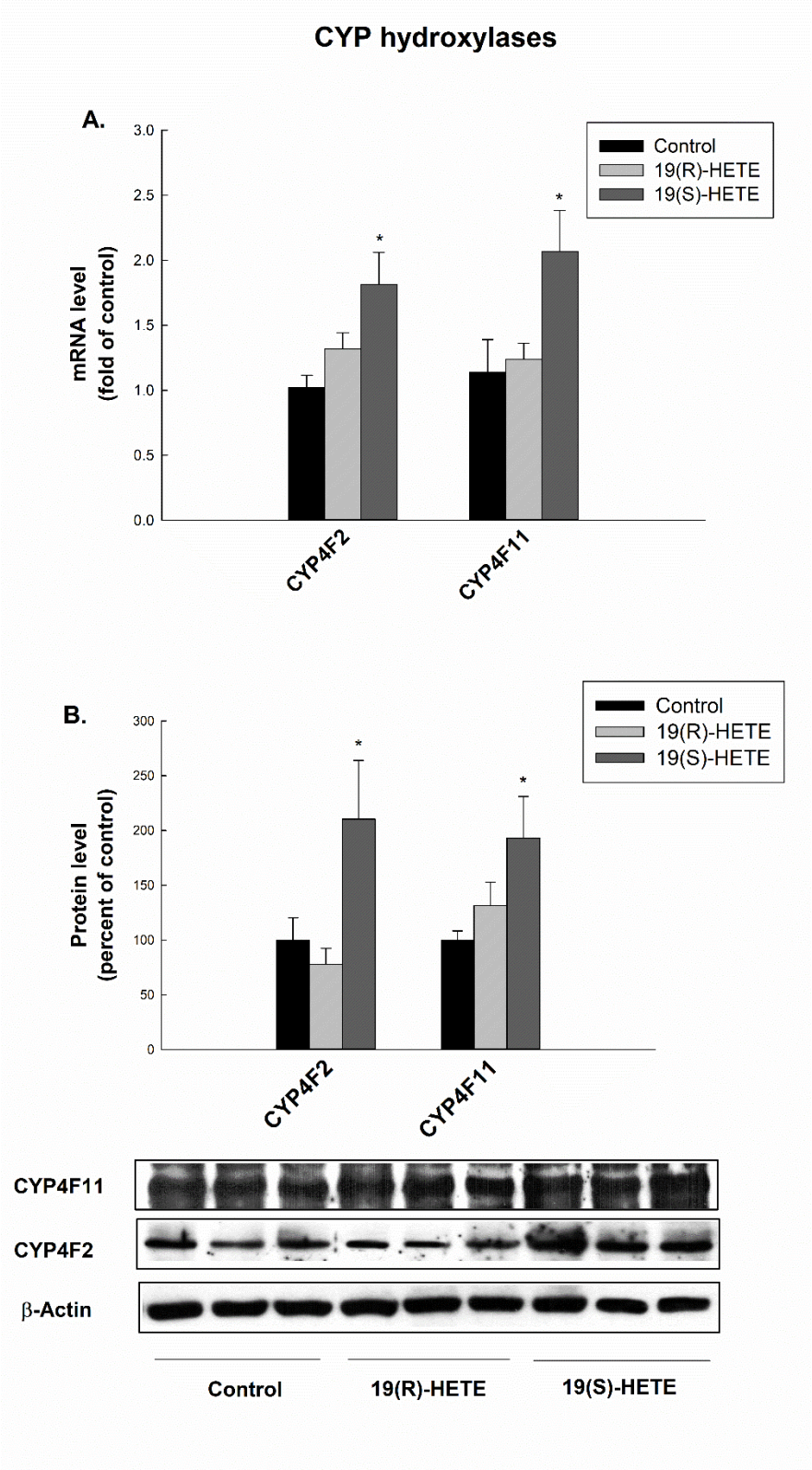
CYP hydroxylases
A.
mRNA level
(fold of control)
3.0
2.5
2.0
1.5
1.0
0.5
0.0
Control
19(R)-HETE
19(S)-HETE
*
*
CYP4F2
CYP4F11
B.
Protein level
(percent of control)
300
250
200
150
100
50
0
Control
19(R)-HETE
19(S)-HETE
*
*
CYP4F2
CYP4F11
CYP4F11
CYP4F2
β-Actin
Control
19(R)-HETE
19(S)-HETE

Figure 3.5. Effect of 19(R)-HETE and 19(S)-HETE on mRNA and protein expression of CYP4F2 and CYP4F11 in RL-14 cells

RL-14 cells were treated for 24 h with 20 μM of 19(R)-HETE or 19(S)-HETE. CYP4F2 and CYP4F11 mRNA (A) and protein (B) expression levels were determined using real-time PCR and Western blot analysis, respectively. For real-time PCR, total RNA was isolated using TRIzol reagent, the mRNA level was quantified and its level was normalized to β-actin housekeeping gene. For Western blot analysis, protein levels were detected using the enhanced chemiluminescence method. The intensity of protein band was normalized to the signals obtained for β-actin protein and quantified using ImageJ®. The results are presented as the mean and SEM on at least 3 individual experiments. Data were analyzed using one-way ANOVA followed by Student–Newman–Keuls as a post hoc test. *$p < 0.05$ significantly different from the control group.

3.1.5 Effect of 19(R)-HETE and 19(S)-HETE on the mRNA, protein expression and enzymatic activity of CYP1B1

The effect of both enantiomers of 19-HETE on CYP1B1 was determined at three levels; first was mRNA expression level and the results showed that R and S enantiomers of 19-HETE did not significantly affect CYP1B1 mRNA expression compared to the control group in RL-14 and H9c2 cells (Figure 3.6A). In agreement with the mRNA results, Western blot analysis showed that protein expression of CYP1B1 was not significantly altered by treatment with both enantiomers compared to the control group in both cell lines, RL-14 and H9c2 cells (Figure 3.6B). To examine the effect of both enantiomers on the functional catalytic activity of CYP1B1, an MROD assay was carried out. Figure 7C showed that, in RL-14 cells, 19(R)-HETE and 19(S)-HETE significantly decreased the formation of resorufin by approximately 80% and 85%, respectively, compared to the control group. In order to confirm this result in different cell line, H9c2 cells were used. The results showed that both R and S enantiomers significantly decreased the resorufin formation by approximately 82% and 85%, respectively (Figure 3.6C).

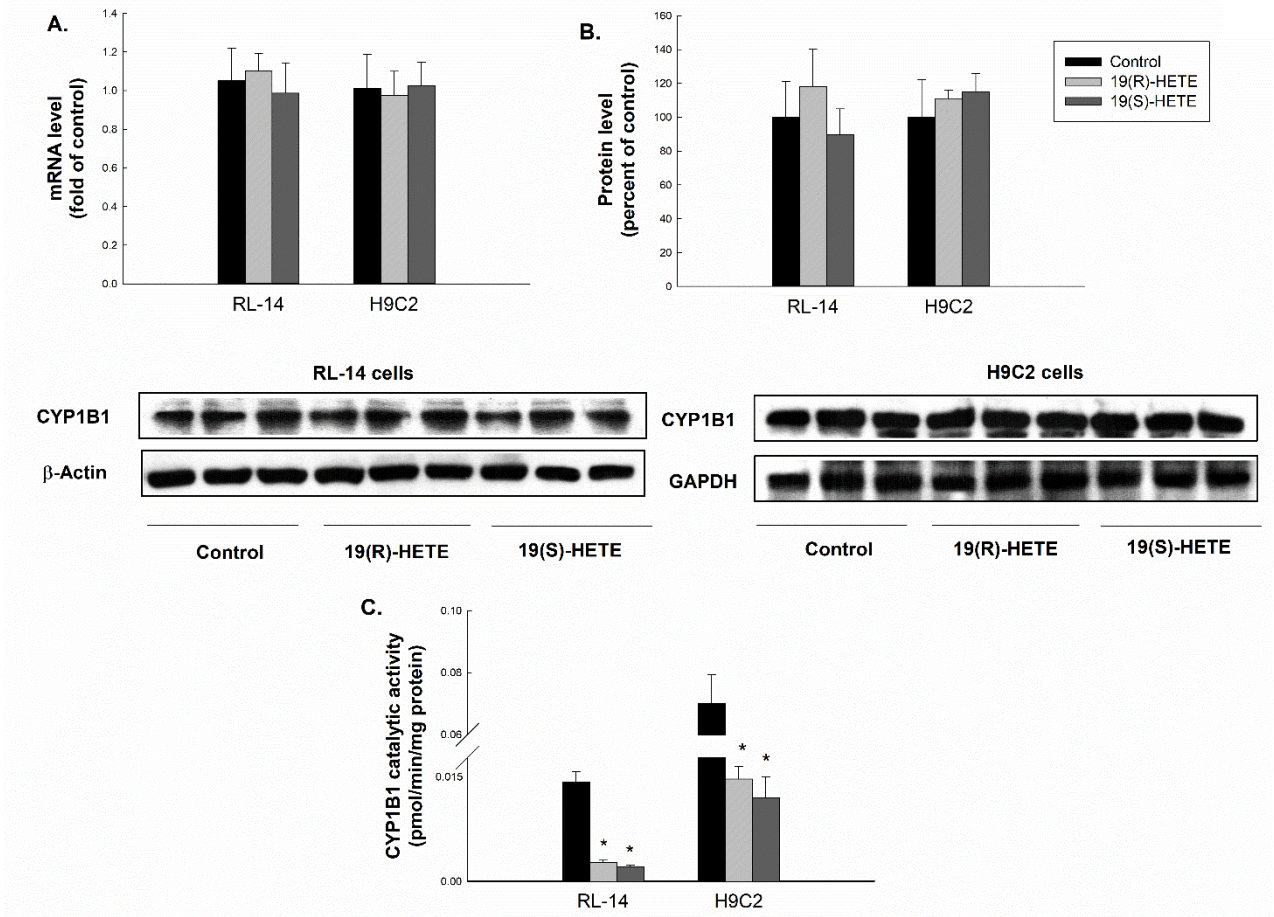

Figure 3.6. Effect of 19(R)-HETE and 19(S)-HETE on mRNA expression, protein expression levels as well as catalytic activity of CYP1B1 in RL-14 and H9c2 cells

RL-14 and H9c2 cells were treated for 24 h with 20 µM of 19(R)-HETE or 19(S)-HETE. CYP1B1 mRNA expression (A), protein expression levels (B) and catalytic activity (C) were determined using real-time PCR, Western blot analysis and MROD assay, respectively. For real-time PCR, the mRNA level was quantified and its level was normalized to β-actin housekeeping gene. For Western blot analysis, the intensity of protein band was normalized to the signals obtained for β-actin or GAPDH protein and quantified using ImageJ®. The results are presented as the mean and SEM based on at least 3 individual experiments. Data were analyzed using one-way ANOVA followed by Student–Newman–Keuls as post hoc test. *$p < 0.05$ significantly different from the control group.

3.1.6 Effect of 19(R)-HETE and 19(S)-HETE on 5-LOX, 12-LOX, 15-LOX and COX-2 protein expression levels

In order to investigate the other two pathways that are involved in the formation of mid-chain HETEs, protein expression levels of 5-LOX, 12-LOX, 15-LOX and COX-2 were assessed using Western blot analysis. For this purpose, RL-14 cells were treated with both enantiomers for 24 h and the results showed that both R and S enantiomers of 19-HETE were able to significantly decrease the protein expression levels of 5-LOX, 12-LOX (Figure 3.7A) and COX-2 (Figure 3.7B**)** by approximately (29%, 44%), (27%, 39%) and (54%, 63%), respectively, compared to the control group. It is worth noting that 15-LOX protein expression level was selectively decreased by the S enantiomer of 19-HETE by approximately 45%, compared to the control group (Figure 3.7A). To further confirm the data obtained from RL-14 cells, rat cardiomyoblast H9c2 cells were treated with 19(R)-HETE and 19(S)-HETE for 24 h. The results showed that both enantiomers significantly decreased protein expression levels of 5-LOX, 12-LOX and 15-LOX by approximately (44%, 54%), (49%, 71%) and (32%, 44%), respectively, compared to the control group (Figure 3.7A). Furthermore, 19(R)-HETE and 19(S)-HETE significantly decreased COX-2 protein expression level by approximately 48% and 55%, respectively, compared to the control group (Figure 3.7B).

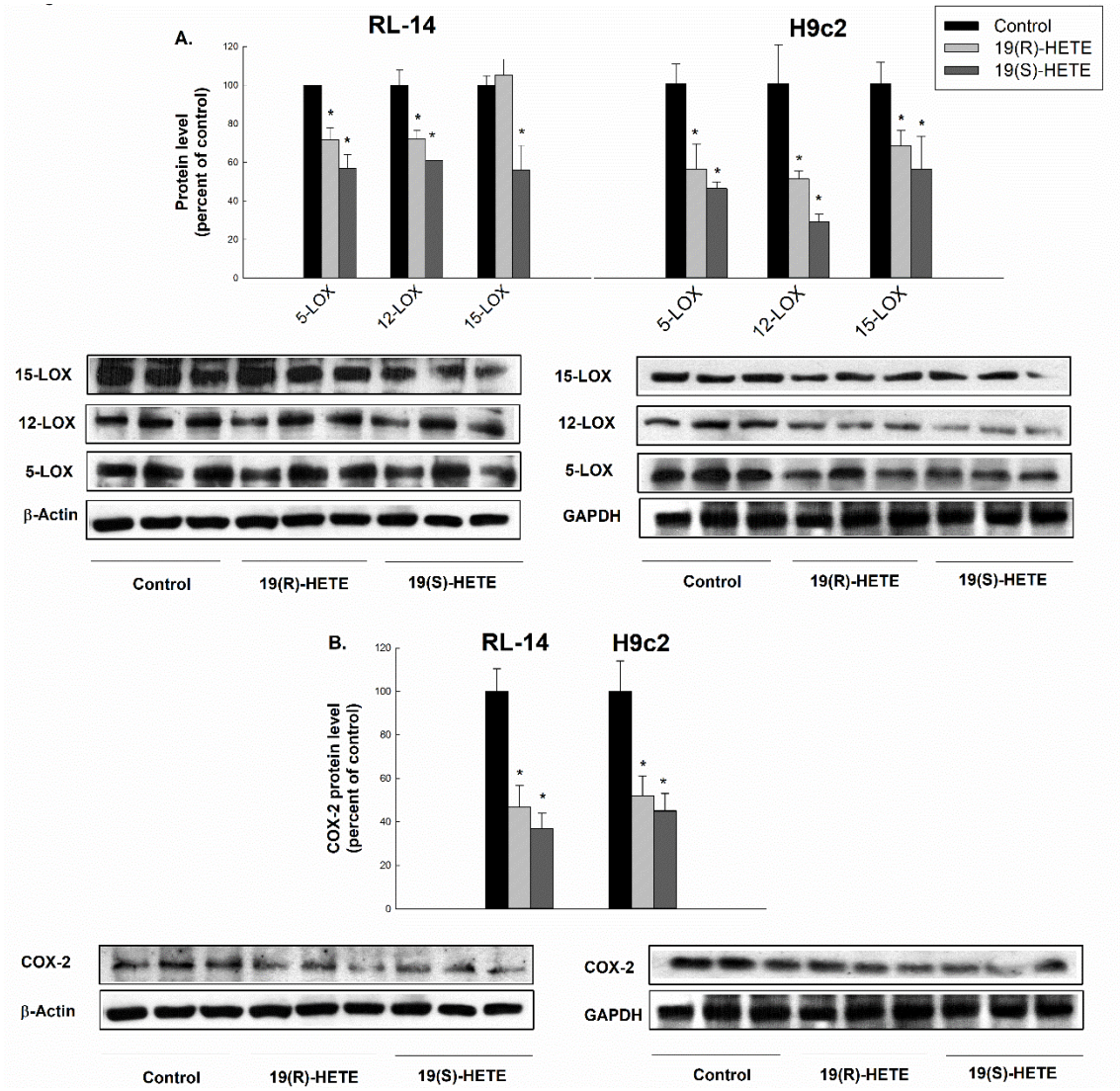

Figure 3.7. Effect of 19(R)-HETE and 19(S)-HETE on protein expression level of 5-LOX, 12-LOX, 15-LOX and COX-2 in RL-14 and H9c2 cells

RL-14 and H9c2 cells were treated for 24 h with 20 μM of 19(R)-HETE or 19(S)-HETE. 5-LOX, 12-LOX, 15-LOX (A) and COX-2 (B) protein expression level were determined using Western blot analysis. The intensity of protein band was normalized to the signals obtained for β-actin or GAPDH protein and quantified using ImageJ®. The results are presented as the mean and SEM based on at least 3 individual experiments. Data were analyzed using one-way ANOVA followed by Student–Newman–Keuls as post hoc test. *$p < 0.05$ significantly different from the control group.

3.1.7 Effect of 19(R)-HETE and 19(S)-HETE on Ang II-induced cellular hypertrophy

To investigate the effect of 19(R)-HETE and 19(S)-HETE on the development of cellular hypertrophy, the cells were treated with Ang II in the absence and presence of both enantiomers of 19-HETE. The results showed that treatment of cells with 10 μM Ang II for 24 h caused cellular hypertrophy as evidenced by a significant increase in β/α-MHC ratio and ANP by approximately 80% and 75%, respectively in RL-14 cells, compared to the control group (Figure 3.8A). Of interest, both R and S enantiomers of 19-HETE significantly attenuated Ang II-mediated increase of β/α-MHC ratio and ANP to nearly the control level. Furthermore, treatment of H9c2 cells with 10 μM Ang II for 24 h significantly increased β/α-MHC ratio and ANP mRNA expression by approximately 97% and 100%, respectively, compared to the control group. On the other hand, 19(R)-HETE and 19(S)-HETE were efficient in significantly returning hypertrophic markers to almost the control levels. These results provide substantial evidence that both R and S enantiomers of 19-HETE protect against Ang II-induced cellular hypertrophy (Figure 3.8B).

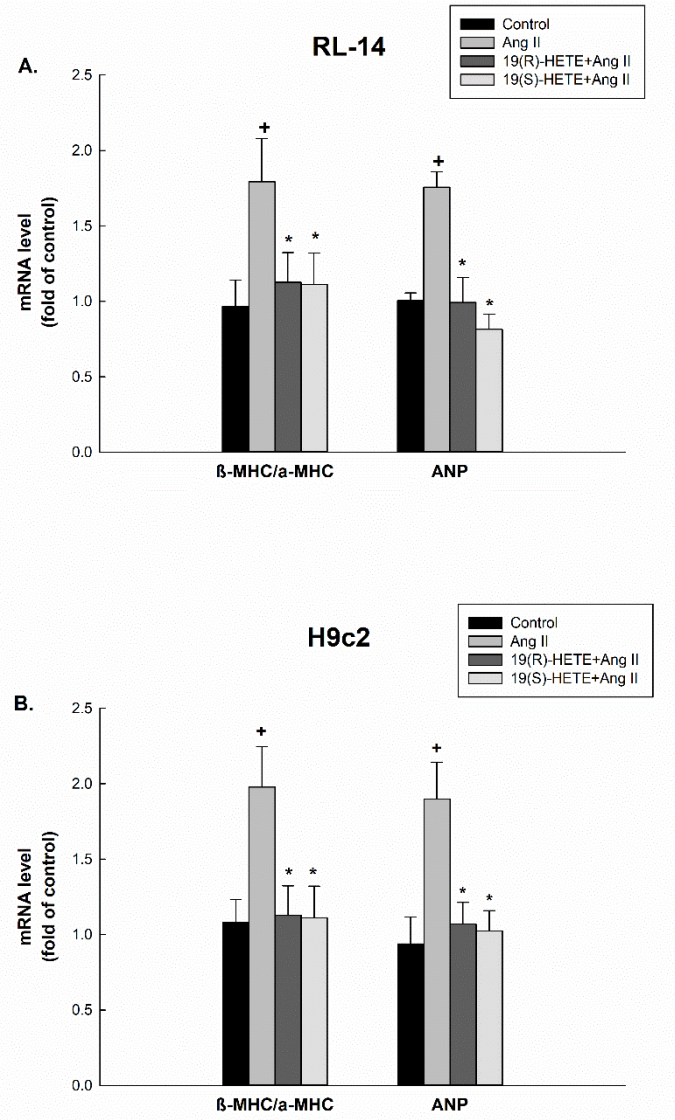

Figure 3.8. Effect of 19(R)-HETE and 19(S)-HETE on Ang II-mediated induction of hypertrophic markers in RL-14 and H9c2 cells

RL-14 (A) and H9c2 (B) cells were treated for 24 h with vehicle or 10 μM Ang II in the absence and presence of 20 μM 19(R)-HETE or 19(S)-HETE. The mRNA expression levels of β-MHC/α-MHC and ANP were assessed using real time-PCR and their levels were normalized to β-actin housekeeping gene. The results are presented as the mean and SEM based on at least 3 individual experiments. Data were analyzed using one-way ANOVA followed by Student–Newman–Keuls as post hoc test. +$p < 0.05$ significantly different from the control group. *$p < 0.05$ significantly different from Ang II-treated group.

3.1.8 Effect of 19(R)-HETE and 19(S)-HETE on Ang II-mediated increase of LOXs, COX-2 and pro-inflammatory cytokines at mRNA level

In order to investigate whether 19(R)-HETE and 19(S)-HETE have the capacity to prevent Ang II-mediated induction of LOXs, COX-2 and pro-inflammatory cytokines, mRNA expression of these markers was determined using real-time PCR. The results showed that treatment of RL-14 cells with 10 μM Ang II for 24 h significantly increased the mRNA expression level of 5-LOX, 12-LOX, 15-LOX and COX-2 by approximately 93%, 60%, 100% and 114%, respectively, compared to the control group (Figure 3.9A and B). Interestingly, R and S enantiomers of 19-HETE significantly prevented the Ang II-mediated induction of mRNA expression of these enzymes to nearly control levels while the mRNA expression of 15-LOX was solely decreased to control levels by the S enantiomer (Figure 3.9A and B). Furthermore, H9c2 cells were used to confirm the results obtained from RL-14 cells and the data showed that Ang II significantly increased the mRNA expression level of 5-LOX, 12-LOX, 15-LOX and COX-2 by approximately 150%, 83%, 100% and 81%, respectively, compared to the control group (Figure 3.9A and B). On the other hand, treatment of H9c2 with 19(R)-HETE and 19(S)-HETE completely prevented the Ang II-mediated induction of LOXs and COX-2 at the mRNA expression level.

Treatment of RL-14 cells with 10 μM Ang II for 24 h significantly increased the gene expression of both IL-6 and IL-8 by approximately 98% and 76%, respectively, compared to the control group (Figure 3.9C). On the other hand, R and S enantiomers reduced the Ang II-mediated induction of these two genes. 19(R)-HETE was able to partially decrease

the mRNA expression level of IL-6 and IL-8 by approximately 47% and 39%, respectively, compared to Ang II-treated group. Interestingly, 19(S)-HETE reduced mRNA expression of IL-6 and IL-8 to nearly control level. To further confirm our results, H9c2 cells were used to represent another species. The results showed that both enantiomers were able to decrease the Ang II-mediated induction of IL-6 and IL-8 gene expression to almost control levels (Figure 3.9C).

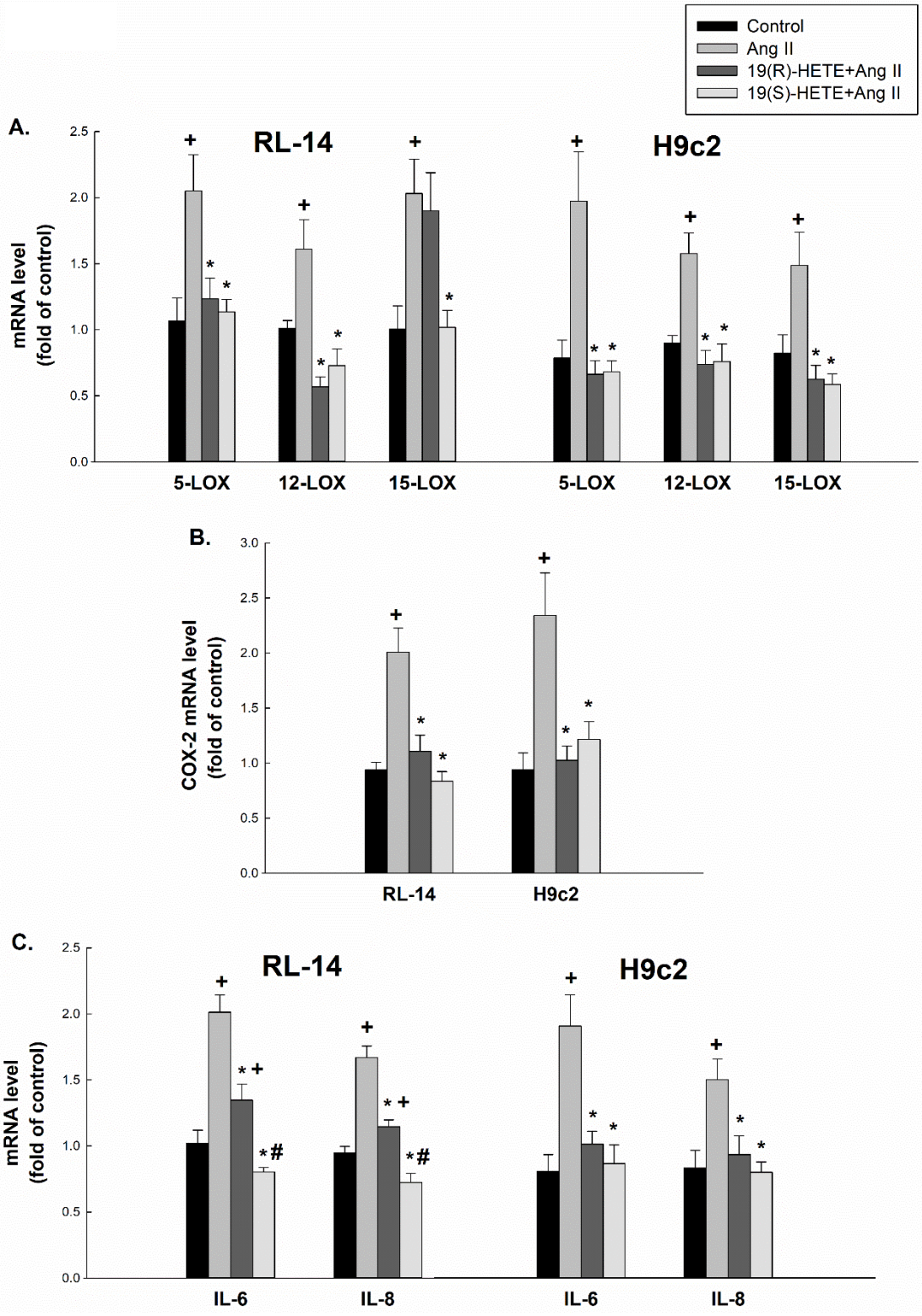
Control
Ang II
19(R)-HETE+Ang II
19(S)-HETE+Ang II
A.
RL-14
H9c2
mRNA level
(fold of control)
5-LOX
12-LOX
15-LOX
5-LOX
12-LOX
15-LOX
B.
COX-2 mRNA level
(fold of control)
RL-14
H9c2
C.
RL-14
H9c2
mRNA level
(fold of control)
IL-6
IL-8
IL-6
IL-8

Figure 3.9. Effect of 19(R)-HETE and 19(S)-HETE on Ang II-mediated induction of LOXs, COX-2 and pro-inflammatory cytokines mRNA expression in RL-14 and H9c2 cells

RL-14 and H9c2 cells were treated for 24 h with vehicle or 10 μM Ang II in the absence and presence of 20 μM 19(R)-HETE or 19(S)-HETE. Total RNA was isolated using TRIzol, the mRNA expression levels of LOXs (A), COX-2 (B) and interleukins (C) were assessed using real time-PCR and their levels were normalized to β-actin housekeeping gene. The results are presented as the mean and SEM based on at least 3 individual experiments. Data were analyzed using one-way ANOVA followed by Student–Newman–Keuls as post hoc test. $+p < 0.05$ significantly different from the control group. $*p < 0.05$ significantly different from Ang II-treated group. $\#p < 0.05$ significantly different from 19(R)-HETE-treated group.

3.2 Identification of 19-(S/R)Hydroxyeicosatetraenoic Acid as the First Endogenous Non-Competitive Inhibitor of Cytochrome P450 CYP1B1 with Enantioselective Activity

3.2.1 Determination of the enzyme kinetics of resorufin formation by human recombinant CYP1B1

Inhibitory activity of 19(R)-HETE (Figure 3.10A) and 19(S)-HETE (Figure 3.10B) on CYP1B1 was studied. Foremost experiments involved the assessment of 7-ER-O-deethylase kinetics by determination of the rate of resorufin formation over time. Based on the nonlinear regression analysis and fitting to simple or sigmoid Michaelis-Menten model, the most probable mode of binding is the sigmoid type of with the maximal EROD activity (V_{max}) in the control containing 0.1% DMSO was 10.6 pmol resorufin/pmol P450/min (R^2 =0.993). The Michaelis-Menten constant (K_m) value for the current EROD reaction is 37 nM (Table 3.1).

3.2.2 Inhibitory effect of 19(R)-HETE and 19(S)-HETE on EROD activity mediated by human recombinant CYP1B1

During the co-incubation of 10 nM of either 19-HETE enantiomers with different concentrations of 7-ER, we observed a significant inhibition of CYP1B1 enzymatic activity. This finding prompted us to test increasing concentrations (0-40 nM) of either 19(R)-HETE or 19(S)-HETE with different concentrations (0-100 nM) of 7-ER in order to characterize the mode of inhibition by 19-HETE enantiomers. Nonlinear regression analysis and comparisons showed that the mode of inhibition for 19(R)-HETE and 19(S)-HETE is noncompetitive inhibition of CYP1B1 enzyme. Dixon

plots showed that 19(R)-HETE (Figure 3.11A) and 19(S)-HETE (Figure 3.11B) have Ki values of 89.1 and 37.3 nM, respectively (Table 3.1).

Table 3.1. The mean values and standard error of kinetic parameters of resorufin formation by human recombinant CYP1B1, in the absence and presence of 19(R)-HETE or 19(S)-HETE

Ki (nM)		19(R)-HETE	19(S)-HETE
		89.1 ± 11.5	37.3 ± 5.5
	Kinetics of resorufin formation		
19-HETE concentration	**Vmax (pmol/pmol P450/min)**	**K_m (nM)**	**Hill coefficient (n)**
No inhibitor	10.6 ± 1.2	37 ± 4.3	1.56
5 nM 19(R)-HETE	10.1 ± 1.3	40.6 ± 5.1	1.41
10 nM 19(R)-HETE	9.6 ± 0.9	40.1 ± 4.1	1.4
20 nM 19(R)-HETE	8.8 ± 1.1	45.4 ± 5.9	1.21
40 nM 19(R)-HETE	8.1 ± 1.4	41.9 ± 4.6	1.22
5 nM 19(S)-HETE	7.6 ± 0.8	35 ± 3.7	1.3
10 nM 19(S)-HETE	7.4 ± 0.8	40.5 ± 4.8	1.22
20 nM 19(S)-HETE	7 ± 0.9	46 ± 4.7	1.16
40 nM 19(S)-HETE	6.4 ± 0.7	47.1 ± 5.4	1.25

Results are presented as mean and SE, based on at least 3 individual experiments. K_m, Vmax and Ki mean ± SE were determined by Enzyme Kinetics module from GraphPad Prism, version 5.01 and Microsoft Excel Solver.

A.

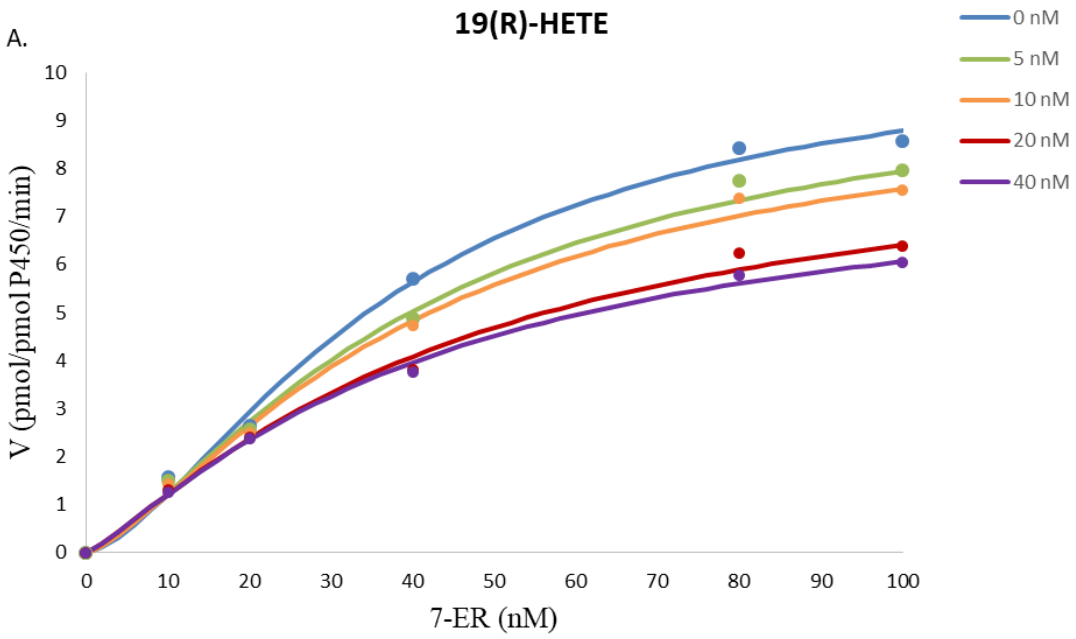
19(R)-HETE
0 nM
5 nM
10 nM
20 nM
40 nM
V (pmol/pmol P450/min)
7-ER (nM)
0
1
2
3
4
5
6
7
8
9
10
0
10
20
30
40
50
60
70
80
90
100

B.

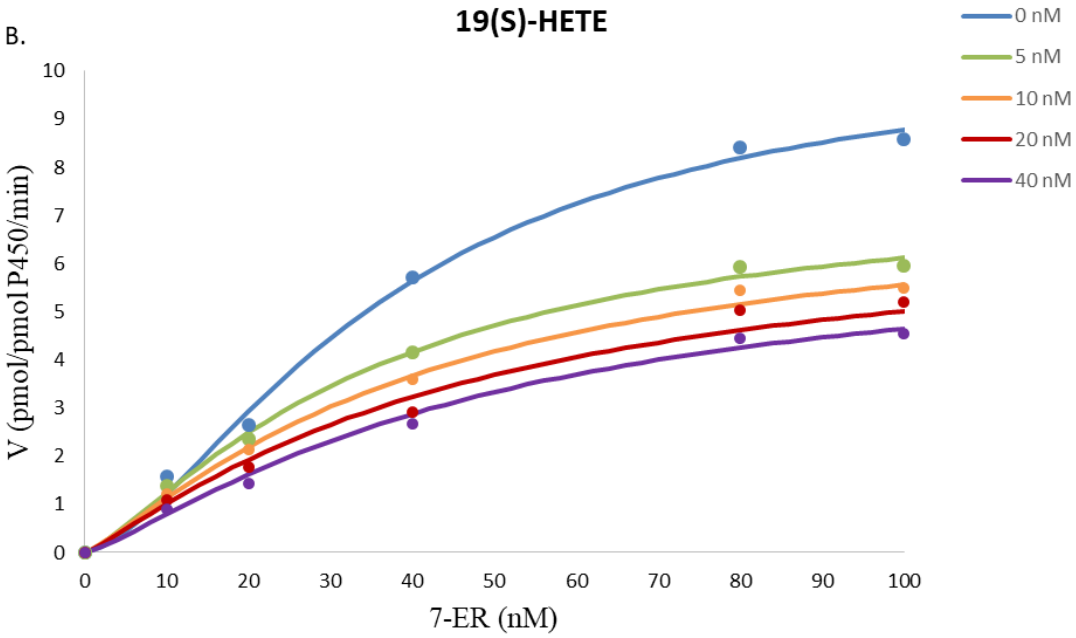
19(S)-HETE
0 nM
5 nM
10 nM
20 nM
40 nM
V (pmol/pmol P450/min)
7-ER (nM)
0
1
2
3
4
5
6
7
8
9
10
0
10
20
30
40
50
60
70
80
90
100

Figure 3.10. Inhibitory effect of 19(R)-HETE and 19(S)-HETE on EROD activity mediated by human recombinant CYP1B1

0, 5, 10, 20, or 40 nM of either 19(R)-HETE (A) or 19(S)-HETE (B) was added to the reaction mixture. The reaction was initiated by the addition of 100 µL of 2 mM NADPH, the fluorescent signal related to the formation of resorufin was measured every min. Each point represents the mean of 6 independent experiments ± SE.

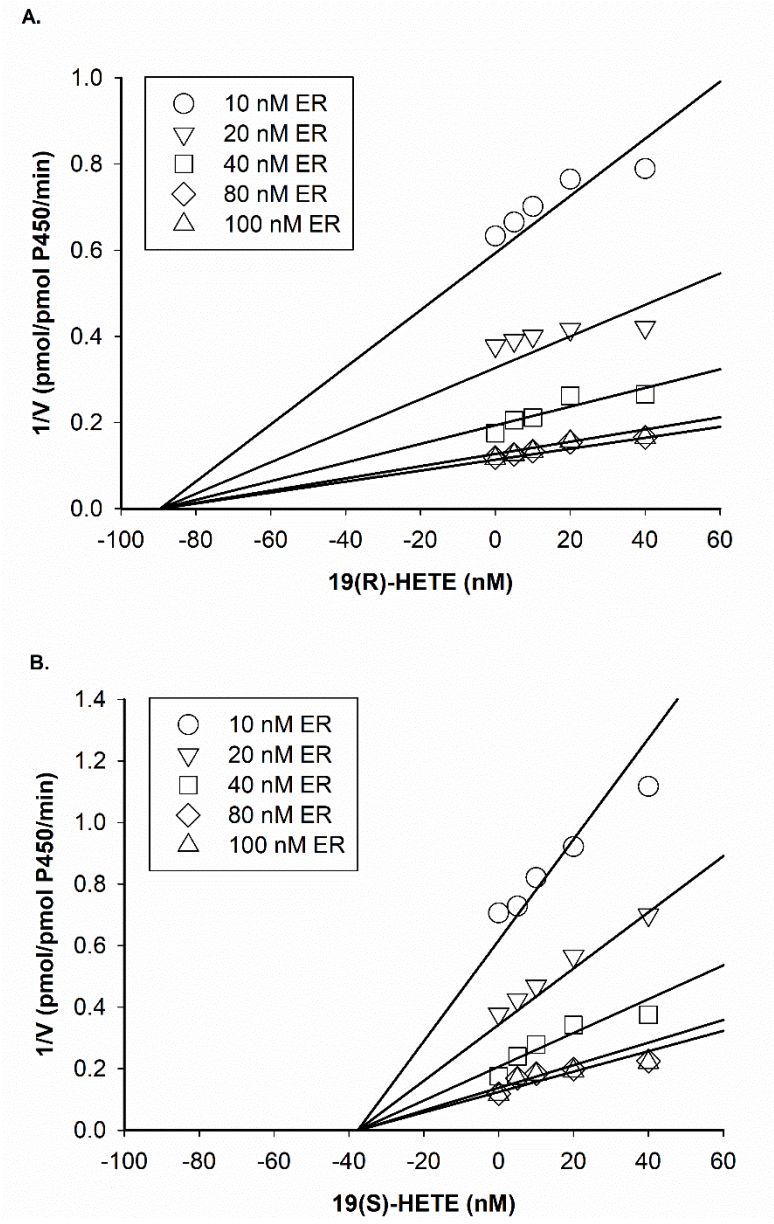

Figure 3.11. Dixon plots representing the inhibitory effect of 19(R)-HETE and 19(S)-HETE on EROD activity mediated by human recombinant CYP1B1

The Y-axis represents the reciprocal of EROD activity expressed in picomoles of resorufin/ pmol CYP1B1/min while the X-axis represents 19(R)-HETE (A) or 19(S)-HETE (B) concentrations in nM in the presence of increasing concentration of the substrate 7-ER (10-100 nM). Each point represents the mean of 6 independent experiments ± SE.

3.2.3 Determination of 19(R)-HETE and 19(S)-HETE in-vitro stability

In order to assess the stability of 19-HETE enantiomers in solution under the same experimental conditions of the kinetic study, the stability experiment has been carried out. In accordance with being noncompetitive inhibitors, the *in vitro* stability study showed that both enantiomers of 19-HETE are metabolically stable in solution during the 30 min time course of the kinetic experiment as there was no significant difference in the level of both enantiomers during the duration of the experiment (Table 3.2, Figures 3.12 & 3.13).

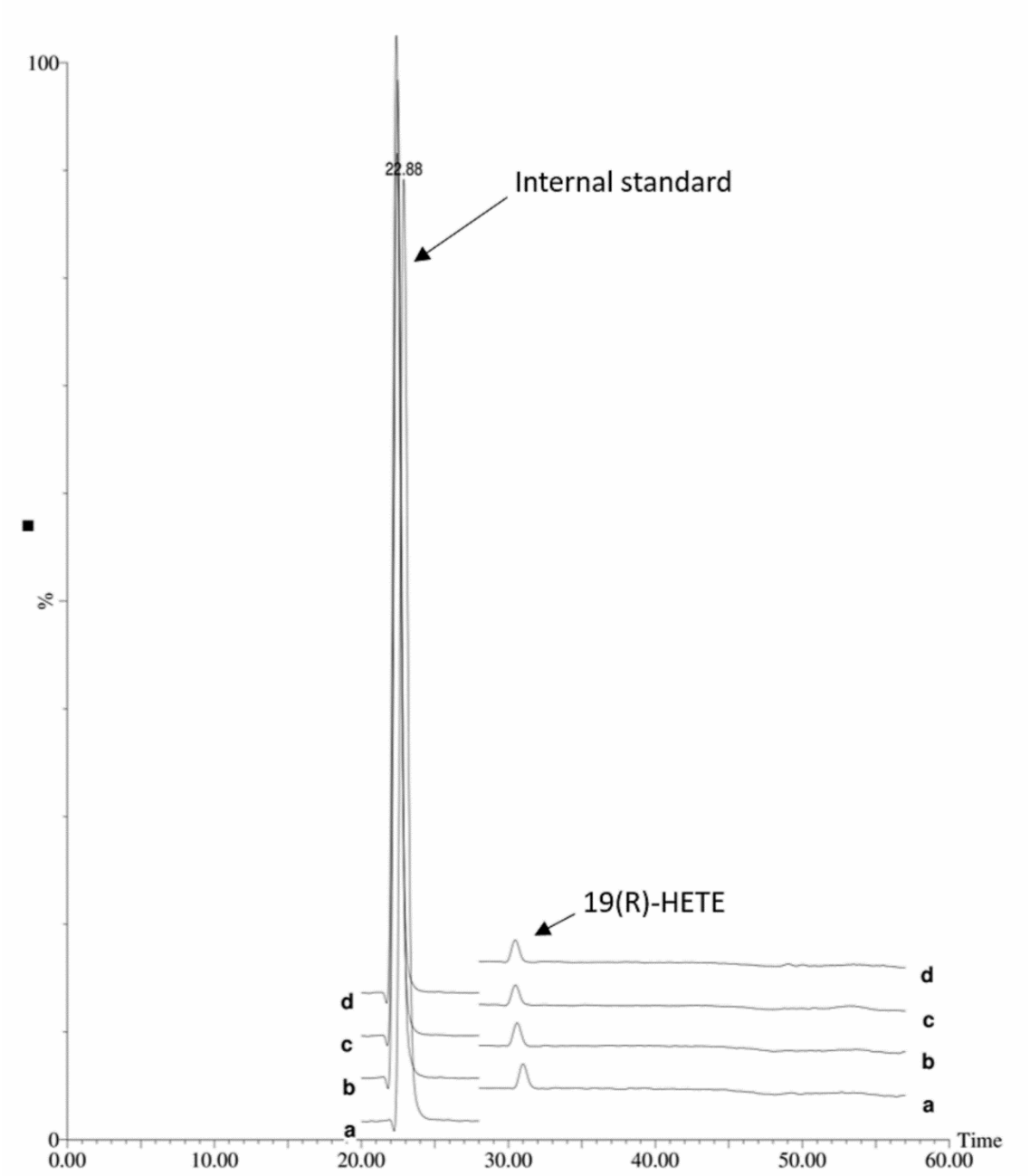

Figure 3. 12. Representative LC-MS chromatograms showing the peaks of 19(R)-HETE and internal standard at the start of the experiment (a), after 10 min (b), 20 min (c) and 30 min (d).

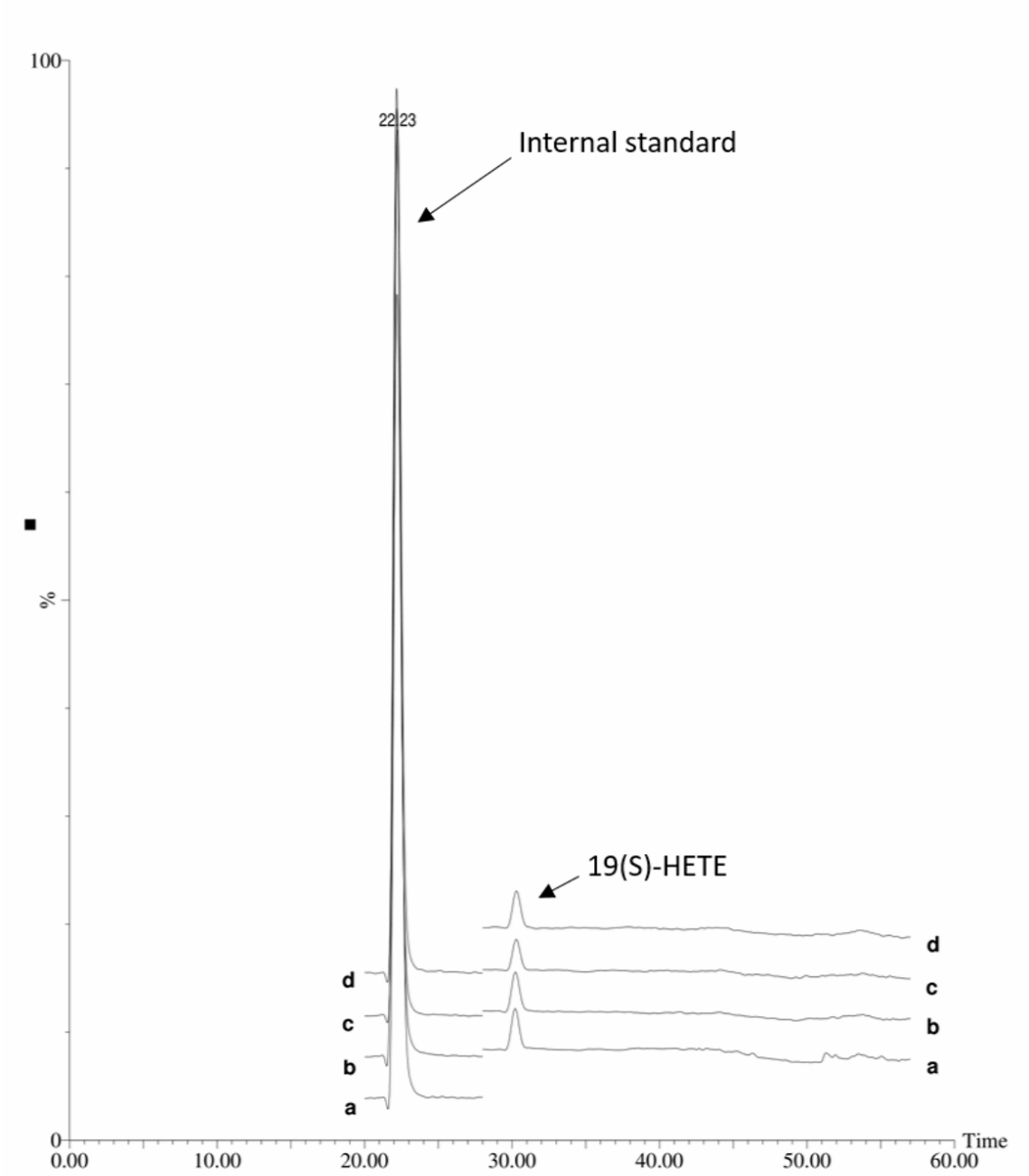

Figure 3. 13. Representative LC-MS chromatograms showing the peaks of 19(R)-HETE and internal standard at the start of the experiment (a), after 10 min (b), 20 min (c) and 30 min (d).

Table 3.2. Determination of 19(R)-HETE and 19(S)-HETE in-vitro stability

The mean values and standard error of 19(R)-HETE or 19(S)-HETE levels calculated as a percentage of the metabolite level at the beginning of the experiment (T_0). Data are represented as mean ± SE where n=3.

	19(R/S)-HETE levels as a percentage of their levels at zero time (%)			
Time Interval (T_{min})	T_0	T_{10}	T_{20}	T_{30}
19(R)-HETE	100 ± 17.1	98.6 ± 7.8	96.3 ± 1.3	98.5 ± 8.9
19(S)-HETE	100 ± 5.9	99.7 ± 1.3	100.1 ± 0.9	98.9 ± 4.6

3.3 Novel Synthetic Analogues of 19(S/R)-Hydroxyeicosatetraenoic Acid Exhibit Noncompetitive Inhibitory Effect on the Activity of Cytochrome P450 1A1 and 1B1

3.3.1 Inhibitory effect of 19(R)-HETE and 19(S)-HETE synthetic analogues on EROD activity mediated by human recombinant CYP1A1

Inhibitory activity of the novel synthetic analogues of 19(R)-HETE and 19(S)-HETE on CYP1A1 (Figure 3.14A and 3.14C) was studied. Initial experiments included the assessment of 7-ER-O-deethylase kinetics by measurement of the rate of fluorescent resorufin formation over time. The reaction mixture containing human recombinant CYP1A1 was incubated with 10-200 nM of 7-ER. In addition, 0, 5, 10, 20, or 40 nM of either the 19(R)-HETE analogue or the 19(S)-HETE analogue was added to the reaction. The reaction was initiated by the addition of 100 µL of 2 mM NADPH. Nonlinear regression analysis and fitting to simple or sigmoid Michaelis-Menten model were applied, the most probable mode of binding is the sigmoid type. The results showed that the maximal EROD activity (V_{max}) for CYP1A1 in the control containing 0.1% DMSO was 58.9 pmol resorufin/pmol P450/min. The value of Michaelis-Menten constant (K_m) for the EROD reaction is 47.6 nM (Table 3.3). Dixon plots demonstrated that the novel analogues of 19(R)-HETE (Figure 3.14B) and 19(S)-HETE (Figure 3.14D) have Ki values of 15.7 and 6.1 nM, respectively, with CYP1A1 (Table 3.3).

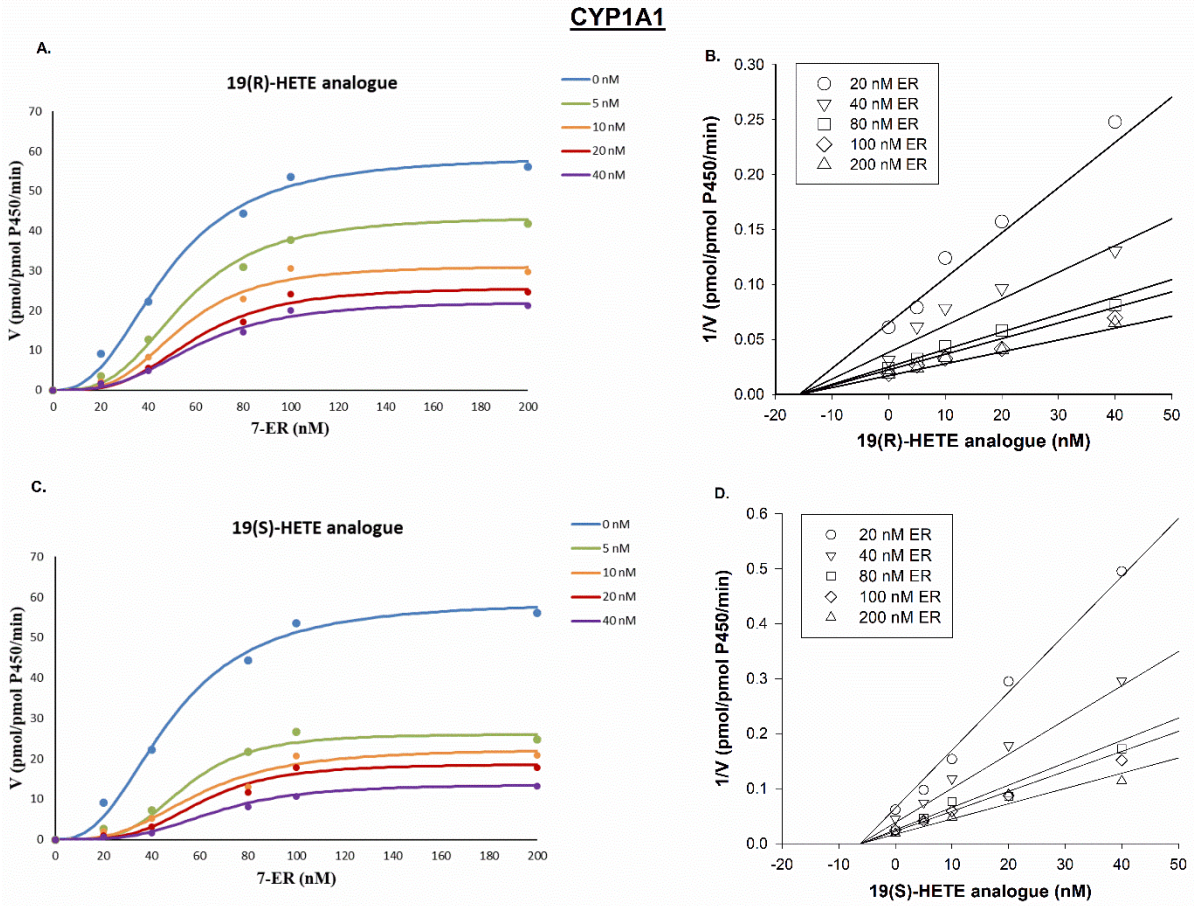

Figure 3.14. Inhibitory effect of 19(R)-HETE and 19(S)-HETE synthetic analogues on EROD activity mediated by human recombinant CYP1A1

In 96-well solid black polystyrene plates, the reaction mixture containing buffer and 1 pmol of human CYP1A1 was incubated with 10-200 nM of 7-ER. In addition, 0, 5, 10, 20, or 40 nM of either 19(R)-HETE analogue **(A)** or 19(S)-HETE analogue **(C)** was added to the reaction. The reaction was initiated by the addition of 100 µL of 2 mM NADPH, the fluorescent signal related to the formation of resorufin was measured. Figures **2B** and **2D** represent the Dixon plots of the inhibitory effect of 19(R)-HETE and 19(S)-HETE synthetic analogues on the EROD activity. The Y-axis represents the reciprocal of EROD activity expressed in picomoles of resorufin/ pmol CYP1A1/min while the X-axis represents 19(R)-HETE analogue **(B)** or 19(S)-HETE analogue **(D)** concentrations in nM. Each point represents the mean of 3 independent experiments ± SEM.

Table 3.3. The kinetic parameters of resorufin formation by human recombinant CYP1A1, CYP1A2 and CYP1B1.The mean values and standard deviation (SD) of kinetic parameters of resorufin formation by human recombinant CYP1A1, CYP1A2 and CYP1B1, in the absence and presence of 19(R)-HETE or 19(S)-HETE synthetic analogues.

Results are presented as mean and SD, based on at least 3 individual experiments. K_m, Vmax and Ki mean ± SD were determined by Enzyme Kinetics module from GraphPad Prism, version 5.01 and Microsoft Excel Solver.

CYP1A1			
Ki (nM)		**19(R)-HETE analogue**	**19(S)-HETE analogue**
		15.7 ± 4.4	6.1 ± 1.5
	Kinetics of resorufin formation		
Synthetic analogue concentration	**Vmax (pmol/pmol P450/min)**	**K_m (nM)**	**Hill coefficient (n)**
No inhibitor	58.9 ± 7.2	47.6 ± 5.3	2.57
5 nM 19(R)-HETE analogue	43.6 ± 5.4	55 ± 6.1	3.14
10 nM 19(R)-HETE analogue	31.1 ± 3.8	53 ± 7.2	3.41
20 nM 19(R)-HETE analogue	25.8 ± 3.2	59.7 ± 6.7	3.34
40 nM 19(R)-HETE analogue	22.3 ± 2.4	60.1 ± 5.2	3

5 nM 19(S)-HETE analogue	26.1 ± 3.5	54 ± 3.9	3.94
10 nM 19(S)-HETE analogue	22.4 ± 3.3	59.3 ± 7.5	3.03
20 nM 19(S)-HETE analogue	18.6 ± 1.6	60.6 ± 8.6	3.8
40 nM 19(S)-HETE analogue	13.6 ± 1.2	66.1 ± 5.8	3.53
CYP1A2			
Ki (nM)		**19(R)-HETE analogue**	**19(S)-HETE analogue**
		-	-
	Kinetics of resorufin formation		
Synthetic analogue concentration	**Vmax (pmol/pmol P450/min)**	**K_m (nM)**	**Hill coefficient (n)**
No inhibitor	7.1 ± 1.1	47.8 ± 5.2	2.19
5 nM 19(R)-HETE analogue	6.9 ± 0.8	49.3 ± 5.6	2.04
10 nM 19(R)-HETE analogue	6.9 ± 0.9	49.6 ± 6.3	2.09
20 nM 19(R)-HETE analogue	7 ± 1.2	48.2 ± 5.7	2.03
40 nM 19(R)-HETE analogue	7 ± 0.9	49.5 ± 5.2	2.2
5 nM 19(S)-HETE analogue	6.9 ± 1.3	45.4 ± 4.9	1.89
10 nM 19(S)-HETE analogue	6.8 ± 0.7	45.4 ± 6.1	1.89

20 nM 19(S)-HETE analogue	6.8 ± 1.6	40.4 ± 4.8	2
40 nM 19(S)-HETE analogue	6.8 ± 1.2	40.5 ± 5.8	2.05
CYP1B1			
Ki (nM)		**19(R)-HETE analogue**	**19(S)-HETE analogue**
		26.1 ± 2.9	9.1 ± 1.8
	Kinetics of resorufin formation		
Synthetic analogue concentration	**Vmax (pmol/pmol P450/min)**	**K_m (nM)**	**Hill coefficient (n)**
No inhibitor	10.1 ± 1.2	32.6 ± 4.8	1.38
5 nM 19(R)-HETE analogue	8.6 ± 0.9	33 ± 4.2	1.27
10 nM 19(R)-HETE analogue	5.8 ± 0.7	25.5 ± 3.4	1.58
20 nM 19(R)-HETE analogue	5.6 ± 0.7	28.1 ± 3.1	1.25
40 nM 19(R)-HETE analogue	4.1 ± 0.6	34.1 ± 4.5	1.3
5 nM 19(S)-HETE analogue	4.8 ± 0.5	28.6 ± 3.4	1.14
10 nM 19(S)-HETE analogue	4.1 ± 0.5	27.7 ± 3.1	1.13
20 nM 19(S)-HETE analogue	3.3 ± 0.3	25.4 ± 4.7	1.23
40 nM 19(S)-HETE analogue	2.4 ± 0.3	27.1 ± 3.4	1.43

3.3.2 Inhibitory effect of 19(R)-HETE and 19(S)-HETE synthetic analogues on MROD activity mediated by human recombinant CYP1A2

The potential inhibitory effect of the synthetic analogs of 19(R)-HETE and 19(S)-HETE on CYP1A2 has been evaluated using the MROD assay. The MROD assay was selected based on previous studies that have extensively used this assay to determine the activity of CYP1A2 enzyme (Kim and Guengerich, 2004). Primary measurements included the determination of 7-MR-O-demethylase kinetics by assessment of the rate of the formation of fluorescent resorufin over time. Data were analyzed through nonlinear regression analysis and fitting to simple or sigmoid Michaelis-Menten model, the most probable mode of binding is the sigmoid type. The results demonstrated that the maximal MROD activity (V_{max}) for CYP1A2 in the control containing 0.1% DMSO was 7.1 pmol resorufin/pmol P450/min. The value of K_m for the MROD reaction is 47.8 nM (Table 3.3). Similar to CYP1A1 and CYP1B1, increasing concentrations (0-40 nM) of either 19-HETE synthetic analogues were co-incubated with varying concentrations of 7-MR. Notably, there was no significant inhibitory effect of both analogues on the CYP1A2 enzymatic activity (Figure 3.15A and 3.15B).

A.

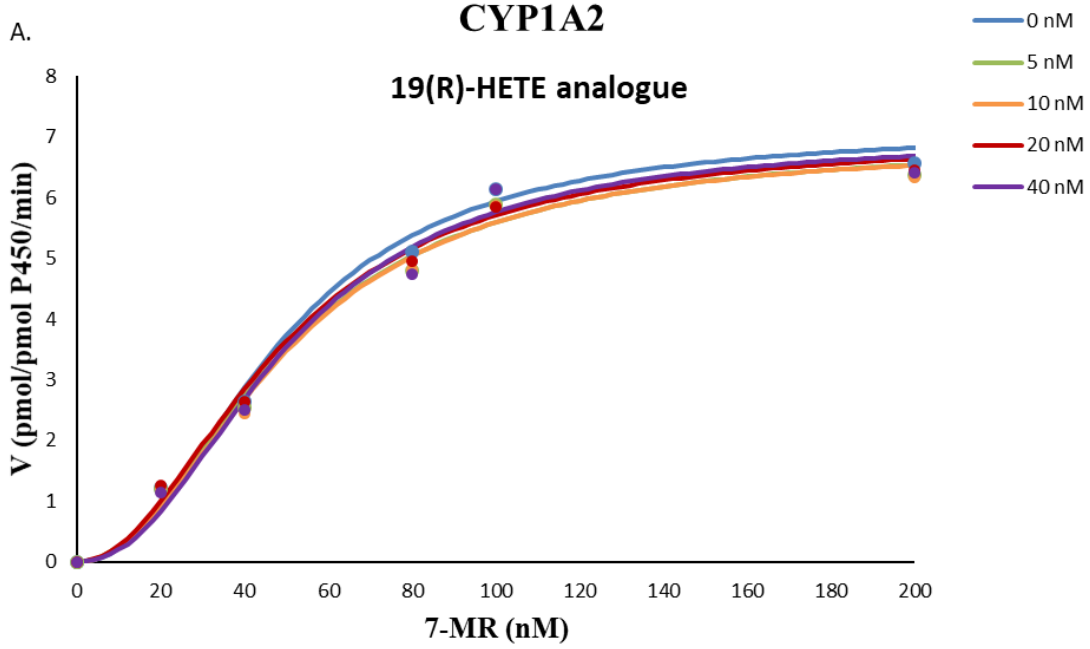
CYP1A2
19(R)-HETE analogue
V (pmol/pmol P450/min)
7-MR (nM)
0 nM
5 nM
10 nM
20 nM
40 nM

B.

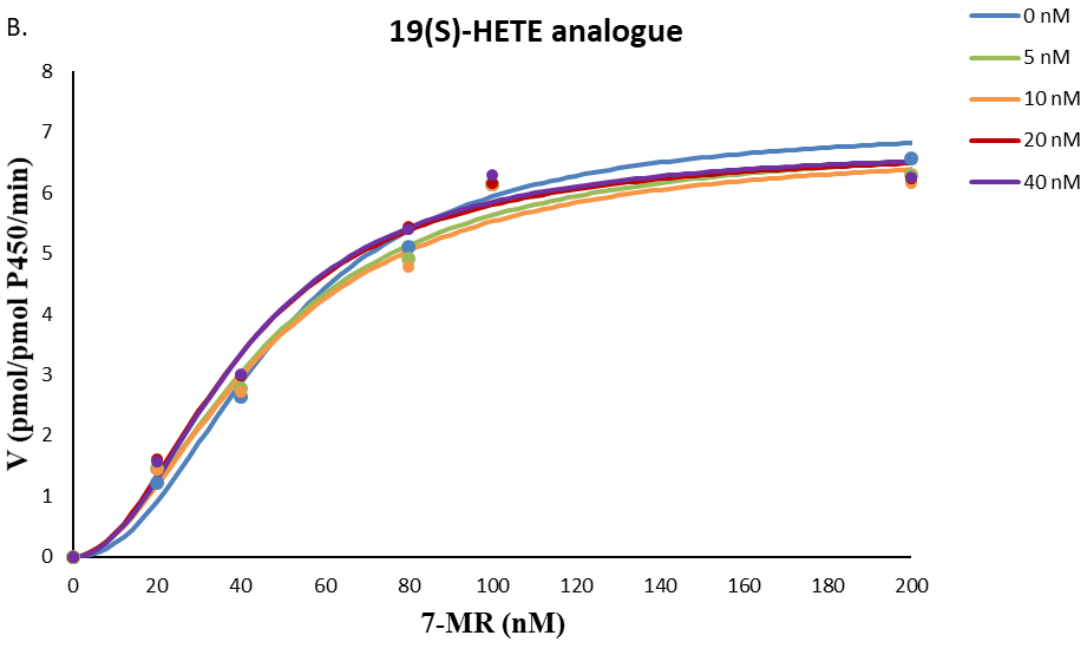
19(S)-HETE analogue
V (pmol/pmol P450/min)
7-MR (nM)
0 nM
5 nM
10 nM
20 nM
40 nM

Figure 3.15. Inhibitory effect of 19(R)-HETE and 19(S)-HETE synthetic analogues on MROD activity mediated by human recombinant CYP1A2

In 96-well solid black polystyrene plates, the reaction mixture containing 100 mM potassium phosphate (pH 7.4) buffer supplemented with 5 mM magnesium chloride hexahydrate and 1 pmol of human CYP1A2, was incubated with 10-200 nM of 7-MR. In addition, 0, 5, 10, 20, or 40 nM of either 19(R)-HETE analogue **(A)** or 19(S)-HETE analogue **(B)** was added to the reaction. The reaction was initiated by the addition of 100 µL of 2 mM NADPH, the fluorescent signal related to the formation of resorufin was measured using a BioTek Synergy H1 Hybrid Reader (BioTek Instruments, Inc.). Each point represents the mean of 3 independent experiments ± SEM.

3.3.3 Inhibitory effect of 19(R)-HETE and 19(S)-HETE synthetic analogues on EROD activity mediated by human recombinant CYP1B1

Inhibitory activity of both synthetic analogues of 19(R)-HETE and 19(S)-HETE on CYP1B1 (Figure 3.16A and 3.16C) was assessed. Initial experiments included the assessment of 7-ER-O-deethylase kinetics by measurement of the rate of fluorescent resorufin formation over time. The reaction mixture containing human recombinant CYP1B1 was incubated with 10-100 nM of 7-ER. Additionally, 0, 5, 10, 20, or 40 nM of either 19(R)-HETE analogue or 19(S)-HETE analogue was added to the reaction. The reaction was initiated by the addition of 100 µL of 2 mM NADPH. Nonlinear regression analysis and fitting to simple or sigmoid Michaelis-Menten model were applied, the most probable mode of binding is the sigmoid type. The results showed that the maximal EROD activity (V_{max}) for CYP1B1 in the control containing 0.1% DMSO was 10.1 pmol resorufin/pmol P450/min. The value of Michaelis-Menten constant (K_m) for the EROD reaction is 32.6 nM (Table 3.3). Dixon plots showed that the synthetic analogues of 19(R)-HETE (Figure 3.16B) and 19(S)-HETE (Figure 3.16D) have Ki values of 26.1 and 9.1 nM, respectively, (Table 3.3).

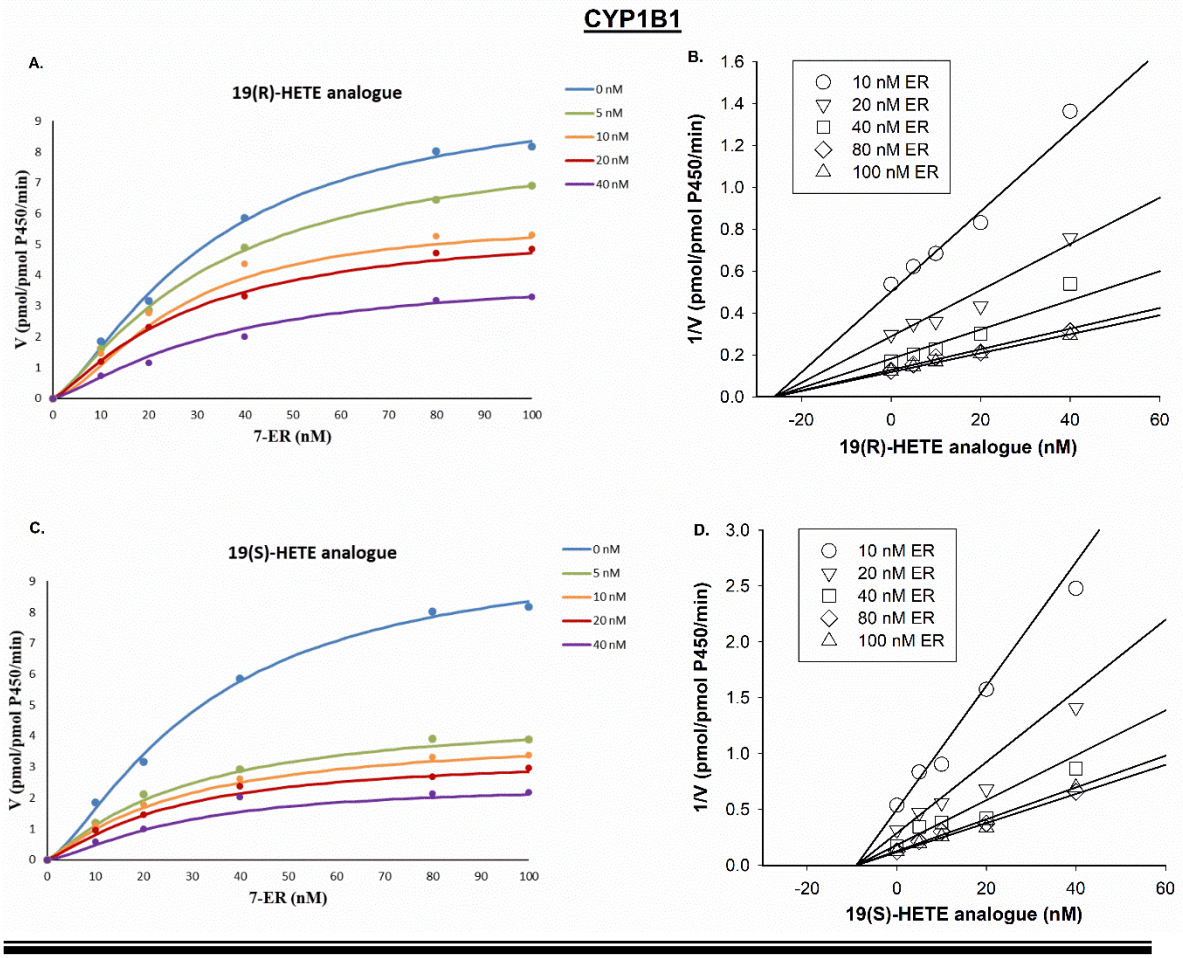

Figure 3.16. Inhibitory effect of 19(R)-HETE and 19(S)-HETE synthetic analogues on EROD activity mediated by human recombinant CYP1B1

In 96-well solid black polystyrene plates, the reaction mixture containing buffer and 1 pmol of human CYP1B1 was incubated with 10-100 nM of 7-ER. In addition, 0, 5, 10, 20, or 40 nM of either 19(R)-HETE analogue **(A)** or 19(S)-HETE analogue **(C)** was added to the reaction. The reaction was initiated by the addition of 100 µL of 2 mM NADPH, the fluorescent signal related to the formation of resorufin was measured. Figures **2B** and **2D** represent the Dixon plots of the inhibitory effect of 19(R)-HETE and 19(S)-HETE synthetic analogues on the EROD activity. The Y-axis represents the reciprocal of EROD activity expressed in picomoles of resorufin/ pmol CYP1B1/min while the X-axis represents 19(R)-HETE analogue **(B)** or 19(S)-HETE analogue **(D)** concentrations in nM. Each point represents the mean of 3 independent experiments ± SEM.

3.3.4 Inhibitory effect of 19(R)-HETE and 19(S)-HETE synthetic analogues on EROD and MROD activity in RL-14 cells

To examine the inhibitory effect of both analogues on the catalytic activity of CYP1A1 and CYP1B1 in a cell-based assay, EROD and MROD were performed in RL-14 cells. Cells were seeded in 24-well plates and synthetic analogues (100 nM) and 7-ER (2 μM) or 7-MR (5 μM) in serum free medium were added. Figure 3.17A and 3.17B show that synthetic analogues of 19(R)-HETE and 19(S)-HETE significantly inhibited the formation of resorufin in both assays, compared to the control group. 19(R)-HETE and 19(S)-HETE synthetic analogues inhibited EROD by approximately 69% and 84%, respectively. In addition, they inhibited MROD by approximately 68% and 75%, respectively.

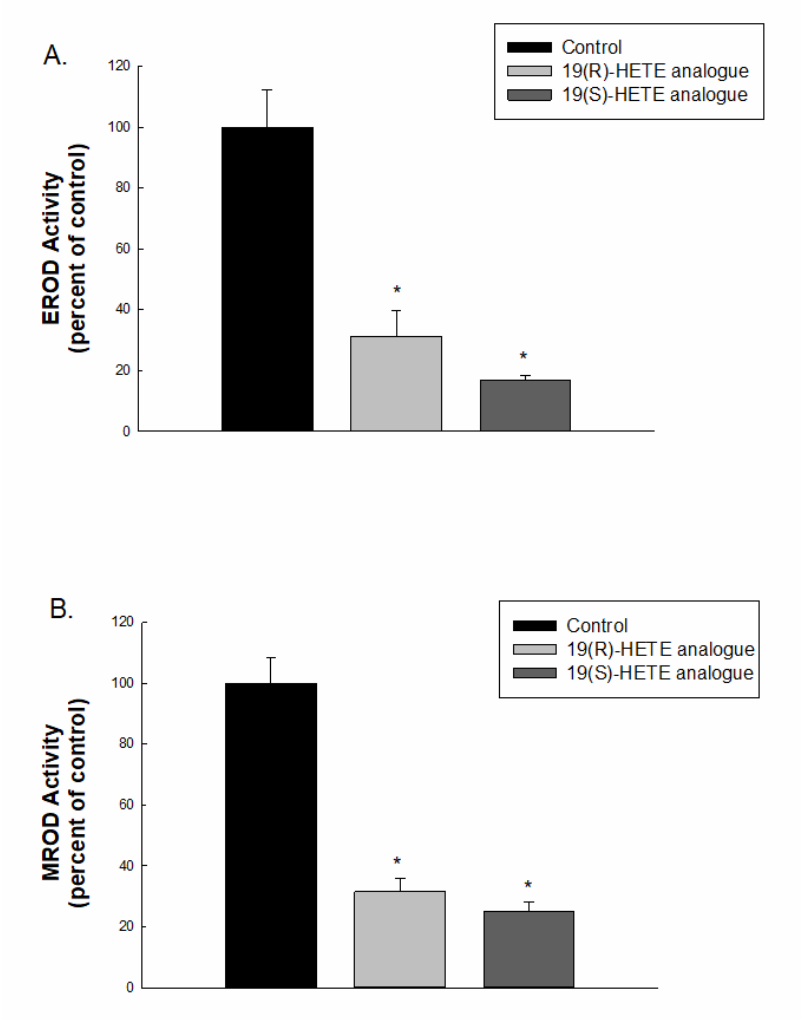

Figure 3.17. Inhibitory effect of 19(R)-HETE and 19(S)-HETE synthetic analogues on EROD and MROD activity in RL-14 cells

RL-14 cells were seeded in 24-well plates and synthetic analogues (100 nM) and 7-ER (2 μM) or 7-MR methoxyresorufin (5 μM) in serum free medium were added. Fluorescence of the samples was recorded every 5 min interval for 40 min using the Bio-Tek Synergy H1 Hybrid Multi-Mode Microplate Readers. The results are presented as the means of three independent experiment ± SEM. *$p < 0.05$ compared to the control group.

3.3.5 Inhibitory effect of 19(R)-HETE and 19(S)-HETE synthetic analogues on EROD and MROD activity in human liver microsomes

To further confirm the results obtained from the recombinant enzymes and cells, we have tested the possible inhibitory effect of both analogues on the catalytic activity of EROD and MROD, using human liver microsomes. Fixed concentration of the substrate was used in each assay with varying concentrations of either 19(R)-HETE or 19(S)-HETE synthetic analogues (0, 20, 40, 80, or 100 nM). The results show that synthetic analogues of 19(R)-HETE and 19(S)-HETE significantly inhibited the formation of resorufin in both assays, compared to the control group. 19(R)-HETE and 19(S)-HETE synthetic analogues have IC_{50} values of 213.1 and 78 nM, respectively, for EROD assay (Figure 3.18A). Additionally, they possess IC_{50} values of 211.8 and 145.2 nM, respectively, for MROD assay (Figure 3.18B).

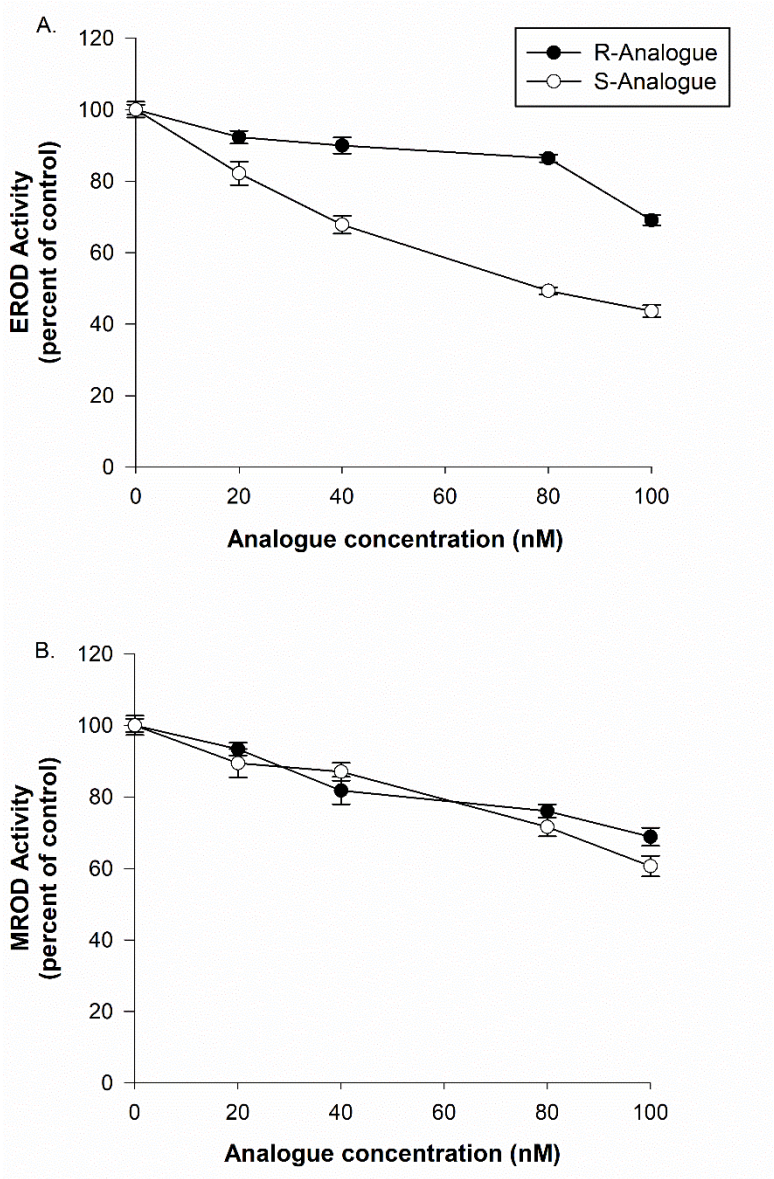

Figure 3.18. Inhibitory effect of 19(R)-HETE and 19(S)-HETE synthetic analogues on EROD and MROD activity in human liver microsomes

Human liver microsomes were used in a concentration of 0.2mg/ml, in the absence and presence of varying concentrations of 19(R)-HETE or 19(S)-HETE synthetic analogues (X axis). In addition, 2 µM of 7-ER for EROD assay or 5 µM of 7-MR for MROD assay were used as substrates. The reaction was initiated by the addition of 100 µL of 2 mM NADPH, the fluorescent signal related to the formation of resorufin was measured. The results are presented as the means of three independent experiment ± SEM.

3.3.6 Inhibitory effect of 19(R)-HETE and 19(S)-HETE synthetic analogues on CYP3A4 activity using human recombinant CYP3A4 enzyme

To further investigate the possible inhibitory effect of both synthetic analogues of 19(R)-HETE and 19(S)-HETE on other important CYP enzymes, we assessed their inhibitory effect on CYP3A4 using human recombinant CYP3A4 enzyme. The final concentration of the analogues for each group was 0, 5, 10, 20 or 40 nM using a fixed concentration of the substrate. The results demonstrated that the CYP3A4 activity in the control group (containing 0 nM of the analogues) was 4.05 and 4.07 pmol D-luciferin/pmol CYP/min for R- and S-analogue, respectively. Notably, there was no significant inhibitory effect of both synthetic analogues of 19-HETE on the CYP3A4 enzymatic activity (Figure 3.19A and 3.19B).

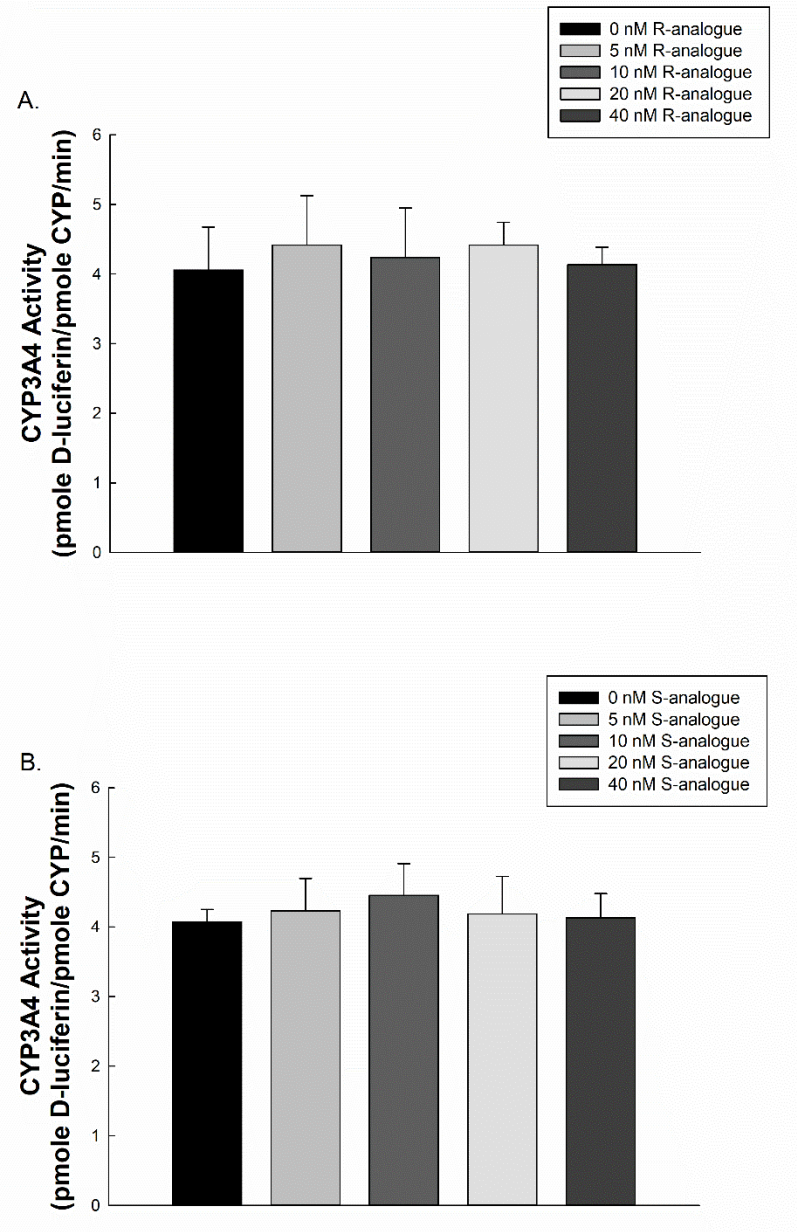

Figure 3.19. Inhibitory effect of 19(R)-HETE and 19(S)-HETE synthetic analogues on CYP3A4 activity using recombinant human enzyme

Purified human recombinant CYP3A4 was used (0.1 pmole/reaction), in the absence and presence of varying concentrations of 19(R)-HETE (A) or 19(S)-HETE (B) synthetic analogues. The reaction was initiated by the addition of 25µL of 200 µM NADPH, the luminscent signal related to the formation of D-luciferin was measured. The results are presented as the means of three independent experiment ± SEM.

3.4 Resveratrol Attenuates Angiotensin II-Induced Cellular Hypertrophy through the Inhibition of CYP1B1 and the Cardiotoxic Mid-Chain HETE Metabolites

3.4.1 Effect of resveratrol on cell viability in RL-14 and H9c2 cells

MTT assay was used to assess the effect of different concentrations of resveratrol on cell viability. RL-14 and H9c2 cells were grown to 80-90% confluency in 96-well culture plates and treated for 24 h with increasing concentrations of resveratrol (0, 1, 10, 25, 50 or 100 μM). Cells in the control group was treated with SFM without resveratrol. After incubation of cells with MTT for 3 h, MTT is reduced by viable cells to produce formazan dye which is then solubilized using isopropyl alcohol. Data in figure 3.20A and B showed that resveratrol, at all concentrations used, did not significantly alter the cell viability of both cell lines (measured cell viability was more than 90%). Therefore, 2, 10 and 50 μM resveratrol concentrations were selected to perform all consequent experiments in the current study based on MTT assay results.

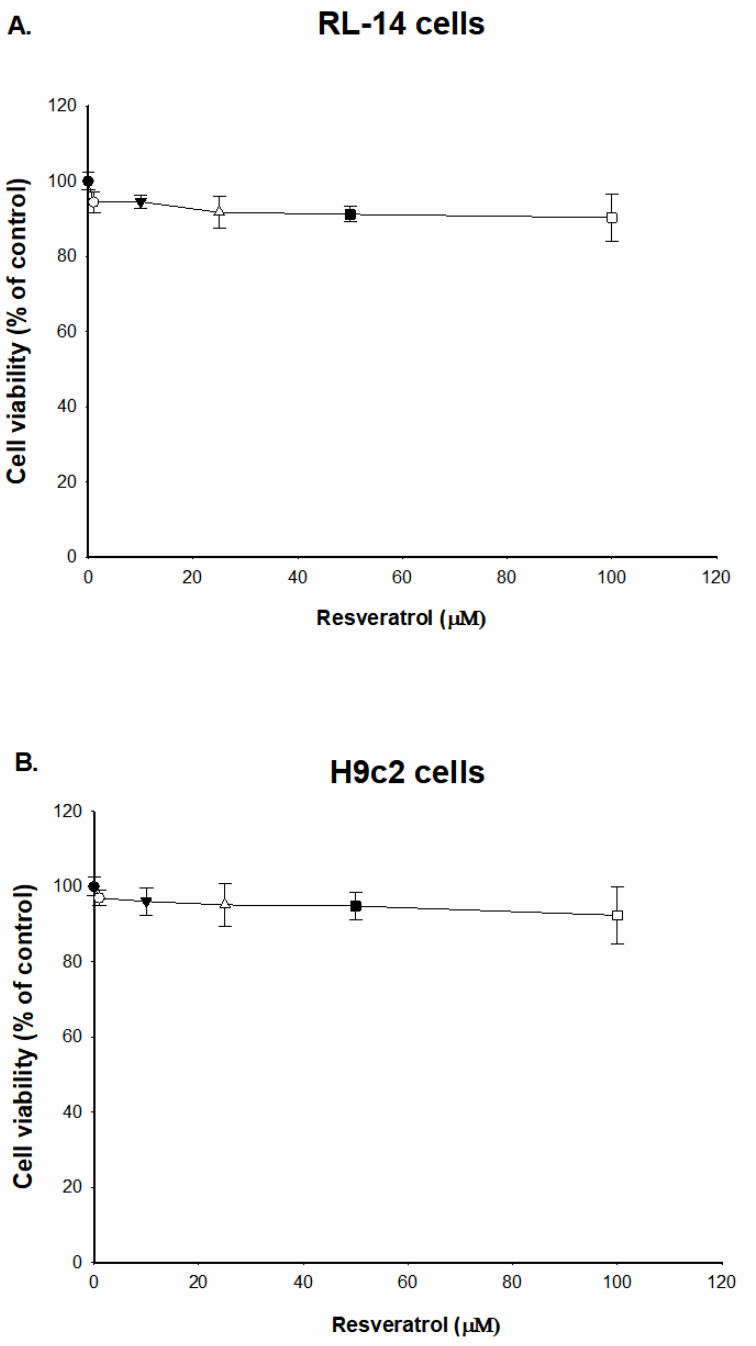

Figure 3.20. Effect of resveratrol on cell viability in RL-14 and H9c2 cells

RL-14 (A) and H9c2 (B) cells were treated for 24 h with 1-100 µM of resveratrol. Cell cytotoxicity was assessed using the MTT assay. Data are presented as the percentage of control (set at 100%) ± SEM (n =4). Data were analyzed using one-way ANOVA followed by Student–Newman–Keuls as post hoc test.

3.4.2 Effect of resveratrol on Ang II-induced cellular hypertrophy in RL-14 and H9c2 cells

To examine the potential protective effect of resveratrol against the development of cellular hypertrophy, RL-14 and H9c2 cells were treated with vehicle, 10 μM Ang II, 10 μM Ang II in combination with resveratrol (2, 10 or 50 μM) or resveratrol alone (2, 10 or 50 μM) in SFM. The results showed that incubation of cells with 10 μM Ang II for 24 h resulted in cellular hypertrophy as demonstrated by significant increase in β/α-MHC ratio and ANP by approximately 123% and 78%, respectively in RL-14 cells, compared to the control group (Figure 3.21A). Also, in H9c2 cells, Ang II caused significant elevation of β/α-MHC ratio and ANP by approximately 226% and 270%, respectively, compared to the control group (Figure 3.21B). While low concentration of resveratrol (2 μM) was not able to revert Ang II- induced effects, co-treatment with higher concentration of 10 and 50 μM was able to significantly protect against Ang II-mediated elevation of β/α-MHC ratio and ANP to approximately control levels in both cell lines. Notably, treatment of cells with low and high concentrations of resveratrol alone did not have any significant effects on hypertrophic markers. These results indicate that resveratrol protects against Ang II-induced cellular hypertrophy as evidenced by a reduction in hypertrophic markers and prompted us to further investigate the effects of resveratrol on CYP1B1 and its cardiotoxic mid-chain HETE metabolites.

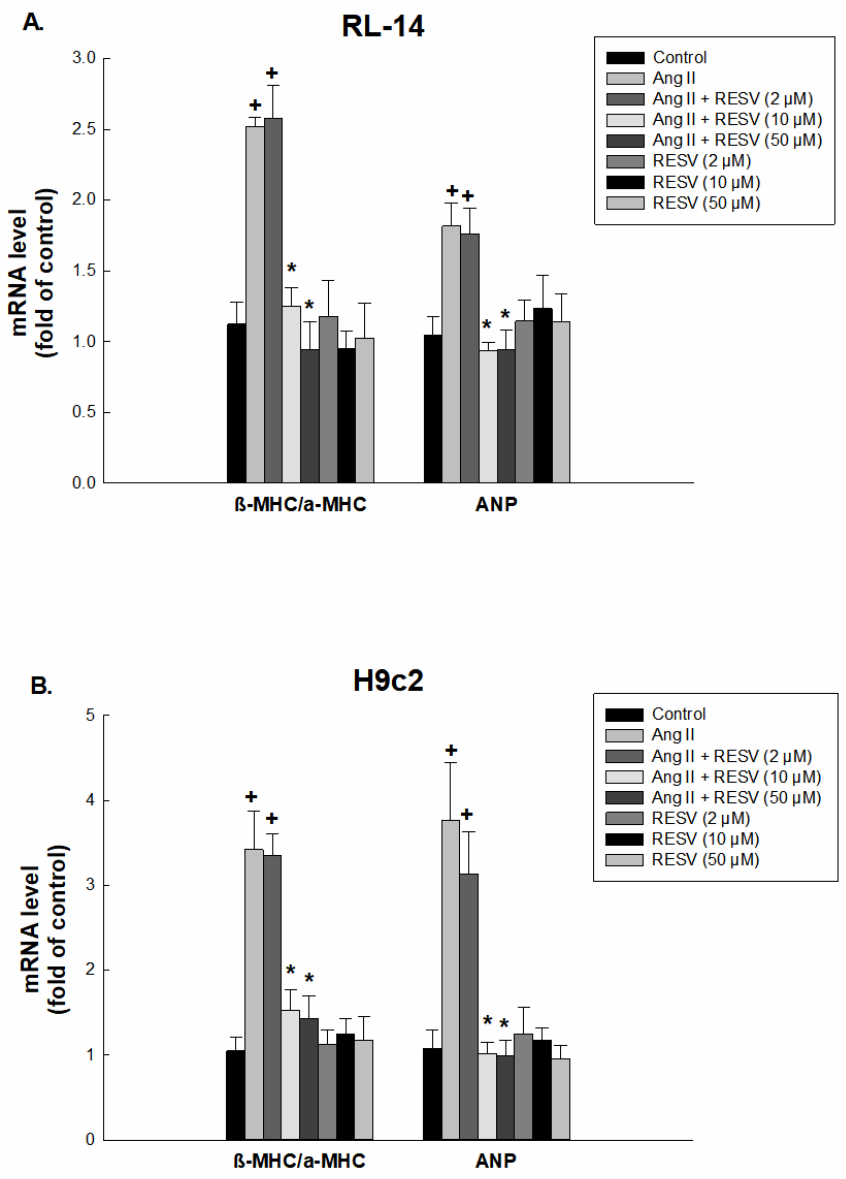

Figure 3.21 Effect of resveratrol on Ang II-mediated induction of hypertrophic markers in RL-14 and H9c2 cells

RL-14 (A) and H9c2 (B) cells were treated for 24 h with vehicle, 10 µM Ang II, 10 µM Ang II in combination with (2, 10 or 50 µM resveratrol) or (2, 10 or 50 µM resveratrol alone) in SFM. The results are presented as the mean and SEM based on at least 3 individual experiments. Data were analyzed using one-way ANOVA followed by Student–Newman–Keuls as post hoc test. +$p < 0.05$ significantly different from the control group. *$p < 0.05$ significantly different from Ang II-treated group.

3.4.3 Effect of resveratrol on the mRNA and protein expression of CYP1B1 in RL-14 and H9c2 cells

We investigated the effect of low and high concentrations of resveratrol on mRNA and protein expression levels of CYP1B1 in RL-14 and H9c2 cells and the results showed that while Ang II (10 μM) had no significant effect on CYP1B1 mRNA level in comparison to the control group in both cell lines, co-treatment with Ang II and resveratrol (2, 10 or 50 μM) or resveratrol alone (2, 10 or 50 μM) significantly decreased the transcription level of CYP1B1, compared to Ang II group, in both cell lines (Figures 3.22A and 3.23A). In RL-14 cells, resveratrol (2, 10 or 50 μM) in combination with Ang II decreased CYP1B1 mRNA expression by approximately 40%, 81% or 89%, respectively, While 2, 10 or 50 μM of resveratrol alone significantly decreased the expression of CYP1B1 by approximately 60%, 80% or 86%, respectively. In H9c2 cells, resveratrol (2, 10 or 50 μM) in combination with Ang II decreased CYP1B1 mRNA expression by approximately 35%, 74% or 88%, respectively. Whereas, 2, 10 or 50 μM resveratrol alone significantly decreased the expression by approximately 64%, 88% or 89%, respectively.

We examined whether different concentrations of resveratrol have a protective effect against Ang II-induced cellular hypertrophy through inhibiting the protein expression of CYP1B1. For this reason, Western blot analysis was performed and the results showed that the protein expression of CYP1B1 was significantly increased by Ang II treatment in comparison to the control group in RL-14 and H9c2 cells, by approximately 570% and 430%, respectively (Figures 3.22B and 3.23B). In RL-14 cells, low and high

concentrations of resveratrol (2, 10 or 50 μM) in combination with Ang II significantly decreased CYP1B1 protein expression by approximately 19%, 28% or 58%, respectively, compared to Ang II group. Interestingly, 2, 10 or 50 μM resveratrol alone significantly induced CYP1B1 protein expression by approximately 2.6, 2.6 or 2 folds, respectively. In H9c2 cells, low concentration of resveratrol (2 μM) did not significantly alter CYP1B1 protein level compared to Ang II group. However, high concentrations of resveratrol (10 or 50 μM) in combination with Ang II significantly decreased CYP1B1 protein expression by approximately 31% or 33%, respectively, compared to Ang II group. Intriguingly, 2, 10 or 50 μM resveratrol alone significantly increased CYP1B1 protein expression by approximately 1.7, 1.6 or 2 folds, respectively.

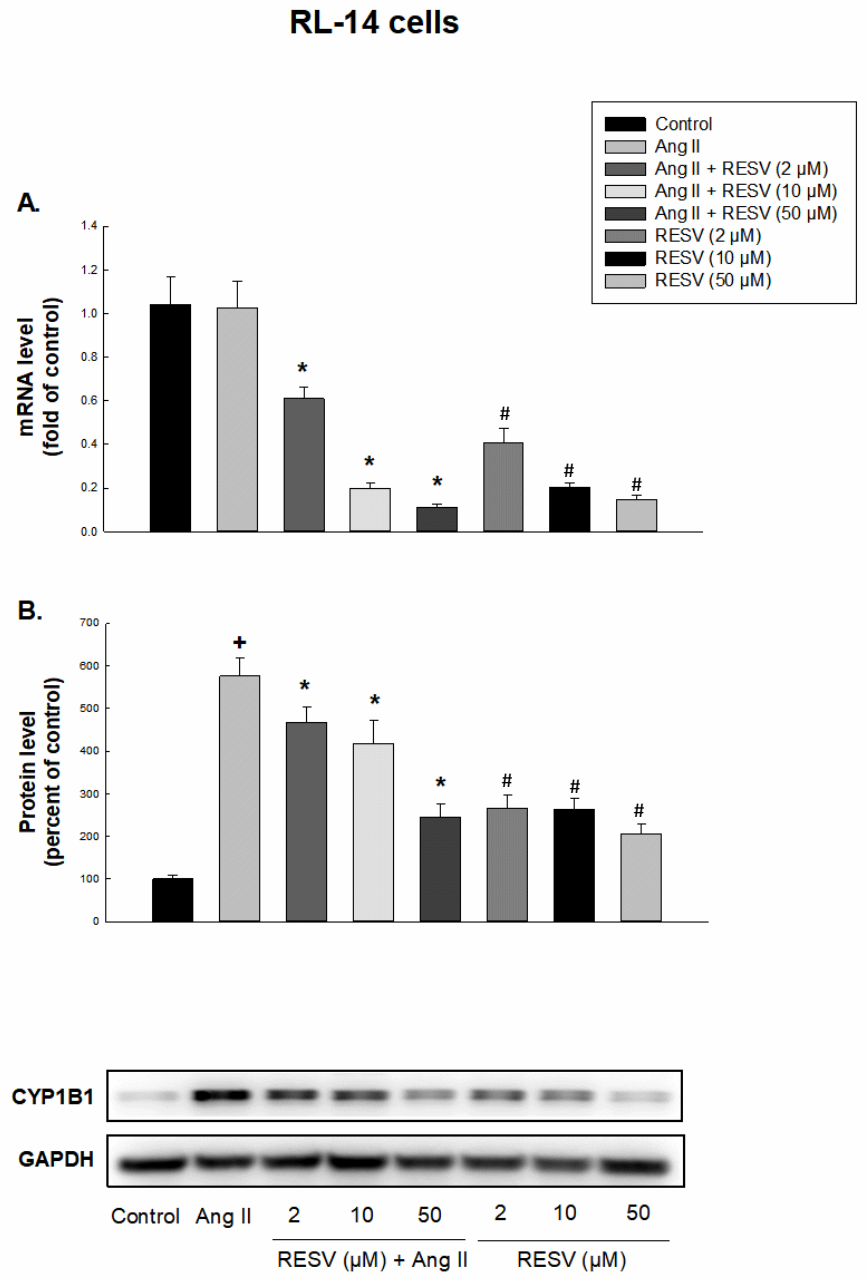

Figure 3.22. Effect of resveratrol on mRNA expression and protein expression levels of CYP1B1 in RL-14 cells

RL-14 cells were treated for 24 h with vehicle, 10 μM Ang II, 10 μM Ang II in combination with (2, 10 or 50 μM resveratrol) or (2, 10 or 50 μM resveratrol alone) in SFM. CYP1B1 mRNA expression (A) and protein expression levels (B) were determined using real-time PCR and Western blot analysis, respectively. For real-time PCR, total

RNA was isolated using TRIzol reagent, the mRNA level was quantified and its level was normalized to β-actin housekeeping gene. For Western blot analysis, protein levels were detected using the enhanced chemiluminescence method. The intensity of protein band was normalized to the signals obtained for β-actin or GAPDH protein and quantified using ImageJ®. The results are presented as the mean and SEM based on at least 3 individual experiments. Data were analyzed using one-way ANOVA followed by Student–Newman–Keuls as post hoc test. $+p < 0.05$ significantly different from the control group. $*p < 0.05$ significantly different from Ang II-treated group. $^{\#}p < 0.05$ significantly different from the control group.

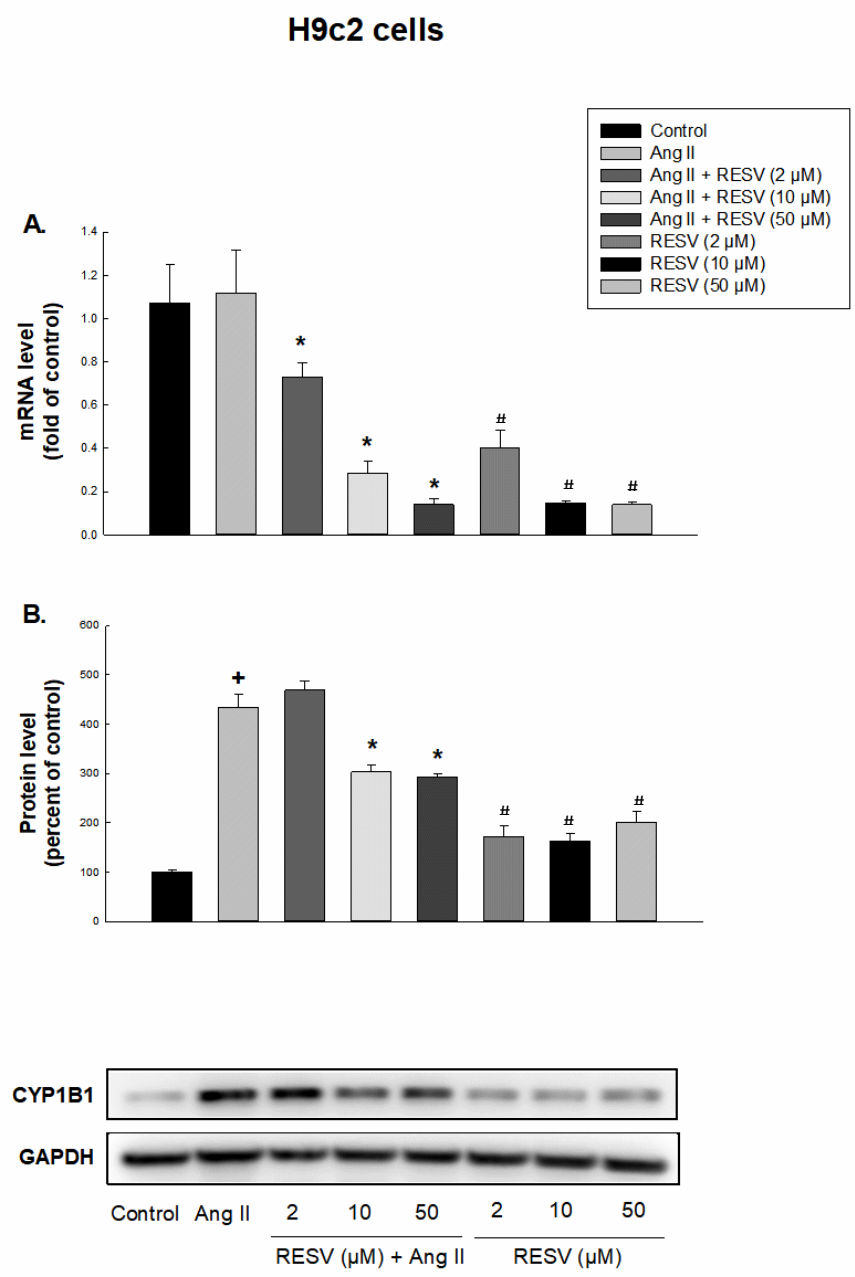

Figure 3.23. Effect of resveratrol on mRNA expression and protein expression levels of CYP1B1 in H9c2 cells

H9c2 cells were treated for 24 h with vehicle, 10 μM Ang II, 10 μM Ang II in combination with (2, 10 or 50 μM resveratrol) or (2, 10 or 50 μM resveratrol alone) in SFM. CYP1B1 mRNA expression (A) and protein expression levels (B) were determined using real-time PCR and Western blot analysis, respectively. For real-time PCR, total RNA was isolated

using TRIzol reagent, the mRNA level was quantified and its level was normalized to β-actin housekeeping gene. For Western blot analysis, protein levels were detected using the enhanced chemiluminescence method. The intensity of protein band was normalized to the signals obtained for β-actin or GAPDH protein and quantified using ImageJ®. The results are presented as the mean and SEM based on at least 3 individual experiments. Data were analyzed using one-way ANOVA followed by Student–Newman–Keuls as post hoc test. $+p < 0.05$ significantly different from the control group. $*p < 0.05$ significantly different from Ang II-treated group. $^{\#}p < 0.05$ significantly different from the control group.

3.4.4 Effect of low and high concentrations of resveratrol on the formation of mid-chain HETEs in RL-14 and H9c2 cells

In order to investigate the effect of low and high concentrations of resveratrol on the formation of mid-chain HETEs metabolites, RL-14 and H9c2 cells were treated for 24 h with vehicle, 10 μM Ang II or 10 μM Ang II in combination with (2, 10 or 50 μM resveratrol). Thereafter, the cells were incubated with 50 μM AA for 3 h and mid-chain HETE metabolites were analyzed using LC–ESI–MS. The results showed that treatment of RL-14 cells with Ang II significantly increased the metabolite formation rate of 5-, 8-, 9-, 12- and 15-HETE by approximately 427%, 303%, 279%, 277% and 425%, respectively, while it had no significant effect on 11-HETE (Figure 3.24A and B). Resveratrol at concentration of 2 μM was able to decrease Ang II-mediated induction of 5- and 12-HETE by approximately 51% and 53%, respectively, compared to Ang II-treated group, while it was not able to reverse this increase in the case of 8-, 9-, and 15-HETE (Figure 3.24A and B). On the other hand, higher doses of resveratrol significantly protected against the increase in cardio-toxic mid-chain HETE metabolites. Resveratrol at concentration of 10 μM significantly inhibited Ang II-mediated increase of the metabolite formation rate of 5-, 8-, 9-, 12- and 15-HETE by approximately 78%, 73%, 65%, 64% and 62%, respectively, compared to Ang II-treated group (Figure 3.24A and B). Also, the highest concentration of resveratrol (50 μM) was able to decrease Ang II-mediated increase of the metabolite formation rate of 5-, 8-, 9-, 12- and 15-HETE by approximately 66%, 73%, 68%, 67% and 66%, respectively, compared to Ang II-treated group (Figure 3.24A and B).

In order to further confirm the results in another species, we have performed the metabolic analysis study in rat H9c2 cells. The results showed that treatment of H9c2 cells with 10 μM Ang II significantly increased the metabolite formation rate of 5-, 8-, 12- and 15-HETE by approximately 362%, 301%, 303% and 344%, respectively, while it had no significant effect on 9- or 11-HETE (Figure 3.25A and 3.25B). Resveratrol at concentration of 2 μM was only able to decrease Ang II-mediated increase of 15-HETE by approximately 34%, compared to Ang II-treated group. While it was not able to reverse this increase in case of 5-, 8- and 12-HETE (Figure 3.25A and 3.25B). Interestingly, higher concentrations of resveratrol also significantly inhibited Ang II-mediated increase in cardio-toxic mid-chain HETE metabolites. Resveratrol at concentration of 10 μM significantly inhibited Ang II-mediated increase of the metabolite formation rate of 5-, 8-, 12- and 15-HETE by approximately 65%, 62%, 65% and 64%, respectively, compared to Ang II-treated group (Figure 3.25A and 3.25B). Moreover, the highest concentration of resveratrol (50 μM) was able to decrease Ang II-mediated increase of the metabolite formation rate of 5-, 8-, 12- and 15-HETE by approximately 67%, 69%, 68% and 68%, respectively, compared to Ang II-treated group (Figure 3.25A and 3.25B).

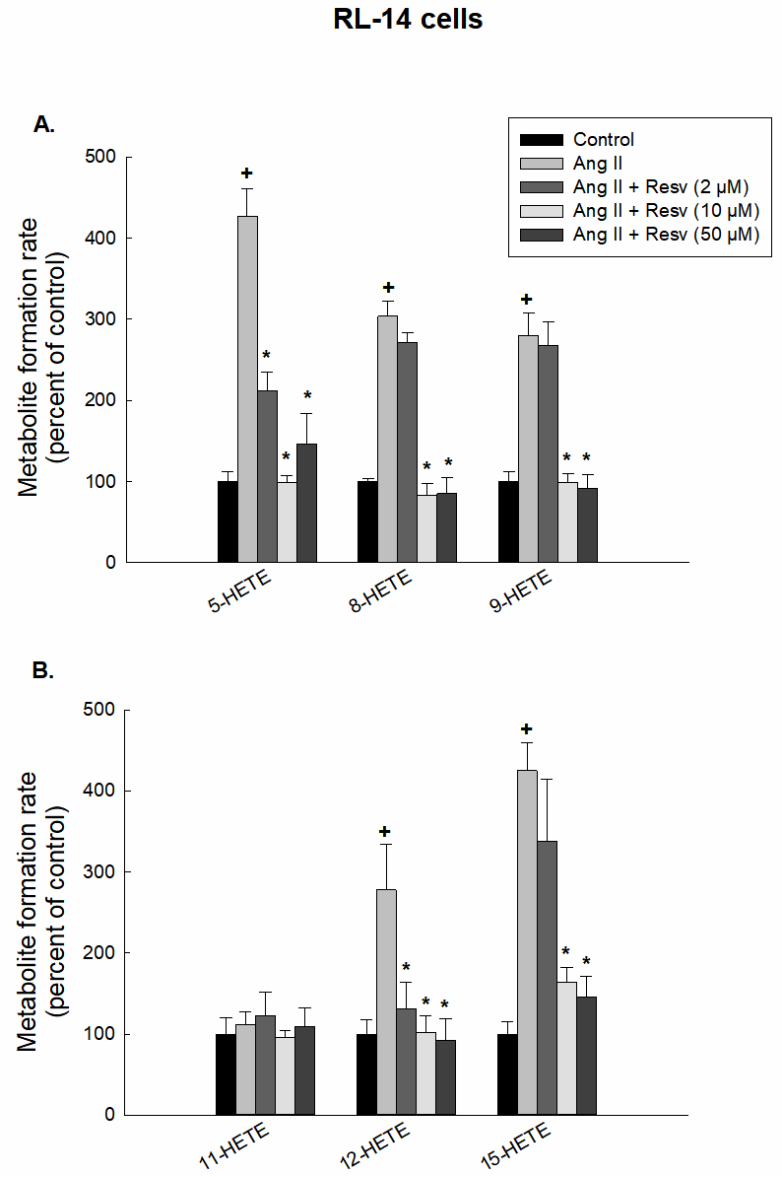

Figure 3.24. Effect of resveratrol on mid-chain HETE metabolite formation rate in RL-14 cells

RL-14 cells were treated for 24 h with vehicle, 10 μM Ang II and 10 μM Ang II in combination with 2, 10 or 50 μM resveratrol. 5-, 8-, 9-HETE (A) and 11-, 12-, 15-HETE (B) metabolites were measured using LC–ESI–MS. The results are presented as the mean and SEM (n=3). Data were analyzed using one-way ANOVA followed by Student–Newman–Keuls as post hoc test. +$p < 0.05$ significantly different from the control group. *$p < 0.05$ significantly different from Ang II-treated group.

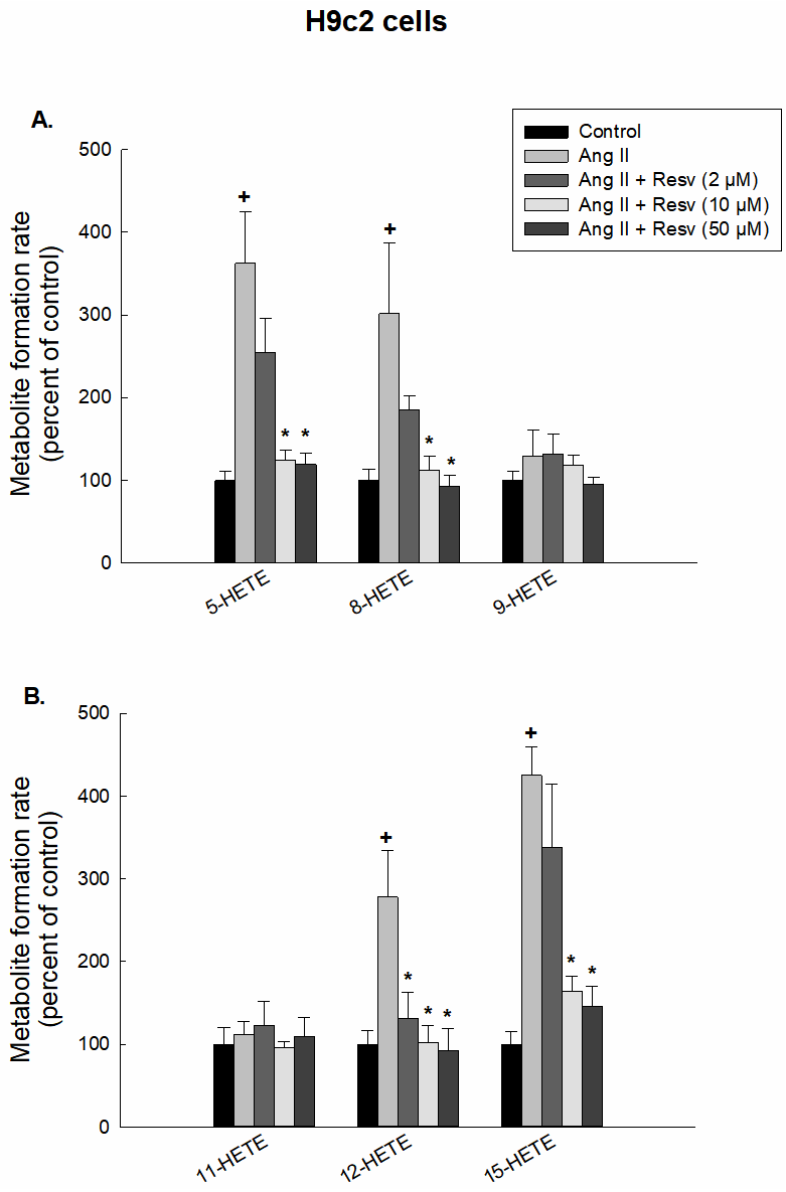

Figure 3.25. Effect of resveratrol on mid-chain HETE metabolite formation rate in H9c2 cells

H9c2 cells were treated for 24 h with vehicle, 10 μM Ang II and 10 μM Ang II in combination with 2, 10 or 50 μM resveratrol. 5-, 8-, 9-HETE (A) and 11-, 12-, 15-HETE (B) metabolites were measured using LC–ESI–MS. The results are presented as the mean and SEM (n=3). Data were analyzed using one-way ANOVA followed by Student–Newman–Keuls as post hoc test. +$p < 0.05$ significantly different from the control group. *$p < 0.05$ significantly different from Ang II-treated group.

3.5 Resveratrol Improves Cardiac Function and Exercise Performance in MI-Induced Heart Failure through the Inhibition of Cardiotoxic HETE Metabolites

The results included in this section have been published as a part of the following study:

Matsumura N, Takahara S, Maayah Z, Parajuli N, Byrne N, Shoieb S, Soltys C-LM, Beker D, Masson G, El-Kadi A, Dyck J. (2018). Resveratrol improves cardiac function and exercise performance in MI-induced heart failure through the inhibition of cardiotoxic HETE metabolites. Journal of Molecular and Cellular Cardiology. 125: 162–173.

3.5.1 Resveratrol treatment inhibits the formation of cardiotoxic HETE metabolites in hearts from rats with established HF

We examined whether low dose resveratrol exerts a cardioprotective effect through inhibiting the expression of CYP1B1 and its associated cardiotoxic mid-chain HETE metabolites. Rats were subjected to either sham surgery or a surgery to ligate the left anterior descending artery to induce a MI and subsequent HF. Three weeks post-surgery, rats with established HF were treated with control diet or administered a diet containing (0.2 g resveratrol/kg AIN-93G diet; Dyets Inc., Bethlehem, PA.). Thereafter, mid-chain HETE metabolites were determined in hearts using LC–ESI–MS. The level of 15-, 12-, 8-, and 5-HETE formation were significantly increased to 180%, 220%, 150% and 190%, respectively, in hearts from rats with established HF in comparison to the sham-operated group with the control diet (Figure 3.26A, C, D, F). On the other hand, 15-, 12-, 8-, and 5-HETE were restored to that of the sham-operated group by 2 weeks resveratrol treatment in the MI-operated group (Figure 3.26A, C, D, F). Furthermore, no significant

differences were observed between the control and the resveratrol treatment alone (Figure 3.26A, C, D, F).

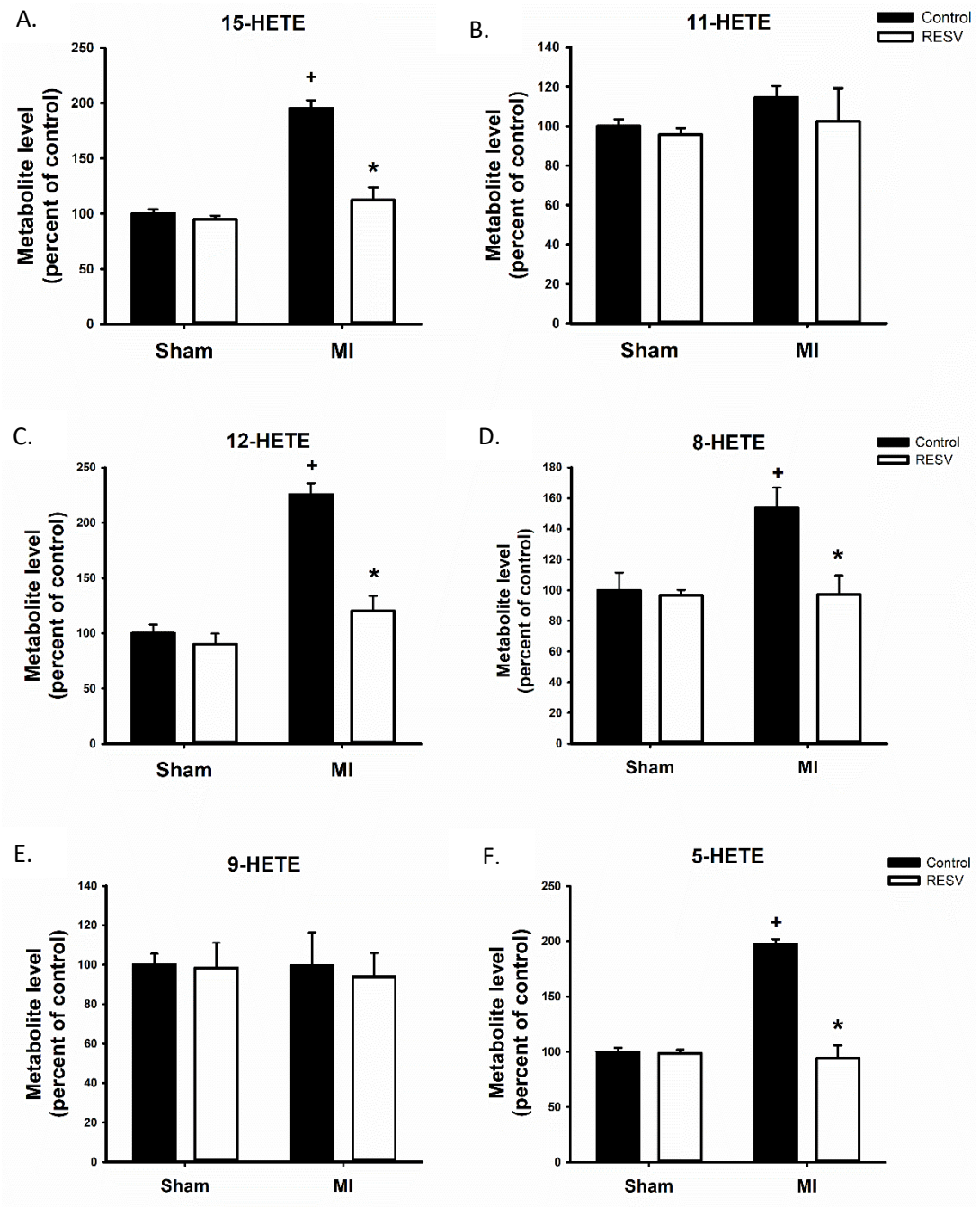

Figure 3.26. Resveratrol treatment inhibits MI-induced formation of cardiotoxic HETE metabolites in hearts from rats with established HF

A: 15-HETE, B: 11-HETE, C: 12-HETE, D: 8-HETE, E: 9-HETE, F: 5-HETE formation levels in hearts of both control diet and resveratrol (RESV)-treated rats that underwent MI surgery or sham (n = 3 per group). Results are shown as means ± SEM. Comparisons between groups were made by one-way ANOVA followed by Student–Newman–Keuls as post hoc test. + $p < .05$ vs its own sham group. * $p < .05$ vs MI-Control. MI: myocardial infarction.

3.5.2 Resveratrol treatment decrease the protein expression level of CYP1B1 in hearts from rats with established HF

We examined whether the decrease in the formation of mid-chain HETEs by resveratrol is due to the inhibition of CYP1B1 enzyme. For this purpose, CYP1B1 protein expression level was determined by Western blot analysis. Our results showed that hearts of rats with HF had a significant increase (400%) in the expression of CYP1B1 compared to the sham-operated group (Figure 3.27). Resveratrol alone caused a significant increase in the expression of CYP1B1 by 200% in comparison to sham-operated group. Importantly, resveratrol significantly inhibited the expression of CYP1B1-induced by HF to 110% compared to control diet-treated rats (Figure 3.27). Overall, these observations suggest that the beneficial effects of resveratrol in HF may be mediated through the inhibition of CYP1B1 and its associated HETE metabolites.

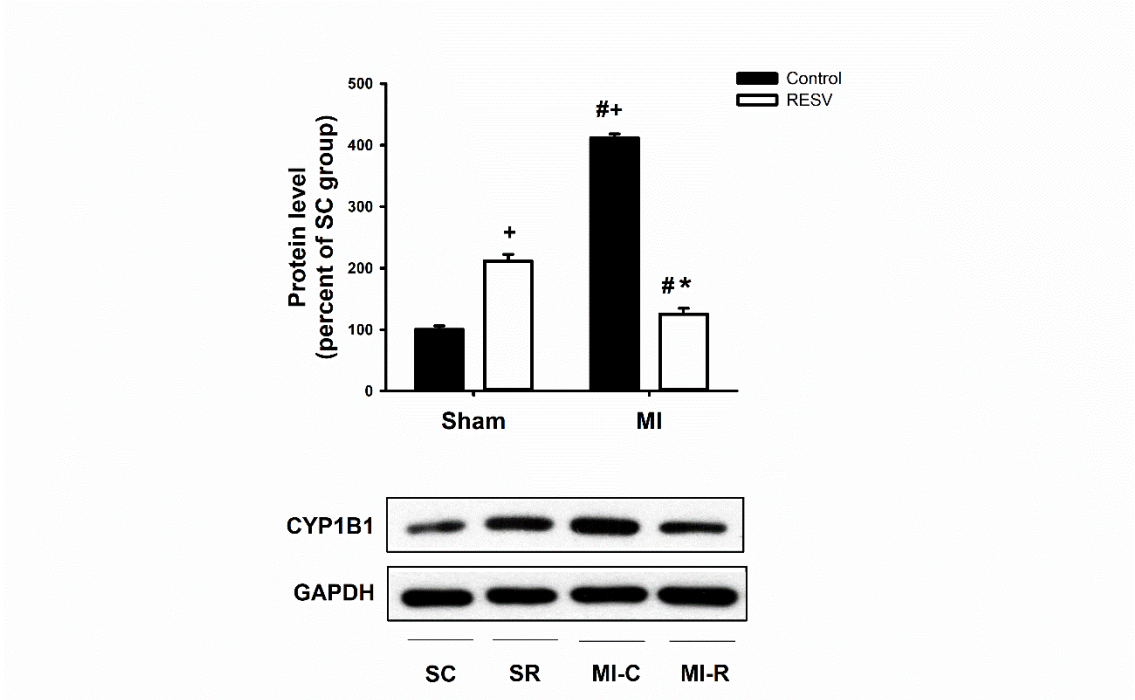

Figure 3.27. Resveratrol treatment decrease the protein expression level of CYP1B1 in hearts from rats with established HF

Microsomes from heart were immunoblotted with antibodies against the following CYP1B1 and GAPDH. Results are shown as means ± SEM. protein levels were detected using the enhanced chemiluminescence method. The intensity of protein band was normalized to the signals obtained for GAPDH protein and quantified using ImageJ®. The results are presented as the mean and SEM based on at least 3 individual experiments. Data were analyzed using one-way ANOVA followed by Student–Newman–Keuls as post hoc test. +$p < 0.05$ significantly different from SC group, #$p < 0.05$ significantly different from SR group, *$p < 0.05$ significantly different from MI-C group. **SC:** Sham with control diet; **SR:** Sham with resveratrol treatment; **MI-C:** Myocardial infarction with control diet; **MI-R:** Myocardial infarction with resveratrol treatment.

3.6 Ameliorative Role of Fluconazole against Abdominal Aortic Constriction-Induced Cardiac Hypertrophy in rats

3.6.1 Fluconazole significantly reversed the abdominal aortic constriction-induced left ventricular hypertrophy in rats

In order to assess whether fluconazole has the ability to protect against AAC-induced cardiac hypertrophy in rats, systolic and diastolic function, and wall measurements were assessed *in vivo* using ultrasound echocardiography. Also, the cardiac hypertrophy was assessed *ex vivo* by measuring heart weight-to-tibial length ratio (HW/TL) and heart weight-to-body weight ratio (HW/BW). The experimental cardiac hypertrophy was evidenced by thickening of the left ventricular wall as shown by an increase in LVPWs, LVPWd (Figure 3.28A, represents m-mode images from 2D echocardiography), IVSd, and IVSs as well as a significant increase in LV mass (Table 3.4). On the other hand, treatment of AAC rats with fluconazole resulted in a substantial reduction in the AAC-induced hypertrophy of the left ventricle to nearly control levels. Moreover, AAC significantly increased the HW/TL and HW/BW, compared to the control group, whereas treatment with fluconazole significantly inhibited the AAC-induced increase in the HW/TL and HW/BW ratios (Figures 3.29A and 3.29B, respectively). It is noteworthy to mention that the echocardiographic assessment showed that heart rate, systolic function parameters including EF% and %FS, diastolic function parameters were not changed across the four treatment groups (Table 3.4). Also, fluconazole-treated rats showed no significant differences in all assessed parameters compared to the control group.

3.6.2 Fluconazole significantly reversed the abdominal aortic constriction-mediated increase in hypertrophic markers

We have examined the effect of AAC surgery and fluconazole treatment on cardiac hypertrophic markers, the results showed that AAC surgery resulted in a significant increase in β/α-MHC ratio and ANP by approximately 30% and 145%, respectively, compared to the control group (Figure 3.29C and 3.29D). Treatment of rats with fluconazole was able to significantly protect against AAC-mediated elevation of β/α-MHC ratio and ANP to approximately control levels. Notably, treatment of rats with fluconazole alone did not have any significant effects on any of the hypertrophic markers. These results, combined with the ultrasound echocardiography data, indicate that fluconazole protects against AAC-induced cardiac hypertrophy as evidenced by a reduction in hypertrophic markers. This prompted us to further study the effects of AAC and fluconazole on CYP enzymes as well as the metabolite formation rate of cardiotoxic mid-chain HETE metabolites.

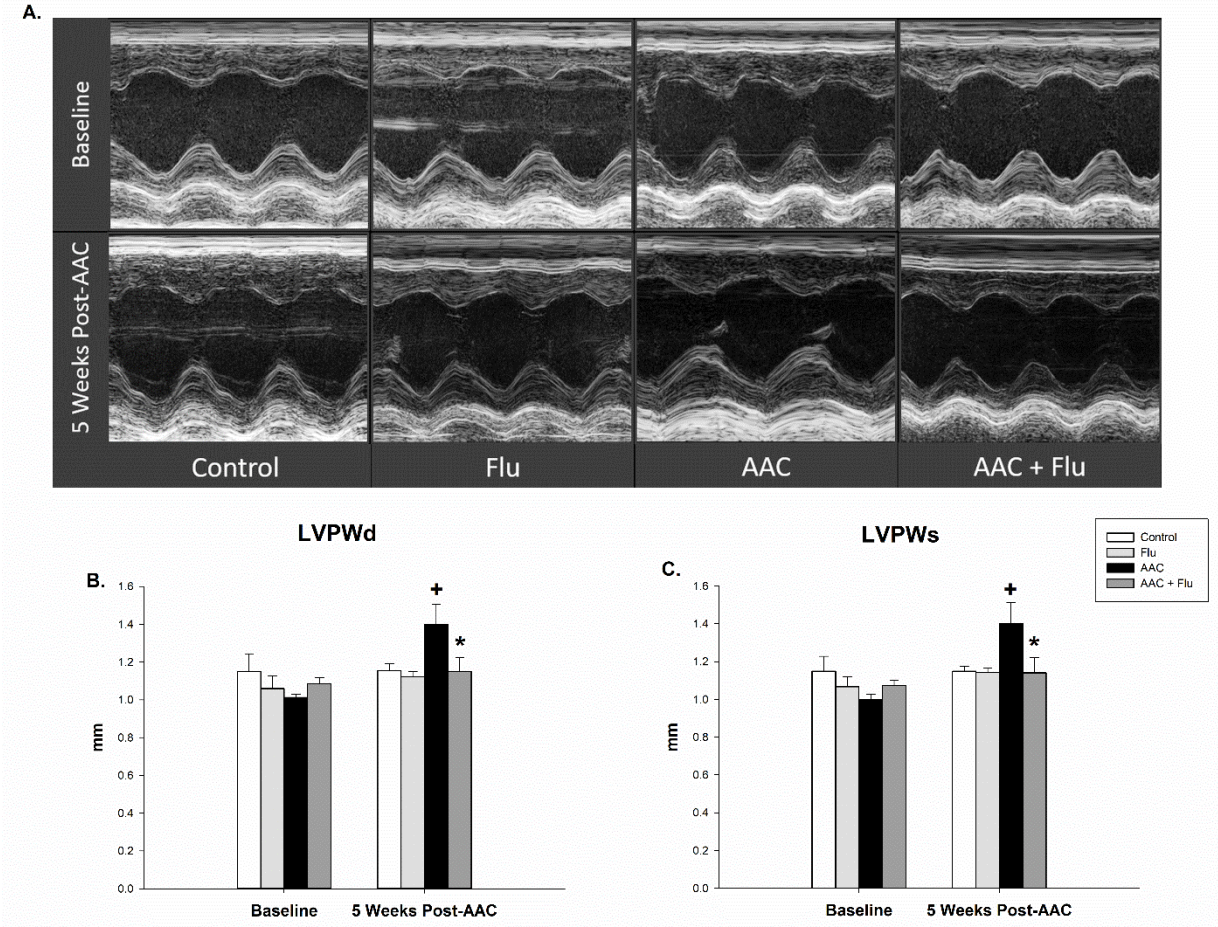

Figure 3.28. Fluconazole significantly reversed the abdominal aortic constriction-induced left ventricular hypertrophy in rats

A, Representative m-mode images from 2D ultrasonic echocardiography, M-mode slices were taken in PLAX mode. **B and C**, Effect of fluconazole on AAC-mediated increase in **LVIDs,** left ventricular internal diameter, systole; and **LVPWd,** left ventricular posterior wall, diastole. **AAC,** abdominal aortic constriction. **Flu**, fluconazole (20 mg/kg/day) intraperitoneally. The values represent mean ± SEM (n = 6). +$p < 0.05$ significantly different from the control group. *$p < 0.05$ significantly different from AAC group.

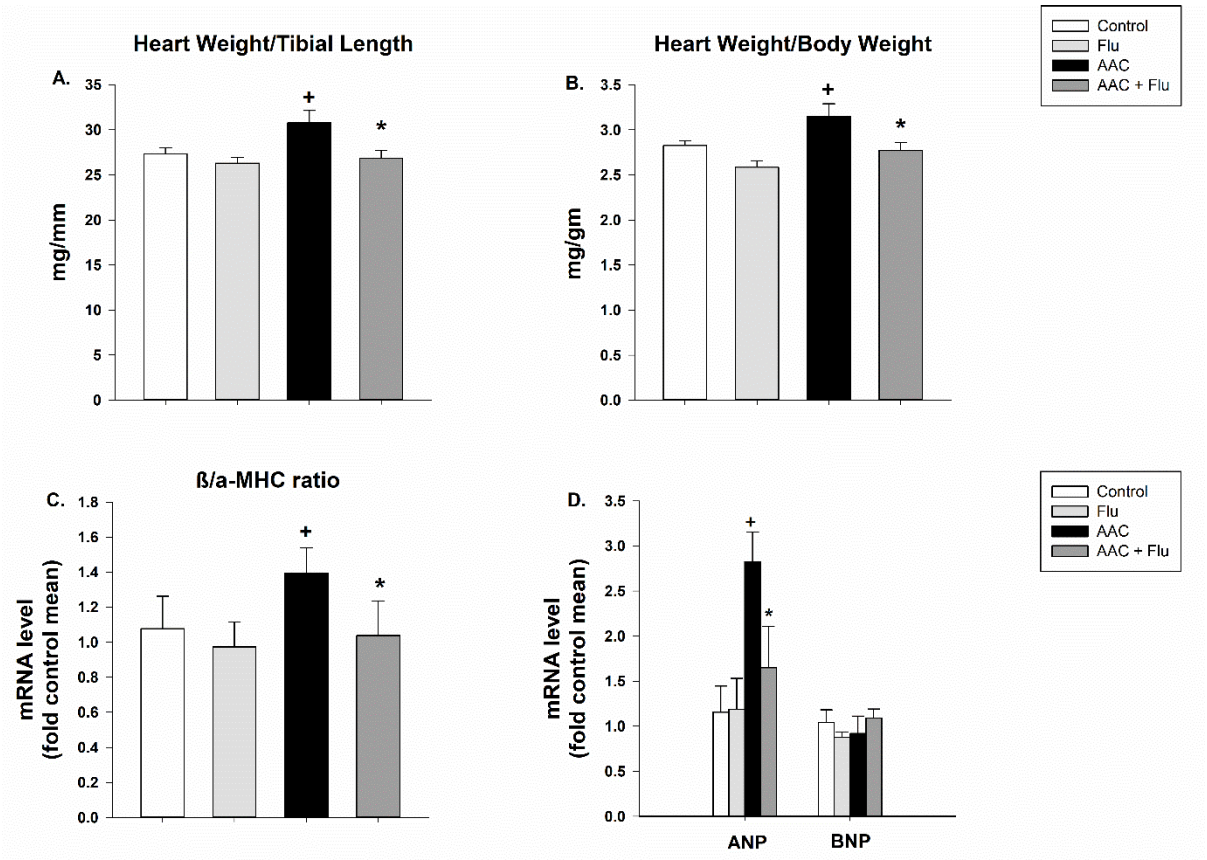

Figure 3.29. Fluconazole significantly reversed the abdominal aortic constriction-mediated increase in hypertrophic markers

Sham and AAC rats were treated with fluconazole (20 mg/kg/day) intraperitoneally. Thereafter, **A,** heart weight/tibial length (mg/mm) and **B,** heart weight/body weight (mg per gm) were determined for each animal. **C** and **D,** the mRNA level of β- MHC, α-MHC and ANP were quantified using real time-PCR. The results are presented as the mean ± SEM (n = 6). +$p < 0.05$ significantly different from the control group. *$p < 0.05$ significantly different from AAC group.

Table 3.4. Ultrasonic echocardiography data representing the cardiac function and haemodynamic parameters.

Echocardiography	Baseline				5 Weeks Post-AAC			
	Control	**Flu**	**AAC**	**Flu+AAC**	**Control**	**Flu**	**AAC**	**Flu+AAC**
Body Weight (gm)	257.9±2.2	378.4 ±11	270.3±7.2	359.3±5.2	538.8±10.3	593.6±17.0	557.0±23.3	554.3±17.1
Heart Rate (bpm)	392 ±13	383 ±9	383 ±13	373 ±9	343 ±17	344 ±13	331 ±11	331 ±12
Systolic and Wall Measurements								
Corrected LV Mass (mg)	397.1 ±58	424.7 ±43	332.6 ±22	429.7 ±30	535.8 ±47	494.5±24.1	697.8 ±53^{+}	529.6 ±35*
IVS;d (mm)	1.1 ±0.08	1.1 ±0.07	1.0 ±0.02	1.1 ±0.03	1.2 ±0.04	1.1 ±0.03	1.4 ±0.11^{+}	1.2 ±0.07*
IVS;s (mm)	1.08±0.09	1.07±0.06	1.02±0.01	1.04±0.02	1.16 ±0.02	1.13 ±0.02	1.45±0.11^{+}	1.18±0.07*
LVID;d (mm)	7.11±0.22	7.79±0.11	7.01±0.21	7.76±0.21	8.32 ±0.38	8.22 ±0.20	8.50 ±0.20	8.33 ±0.27
LVID;s (mm)	3.92±0.12	4.06±0.20	3.59±0.20	4.60±0.26	4.49 ±0.30	4.31 ±0.34	4.53 ±0.33	4.63 ±0.31
LVPW;d (mm)	1.15±0.10	1.06±0.07	1.01±0.02	1.08±0.03	1.16±0.03	1.12±0.03	1.40±0.11^{+}	1.15±0.07*
LVPW;s (mm)	1.15±0.08	1.07±0.05	1.00±0.03	1.07±0.03	1.15 ±0.03	1.14 ±0.02	1.40±0.11^{+}	1.15±0.08*
%EF	75.49±1.7	76.90±2.4	78.37±1.7	70.27±2.7	74.91±1.61	77.00±2.98	75.08±3.02	73.51±2.65
%FS	45.66±1.7	47.47±2.3	48.44±1.7	41.39±2.2	45.53 ±1.5	47.81 ±2.6	46.15 ±2.9	44.50 ±2.5
Doppler Imaging								

TEI Index	0.64±0.05	0.71±0.03	0.67±0.02	0.70±0.04	0.70 ±0.04	0.81 ±0.08	0.73 ±0.04	0.84 ±0.05
Mitral E/A	1.32±0.12	1.2 ±0.03	1.4 ±0.07	1.3 ±0.06	1.24 ±0.16	1.2 ±0.06	1.1 ±0.12	1.5 ±0.10
E'/A'	1.2 ±0.24	1.4 ±0.07	1.1 ±0.24	1.5 ±0.07	1.1 ±0.18	1.1 ±0.13	1.3 ±0.11	1.3 ±0.19
A'/E'	1.05±0.19	0.72±0.03	1.14±0.20	0.69±0.03	1.02 ±0.19	1.04 ±0.16	0.84 ±0.08	0.87 ±0.16
E/E'	22.82±4.0	16.04±1.25	21.60±3.43	16.51±1.36	15.67±2.18	14.83±1.42	14.83±1.91	15.44±2.90
S Wave	46.85±2.6	47.08±1.40	51.38±2.33	48.04±1.35	52.26±1.65	52.82±2.40	56.97±2.78	50.56±2.16
Abdominal Aorta								
Pressure Gradient	1.17±0.14	1.22 ±0.19	1.79 ±0.41	1.42 ±0.21	1.46 ±0.18	1.21 ±0.39	$5.69\pm1.57^{+}$	$5.96\pm1.11^{+}$
Peak Velocity	525 ±32	543 ±40	648 ±74	585 ±48	596 ±43	528 ±74	$1145\pm157^{+}$	$1193\pm128^{+}$

The values represent mean ± SEM ($n = 6$). $^{+}P < 0.05$ compared to control. $*P < 0.05$ compared to AAC. **LV mass**, left ventricular mass; **IVS;d,** intraventricular septum, diastole; **IVS;s,** intraventricular septum, systole; **LVID;d** left ventricular internal diameter, diastole; **LVID;s** left ventricular internal diameter, systole; **LVPW;d,** left ventricular posterior wall, diastole; **LVPW;s,** left ventricular posterior wall, systole; **EF,** ejection fraction; **FS,** fractional shortening; **TEI index** = (isovolumic relaxation time + isovolumic contraction time)/ ejection time; **E, A,** wave velocity; **E′, A′,** tissue doppler wave; **S,** sytolic tissue movement.

3.6.3 Chronic treatment with fluconazole did not significantly impact the level of serum hepatotoxicity markers, however it decreased weight gain percentage in rats

In order to investigate whether chronic treatment with fluconazole would have a negative effect on the liver or weight gain, we have assessed the levels of serum hepatotoxicity markers including ALT, AST and albumin in addition to the calculation of the percentage of weight gain for rats. The results showed that fluconazole treatment of 20mg/kg for 4 w showed no significant effect on the level of serum hepatotoxicity markers (Figures 3.30A, B and C). Interestingly, as shown in figure 3.30D, rat groups that received fluconazole treatment gained less weight than control or AAC rats over the five-week period of the experiment. Fluconazole-treated rats showed 56% weight gain from baseline weight compared to 109% weight gain in the control group. Also, fluconazole-treated AAC rats gained approximately 54% in their weight in comparison to 106% gain in weight acquired by AAC rats.

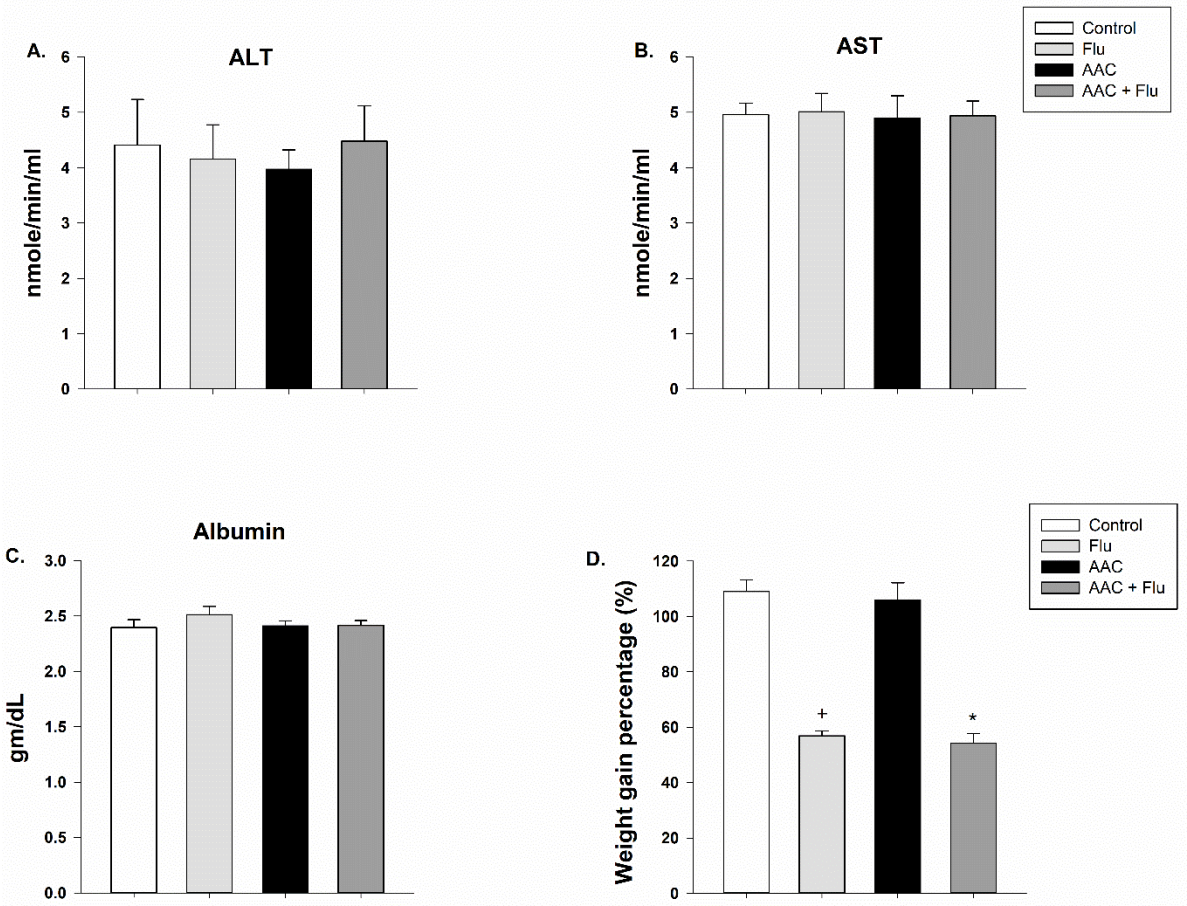

Figure 3.30. Effect of chronic treatment with fluconazole on the level of serum hepatotoxicity markers and weight gain percentage in rats

Serum activities of **A,** ALT and **B,** AST, and **C,** albumin level were assessed using colorimetric assays. Also, the weight gain percentage (**D**) was calculated for each rat using the weights of rats at baseline and 5 weeks post-AAC surgery. The results are presented as the mean ± SEM (n = 6). +$p < 0.05$ significantly different from the control group. *$p < 0.05$ significantly different from AAC group.

3.6.4 Fluconazole significantly decreased the mRNA expression of CYP2C23 and CYP3A2 in the heart.

To better elucidate the effects of fluconazole on CYP enzymes in the heart and to further elucidate the correlate its effects on CYP enzymes with its antihypertrophic effect, screening of the CYP isoforms has been carried out using RT-PCR. The results showed that fluconazole has no significant effect on CYP1A1, CYP1A2, CYP2E1, CYP2J3, CYP4A1 or CYP4F6 on the mRNA (Figures 3.31A and B) level compared to the control group. On the other hand, the mRNA expression of CYP2C23, which is catalytically equivalent to CYP2C9 and CYP2C19 in humans, was significantly decreased by approximately 49% and 45% in the fluconazole-treated sham rats and fluconazole-treated AAC rats, respectively, compared to the control group (Figure 3.31A). Also, there was a significant reduction in the mRNA expression of CYP3A2, which is catalytically equivalent to CYP3A4 in humans, by approximately 42% and 46% in the fluconazole-treated sham rats and fluconazole-treated AAC rats, respectively, compared to the control group (Figure 3.31B).

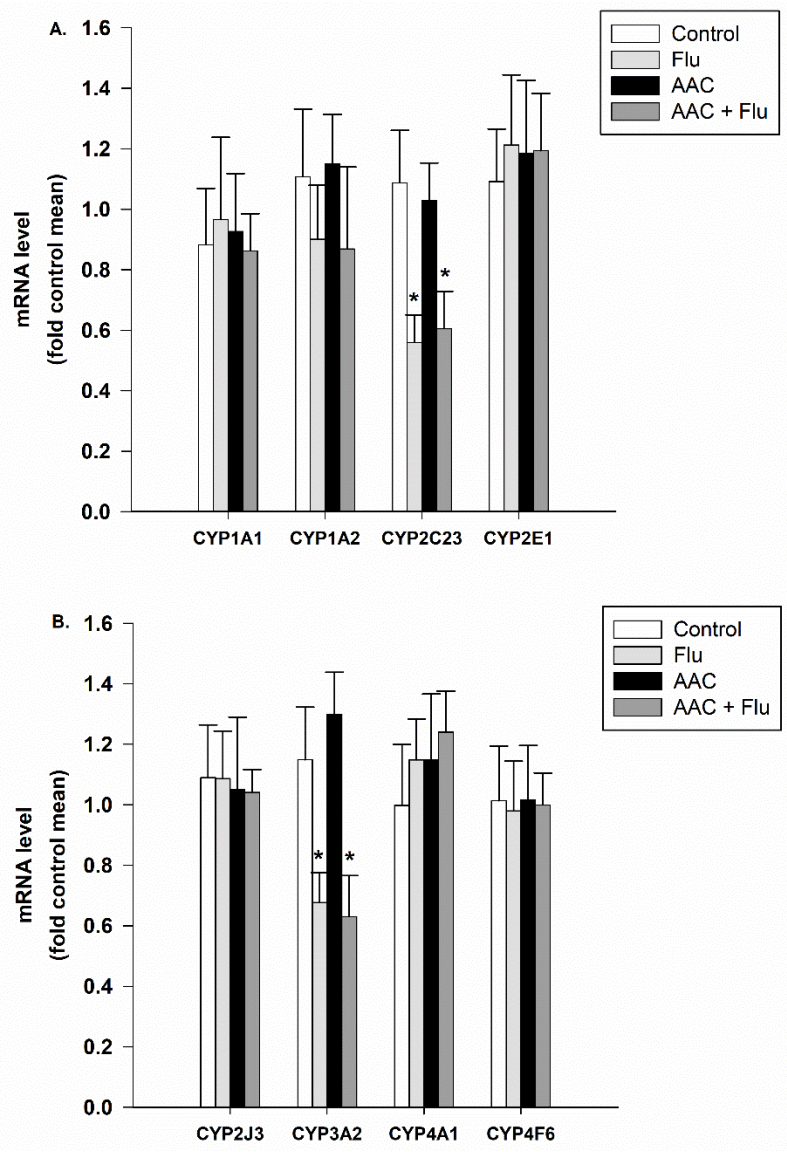

Figure 3.31. Fluconazole significantly decreased the mRNA expression of CYP2C23 and CYP3A2 in the heart.

Sham and AAC rats were treated with fluconazole (20 mg/kg/day) intraperitoneally for four weeks. Thereafter, the mRNA level of CYP1A1, CYP1A2, CYP2C23, CYP2E1 (**A**) and CYP2J3, CYP3A2, CYP4A1 and CYP4F6 (**B**) were quantified using real time-PCR. The results are presented as the mean ± SEM (n = 6). +$p < 0.05$ significantly different from the control group. *$p < 0.05$ significantly different from AAC group.

3.6.5 Fluconazole inhibited abdominal aortic constriction-mediated induction of CYP1B1 on the mRNA and protein expression levels in the heart.

The effect of both AAC surgery and fluconazole treatment on CYP1B1 was determined at two levels; the mRNA expression level and the protein expression level. The results showed that hearts of rats with cardiac hypertrophy had a significant increase (149%) in the mRNA expression of CYP1B1 compared to the control group (Figure 3.32A). Importantly, fluconazole was able to ameliorate the AAC-mediated induction of CYP1B1 mRNA to 73%, compared to the control group. Also, fluconazole-treated sham rats showed a decrease of the mRNA expression of CYP1B1 to 60% compared to the control group (Figure 3.32A). In agreement with the mRNA results, Western blot analysis followed the same trend, the results showed that hearts of the AAC rats has a significant induction (176%) of CYP1B1 protein expression compared to the control group (Figures 3.32B and C). However, fluconazole was able to protect against the AAC-mediated induction of CYP1B1 protein expression and reversed it to nearly control level. Also, fluconazole-treated sham rats showed a significant inhibition of the protein expression of CYP1B1 to 74% compared to the control group (Figures 3.32B and C).

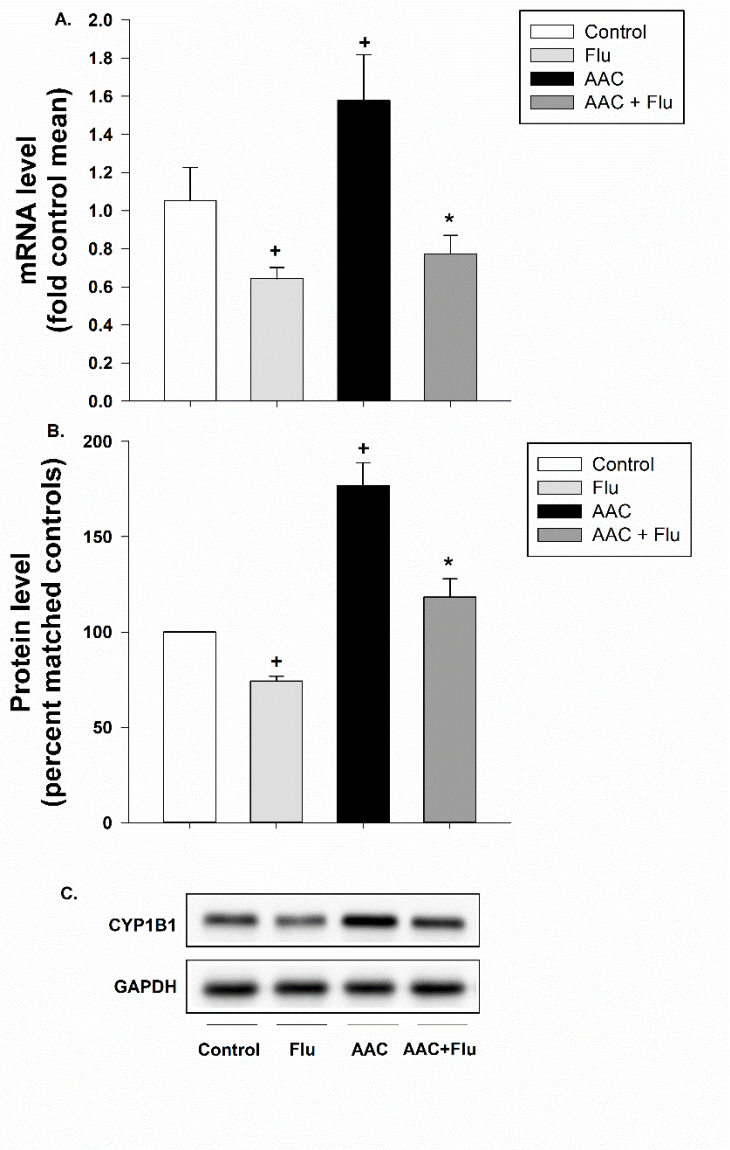

Figure 3.32. Fluconazole inhibited abdominal aortic constriction-mediated induction of CYP1B1 on the mRNA and protein expression levels in the heart.

Sham and AAC rats were treated with fluconazole (20 mg/kg/day) intraperitoneally for four weeks. Thereafter, the mRNA level of CYP1B1 (**A**) was quantified using real time-PCR. **B** and **C**, CYP1B1 protein expression level was determined using Western blot analysis. The results are presented as the mean ± SEM (n = 6). +$p < 0.05$ significantly different from the control group. *$p < 0.05$ significantly different from AAC group.

3.6.6 Fluconazole inhibited abdominal aortic constriction-mediated increase of mid-chain HETEs formation in the heart.

In order to investigate the effect of AAC surgery and fluconazole treatment on the formation of the cardiotoxic mid-chain HETEs metabolites, LC-ESI–MS was used. The results showed that hypertrophied hearts microsomes in the AAC group had a significant increase of the metabolite formation rate of 5-, 12- and 15-HETE by approximately 137%, 143% and 144%, respectively, compared to the heart microsomes in the control group (Figures 3.33A and B). However, AAC surgery had no significant effect on the formation rate of 8-, 9- and 11-HETE (Figures 3.33A and B). Interestingly, fluconazole decreased the AAC-mediated induction of 5-, 12- and 15-HETE formation rate to 93%, 120% and 112%, respectively, compared to the heart microsomes in the control group. It had no significant effect on the formation rate of 8-, 9- and 11-HETE (Figures 3.33A and B). Also, fluconazole-treated sham rats had a significant decrease of the 5-, 12- and 15-HETE formation rate to 70%, 66% and 75%, respectively, compared to the heart microsomes in the control group. Together, these findings suggest that the protective role of fluconazole against experimentally-induced cardiac hypertrophy might be mediated through the inhibition of CYP1B1 and its associated mid-chain HETE metabolites.

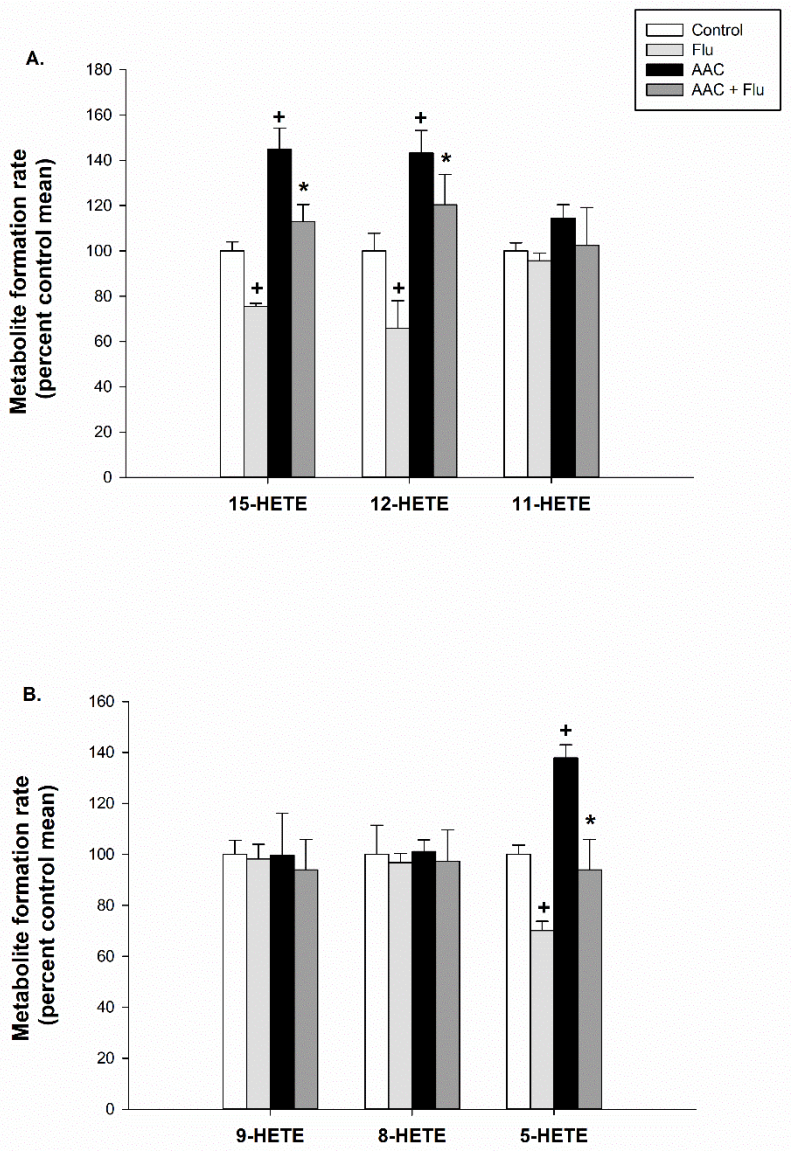

Figure 3.33. Fluconazole inhibited abdominal aortic constriction-mediated increase of mid-chain HETEs formation in the heart.

Sham and AAC rats were treated with fluconazole (20 mg/kg/day) intraperitoneally for four weeks. **A,** 15-, 12-, 11-HETE and **B,** 9-, 8-, 5-HETE metabolites were measured using LC–ESI–MS. The results are presented as the mean ± SEM (n = 6). +$p < 0.05$ significantly different from the control group. *$p < 0.05$ significantly different from AAC group.

CHAPTER 4: DISCUSSION

Portions of this chapter have been published in:

1- **Shoieb SM,** Dakarapu R, Falck JR, El-Kadi AOS. (2021). Novel Synthetic Analogues of 19(S/R)-Hydroxyeicosatetraenoic Acid Exhibit Noncompetitive Inhibitory Effect on the Activity of Cytochrome P450 1A1 and 1B1. European Journal of Drug Metabolism and Pharmacokinetics. In Press.

2- **Shoieb SM,** El-Kadi A. (2020). Resveratrol attenuates angiotensin II-induced cellular hypertrophy through the inhibition of CYP1B1 and the cardiotoxic mid-chain HETE metabolites.Molecular and Cellular Biochemistry. 471: 165–176.

3- **Shoieb SM,** El-Sherbeni A, El-Kadi A. (2019). Identification of 19-(s/r) hydroxyeicosatetraenoic acid as the first endogenous noncompetitive inhibitor of cytochrome P450 1B1 with enantioselective activity. Drug Metabolism and Disposition. 47: 67–70.

4- **Shoieb SM,** El-Kadi A. (2018). S-enantiomer of 19-hydroxyeicosatetraenoic acid preferentially protects against angiotensin II-induced cardiac hypertrophy. Drug Metabolism and Disposition. 46: 1157–1168.

5- Matsumura N, Takahara S, Maayah Z, Parajuli N, Byrne N, **Shoieb SM,** Soltys C-LM, Beker D, Masson G, El-Kadi A, Dyck J. (2018). Resveratrol improves cardiac function and exercise performance in MI-induced heart failure through the inhibition of cardiotoxic HETE metabolites. Journal of Molecular and Cellular Cardiology. 125: 162–173.

4.1 S-Enantiomer of 19-Hydroxyeicosatetraenoic Acid Preferentially Protects Against Angiotensin II-Induced Cardiac Hypertrophy

Recent studies provide strong evidence that CYP enzymes and their AA metabolites play differential roles in most of cardiac diseases, while some of these metabolites are cadiotoxic, others showed cardioprotective effects (Westphal et al., 2015; Zu et al., 2016). One group of AA metabolites that are not fully studied in case of cardiac hypertrophy are subterminal HETEs, specifically 16-, 17-, 18- and 19-HETE. Each member of subterminal HETEs has two enantiomers; R and S enantiomers. Various enantiomers of a chiral drug may be different in their properties such as drug absorption, metabolism, CYP induction or inhibition and excretion (Brocks, 2006; Nguyen et al., 2006). Among the subterminal HETEs, 19-HETE, is considered the main subterminal HETEs in the heart and has been given the highest attention (El-Sherbeni and El-Kadi, 2014c). Therefore, in the current study, we examined the effects of R and S enantiomers of 19-HETE on cardiac CYP enzymes and their associated AA metabolites (subterminal/terminal HETEs, mid-chain HETEs and EETs). Since there was no change in the level of AA metabolites except for mid-chain HETEs, we characterized the three different pathways involved in the formation of mid-chain HETEs and tested whether R- or S-enantiomer have cardioprotective effect against Ang II-induced cellular hypertrophy.

To determine the non-toxic concentration of both enantiomers that will be used in the current study, we examined the effect of increasing concentration both enantiomers on cell viability. Based on the MTT assay results as well as our previously published study,

20 μM of R and S enantiomers was selected for further investigations (Elkhatali et al., 2015). The novel finding of the current study is that both 19(R)-HETE and 19(S)-HETE significantly decreased the metabolite formation rate of most of mid-chain HETEs while the level of 5-HETE was selectively decreased by S-enantiomer. Several pieces of evidence strongly suggest the role of mid-chain HETEs in the pathogenesis of cardiac hypertrophy. It has been reported that 15-HETE is able to increase the sensitivity of isoproterenol-induced β-adrenergic response in rat neonatal cardiomyocytes. In addition, 5-, 12-, and 15-HETE were able to induce cellular hypertrophy in human ventricular cardiomyocytes RL-14 cells through MAPK- and NF-κB-dependent pathways (Zhang et al., 2014a; Maayah and El-Kadi, 2016a).

In the current study, the concentration of AA was chosen based on the fact that intracellular concentrations of the unesterified AA is widely believed to be in the micromolar range, based on reports where the total concentration of unesterified AA has been determined in different tissues. For example, AA concentration has been reported to be 13–44 μM in umbilical cord and intervillous space (Benassayag et al., 1997), 18.9 μg/g (approximately equivalent to 60 μM) in skin (Hammarström et al., 1975), and 75 μg/g (approximately equivalent to 250 μM) in liver (Edpuganti and Mehvar, 2014). Therefore, 50–100 μM of AA was used in several published studies performed in AA and CYP incubation experiments (Xu et al., 2004; Imaoka et al., 2005).

Inhibiting the formation of 5-HETE metabolite significantly protected against Ang II-induced cardiac hypertrophy in mice suggesting that inhibiting its formation could be a novel strategy to treat cardiac hypertrophy (Revermann et al., 2011). The results of the

current study highlight the preferential effect of the S-enantiomer of 19-HETE in decreasing the formation of 5-HETE.

In order to determine the pathway that is involved in the decrease in the level of mid-chain HETEs, three pathways were examined in this study. In the heart, mid-chain HETEs are formed through three different metabolic pathways (Konkel and Schunck, 2011). The first metabolic pathway is CYP enzymes, particularly CYP1B1. CYP1B1 is constitutively expressed in the cardiac tissue and several reports have confirmed the association between this enzyme and cardiovascular disease states (Zordoky and El-Kadi, 2008; Chung et al., 2012). For example, blood pressure elevation induced by Ang II was reduced in Cyp1b1-null mice compared to wild-type mice (Jennings et al., 2010). Protein expression and catalytic activity of CYP1B1 were significantly increased in three different experimental models of cardiac hypertrophy including: pressure overload-induced, isoproterenol-induced and Ang II-induced cardiac hypertrophy (Jennings et al., 2010; El-Sherbeni and El-Kadi, 2014c; Maayah et al., 2017). Recently, we demonstrated that 2-methoxyestradiol, selective CYP1B1 inhibitor, protected against pressure overload-induced left ventricular hypertrophy in rats (Maayah et al., 2018).

One of the important findings of the current study is that both enantiomers of 19-HETE significantly inhibited CYP1B1 catalytic activity in both cell lines (RL-14 and H9c2) without altering its mRNA or protein levels suggesting direct inhibition of its catalytic activity (Li et al., 2017). Interestingly, 19(S)-HETE selectively induced the mRNA and protein expression levels of CYP4F2 and CYP4F11 which have been reported to be involved in the degradation of mid-chain HETEs (Maayah and El-Kadi, 2016b). It is

important to mention that CYP4F2 and CYP4F11 are involved in 20-HETE as well as 19-HETE formation in human. Therefore, our data suggest that 19(S)-HETE may inhibit the catalytic activity of 20-HETE forming enzymes (CYP4F2 and CYP4F11) which may explain the unchanged level of 20-HETE. These data were substantiated by the fact that 19-HETE is a well-known endogenous antagonist of 20-HETE which may explain the cardioprotective effect of 19(S)-HETE (El-Sherbeni and El-Kadi, 2016). On the other hand, both enantiomers did not affect CYP2B6, CYP2C8 or CYP2J2 at gene or protein expression levels. This was further supported by the unchanged metabolite formation rate of EETs, the major products of these enzymes (Zhou et al., 2018).

The other two pathways that are involved in the formation of mid-chain HETEs are LOXs and COX-2 enzymes. 5-LOX, 12-LOX and 15-LOX enzymes metabolize AA to produce 5-, 12- and 15-HETE, respectively (Porro et al., 2014; Radmark et al., 2015; Mao et al., 2016). In addition, it has been reported that minor quantities of mid-chain HETEs are produced by COX-2 enzyme (Bai and Zhu, 2008). Several studies highlighted the role of LOXs in the pathogenesis of cardiovascular diseases including stroke, atherosclerosis and myocardial infarction (Pergola and Werz, 2010). For instance, products of the LOXs pathway are involved in cell proliferation regulation and cell survival. Cardiovascular events such as coronary arteries vasoconstriction leading to compromised ventricular contraction, decrease in blood flow to coronary arteries and depressed cardiac output have also been associated with different metabolites of these enzymes (Vila, 2004; Werz and Steinhilber, 2006). 15-LOX was involved in the pathogenesis of Ang II-induced cardiac hypertrophy in mice. Treatment with the 15-LOX inhibitor, baicalein, showed

cardioprotective effect through inhibition of 15-LOX (Wang et al., 2015a). Furthermore, COX-2 enzyme activation leads to cardiac cell death, decrease in myocardial function and consequently leads to heart failure (Lamon et al., 2010).

In the current study, S-enantiomer of 19-HETE selectively decreased the protein expression level of 15-LOX in human cardiomyocytes while 5-LOX, 12-LOX and COX-2 protein expression was decreased by both enantiomers in RL-14 and H9c2 cells. To the best of our knowledge, this is the first study to reveal how 19(R)-HETE and 19(S)-HETE modulate CYP, LOXs and COX-2 enzymes in cardiac cells. The ability of 19(S)-HETE to inhibit CYP1B1, LOXs and COX-2 pathways and their associated pro-inflammatory metabolites is of significant benefit in the process of designing novel therapeutic modalities for cardiac hypertrophy.

In the present study, both enantiomers of 19-HETE protected against Ang II-induced cellular hypertrophy as evidenced by a substantial decrease in β-MHC/α-MHC ratio and ANP mRNA expression, in RL-14 and H9c2 cells. The protective effect of each enantiomer of 19-HETE against cellular hypertrophy has never been reported before, however we have previously demonstrated that racemic mixture of 19-HETE protected against Ang II-induced cardiac hypertrophy (Elkhatali et al., 2015).

In the current study, both enantiomers of 19-HETE inhibited Ang II-mediated increase of both IL-6 and IL-8 compared to the control group with preferential effect of the S-enantiomer. Interleukins are group of cytokines that have a central role in pathogenesis of cardiac hypertrophy. IL-6 and IL-8 are considered as the main hypertrophic cytokines which mediate their effects through JAK/STAT, MAPK and PI3K pathways (Rohini et

al., 2010). IL-8 was significantly higher in the thoracic aorta of spontaneously hypertensive rats (SHRs) compared to normotensive rats. This finding suggests that IL-8 plays an important role in the pathogenesis of hypertension and cardiac hypertrophy (Apostolakis et al., 2009). Treatment of hypertensive rats with reparixin, an IL-8 receptor inhibitor, caused a significant reduction in blood pressure (Martynowicz *et al.*, 2014).

In summary, our data demonstrated that both enantiomers of 19-HETE protected against Ang II-induced cardiac hypertrophy via decreasing the level of mid-chain HETEs, inhibiting the catalytic activity of CYP1B1, decreasing the protein expression level of LOX and COX-2 enzymes and decreasing the mRNA expression level of pro-inflammatory markers IL-6 and IL-8. It is noteworthy that the S-enantiomer demonstrated more protection than the R-enantiomer reflected by its ability to decrease the level of 5-HETE, decrease the protein expression of 15-LOX, increase the protein expression level of CYP4F2 and CYP4F11 and its preferential effect on IL-6 and IL-8 compared to the R-enantiomer.

Limitations: we acknowledge that the described effects of both enantiomers of 19-HETE were only investigated in an *in vitro* model of cellular hypertrophy. It is challenging to address 19-HETE metabolism into *in vitro* assays and how its metabolic profile would affect its actions on the cardiac cells. We suggest that the anti-hypertrophic effect of these metabolites could be tested in an *in vivo* model of cardiac hypertrophy such as AAC-induced cardiac hypertrophy experimental model in rats.

4.2 Identification of 19-(S/R)Hydroxyeicosatetraenoic Acid as the First Endogenous Non-Competitive Inhibitor of Cytochrome P450 CYP1B1 with Enantioselective Activity

Inhibition of CYP1B1 is proposed as one of the strategies in the treatment of cardiovascular diseases and cancer chemoprevention (Mikstacka et al., 2007). In this regard, we tested the capacity of both enantiomers of 19-HETE to inhibit the catalytic activity of human recombinant CYP1B1, based on our previous finding that 19(R)- and 19(S)-HETE protected against the Ang II-induced cellular hypertrophy via decreasing the level of cardiotoxic mid-chain HETEs; the major metabolites of CYP1B1 (Shoieb and El-Kadi, 2018b). For that purpose, the inhibition kinetics of both enantiomers of 19-HETE on CYP1B1 activity were carried out using CYP1B1 substrate 7-ER, a compound that is metabolized via oxidative reaction by this enzyme (Shimada et al., 1997). The experimental conditions such as the concentrations of 7-ER, concentration of the recombinant enzyme in addition to the incubation time were all optimized before the addition of either 19(R)-HETE or 19(S)-HETE.

Inhibition of EROD is a well-reported assay carried out predominantly to examine the inhibitory potencies of CYP1B1 inhibitors (Androutsopoulos et al., 2011). Inhibitory activity of 19(R)-HETE and 19(S)-HETE on CYP1B1 was studied. Foremost experiments involved the assessment of 7-ER-O-deethylase kinetics by determination of the rate of resorufin formation over time. Based on the nonlinear regression analysis and fitting to simple or sigmoid Michaelis-Menten model, the maximal EROD activity (V_{max}) in the control containing 0.1% DMSO was 10.6 pmol resorufin/pmol P450/min (R^2

=0.993). The Michaelis-Menten constant (K_m) value for the current EROD reaction is 37 nM. During the co-incubation of 10 nM of either 19-HETE enantiomers with different concentrations of 7-ER, we observed a significant inhibition of CYP1B1 enzymatic activity. This finding prompted us to test increasing concentrations (0-40 nM) of either 19(R)-HETE or 19(S)-HETE with different concentrations (0-100 nM) of 7-ER in order to characterize the mode of inhibition by 19-HETE enantiomers.

Nonlinear regression analysis and comparisons showed that the mode of inhibition for 19(R)-HETE and 19(S)-HETE is noncompetitive inhibition of CYP1B1 enzyme. Dixon plots showed that 19(R)-HETE and 19(S)-HETE have Ki values of 89.1 and 37.3 nM, respectively. The Ki values of both enantiomers showed that the S-enantiomer is more potent than the R-enantiomer by approximately 2.4 fold. This comes in agreement with our previous work demonstrating that the S-enantiomer of 19-HETE has a preferential effect over the R-enantiomer in inhibiting the formation of mid-chain HETEs (Shoieb and El-Kadi, 2018a). In accordance with being noncompetitive inhibitors, the *in vitro* stability study showed that both enantiomers of 19-HETE are metabolically stable in solution during the 30 min-time course of the kinetic experiment as there was no significant difference in the level of both enantiomers during the duration of the experiment. Discovery of selective and potent inhibitors of CYP1B1 enables for the design of CYP1B1-targeted cardiovascular treatment and prevention in addition to cancer chemotherapy (Pingili et al., 2017; Ware, 2017).

To date, more than 50 synthetic and natural compounds have been designed or recognized as inhibitors of CYP1B1 (Li et al., 2017). Various CYP1B1 inhibitors with varying mode

of inhibition have been identified. For instance, trans-resveratrol inhibited CYP1B1 enzymatic activity via mixed-type inhibitory mechanism and the Ki was 0.75 μM (Chang et al., 2000). Also, myricetin and quercetin with Ki 230 and 120 nM, respectively exhibited mixed-type inhibition while apigenin with Ki 60 nM acted as a competitive inhibitor of CYP1B1 (Chaudhary and Willett, 2006). Moreover, tetramethoxystilbene (TMS) noncompetitively inhibited EROD activity of CYP1B1 with IC_{50} value of 2 nM when using 2 μM of 7-ER as a substrate (Chun et al., 2009). In the present study, both enantiomers of 19-HETE inhibited CYP1B1 enzymatic activity in the nanomolar range and more potently than some of the previously mentioned CYP1B1 inhibitors proposing them to be introduced as therapeutic and preventive modalities in CYP1B1-targeted therapies.

In the current study, there is a significant difference in the inhibitory activity between R- and S-enantiomers of 19-HETE. To the best of our knowledge, the current study is the first to characterize the enantioselective pattern of inhibition of CYP1B1 by enantiomers of 19-HETE. Enantioselective inhibition of CYP enzymes has been previously documented. S002-333, a novel and potent antithrombotic agent, inhibited CYP2B6-mediated bupropion 6-hydroxylation in a stereoselective manner. While the S-enantiomer showed strong inhibition with IC_{50} value of 5.28 μM, the R-enantiomer showed much less inhibition on CYP2B6 catalytic activity with IC_{50} value of more than 50 μM (Bhateria et al., 2016).

It is noteworthy that CYP1B1 regulates several metabolic pathways. For example, AA is oxidized by CYP1B1 to produce the cardiotoxic mid-chain HETEs metabolites. In rat

neonatal cardiomyocytes, 15-HETE has been reported to be capable of elevating isoproterenol-induced β-adrenergic response sensitivity. Moreover, 5-, 12-, and 15-HETE were capable of inducing cellular hypertrophy in RL-14 cells, human ventricular cardiomyocytes, via MAPK- and NF-κB-dependent pathways (Zhang et al., 2014a; Maayah and El-Kadi, 2016a). Furthermore, CYP1B1 is responsible for some vital physiological processes in blood vessels, importantly the development and progression of hypertension. In Ang II-induced hypertension, CYP1B1 mediates cell migration, induces proliferation and increases protein synthesis in vascular smooth muscle cells through regulation of the metabolism of AA (Yaghini et al., 2010). The fact that CYP1B1 expression is vastly enhanced in several tumors such as prostate, breast and colon cancers, suggests that CYP1B1 inhibitors could be considered as an accepted therapeutic strategy in treatment and prevention of cancer (Gibson et al., 2003; Tokizane et al., 2005a).

In summary, CYP1B1 is considered one of the important CYPs. It is involved in the metabolism of many endobiotics, xenobiotics and in the activation pathways of various procarcinogens. The findings of the current study show that both enantiomers of 19-HETE noncompetitively inhibited CYP1B1 enzymatic activity with higher potency of the S-enantiomer. The current study suggests that 19(R)-HETE and 19(S)-HETE could be considered as a novel therapeutic modality in the treatment of hypertension, cardiac hypertrophy and cancer. Moreover, given that a noncompetitive inhibitor might bind to the enzyme regulatory region, 19(R)-HETE and 19(S)-HETE could be considered to unravel the obscure mechanisms of CYP1B1 enzymatic reaction.

Limitations: The inhibitory effect of 19(R)-HETE and 19(S)-HETE on the enzymatic activity of CYP1B1 has been investigated in a cell-free system using the human recombinant CYP1B1 enzyme. These system exclude the effect of the drug transport through the cell membrane, therefore, we suggest that the inhibitory effect of 19-HETE enantiomers could be tested on cell lines expressing CYP1B1 using an assay that possess high selectivity against CYP1B1. Also, the inhibitory effect could be tested on other CYP enzymes including CYP3A4.

4.3 Novel Synthetic Analogues of 19(S/R)-Hydroxyeicosatetraenoic Acid Exhibit Noncompetitive Inhibitory Effect on the Activity of Cytochrome P450 1A1 and 1B1

CYPs comprise a superfamily of either constitutive or inducible enzymes that are involved in the oxidative biotransformation of different xenobiotics and several endogenous substances (Zanger and Schwab, 2013). Inhibition of CYP family 1 enzymes is suggested as one of the possible strategies in the search for novel treatments of several cardiovascular diseases as well as cancer chemoprevention (Liu et al., 2013a). In this regard, we examined the possible inhibitory effect of novel synthetic 19-HETE analogues (R- and S-analogues) on the activity of CYP1A1, CYP1A2 and CYP1B1 recombinant human enzymes. For this purpose, EROD reaction rate by recombinant human CYP1A1 and CYP1B1, and MROD reaction rate by recombinant human CYP1A2 were measured in the absence and presence of increasing concentrations (0-40 nM) of the synthetic analogues of 19(R)- and 19(S)-HETE. The results of the current study showed that both synthetic analogues of 19(R)- and 19(S)-HETE exhibited direct noncompetitive inhibitory effect on the activity of CYP1A1 and CYP1B1 with preferential inhibitory effect associated with the S-analogue. However, both synthetic analogues failed to show any significant effect on CYP1A2 and CYP3A4 activity.

In accordance with structural homology, CYP enzymes should be assigned to the same family in case they have a more than 40% homology of the amino acid sequence. In addition, isozymes that have more than 55% sequence homology should be assigned to the same subfamily (Sello et al., 2015). Family 1 (CYP1) includes three isoenzymes

known as CYP1A1, CYP1A2, and CYP1B1. The sequence homology of CYP1A2 is 72% similar to that of CYP1A1, however the sequence homology of CYP1B1 is lower with either CYP1A1 (38%) or CYP1A2 (37%) (Jorge-Nebert et al., 2010). Nevertheless, CYP1B1 is assigned to CYP1 family on the basis of comparable substrate specificity and the mutual induction of CYP1 family members by the aryl hydrocarbon receptor (Nebert et al., 2004).

The enzyme kinetic profile of subterminal HETEs limits the utility of these metabolites in the clinical and experimental settings. Consequently, there is a critical need for development of novel synthetic analogues that possess improved bioavailability and have higher metabolic stability in comparison with their parent compounds. With the intention of designing robust 19-HETE analogues, the carbon backbone of 20-hydroxyeicosa-5(Z),14(Z)-dienoic acid (20–5,14-HEDE) has been utilized for the synthesis of 19(R)- and 19(S)-HETE synthetic analogues through introduction of hydroxyl group to C(19) position. These analogues are protected from the auto-oxidation process and metabolism by lipoxygenase and cyclooxygenase branches of the AA pathway. Both R- and S-analogues share the same pharmacological activity as their parent 19(R)- and 19(S)-HETE metabolites; they have showed the capability to antagonize the actions induced by 20-HETE in rat renal preglomerular microvessels (Dakarapu et al., 2019).

The O-dealkylation of ethoxyresorufin is widely available and highly sensitive activity assay used for measuring the activity of both CYP1A1 and CYP1B1. Inhibition of this reaction has been utilized as a predominant measure to assess the possible inhibitory effects of potential candidates (Pastrakuljic et al., 1997; Kapelyukh et al., 2019). Initially,

10 nM of either 19-HETE synthetic analogues was co-incubated with varying concentrations of 7-ER, there was a significant inhibition of both CYP1A1 and CYP1B1 enzymatic activities. This result was encouraging enough to test various concentrations (0-40 nM) of either 19(R)-HETE or 19(S)-HETE synthetic analogues with increasing concentrations of 7-ER (0-200 nM) and (0-100 nM) for CYP1A1 and CYP1B1, respectively, for the purpose of determination of the most probable mode of inhibition by 19-HETE novel synthetic analogues. After application of nonlinear regression analysis and comparisons, the data demonstrated that both synthetic analogues of 19(R)-HETE and 19(S)-HETE inhibit CYP1A1 and CYP1B1 through noncompetitive mode of inhibition.

The results of the present study demonstrated that the enzyme kinetics of CYP1A1, CYP1A2 and CYP1B1 are not consistent with the classical Michaelis-Menten model. Instead, the kinetic profile of resurofin formation versus substrate concentration conformed best to the sigmoid Michaelis-Menten model. One of the assumptions of the simple Michaelis-Menten model is that the interactions between the substrate and the enzyme happen at only one binding site. However, several lines of evidence showed that this is not the case for some CYP enzymes including the major CYP3A4 (Yune-Fang Ueng et al., 1997; Davydov and Halpert, 2008). Kinetic features of a number of CYP3A4 substrates were not in line with the context of the simple Michaelis-Menten model. Therefore, they showed the best fitting to a sigmoid enzyme model with multiple sites demonstrating allosteric modulation for the enzyme substrate, meaning that the affinity of the binding site for a ligand is increased, positive cooperativity, or decreased,

negative cooperativity, upon the binding of a ligand to an alternative binding site. (Houston et al., 2000). In agreement with the aforementioned phenomenon, the kinetic profile of CYP1A1, CYP1A2 and CYP1B1 follow the same pattern of allosteric binding and best conform with the sigmoid model of Michaelis-Menten equation.

The results of the current study demonstrated that the synthetic analog of 19(S)-HETE is a more potent inhibitor than the synthetic analog of 19(R)-HETE by approximately 2.6 and 2.9 fold for CYP1A1 and CYP1B1, respectively. These findings are strongly in support of our former conclusions that 19(S)-HETE possess stronger inhibitory effect than 19(R)-HETE on the formation of mid-chain HETE (Shoieb and El-Kadi, 2018b). Moreover, the results of the present study come in accordance with what we have reported in our previous study that both enantiomers of 19-HETE are identified as the first endogenous noncompetitive inhibitors of CYP1B1 with the S-enantiomer having more inhibitory effect (Shoieb et al., 2019b). Invention of dual and selective inhibitors of both CYP1A1 and CYP1B1 will allow for development of novel therapeutic modalities that could be used for the prevention and treatment of malignant tumors and CVD (Chang et al., 2010; Zou et al., 2014).

Selectivity towards specific enzymes of CYP1 family has been previously reported. 5-Hydroxy-4′-propargyloxyflavone was characterized as a strongly selective CYP1B1 inhibitor. α-Naphthoflavone-like and 5-hydroxyflavone derivatives have shown preferential inhibition of CYP1A2. Likewise, derivatives of β-Naphthoflavone-like flavone demonstrated eclectic inhibition of CYP1A1 (Liu et al., 2013b). Also, some of the CYP enzymes' inhibitors showed enantio-specificity in their action. For instance, S-

amlodipine demonstrated more potent inhibitory effect on midazolam hydroxylation than R-amlodipine with Ki values of 8.95 μM, 14.85 μM, respectively (Krasulova et al., 2017). Here we report a difference in the inhibitory activity between the synthetic analogues of 19(R)-HETE and 19(S)-HETE as the S-enantiomer demonstrated a stronger inhibitory effect. To further confirm the data obtained from the current studies on recombinant enzymes, we have tested the inhibitory effect of 19(R)-HETE and 19(S)-HETE synthetic analogues on EROD and MROD activity in both RL-14 cell line and human liver microsomes. Consistent with our findings that both analogues have the ability to inhibit CYP1A1 and CYP1B1, the results of these assays demonstrated their inhibitory activity in a cell-based assay and human liver miscrosomes. While there was no significant differences between the R- and S-analogues in inhibiting EROD and MROD activities in RL-14 cells, the S-analogue appears to possess more potent inhibitory effect than the R-analogue on EROD activity in human liver microsomes with approximately 2.7 fold.

The findings of the present study demonstrate that the synthetic analogues of 19(R)-HETE and 19(S)-HETE noncompetitively inhibited CYP1A1 and CYP1B1 enzymatic activity with preferential selectivity of the S-analogue. Taking into consideration their previously reported ability to antagonize the vasoconstrictor effect of 20-HETE (Dakarapu et al., 2019), the current study builds on the beneficial biological activities attributed to these synthetic analogues. Given the crucial role of CYP1A1 and CYP1B1 in cancer and CVD including hypertension, cardiac hypertrophy and heart failure, the current work proposes that the novel synthetic analogues of 19(R)-HETE and 19(S)-

HETE offer new insights for the establishment of pharmacological agents based on 19-HETE structure that could serve as a future clinical drug candidates.

Limitations: While the synthetic analogues of 19-HETE have been tested in a cell-free system such as the human recombinant enzymes and human liver microsomes in addition to RL-14 cell line, their inhibitory effect on CYP1A1 and CYP1B1 has not been investigated on cancer cell lines such as MCF-7 and Hep G2. In order to confirm that these compounds could be used as novel therapeutic modalities in case of cancer. Their actions could be further investigated on cancer cell lines and other models of malignancy.

4.4 Resveratrol Attenuates Angiotensin II-Induced Cellular Hypertrophy through the Inhibition of CYP1B1 and the Cardiotoxic Mid-Chain HETE Metabolites

According to World Health Organization (WHO), CVD are the leading cause of death worldwide, they are responsible for the death of approximately 17.9 million people each year representing 31% of all deaths globally. Accumulating studies have demonstrated that CYP enzymes and their associated AA metabolites play a central role in the maintenance of cardiovascular health and also in the pathogenesis of CVD (Elbekai and El-Kadi, 2006; Ong et al., 2017). Interestingly, CYP1B1 and its associated cardiotoxic mid-chain HETE metabolites have been given a considerable attention due to their evident role in the pathogenesis of CVD such as pathological cardiac hypertrophy, atherosclerosis, hypertension and HF (Malik et al., 2012; Maayah and El-Kadi, 2016b). Moreover, several studies have established an inverse relationship between developing CVD and the dietary consumption of vegetables and fruits. These protective effects have been attributed to polyphenols including flavonoids (such as resveratrol) and stilbenoids that are naturally present in high concentration in heart-healthy diets. Nevertheless, the molecular cardioprotective mechanisms for some of these natural compounds have not yet been elucidated (Hartley et al., 2013; Pallazola et al., 2019).

Resveratrol has been widely studied as a protective agent against many CVD. Also, resveratrol has been demonstrated to possess an inhibitory effect on CYP1B1 (MacPherson and Matthews, 2010). However, the possible beneficial effects of resveratrol as an inhibitor of CYP1B1 in case of cardiac hypertrophy have never been

investigated. Therefore, in the current study, we evaluated the effects of three different concentrations of resveratrol (2, 10 and 50 μM) on cardiac CYP1B1 and its associated cardiotoxic midchain HETE metabolites. Using two different cell lines, we investigated whether resveratrol is able to protect against Ang II-induced cellular hypertrophy. Moreover, we characterized the effect of resveratrol on both transcriptional and translational levels of CYP1B1 and its effect on the metabolite formation of cardiotoxic mid-chain HETEs including 5-, 8-, 9-, 11-, 12- and 15-HETE.

Prior to investigating the effect of resveratrol on Ang II-induced cellular hypertrophy, we tested the effect of increasing concentrations of resveratrol on cell viability. Based on the MTT assay results, resveratrol did not have any toxic effect on cell viability following treatment for 24 h at concentrations of 2–50 μM, suggesting that the concentrations used in the current study have no cytotoxic effects. This comes in agreement with previous studies that reported the safe use of resveratrol at concentration up to 100 μM without observing toxic effects (Chang et al., 2007; Hwang et al., 2008). Therefore, we tested the potential protective effect of resveratrol concentrations (2, 10 and 50 μM) against Ang II-induced cellular hypertrophy. Treatment of both cell lines with Ang II resulted in cellular hypertrophy as evidenced by the elevation in β-MHC/α-MHC ratio and ANP. The concentration of Ang II has been chosen based on previous work done in our lab. RL-14 cells were treated for 24 h with various concentrations of Ang II (0, 1, 2.5, 5, and 10 μM) and cellular hypertrophy markers were measured using real-time PCR. Ang II increased the expression of hypertrophic markers in a concentration-dependent manner. The maximum induction was observed at the highest concentration tested, 10 μM, and it was

associated with increase in the cell surface area without affecting cell viability (Maayah et al., 2015a). In another study, Ang II has been shown to induce CYP1B1 protein expression at 10 μM concentration without negatively affecting cell viability in two different cell lines (Alammari et al., 2020).

The ratio of β-MHC to α-MHC is regarded as a sensitive marker of cardiac hypertrophy in several models (Wang et al.; Chassagne et al., 1993; Qi et al., 2015). The mechanical properties of the cardiac muscle are largely dependent on the expressed isoform of MHC (Alpert et al., 2002). Several studies have reported that α-MHC isoform has greater ATPase activity than β-MHC, and shifting from α-MHC to β-MHC isoform during cardiac hypertrophy is considered as an adaptive response for improved energy economy. However, it also leads to disruption in the contractile machinery of the heart resulting in impaired cardiac function and promoting diseases progression (Gupta, 2007). Furthermore, treatment of cells with Ang II caused a significant increase in ANP, a hypertrophic marker that is found to be increased at the mRNA and protein levels in human hypertrophic hearts supporting the correlation between higher ANP expression and cellular hypertrophy (Kessler-Icekson et al., 2002). In the current study, low concentration of resveratrol (2 μM) was not able to significantly protect against Ang II-induced increase in β-MHC/α-MHC ratio and ANP. On the other hand, higher concentrations (10 and 50 μM) were able to reverse Ang II-mediated increase of hypertrophic markers to nearly control level, with no significant difference between the 2 concentrations. Notably, resveratrol-alone groups did not have any significant effects on the mRNA level of hypertrophic markers in both cell lines, RL-14 and H9c2.

CYP1B1 is a heme-thiolate monooxygenase enzyme that is constitutively expressed in non-hepatic tissues including cardiovascular system, and is responsible for NADPH-dependent metabolism of endobiotics and xenobiotics (Jennings et al., 2014). Moreover, CYP1B1 expression was found to be induced in several experimental models of cardiac hypertrophy such as isoproterenol-induced, pressure overload-induced and Ang II-induced cardiac hypertrophy, pointing out to the role of Ang II in the progression of cardiac hypertrophy (Jennings et al., 2010; El-Sherbeni and El-Kadi, 2014a; Maayah et al., 2017). In the current study, while treatment of cells with Ang II did not show significant effects on mRNA expression level of CYP1B1, it significantly induced the protein expression of CYP1B1. This comes in agreement with previous study that used Ang II as an inducer of cardiac hypertrophy (Elkhatali et al., 2017).

Several cardioprotective effects of resveratrol have been previously reported in various experimental and clinical settings. Experimentally, it attenuated pressure overload-induced cardiac fibrosis and diastolic dysfunction, it protected against chronic intermittent hypoxia-induced cardiac hypertrophy and it also restored the cardiac function and structure in case of pressure overload-induced cardiac hypertrophy (Dong et al., 2014; Guan et al., 2019; Zou et al., 2019). Clinically, multiple reports provided evidences that resveratrol exerts protective effects on the cardiovascular system in patient with coronary artery diseases in the secondary prevention against myocardial infarction. Resveratrol prevented platelet aggregation, reduced LDL cholesterol level and enhanced left ventricular diastolic function (Magyar et al., 2012; Bonnefont-Rousselot, 2016). While several molecular mechanisms have been proposed to be responsible for the

cardioprotective effects of resveratrol, this study is focusing on the effect of resveratrol on CYP1B1 and its associated cardiotoxic mid-chain HETEs. In the current study, resveratrol at concentrations of 10 and 50 μM was able to significantly decrease protein expression of CYP1B1 compared to Ang II group, in both cell lines. This comes in agreement with previous reports demonstrating the inhibitory effect of resveratrol on protein expression of CYP1B1 in several tissues (Ghosh et al., 2018; Huderson et al., 2019). Although resveratrol inhibits CYP1B1 on the protein expression and activity levels, it has been found to inhibit other cytochrome CYP enzymes such as CYP1A1 and CYP1A2 with higher affinity to CYP1A1 (Chun et al., 1999). Moreover, our lab has shown that resveratrol also inhibits the activity of human recombinant CYP4A11, CYP4F2 and CYP4F3B enzymes with higher potency on CYP4F2 (El-Sherbeni and El-Kadi, 2016).

Interestingly, in the current study, the effect of resveratrol alone on the level of mRNA and protein expression of CYP1B1 did not show a positive correlation. While resveratrol alone significantly decreased the level of mRNA of CYP1B1 compared to the control group, it surprisingly increased the level of CYP1B1 protein expression. This discrepancy between the level of mRNA and protein expression is presumably attributed to different reasons. Here we highlight the effect of resveratrol on CYP1B1 on three different levels, mRNA, protein expression levels and the enzymatic activity. CYP1B1 gene transcription is regulated by the aryl hydrocarbon receptor (AhR), resveratrol is a well-known natural inhibitor of AhR, hence decreasing the mRNA expression of CYP1B1 (Saini et al., 2009; Hong et al., 2014). Chemical suppression of constitutive CYP1B1 expression by

resveratrol and other polyphenols has been previously reported (Yang et al., 2008; Rajaraman et al., 2009). Although the mechanism of constitutive CYP1B1 suppression is not fully unravelled, it is proposed to involve the AhR repressor, which acts as a negative modulator of AhR function (Hahn et al., 2009).

On the other hand, the protein level of CYP1B1 was surprisingly increased in the 3 groups treated with resveratrol alone compared to the control group. The discrepancy between the mRNA and protein levels might result from the multi-target profile of resveratrol. For instance, it has been reported that resveratrol possess an estrogenic effect and it was shown to bind to estrogen receptors in cytosolic extracts from breast cancer cell line, MCF-7, and rat uteri (Gehm et al., 1997). Of particular interest, CYP1B1 has been previously reported to be regulated by estrogen via the estrogen receptors and independent from the AhR pathway. Due to the fact that endometrial tissue is highly regulated by estrogens, CYP1B1 protein expression in human endometrial samples was determined using immunohistochemistry. The expression of CYP1B1 was higher in glandular epithelial cells during a proliferative phase than those during a secretory phase, in agreement with the pattern of estrogen secretion in these cells (Tsuchiya et al., 2004). Taken together, these findings may explain why resveratrol has increased the protein expression level of CYP1B1 while decreased the mRNA level. Another point to consider is that there are several complicated and varied post-transcriptional and post-translational mechanisms, including decreased ubiquitination and proteasomal degradation, that may disturb the correlation between mRNA and protein expression levels that would lead to a huge differences in stability and half-lives (De Sousa Abreu et al., 2009).

It is noteworthy to mention that the induction of CYP1B1 protein expression was not associated with an increase in the level of cardiotoxic midchain HETEs. In fact, this observation might be reasoned by the well-known inhibitory effect of resveratrol on the catalytic activity of CYP1B1 (Chang et al., 2000; Mikstacka et al., 2007). Therefore, the increase in the protein expression of CYP1B1 has not led to induction of cellular hypertrophy because it was not associated with increase in the catalytic activity of CYP1B1 as there was no significant increase in the level of cardiotoxic midchain HETEs.

Several lines of evidence previously demonstrated the role of cardiotoxic mid-chain HETEs in the pathogenesis of CVD such cardiac hypertrophy and heart failure. 15-HETE has been reported to elevate rat neonatal cardiomyocytes sensitivity to isoproterenol-induced β-adrenergic response. Moreover, 5-, 12-, and 15-HETE showed a direct inducing effect of cellular hypertrophy in RL-14 cells via MAPK- and NF-κB-dependent pathways (Zhang et al., 2014b; Maayah and El-Kadi, 2016a). Inhibiting the formation of 5-HETE metabolite reduced AngII-induced vascular remodelling and cardiac hypertrophy in mice proposing that inhibition of the 5-HETE formation might be considered as a new therapeutic target in the treatment of cardiac hypertrophy (Revermann et al., 2011). In the present study, treatment of cells with Ang II significantly induced the metabolite formation rate of the majority of mid-chain HETE metabolites including 5-, 8-, 12- and 15-HETE. Interestingly, treatment of cells with resveratrol at concentrations of 10 and 50 μM was able to significantly decrease the metabolite formation rate of mid-chain HETEs compared to Ang II-treated group, in both cell lines. These results are in line with previous study showing that resveratrol improved cardiac

function and exercise performance in MI-induced heart failure through the inhibition of CYP1B1 and cardiotoxic HETE metabolites (Matsumura et al., 2018). Moreover, our laboratory has previously shown that resveratrol was able to inhibit the formation of 20-HETE generated by incubation of arachidonic acid with human liver microsomes. Resveratrol has shown concertation-dependent inhibition of the 20-HETE formation with maximum inhibition I_{max} of 54% and IC_{50} of 3 μM. These data suggests that inhibition of the pro-fibrotic 20-HETE may contribute to the beneficial and protective effects of resveratrol in case of cardiac hypertrophy (El-Sherbeni and El-Kadi, 2016).

In conclusion, the results of the current study showed that resveratrol, at concentrations of 10 and 50 μM, was able to protect against Ang-II- induced cellular hypertrophy as evidenced by significant inhibition of β-MHC/α-MHC ratio and ANP. While Ang II significantly induced the protein expression of CYP1B1 and increased the metabolite formation rate of its associated mid-chain HETEs, resveratrol was able to attenuate Ang II-mediated effects and caused a significant decrease of CYP1B1 protein expression and mid-chain HETEs. Our results provide the first demonstration that resveratrol protects against Ang II-induced cellular hypertrophy, at least in part, through CYP1B1/mid-chain HETEs-dependent mechanism.

Limitations: While there was an anti-hypertrophic effect of resveratrol against cellular hypertrophy and it caused an improvement of the cardiac function, these beneficial effects might not be necessarily due to suppression of midchain HETEs. Owing to the multi-target profile of resveratrol, we acknowledge that further experiments using, for instance, CYP1B1 knockout model are needed in order to demonstrate a causal relationship

between inhibition of CYP1B1 and its associated midchain HETEs and improvement of cardiac function by resveratrol.

4.5 Ameliorative Role of Fluconazole against Abdominal Aortic Constriction-Induced Cardiac Hypertrophy in rats

CYP1B1 is known to be involved in the pathogenesis of several cardiovascular diseases including hypertension and cardiac hypertrophy, through the formation of cardiotoxic metabolites named as mid-chain HETEs. CYP1B1 gene disruption was able to ameliorate deoxycorticosterone acetate-salt-induced hypertension and its associated cardiac hypertrophy in mice. Also, CYP1B1 was proven to mediate angiotensin II-induced vascular smooth muscle cell migration and hypertrophy through the metabolism of arachidonic acid (Zordoky et al., 2008; Yaghini et al., 2010; Jennings et al., 2012). Recently, we have demonstrated that fluconazole, a clinically-approved antifungal agent, decreased the level of mid-chain HETEs in human liver microsomes, inhibited human recombinant CYP1B1 activity in vitro and protected against angiotensin II-induced cellular hypertrophy in H9c2 cells (El-Sherbeni and El-Kadi, 2016; Alammari et al., 2020). To further investigate the possible protective role of fluconazole against experimentally-induced cardiac hypertrophy *in vivo*, we experimentally induced cardiac hypertrophy in rats using AAC model. Our results demonstrated the protective role of fluconazole against AAC-induced cardiac hypertrophy in rats. The anti-hypertrophic effect of fluconazole was associated with a significant inhibition of CYP1B1 at the gene and protein levels and a reduction in the formation rate of mid-chain HETEs. Taken together, the data presented in the current study suggest that fluconazole could be potentially repurposed as a CYP1B1 inhibitor for the protection against cardiac hypertrophy.

For the purpose of mimicking human conditions in case of cardiac hypertrophy, animal models including rats are established using surgical procedures because the hypertrophy is developed over a long period of time. Particularly, abdominal aorta undergoes a distinctive surgical ligation in order to be constricted and to elevate the resistance against the left ventricle, therefore a pressure overload will be developed in the heart. Consequently, this event leads to the pathogenesis of cardiac hypertrophy within weeks after the surgical procedure (Ni et al., 2011; Ku et al., 2016). In the current study, AAC experimental model of cardiac hypertrophy was used, the ligation of the abdominal aorta led to increase in the left ventricular mass and wall measurements. Importantly, the experimental model showed no significant impact on the cardiac function, both systolic and diastolic functions, as evidenced data obtained by the ultrasonic echocardiography that showed there was no change in EF%, %FS or TEI index. The characteristic molecular and echocardiography data pertinent to the AAC model in rats in this study completely aligned with previous studies that have used the same model for induction of cardiac hypertrophy in rats (Phrommintikul et al., 2008; Wang et al., 2015b, 2017).

The initial novel finding of the current study was that fluconazole was able ameliorate the AAC-induced cardiac hypertrophy. This finding is evidenced by the capability of fluconazole to normalize all the changes of the cardiac hypertrophic markers to nearly control levels. To the best of the available evidence, this is the first study to report the anti-hypertrophic effect of fluconazole against cardiac hypertrophy. Based on the results obtained by ultrasonic echocardiography, the anti-hypertrophic effect of fluconazole was not mediated through antihypertensive effect as it was not able to alleviate the pressure

gradient increase that resulted from the aortic constriction. Therefore, here we propose that fluconazole possesses a direct anti-hypertrophic effect against the cardiac hypertrophy. In addition, in agreement with previous studies, AAC surgery led to a significant increase in the HW/TL and HW/BW ratios as well as the mRNA levels of β/α-MHC ratio and ANP (Harada, 1998; Nicks et al., 2020). Importantly, fluconazole was able to protect against the AAC-mediated increase in the aforementioned parameters. In a previous *in vitro* model of cellular hypertrophy, fluconazole protected against angiotensin II-induced cellular hypertrophy as evidenced by a significant down-regulation of hypertrophic markers; β-MHC/α-MHC and as well as cell surface area (Alammari et al., 2020).

It is recommended that fluconazole should be administered with caution to patients with liver dysfunction (Joseph et al., 2019; Zhang et al., 2020a). Its administration has been associated with very rare cases of severe hepatic injuries (Diflucan®, product monograph). The toxic effects have been mostly reversible after discontinuation of the drug. Therefore, in the current study we have assessed whether chronic treatment with fluconazole for four weeks at a dose of 20 mg/kg would have a negative effect on the liver. Fluconazole showed no significant effect on the serum levels of hepatotoxicity markers including ALT, AST and albumin. These results come in agreement with previous studies that reported the safe use of fluconazole in doses similar to that was used in the current study (Diflucan®, product monograph; Somchit et al., 2004; Dadarkar et al., 2011).

Another interesting observation in the current study is that rat groups which received fluconazole gained less weight than control or AAC rats over the five-week period of the experiment. The anorexia effect that results from the chronic treatment with fluconazole has been previously reported. One study that assessed the in vivo toxicity of fluconazole in rats showed that fluconazole-treated group that received 19.6 mg/kg of fluconazole a week for four weeks had a significantly lower body weight gain compared to the control group (Sülo؛lu et al., 2015). Another study assessed the probable adverse effects of chronic fluconazole therapy in a multicenter, dose-escalating study of the therapy of invasive mycoses. The study included 93 adult patients, about 50% of them have received fluconazole for more than 6 months. Anorexia was one of the most common symptoms experienced (3% of patients) (Stevens et al., 1997). Reasons for fluconazole-mediated anorexia and a decrease in weight gain have not been previously reported. Further studies are need in order to elucidate the underlying mechanism of action, as this effect may add a significant benefit in case of CVD (Wing et al., 2011). It is noteworthy to mention that the rats' average weight in the control and AAC groups at baseline was lower than their average weight in the fluconazole-treated sham and fluconazole-treated AAC rats. Therefore, the effect on weight gain, 5 w post-surgery, might not be due to fluconazole treatment and it could be as result of a different rate of growth between the four groups.

Fluconazole is classified as a moderate inhibitor of CYP2C9 and CYP3A4 isoenzymes. Also, it is a strong inhibitor of the isoenzyme CYP2C19 (Malhotra et al., 2011). In the current study, we have carried out a screening study to the effects of fluconazole on a different members of the CYP enzymes families. While fluconazole showed no

significant effect on the mRNA levels of CYP1A1, CYP1A2, CYP2E1, CYP2J3, CYP4A1 or CYP4F6, it significantly decreased the mRNA levels of CYP2C23 (which is catalytically equivalent to human CYP2C9 and CYP2C19) in the heart (Imaoka et al., 2005). In consonance with the results of the current study, fluconazole has been previously reported to decrease the mRNA level of CYP2C23 in rat heart. CYP2C23 represents the major epoxygenase enzyme expressed in the heart of rats , this enzyme is responsible for the formation of EETs via the biotransformation of AA (Roman, 2002). However, immuno-inhibition studies of CYP2C23 in the heart have shown a negligible inhibitory effect on the cardiac epoxygenation activity (El-Sherbeni et al., 2013). Therefore, the inhibitory effect of fluconazole on CYP2C23 is not expected to impact the CYP-mediated AA metabolism into EETs in the heart. Although, fluconazole significantly decreased the mRNA level of CYP3A2, the rat homologue of human CYP3A4 in the heart, this enzyme has a low cardiac expression level and its involvement in the AA metabolism is still unknown (Chaudhary et al., 2009; Miyajima et al., 2020).

Importantly, the ameliorative effect of fluconazole against AAC-induced cardiac hypertrophy was associated with a significant down-regulation of CYP1B1 enzyme at both mRNA and protein levels. In the current study, AAC surgery resulted in a significant induction of CYP1B1 at both mRNA and protein levels, similar to previous studies that showed the same effect in experimentally-induced cardiac hypertrophy models (Jennings et al., 2010; El-Sherbeni and El-Kadi, 2014a; Maayah et al., 2017). Also, CYP1B1 protein expression was found to be involved in the development of other experimental model of CVD including myocardial infarction-induced heart failure, angiotensin II-induced

hypertension, L-arginine methyl ester-induced hypertension and in spontaneously hypertensive rats (Malik et al., 2012; Matsumura et al., 2018). In blood vessels, CYP1B1 is mainly expressed in vascular smooth muscle cell with very low expression in endothelial cells, however shear stress increase its expression in endothelial cells (Conway et al., 2009). This may at least in part illustrate the reason why upregulation of CYP1B1 is associated with the pressure overload inflicted by the AAC surgery. In addition to its effects on CYP1B1 at the mRNA and protein levels, fluconazole has been previously shown to noncompetitively inhibit CYP1B1 at the activity level with K_i value of 130.9 nM (Alammari et al., 2020).

In addition to the induction of CYP1B1, rats with cardiac hypertrophy demonstrated a significant increase in the expression of the formation of mid-chain HETE metabolites. Interestingly, the inhibitory effect of fluconazole on CYP1B1 in the heart was associated with a significant decrease in the level of cardiotoxic mid-chain HETEs including 5-, 12- and 15-HETE. These observations are consistent with previous studies that reported an increase in the level of mid-chain HETEs in AAC-induced cardiac hypertrophy model and an experimental model of heart failure (Maayah et al., 2018; Matsumura et al., 2018). Interestingly, fluconazole ameliorated the AAC-induced CYP1B1 and mid-chain HETE metabolites in rats with cardiac hypertrophy. Therefore, it is speculated that some of the cardioprotective effects of fluconazole are achieved through decreased expression of CYP1B1 and a dependent lowering in the mid-chain HETE metabolites levels.

In summary, the results of the current study highlighted the role of CYP1B1 and its associated cardiotoxic mid-chain HETEs metabolite in the pathogenesis of cardiac

hypertrophy. Also, our data showed that the protective role of fluconazole against pressure overload-induced cardiac hypertrophy is associated with a significant inhibition of CYP1B1 at the gene and protein levels and a reduction in the formation rate of mid-chain HETEs. The findings of the present work highlight the potential repurposing of fluconazole as a CYP1B1 inhibitor for the protection against cardiac hypertrophy and a possible treatment for heart failure in the future.

Limitations: Although fluconazole has showed a protective role against pressure overload-induced cardiac hypertrophy, it might not be the perfect choice for further investigations in clinical trials due to its side effects including hepatotoxicity that may limit its future use. Also, it has multiple drug-drug interactions that lead to slowing down of the metabolism of other drugs due to its inhibitory effect on CYP enzymes. Therefore, we suggest that this study could serve as a proof of concept for future development of more selective agents that has lower number of side effects.

4.6 Summary and general conclusions

In the current work, our goal was to investigate the possible cardioprotective roles of a group of CYP-mediated AA metabolites known as subterminal HETEs in case of cardiac hypertrophy. Also, we aimed to test the potential of some clinically-approved drugs to be repurposed, and potentially could be used as pharmacological CYP-modulators in the prevention and treatment of CVD including cardiac hypertrophy and HF.

First, we investigated the effects of 19(R)-HETE and 19(S)-HETE on cardiac CYP enzymes as well as their associated AA metabolites, elucidated the pathway involved and examined whether both enantiomers of 19-HETE have a cardioprotective effect in an *in vitro* model of cellular hypertrophy. We have demonstrated that both enantiomers of 19-HETE protected against Ang II-induced cardiac hypertrophy via decreasing the level of cardiotoxic mid-chain HETEs, inhibiting the catalytic activity of CYP1B1, decreasing the protein expression level of LOX and COX-2 enzymes and decreasing the mRNA expression level of pro-inflammatory markers IL-6 and IL-8. It is noteworthy that the S-enantiomer demonstrated more protection than the R-enantiomer reflected by its ability to decrease the level of 5-HETE, decrease the protein expression of 15-LOX, increase the protein expression level of CYP4F2 and CYP4F11 and its preferential effect on IL-6 and IL-8 compared to the R-enantiomer.

The results of the previous study have prompted us to perform another study to obtain a comprehensive understanding of the protective role of R- and S-enantiomers of 19-HETE in case of cardiac hypertrophy, in this study we examined the inhibitory effect of both enantiomers on human recombinant CYP1B1 enzyme using EROD assay. CYP1B1 is

considered one of the important CYPs. It is involved in the metabolism of many endobiotics, xenobiotics and in the activation pathways of various procarcinogens in addition to the generation of cardiotoxic mid-chaun HETEs in the heart. We have showed that both enantiomers of 19-HETE noncompetitively inhibited CYP1B1 enzymatic activity with higher potency of the S-enantiomer. The current work suggests that 19(R)-HETE and 19(S)-HETE could be considered as a novel therapeutic modality in the treatment of cardiac hypertrophy, HF and cancer. Moreover, given that a noncompetitive inhibitor might bind to the enzyme regulatory region, 19(R)-HETE and 19(S)-HETE could be considered to unravel the obscure mechanisms of CYP1B1 enzymatic reaction.

Despite the discovered beneficial effects of subterminal HETEs, they are metabolically labile agents. This would limit their usefulness as a possible therapeutic modality experimentally or clinically. Therefore, we have tested the potential inhibitory effect of synthetic 19-HETE analogs (R- and S-analogues) on CYP1A1, CYP1A2 and CYP1B1 recombinant human enzymes. Also, we have investigated whether they possess an inhibitory effect on a major CYP enzyme, CYP3A4. The results showed that the synthetic analogues of 19(R)-HETE and 19(S)-HETE noncompetitively inhibited CYP1A1 and CYP1B1 enzymatic activity with preferential selectivity of the S-analogue. Given the crucial role of CYP1A1 and CYP1B1 in cancer and CVD including hypertension, cardiac hypertrophy and HF, the current work proposes that the novel synthetic analogues of 19(R)-HETE and 19(S)-HETE offer new insights for the establishment of pharmacological agents based on 19-HETE structure that could serve as a future clinical drug candidates.

In an attempt to repurpose some of the available clinically-approved drugs, we have investigated whether resveratrol is able to protect against Ang II-induced cellular hypertrophy, and also participated in a study to test its protective role against HF in a mouse model of MI-induced HF. We have demonstrated that resveratrol was able to protect against Ang-II- induced cellular hypertrophy as evidenced by significant inhibition of β-MHC/α-MHC ratio and ANP. While Ang II significantly induced the protein expression of CYP1B1 and increased the metabolite formation rate of its associated mid-chain HETEs, resveratrol was able to attenuate Ang II-mediated effects and caused a significant decrease of CYP1B1 protein expression and mid-chain HETEs. Also, the in vivo work has showed that low dose resveratrol reduces the severity of MI-induced HF, at least in part, through the inhibition of CYP1B1 and cardiotoxic mid-chain HETE metabolites.

Lastly, we tested the potential ameliorative role of another pharmacological CYP-modulator, fluconazole, against cardiac hypertrophy in an *in vivo* model of AAC-induced cardiac hypertrophy in rats. The results of this study highlighted the role of CYP1B1 and its associated cardiotoxic mid-chain HETEs metabolite in the pathogenesis of cardiac hypertrophy. Also, they showed that the protective role of fluconazole against pressure overload-induced cardiac hypertrophy is associated with a significant inhibition of CYP1B1 at the gene and protein levels and a reduction in the formation rate of mid-chain HETEs. The findings of this work highlight the potential repurposing of fluconazole as a CYP1B1 inhibitor for the protection against cardiac hypertrophy and a possible treatment for heart failure in the future.

In the current work, both resveratrol and fluconazole had a significant inhibition of CYP1B1 protein expression in addition to their inhibitory effect on the formation of cardiotoxic mid-chain HETEs. Of interest, members of mid-chain HETEs including 5-, 12-, 8-, and 15-HETE showed the capability to induce cellular hypertrophy in RL-14 cells via MAPK- and NF-κB-dependent pathways (Zhang et al., 2014a; Maayah and El-Kadi, 2016a). Mounting evidence has demonstrated the detrimental role of prolonged activation of NF-κB in the pathogenesis of cardiac hypertrophy and HF. In that sense, $p50^{-/-}$ mice showed ameliorated cardiac hypertrophy following myocardial infarction or during tumour necrosis factor (TNF) α-induced cardiomyopathy (Kawamura et al., 2005; Kawano et al., 2006). In addition, treatment of RL-14 cells with 5-, 8-, 12-, and 15-HETE resulted in a significant increase of of NF-κB binding activity through its p50 and p65 subunits and evident NF-κB-dependent induction of the cellular hypertrophy (Maayah et al., 2015a; Maayah and El-Kadi, 2016a).

In addition, mid-chain HETEs have been demonstrated to induce cardiac hypertrophy through MAPK, this pathway can be classified into three major subfamilies: ERKs, JNKs, and p38 MAPKs (Roux and Blenis, 2004). Interestingly, Harris et al. have showed that inhibition of the ERK pathway successfully prevented against hypertrophy and fetal gene induction in response to pressure overload (Harris et al., 2004). Also, constitutive expression of MKP-1, counteracting factor of MAPKs, in cultured primary cardiomyocytes using adenovirus-mediated gene transfer halted the activation of p38, JNK1/2, and ERK1/2 and protected against agonist-induced hypertrophy. Interestingly, incubation of RL-14 cells with mid-chain HETEs including 5-, 8-, 12- and 15-HETE

significantly induced the phosphorylated ERK1/2 while they showed no significant changes on phosphorylated P38 or JNK (Maayah et al., 2015a; Maayah and El-Kadi, 2016a). Therefore, the protective action of both resveratrol and fluconazole against cardiac hypertrophy and HF could be attributed to their inhibitory effect on CYP1B1 and subsequent decrease in the level of mid-chain HETEs. Inhibition of the formation of these cardiotoxic metabolites ameliorated the mid-chain HETEs-mediated activation of MAPK- and NF-κB pathways and prevented against cardiac hypertrophy and HF.

The protective effect of resveratrol and fluconazole, in case of cardiac hypertrophy and HF, might have been also mediated through other signalling pathways due to the multi-target profile of both drugs, especially resveratrol. For instance, AMPK activation has been reported to be necessary for the antihypertrophic effects of resveratrol, as resveratrol showed less efficacy at inhibiting hypertrophic signaling in AMPK null mouse embryonic fibroblasts. In addition, the antihypertrophic effect of resveratrol was negated by the AMPK inhibitor, compound C (Chan et al., 2008; Thandapilly et al., 2011). Activation of AMPK is mediated by the liver kinase B1 (LKB1), the upstream activator kinase of AMPK. Inhibition of LKB1 results in a decrease in AMPK phosphorylation and subsequent increase in cardiomyocyte hypertrophy (Dolinsky et al., 2009). Interestingly, resveratrol-mediated activation of AMPK is regulated by activation of another target of resveratrol, SIRT1. Activation of SIRT1 by resveratrol has been shown to be associated with a reduction in cardiac hypertrophy (Sundaresan et al., 2011). For instance, treatment of rats with resveratrol led to enhancement of the cardiac function and higher expression levels of SIRT1 in an MI model of heart failure (Gu et al., 2014). Additionally, resveratrol

protected against cardiac hypertrophy in a diabetic model of cardiomyopathy in mice through activation of SIRT1 and subsequent augmentation of autophagy (Wang et al., 2014a).

As mentioned earlier, several reports have previously demonstrated that activation of the PI3K/AKT/mTOR signaling pathway is associated with cardiac hypertrophy. Both resveratrol and fluconazole have been reported to inhibit this signalling pathway. For example, in a chronic intermittent hypoxia-induced cardiac hypertrophy in rats, resveratrol treatment was able to inhibit the PI3K/AKT/mTOR signalling pathway and restored autophagy levels in a heart of cardiac hypertrophy rats (Guan et al., 2019). Also, azole antifungal agents have been demonstrated to induce apoptosis, cell cycle and autophagy by suppressing mTOR via the inhibition of PI3K/Akt pathway in human breast cancer cells, suggesting that fluconazole might also exert its antihypertrophic effect through the same pathway (Park et al., 2018). The following diagram highlights the possible signalling pathways through which resveratrol and fluconazole prevented against cardiac hypertrophy and HF.

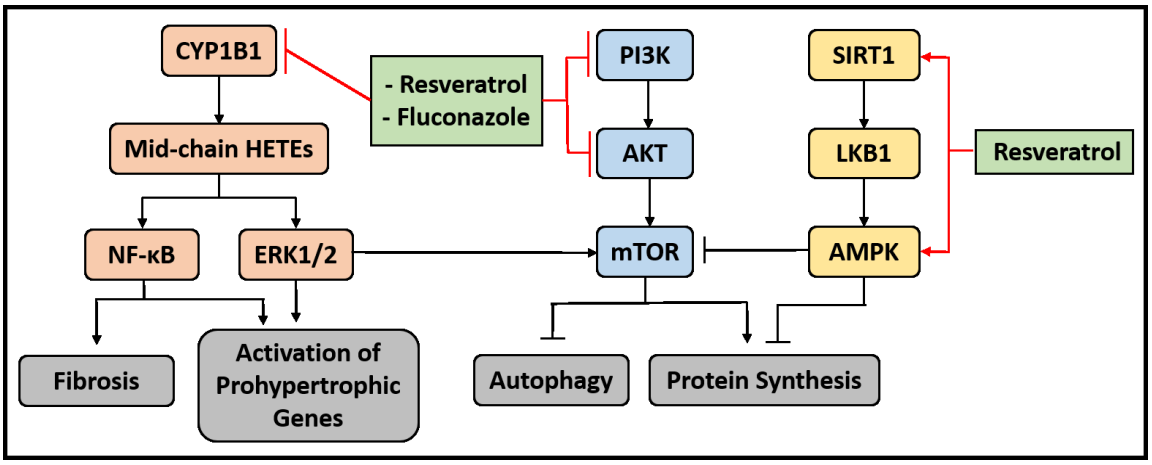

Figure 4.1. Schematic diagram showing the possible signalling pathways through which resveratrol and fluconazole prevented against cardiac hypertrophy and HF

4.7 Future Research Directions

The findings of the present work have focused on revealing the cardioprotective effects of subterminal HETEs against the progression of cardiac hypertrophy and their inhibitory effect on CYP1B1 and its associated AA metabolites. Also, we have identified new promising therapeutic targets in case of cardiac hypertrophy and HF, and presented a novel therapeutic strategy based on the repurposing of clinically-approved drugs to modulate CYP-mediated AA metabolism in humans. However, further studies are needed in order to elaborate more on the underlying mechanisms and translate these findings into clinical practice. Therefore, we propose the following interesting points:

1. To investigate whether cardiac hypertrophy has an effect on the formation of subterminal HETEs enantiomers, and if they have different ratios compared to healthy hearts.

2. To confirm our *in vitro* protective role of synthetic 19-HETE analogs (R- and S-analogues) against cardiac hypertrophy and HF in *in vivo* models of these conditions. In addition to the assessment of their effect on CYP1B1 and its associated AA metabolites including mid-chain HETEs.

3. To carry out *in silico* screening to identify novel bioactive molecules, from large compound library collections, that possess the capability to selectively modulate CYP1B1 and could be used as lead compounds for further development of new selective CYP1B1 modulators.

4. To investigate the protective role of resveratrol against cardiac hypertrophy in animal models of the condition such as AAC-mediated, isoproterenol-induced and Ang II-

induced cardiac hypertrophy. The effect of resveratrol on CYP1B1 and its associated mid-chain HETE metabolites should be confirmed.

5. To explore the mechanisms by which fluconazole inhibits CYP1B1 at the gene and protein levels and protect against cardiac hypertrophy.

6. To investigate whether people who are getting resveratrol as a nutritional supplement or fluconazole as an antifungal agent have a lower risk of developing cardiac hypertrophy. Retrospective cohort studies could be carried out using the immediately available information in databases. The results of this work might prompt to further investigate the effect of resveratrol and fluconazole in randomized controlled trials.

REFERENCES

Abbate, A., Arena, R., Abouzaki, N., Tassell, B.W. Van, Canada, J., Shah, K., et al. (2015). Heart failure with preserved ejection fraction: Refocusing on diastole. Int. J. Cardiol. *179*: 430–440.

Abdelgawad, I.Y., Grant, M.K.O., and Zordoky, B.N. (2019). Leveraging the cardio-protective and anticancer properties of resveratrol in cardio-oncology. Nutrients *11*:.

Aboutabl, M.E., Zordoky, B.N.M., and El-Kadi, A.O.S. (2009). 3-Methylcholanthrene and benzo(a)pyrene modulate cardiac cytochrome P450 gene expression and arachidonic acid metabolism in male Sprague Dawley rats. Br. J. Pharmacol. *158*: 1808–1819.

Adeagbo, A.S. (1997). Endothelium-derived hyperpolarizing factor: characterization as a cytochrome P450 1A-linked metabolite of arachidonic acid in perfused rat mesenteric prearteriolar bed. Am. J. Hypertens. *10*: 763–71.

Agbor, L.N., Walsh, M.T., Boberg, J.R., and Walker, M.K. (2012). Elevated blood pressure in cytochrome P4501A1 knockout mice is associated with reduced vasodilation to omega-3 polyunsaturated fatty acids. Toxicol. Appl. Pharmacol. *264*: 351–60.

Ai, D., Pang, W., Li, N., Xu, M., Jones, P.D., Yang, J., et al. (2009). Soluble epoxide hydrolase plays an essential role in angiotensin II-induced cardiac hypertrophy. Proc. Natl. Acad. Sci. U. S. A. *106*: 564–569.

Aiello, E.A., Villa-Abrille, M.C., Dulce, R.A., Cingolani, H.E., and Pérez, N.G. (2005). Endothelin-1 stimulates the Na+/Ca2+ exchanger reverse mode through intracellular Na+ (Na+i) - Dependent and Na+i-independent pathways. Hypertension *45*: 288–293.

Aikawa, R., Nagai, T., Tanaka, M., Zou, Y., Ishihara, T., Takano, H., et al. (2001). Reactive oxygen species in mechanical stress-induced cardiac hypertrophy. Biochem. Biophys. Res. Commun. *289*: 901–907.

Alammari, A.H., Shoieb, S.M., Maayah, Z.H., and El-Kadi, A.O.S. (2020). Fluconazole Represses Cytochrome P450 1B1 and Its Associated Arachidonic Acid Metabolites in the Heart and Protects Against Angiotensin II-Induced Cardiac Hypertrophy. J. Pharm. Sci. *109*: 2321–2335.

Almeida, L., Vaz-da-Silva, M., Falcão, A., Soares, E., Costa, R., Loureiro, A.I., et al. (2009). Pharmacokinetic and safety profile of trans-resveratrol in a rising multiple-dose study in healthy volunteers. Mol. Nutr. Food Res. *53*:.

Alonso-Galicia, M., Falck, J.R., Reddy, K.M., and Roman, R.J. (1999). 20-HETE agonists and antagonists in the renal circulation. Am. J. Physiol. *277*: F790-6.

Alpert, N.R., Brosseau, C., Federico, A., Krenz, M., Robbins, J., and Warshaw, D.M. (2002). Molecular mechanics of mouse cardiac myosin isoforms. Am. J. Physiol. - Hear. Circ. Physiol. *283*: H1446-54.

Alsaad, A.M.S., Zordoky, B.N.M., Tse, M.M.Y., and El-Kadi, A.O.S. (2013). Drug Metabolism Reviews Role of cytochrome P450-mediated arachidonic acid metabolites

in the pathogenesis of cardiac hypertrophy Role of cytochrome P450-mediated arachidonic acid metabolites in the pathogenesis of cardiac hypertrophy. Drug Metab Rev *45*: 173–195.

Altara, R., Giordano, M., Nordén, E.S., Cataliotti, A., Kurdi, M., Bajestani, S.N., et al. (2017). Targeting Obesity and Diabetes to Treat Heart Failure with Preserved Ejection Fraction. Front. Endocrinol. (Lausanne). *8*: 160.

Althurwi, H.N., Maayah, Z.H., Elshenawy, O.H., and El-Kadi, A.O.S. (2015). Early changes in cytochrome P450s and their associated arachidonic acid metabolites play a crucial role in the initiation of cardiac hypertrophy induced by isoproterenol. Drug Metab. Dispos. *43*: 1254–1266.

Anderson, G., and Mazzoccoli, G. (2019a). Left ventricular hypertrophy: Roles of mitochondria CYP1B1 and melatonergic pathways in co-ordinatingwider pathophysiology. Int. J. Mol. Sci. *20*:.

Anderson, G., and Mazzoccoli, G. (2019b). Left ventricular hypertrophy: Roles of mitochondria CYP1B1 and melatonergic pathways in co-ordinatingwider pathophysiology. Int. J. Mol. Sci. *20*:.

Androutsopoulos, V.P., Papakyriakou, A., Vourloumis, D., and Spandidos, D.A. (2011). Comparative CYP1A1 and CYP1B1 substrate and inhibitor profile of dietary flavonoids. Bioorg. Med. Chem. *19*: 2842–2849.

Androutsopoulos, V.P., Tsatsakis, A.M., and Spandidos, D.A. (2009). Cytochrome P450 CYP1A1: Wider roles in cancer progression and prevention. BMC Cancer *9*: 1–17.

Anwar-Mohamed, A., Elshenawy, O.H., El-Sherbeni, A.A., Abdelrady, M., and El-Kadi, A.O.S. (2014). Acute arsenic treatment alters arachidonic acid and its associated metabolite levels in the brain of C57Bl/6 mice. Can. J. Physiol. Pharmacol. *92*: 693–702.

Aoyagi, T., and Matsui, T. (2011). Phosphoinositide-3 Kinase Signaling in Cardiac Hypertrophy and Heart Failure. Curr. Pharm. Des. *17*: 1818–1824.

Apostolakis, S., Vogiatzi, K., Amanatidou, V., and Spandidos, D.A. (2009). Interleukin 8 and cardiovascular disease. Cardiovasc. Res. *84*: 353–360.

Asakawa, M., Takano, H., Nagai, T., Uozumi, H., Hasegawa, H., Kubota, N., et al. (2002). Peroxisome proliferator-activated receptor γ plays a critical role in inhibition of cardiac hypertrophy in vitro and in vivo. Circulation *105*: 1240–1246.

Baartscheer, A., Schumacher, C.A., Borren, M.M.G.J. Van, Belterman, C.N.W., Coronel, R., Opthof, T., et al. (2005). Chronic inhibition of Na +/H +-exchanger attenuates cardiac hypertrophy and prevents cellular remodeling in heart failure. Cardiovasc. Res. *65*: 83–92.

Badal, S., and Delgoda, R. (2014). Role of the modulation of CYP1A1 expression and

activity in chemoprevention. J. Appl. Toxicol. *34*: 743–753.

Bai, H.W., and Zhu, B.T. (2008). Strong activation of cyclooxygenase I and II catalytic activity by dietary bioflavonoids. J Lipid Res *49*: 2557–2570.

Bak, M.I., and Ingwall, J.S. (2003). Contribution of Na+/H+ exchange to Na+ overload in the ischemic hypertrophied hyperthyroid rat heart. Cardiovasc. Res. *57*: 1004–1014.

Bak, S., Beisson, F., Bishop, G., Hamberger, B., Höfer, R., Paquette, S., et al. (2011). Cytochromes p450. Arab. B. *9*: e0144.

Bannenberg, G.L., Chiang, N., Ariel, A., Arita, M., Tjonahen, E., Gotlinger, K.H., et al. (2005). Molecular circuits of resolution: formation and actions of resolvins and protectins. J. Immunol. *174*: 5884c – 5884.

Barauna, V.G., Rosa, K.T., Irigoyen, M.C., and Oliveira, E.M. de (2007). Effects of resistance training on ventricular function and hypertrophy in a rat model. Clin. Med. Res. *5*: 114–120.

Barouki, R., and Morel, Y. (2001). Repression of cytochrome P450 1A1 gene expression by oxidative stress: Mechanisms and biological implications. Biochem. Pharmacol. *61*: 511–516.

Bass-Stringer, S., Tai, C.M.K., and McMullen, J.R. (2021). IGF1–PI3K-induced physiological cardiac hypertrophy: Implications for new heart failure therapies, biomarkers, and predicting cardiotoxicity. J. Sport Heal. Sci.

Bednar, M.M., Gross, C.E., Balazy, M., and Falck, J.R. (1997). Antineutrophil strategies. Neurology *49*: S20-2.

Bednar, M.M., Gross, C.E., Balazy, M.K., Belosludtsev, Y., Colella, D.T., Falck, J.R., et al. (2000a). 16(R)-hydroxy-5,8,11,14-eicosatetraenoic acid, a new arachidonate metabolite in human polymorphonuclear leukocytes. Biochem. Pharmacol. *60*: 447–55.

Bednar, M.M., Gross, C.E., Russell, S.R., Fuller, S.P., Ahern, T.P., Howard, D.B., et al. (2000b). 16(R)-hydroxyeicosatetraenoic acid, a novel cytochrome P450 product of arachidonic acid, suppresses activation of human polymorphonuclear leukocyte and reduces intracranial pressure in a rabbit model of thromboembolic stroke. Neurosurgery *47*: 1410–8; discussion 1418-9.

Beedanagari, S.R., Bebenek, I., Bui, P., and Hankinson, O. (2009). Resveratrol inhibits dioxin-induced expression of human CYP1A1 and CYP1B1 by inhibiting recruitment of the aryl hydrocarbon receptor complex and RNA polymerase II to the regulatory regions of the corresponding genes. Toxicol. Sci. *110*: 61–67.

Behrendorff, J.B.Y.H. (2021). Reductive Cytochrome P450 Reactions and Their Potential Role in Bioremediation. Front. Microbiol. *0*: 837.

Benassayag, C., Mignot, T.M., Haourigui, M., Civel, C., Hassid, J., Carbonne, B., et al. (1997). High polyunsaturated fatty acid, thromboxane A2, and alpha-fetoprotein

concentrations at the human feto-maternal interface. J. Lipid Res. *38*: 276–86.

Benjamin, E.J., Blaha, M.J., Chiuve, S.E., Cushman, M., Das, S.R., Deo, R., et al. (2017). Heart Disease and Stroke Statistics'2017 Update: A Report from the American Heart Association. Circulation *135*: e146–e603.

Bergmann, O., Zdunek, S., Felker, A., Salehpour, M., Alkass, K., Bernard, S., et al. (2015). Dynamics of Cell Generation and Turnover in the Human Heart. Cell *161*: 1566–1575.

Berlo, J.H. Van, Maillet, M., and Molkentin, J.D. (2013). Signaling effectors underlying pathologic growth and remodeling of the heart. J. Clin. Invest. *123*: 37–45.

Berman, A.Y., Motechin, R.A., Wiesenfeld, M.Y., and Holz, M.K. (2017). The therapeutic potential of resveratrol: a review of clinical trials. Npj Precis. Oncol. *1*: 1–9.

Bernardo, B.C., Weeks, K.L., Pretorius, L., and McMullen, J.R. (2010). Molecular distinction between physiological and pathological cardiac hypertrophy: experimental findings and therapeutic strategies. Pharmacol Ther *128*: 191–227.

Bhateria, M., Ramakrishna, R., Puttrevu, S.K., Saxena, A.K., and Bhatta, R.S. (2016). Enantioselective inhibition of Cytochrome P450-mediated drug metabolism by a novel antithrombotic agent, S002-333: Major effect on CYP2B6. Chem. Biol. Interact. *256*: 257–265.

Bièche, I., Narjoz, C., Asselah, T., Vacher, S., Marcellin, P., Lidereau, R., et al. (2007). Reverse transcriptase-PCR quantification of mRNA levels from cytochrome (CYP)1, CYP2 and CYP3 families in 22 different human tissues. Pharmacogenet. Genomics *17*: 731–42.

Bonnefont-Rousselot, D. (2016). Resveratrol and cardiovascular diseases. Nutrients *8*:.

Braz, J.C., Bueno, O.F., Windt, L.J. De, and Molkentin, J.D. (2002). PKCα regulates the hypertrophic growth of cardiomyocytes through extracellular signal-regulated kinase1/2 (ERK1/2). J. Cell Biol. *156*: 905–919.

Braz, J.C., Gregory, K., Pathak, A., Zhao, W., Sahin, B., Klevitsky, R., et al. (2004). PKC-α regulates cardiac contractility and propensity toward heart failure. Nat. Med. *10*: 248–254.

Brocks, D.R. (2006). Drug disposition in three dimensions: An update on stereoselectivity in pharmacokinetics. Biopharm. Drug Dispos. *27*: 387–406.

Brown, D.W., Giles, W.H., and Croft, J.B. (2000). Left ventricular hypertrophy as a predictor of coronary heart disease mortality and the effect of hypertension. Am Hear. J *140*: 848–856.

Bubb, K.J., Wen, H., Panayiotou, C.M., Finsterbusch, M., Khan, F.J., Chan, M. V., et al. (2013). Activation of neuronal transient receptor potential vanilloid 1 channel underlies 20-hydroxyeicosatetraenoic acid-induced vasoactivity: Role for protein kinase

A. Hypertension *62*: 426–433.

Bueno, O.F., Windt, L.J. De, Lim, H.W., Tymitz, K.M., Witt, S.A., Kimball, T.R., et al. (2001). The dual-specificity phosphatase MKP-1 limits the cardiac hypertrophic response in vitro and in vivo. Circ. Res. *88*: 88–96.

Bui, A.L., Horwich, T.B., and Fonarow, G.C. (2011). Epidemiology and risk profile of heart failure. Nat. Rev. Cardiol. *8*: 30–41.

Bui, N.T., Livolsi, A., Peyron, J.F., and Prehn, J.H.M. (2001). Activation of nuclear factor κB and bcl-x survival gene expression by nerve growth factor requires tyrosine phosphorylation of IκBα. J. Cell Biol. *152*: 753–763.

Byrd, B.F., Abraham, T.P., Buxton, D.B., Coletta, A. V., Cooper, J.H.S., Douglas, P.S., et al. (2015). A Summary of the American Society of Echocardiography Foundation Value-Based Healthcare: Summit 2014: The Role of Cardiovascular Ultrasound in the New Paradigm. J. Am. Soc. Echocardiogr. *28*: 755–769.

Caldwell, J. (1996). Importance of stereospecific bioanalytical monitoring in drug development. J. Chromatogr. A *719*: 3–13.

Caligiuri, S.P.B., Rodriguez-Leyva, D., Aukema, H.M., Ravandi, A., Weighell, W., Guzman, R., et al. (2016). Dietary Flaxseed Reduces Central Aortic Blood Pressure Without Cardiac Involvement but Through Changes in Plasma Oxylipins. Hypertens. (Dallas, Tex. 1979) *68*: 1031–8.

Camilión De Hurtado, M.C., Portiansky, E.L., Pérez, N.G., Rebolledo, O.R., and Cingolani, H.E. (2002). Regression of cardiomyocyte hypertrophy in SHR following chronic inhibition of the Na+/H+ exchanger. Cardiovasc. Res. *53*: 862–868.

Campo, V.L., Bernardes, L.S.C., and Carvalho, I. (2009). Stereoselectivity in drug metabolism: molecular mechanisms and analytical methods. Curr Drug Metab *10*: 188–205.

Capdevila, J.H., Falck, J.R., and Estabrook, R.W. (1992). Cytochrome P450 and the arachidonate cascade. FASEB J. *6*: 731–6.

Cargnello, M., and Roux, P.P. (2011). Activation and Function of the MAPKs and Their Substrates, the MAPK-Activated Protein Kinases. Microbiol. Mol. Biol. Rev. *75*: 50–83.

Carlson, S.E., and Colombo, J. (2016). Docosahexaenoic Acid and Arachidonic Acid Nutrition in Early Development. Adv. Pediatr. *63*: 453–71.

Carroll, M.A., Balazy, M., Huang, D.D., Rybalova, S., Falck, J.R., and McGiff, J.C. (1997). Cytochrome P450-derived renal HETEs: storage and release. Kidney Int. *51*: 1696–702.

Carroll, M.A., Balazy, M., Margiotta, P., Huang, D.D., Falck, J.R., and McGiff, J.C. (1996). Cytochrome P-450-dependent HETEs: profile of biological activity and

stimulation by vasoactive peptides. Am. J. Physiol. *271*: R863-9.

Chadderdon, S.M., Belcik, J.T., Bader, L., Kievit, P., Grove, K.L., and Lindner, J.R. (2016). Vasoconstrictor eicosanoids and impaired microvascular function in inactive and insulin-resistant primates. Int. J. Obes. (Lond). *40*: 1600–1603.

Chahine, M., Bkaily, G., Nader, M., Al-Khoury, J., Jacques, D., Beier, N., et al. (2005). NHE-1-dependent intracellular sodium overload in hypertrophic hereditary cardiomyopathy: Prevention by NHE-1 inhibitor. J. Mol. Cell. Cardiol. *38*: 571–582.

Chan, A.Y.M., Dolinsky, V.W., Soltys, C.L.M., Viollet, B., Baksh, S., Light, P.E., et al. (2008). Resveratrol Inhibits Cardiac Hypertrophy via AMP-activated Protein Kinase and Akt. J. Biol. Chem. *283*: 24194–24201.

Chandrasekharan, J.A., Marginean, A., and Sharma-Walia, N. (2016). An insight into the role of arachidonic acid derived lipid mediators in virus associated pathogenesis and malignancies. Prostaglandins Other Lipid Mediat. *126*: 46–54.

Chang, E.P., Kim, M.J., Jong, H.L., Min, B. Il, Bae, H., Choe, W., et al. (2007). Resveratrol stimulates glucose transport in C2C12 myotubes by activating AMP-activated protein kinase. Exp. Mol. Med. *39*: 222–229.

Chang, T.K., Lee, W.B., and Ko, H.H. (2000). Trans-resveratrol modulates the catalytic activity and mRNA expression of the procarcinogen-activating human cytochrome P450 1B1. Can. J. Physiol. Pharmacol. *78*: 874–81.

Chang, T.K.H., Chen, J., Yang, G., and Yeung, E.Y.H. (2010). Inhibition of procarcinogen-bioactivating human CYP1A1, CYP1A2 and CYP1B1 enzymes by melatonin. J. Pineal Res. *48*: 55–64.

Chassagne, C., Wisnewsky, C., and Schwartz, K. (1993). Antithetical accumulation of myosin heavy chain but not α-actin mRNA isoforms during early stages of pressure-overload-induced rat cardiac hypertrophy. Circ. Res. *72*: 857–864.

Chaudhary, A., and Willett, K.L. (2006). Inhibition of human cytochrome CYP1 enzymes by flavonoids of St. John's wort. Toxicology *217*: 194–205.

Chaudhary, K.R., Batchu, S.N., and Seubert, J.M. (2009). Cytochrome P450 enzymes and the heart. IUBMB Life *61*: 954–960.

Chen, C., Zou, L.X., Lin, Q.Y., Yan, X., Bi, H.L., Xie, X., et al. (2019). Resveratrol as a new inhibitor of immunoproteasome prevents PTEN degradation and attenuates cardiac hypertrophy after pressure overload. Redox Biol. *20*: 390–401.

Chen, X.-P., Tan, Z.-R., Huang, S.-L., Huang, Z., Ou-Yang, D.-S., and Zhou, H.-H. (2003). Isozyme-specific induction of low-dose aspirin on cytochrome P450 in healthy subjects. Clin. Pharmacol. Ther. *73*: 264–71.

Chen, Y., Zeng, L., Wang, Y., Tolleson, W.H., Knox, B., Chen, S., et al. (2017). The expression, induction and pharmacological activity of CYP1A2 are post-

transcriptionally regulated by microRNA hsa-miR-132-5p. Biochem. Pharmacol. *145*: 178–191.

Chen, Z.-H. (2004). Resveratrol inhibits TCDD-induced expression of CYP1A1 and CYP1B1 and catechol estrogen-mediated oxidative DNA damage in cultured human mammary epithelial cells. Carcinogenesis *25*: 2005–2013.

Cheng, J., Ou, J.-S., Singh, H., Falck, J.R., Narsimhaswamy, D., Pritchard, K.A., et al. (2008). 20-Hydroxyeicosatetraenoic acid causes endothelial dysfunction via eNOS uncoupling. Am. J. Physiol. Circ. Physiol. *294*: H1018–H1026.

Choudhary, D., Jansson, I., Stoilov, I., Sarfarazi, M., and Schenkman, J.B. (2004). Metabolism of retinoids and arachidonic acid by human and mouse cytochrome P450 1B1. Drug Metab. Dispos. *32*: 840–847.

Choudhary, D., Jansson, I., Stoilov, I., Sarfarazi, M., and Schenkman, J.B. (2005). Expression patterns of mouse and human CYP orthologs (families 1-4) during development and in different adult tissues. Arch. Biochem. Biophys. *436*: 50–61.

Chuang, S.S., Helvig, C., Taimi, M., Ramshaw, H.A., Collop, A.H., Amad, M., et al. (2004). CYP2U1, a novel human thymus- and brain-specific cytochrome P450, catalyzes omega- and (omega-1)-hydroxylation of fatty acids. J. Biol. Chem. *279*: 6305–14.

Chun, Y.-J., Oh, Y.-K., Kim, B.J., Kim, D., Kim, S.S., Choi, H.-K., et al. (2009). Potent inhibition of human cytochrome P450 1B1 by tetramethoxystilbene. Toxicol. Lett. *189*: 84–89.

Chun, Y.J., Kim, M.Y., and Guengerich, F.P. (1999). Resveratrol is a selective human cytochrome P450 1A1 inhibitor. Biochem. Biophys. Res. Commun. *262*: 20–24.

Chung, E., Heimiller, J., and Leinwand, L.A. (2012). Distinct cardiac transcriptional profiles defining pregnancy and exercise. PLoS One *7*: e42297.

Ciepiela, P., Bączkowski, T., Drozd, A., Kazienko, A., Stachowska, E., and Kurzawa, R. (2015). Arachidonic and linoleic acid derivatives impact oocyte ICSI fertilization--a prospective analysis of follicular fluid and a matched oocyte in a 'one follicle--one retrieved oocyte--one resulting embryo' investigational setting. PLoS One *10*: e0119087.

Cingolani, H.E., and Ennis, I.L. (2007). Sodium-hydrogen exchanger, cardiac overload, and myocardial hypertrophy. Circulation *115*: 1090–1100.

Cione, E., Torre, C. La, Cannataro, R., Caroleo, M.C., Plastina, P., and Gallelli, L. (2019). Quercetin, Epigallocatechin Gallate, Curcumin, and Resveratrol: From Dietary Sources to Human MicroRNA Modulation. Molecules *25*:.

Conway, D.E., Sakurai, Y., Weiss, D., Vega, J.D., Taylor, W.R., Jo, H., et al. (2009). Expression of CYP1A1 and CYP1B1 in human endothelial cells: Regulation by fluid shear stress. Cardiovasc. Res. *81*: 669–677.

Cornelis, M.C., El-Sohemy, A., and Campos, H. (2004). Genetic polymorphism of CYP1A2 increases the risk of myocardial infarction. J. Med. Genet. *41*: 758–762.

Cottart, C.H., Nivet-Antoine, V., Laguillier-Morizot, C., and Beaudeux, J.L. (2010). Resveratrol bioavailability and toxicity in humans. Mol. Nutr. Food Res. *54*: 7–16.

Crozatier, B., and Hittinger, L. (1988). Mechanical adaptation to chronic pressure overload. Eur. Heart J. *9*: 7–11.

Dadarkar, S.S., Fonseca, L.C., Mishra, P.B., Lobo, A.S., Doshi, L.S., Dagia, N.M., et al. (2011). Phenotypic and genotypic assessment of concomitant drug-induced toxic effects in liver, kidney and blood. J. Appl. Toxicol. *31*: 117–130.

Dakarapu, R., Errabelli, R., Manthati, V.L., Michael Adebesin, A., Barma, D.K., Barma, D., et al. (2019). 19-Hydroxyeicosatetraenoic acid analogs: Antagonism of 20-hydroxyeicosatetraenoic acid-induced vascular sensitization and hypertension. Bioorganic Med. Chem. Lett. *29*: 126616.

Davydov, D.R., and Halpert, J.R. (2008). Allosteric P450 mechanisms: multiple binding sites, multiple conformers, or both? Expert Opin. Drug Metab. Toxicol. *4*: 1523.

DeFilippis, A.P., Chapman, A.R., Mills, N.L., Lemos, J.A. De, Arbab-Zadeh, A., Newby, L.K., et al. (2019). Assessment and treatment of patients with type 2 myocardial infarction and acute nonischemic myocardial injury. Circulation *140*: 1661–1678.

DeLozier, T.C., Kissling, G.E., Coulter, S.J., Dai, D., Foley, J.F., Bradbury, J.A., et al. (2007). Detection of human CYP2C8, CYP2C9, and CYP2J2 in cardiovascular tissues. Drug Metab. Dispos. *35*: 682–688.

Desai, A., and Fang, J.C. (2008). Heart Failure with Preserved Ejection Fraction: Hypertension, Diabetes, Obesity/Sleep Apnea, and Hypertrophic and Infiltrative Cardiomyopathy. Heart Fail. Clin. *4*: 87–97.

Diflucan, P. DIFLUCAN-Product Monograph PRODUCT MONOGRAPH.

Divanovic, S., Dalli, J., Jorge-Nebert, L.F., Flick, L.M., Gálvez-Peralta, M., Boespflug, N.D., et al. (2013). Contributions of the Three CYP1 Monooxygenases to Pro-Inflammatory and Inflammation-Resolution Lipid Mediator Pathways. J. Immunol. *191*: 3347–3357.

Dolinsky, V.W., Chan, A.Y.M., Frayne, I.R., Light, P.E., Rosiers, C. Des, and Dyck, J.R.B. (2009). Resveratrol Prevents the Prohypertrophic Effects of Oxidative Stress on LKB1. Circulation *119*: 1643–1652.

Dong, Q., Wu, Z., Li, X., Yan, J., Zhao, L., Yang, C., et al. (2014). Resveratrol ameliorates cardiac dysfunction induced by pressure overload in rats via structural protection and modulation of Ca2+ cycling proteins. J. Transl. Med. *12*: 323.

Dorn, G.W. (2007). The fuzzy logic of physiological cardiac hypertrophy. Hypertension

49: 962–970.

Drazner, M.H. (2011). The progression of hypertensive heart disease. Circulation *123*: 327–334.

Dreisbach, A.W., Smith, S. V, Kyle, P.B., Ramaiah, M., Amenuke, M., Garrett, M.R., et al. (2014). Urinary CYP eicosanoid excretion correlates with glomerular filtration in African-Americans with chronic kidney disease. Prostaglandins Other Lipid Mediat. *113–115*: 45–51.

Du, X.J. (2007). Divergence of hypertrophic growth and fetal gene profile: The influence of β-blockers. Br. J. Pharmacol. *152*: 169–171.

Dubey, R.K., Gillespie, D.G., Zacharia, L.C., Barchiesi, F., Imthurn, B., and Jackson, E.K. (2003). CYP450- and COMT-derived estradiol metabolites inhibit activity of human coronary artery SMCs. Hypertension *41*: 807–813.

Dunn, K.M., Renic, M., Flasch, A.K., Harder, D.R., Falck, J., and Roman, R.J. (2008). Elevated production of 20-HETE in the cerebral vasculature contributes to severity of ischemic stroke and oxidative stress in spontaneously hypertensive rats. Am. J. Physiol. - Hear. Circ. Physiol. *295*: H2455.

Dyck, J.R.B., and Lopaschuk, G.D. (2006). AMPK alterations in cardiac physiology and pathology: Enemy or ally? J. Physiol. *574*: 95–112.

Edpuganti, V., and Mehvar, R. (2014). UHPLC-MS/MS analysis of arachidonic acid and 10 of its major cytochrome P450 metabolites as free acids in rat livers: effects of hepatic ischemia. J. Chromatogr. B. Analyt. Technol. Biomed. Life Sci. *964*: 153–63.

Edson, K., and Rettie, A. (2013). CYP4 Enzymes As Potential Drug Targets: Focus on Enzyme Multiplicity, Inducers and Inhibitors, and Therapeutic Modulation of 20-Hydroxyeicosatetraenoic Acid (20-HETE) Synthase and Fatty Acid ω-Hydroxylase Activities. Curr. Top. Med. Chem. *13*: 1429–1440.

El-Kadi, A., and Zordoky, B. (2008). Modulation of Cardiac and Hepatic Cytochrome P450 Enzymes During Heart Failure. Curr. Drug Metab. *9*: 122–128.

El-Sherbeni, A.A., Aboutabl, M.E., Zordoky, B.N.M., Anwar-Mohamed, A., and El-Kadi, A.O.S. (2013). Determination of the dominant arachidonic acid cytochrome P450 monooxygenases in rat heart, lung, kidney, and liver: Protein expression and metabolite kinetics. AAPS J. *15*: 112–122.

El-Sherbeni, A.A., and El-Kadi, A.O.S. (2014a). Alterations in cytochrome P450-derived arachidonic acid metabolism during pressure overload-induced cardiac hypertrophy. Biochem. Pharmacol. *87*: 456–66.

El-Sherbeni, A.A., and El-Kadi, A.O.S. (2014b). Characterization of arachidonic acid metabolism by rat cytochrome P450 enzymes: the involvement of CYP1As. Drug Metab. Dispos. *42*: 1498–507.

El-Sherbeni, A.A., and El-Kadi, A.O.S. (2016). Repurposing Resveratrol and Fluconazole to Modulate Human Cytochrome P450-Mediated Arachidonic Acid Metabolism. Mol. Pharm. *13*: 1278–1288.

El-Sherbeni, A.A., and El-Kadi, A.O.S. (2017a). Microsomal cytochrome P450 as a target for drug discovery and repurposing. Drug Metab. Rev. *49*: 1–17.

El-Sherbeni, A.A., and El-Kadi, A.O.S. (2017b). Microsomal cytochrome P450 as a target for drug discovery and repurposing. Drug Metab. Rev. *49*: 1–17.

El-Sherbeni, A.A., and El-Kadi, A.O.S.S. (2014c). Alterations in cytochrome P450-derived arachidonic acid metabolism during pressure overload-induced cardiac hypertrophy. Biochem Pharmacol *87*: 456–466.

Elbekai, R.H., and El-Kadi, A.O.S. (2006). Cytochrome P450 enzymes: central players in cardiovascular health and disease. Pharmacol Ther *112*: 564–587.

Elkhatali, S., El-Sherbeni, A.A., Elshenawy, O.H., Abdelhamid, G., and El-Kadi, A.O.S.S. (2015). 19-Hydroxyeicosatetraenoic acid and isoniazid protect against angiotensin II-induced cardiac hypertrophy. Toxicol Appl Pharmacol *289*: 550–559.

Elkhatali, S., Maayah, Z.H., El-Sherbeni, A.A., Elshenawy, O.H., Abdelhamid, G., Shoieb, S.M., et al. (2017). Inhibition of Mid-chain HETEs Protects Against Angiotensin II-induced Cardiac Hypertrophy. J. Cardiovasc. Pharmacol. *70*: 16–24.

Elshenawy, O., Shoieb, S., Mohamed, A., and El-Kadi, A. (2017a). Clinical Implications of 20-Hydroxyeicosatetraenoic Acid in the Kidney, Liver, Lung and Brain: An Emerging Therapeutic Target. Pharmaceutics *9*: 9.

Elshenawy, O.H., Shoieb, S.M., Mohamed, A., and El-Kadi, A.O.S. (2017b). Clinical implications of 20-hydroxyeicosatetraenoic acid in the kidney, liver, lung and brain: An emerging therapeutic target. Pharmaceutics *9*:.

Ergatoudes, C., Schaufelberger, M., Andersson, B., Pivodic, A., Dahlström, U., and Fu, M. (2019). Non-cardiac comorbidities and mortality in patients with heart failure with reduced vs. preserved ejection fraction: a study using the Swedish Heart Failure Registry. Clin. Res. Cardiol. *108*: 1025–1033.

Farías, J.G., Molina, V.M., Carrasco, R.A., Zepeda, A.B., Figueroa, E., Letelier, P., et al. (2017). Antioxidant therapeutic strategies for cardiovascular conditions associated with oxidative stress. Nutrients *9*: 1–23.

Fidelis, P., Wilson, L., Thomas, K., Villalobos, M., and Oyekan, A.O. (2010). Renal function and vasomotor activity in mice lacking the Cyp4a14 gene. Exp. Biol. Med. (Maywood). *235*: 1365–74.

Florea, V.G., Rector, T.S., Anand, I.S., and Cohn, J.N. (2016). Heart failure with improved ejection fraction: clinical characteristics, correlates of recovery, and survival. Circ. Hear. Fail. *9*:.

Fox, K.F., Cowie, M.R., Wood, D.A., Coats, A.J.S., Gibbs, J.S.R., Underwood, S.R., et al. (2001). Coronary artery disease as the cause of incident heart failure in the population. Eur. Heart J. *22*: 228–236.

French, B.A., and Kramer, C.M. (2007). Mechanisms of postinfarct left ventricular remodeling. Drug Discov. Today Dis. Mech. *4*: 185–196.

Frey, N., Katus, H.A., Olson, E.N., and Hill, J.A. (2004). Hypertrophy of the Heart: A New Therapeutic Target? Circulation *109*: 1580–1589.

Funk, C.D. (2001). Prostaglandins and leukotrienes: advances in eicosanoid biology. Science *294*: 1871–5.

Gainer, J. V, Lipkowitz, M.S., Yu, C., Waterman, M.R., Dawson, E.P., Capdevila, J.H., et al. (2008). Association of a CYP4A11 variant and blood pressure in black men. J. Am. Soc. Nephrol. *19*: 1606–12.

Gaspar-Pereira, S., Fullard, N., Townsend, P.A., Banks, P.S., Ellis, E.L., Fox, C., et al. (2012). The NF-κB subunit c-Rel stimulates cardiac hypertrophy and fibrosis. Am. J. Pathol. *180*: 929–939.

Gehm, B.D., McAndrews, J.M., Chien, P.Y., and Jameson, J.L. (1997). Resveratrol, a polyphenolic compound found in grapes and wine, is an agonist for the estrogen receptor. Proc. Natl. Acad. Sci. U. S. A. *94*: 14138–14143.

Ghosh, J., Chowdhury, A.R., Srinivasan, S., Chattopadhyay, M., Bose, M., Bhattacharya, S., et al. (2018). Cigarette Smoke Toxins-Induced Mitochondrial Dysfunction and Pancreatitis Involves Aryl Hydrocarbon Receptor Mediated Cyp1 Gene Expression: Protective Effects of Resveratrol. Toxicol. Sci. *166*: 428–440.

Ghosh, S., May, M.J., and Kopp, E.B. (1998). NF-κB and rel proteins: Evolutionarily conserved mediators of immune responses. Annu. Rev. Immunol. *16*: 225–260.

Gibson, P., Gill, J.H., Khan, P.A., Seargent, J.M., Martin, S.W., Batman, P.A., et al. (2003). Cytochrome P450 1B1 (CYP1B1) is overexpressed in human colon adenocarcinomas relative to normal colon: implications for drug development. Mol. Cancer Ther. *2*: 527–34.

Gitau, S.C., Li, X., Zhao, D., Guo, Z., Liang, H., Qian, M., et al. (2015). Acetyl salicylic acid attenuates cardiac hypertrophy through Wnt signaling. Front. Med. *9*: 444–56.

González, A., Ravassa, S., Beaumont, J., López, B., and Díez, J. (2011). New targets to treat the structural remodeling of the myocardium. J. Am. Coll. Cardiol. *58*: 1833–1843.

Gordon, J.A., Heller, S.K., Kaduce, T.L., and Spector, A.A. (1994). Formation and release of a peroxisome-dependent arachidonic acid metabolite by human skin fibroblasts. J. Biol. Chem. *269*: 4103–4109.

Gradman, A.H., and Alfayoumi, F. (2006). From Left Ventricular Hypertrophy to

Congestive Heart Failure: Management of Hypertensive Heart Disease (Prog Cardiovasc Dis).

Grant, M.K.O., Seelig, D.M., Sharkey, L.C., and Zordoky, B.N. (2017). Sex-dependent alteration of cardiac cytochrome P450 gene expression by doxorubicin in C57Bl/6 mice. Biol. Sex Differ. *8*: 1.

Grossman, W., Jones, D., and McLaurin, L.P. (1975). Wall stress and patterns of hypertrophy in the human left ventricle. J. Clin. Invest. *56*: 56–64.

Gu, X.S., Wang, Z.B., Ye, Z., Lei, J.P., Li, L., Su, D.F., et al. (2014). Resveratrol, an activator of SIRT1, upregulates AMPK and improves cardiac function in heart failure. Genet. Mol. Res. *13*: 323–335.

Guan, P., Sun, Z.M., Wang, N., Zhou, J., Luo, L.F., Zhao, Y.S., et al. (2019). Resveratrol prevents chronic intermittent hypoxia-induced cardiac hypertrophy by targeting the PI3K/AKT/mTOR pathway. Life Sci. *233*: 116748.

Guengerich, F.P. (2018). Mechanisms of Cytochrome P450-Catalyzed Oxidations. ACS Catal. *8*: 10964–10976.

Gupta, M.P. (2007). Factors controlling cardiac myosin-isoform shift during hypertrophy and heart failure. J. Mol. Cell. Cardiol. *43*: 388–403.

Gupta, S., Young, D., Maitra, R.K., Gupta, A., Popovic, Z.B., Yong, S.L., et al. (2008). Prevention of Cardiac Hypertrophy and Heart Failure by Silencing of NF-κB. *375*:.

Haeggström, J.Z., and Funk, C.D. (2011). Lipoxygenase and leukotriene pathways: biochemistry, biology, and roles in disease. Chem. Rev. *111*: 5866–98.

Hahn, M.E., Allan, L.L., and Sherr, D.H. (2009). Regulation of constitutive and inducible AHR signaling: Complex interactions involving the AHR repressor. Biochem. Pharmacol. *77*: 485–497.

Hammarström, S., Hamberg, M., Samuelsson, B., Duell, E.A., Stawiski, M., and Voorhees, J.J. (1975). Increased concentrations of nonesterified arachidonic acid, 12L-hydroxy-5,8,10,14-eicosatetraenoic acid, prostaglandin E2, and prostaglandin F2alpha in epidermis of psoriasis. Proc. Natl. Acad. Sci. U. S. A. *72*: 5130–4.

Harada, K. (1998). Pressure overload induces cardiac hypertrophy in angiotensin II type 1a receptor knockout mice. Circulation *97*: 1952–1959.

Hardwick, J.P. (2008). Cytochrome P450 omega hydroxylase (CYP4) function in fatty acid metabolism and metabolic diseases. Biochem. Pharmacol. *75*: 2263–2275.

Harris, I.S., Zhang, S., Treskov, I., Kovacs, A., Weinheimer, C., and Muslin, A.J. (2004). Raf-1 kinase is required for cardiac hypertrophy and cardiomyocyte survival in response to pressure overload. Circulation *110*: 718–723.

Hartley, L., Igbinedion, E., Holmes, J., Flowers, N., Thorogood, M., Clarke, A., et al.

(2013). Increased consumption of fruit and vegetables for the primary prevention of cardiovascular diseases. Cochrane Database Syst. Rev. *2013*:.

Hassan, H.M., Guo, H., Yousef, B.A., Guerram, M., Hamdi, A.M., Zhang, L., et al. (2016). Role of Inflammatory and Oxidative Stress, Cytochrome P450 2E1, and Bile Acid Disturbance in Rat Liver Injury Induced by Isoniazid and Lipopolysaccharide Cotreatment. Antimicrob. Agents Chemother. *60*: 5285–93.

Heart and Stroke Foundation (2016). 2016 REPORT ON THE HEALTH OF CANADIANS.

Heineke, J., and Molkentin, J.D. (2006). Regulation of cardiac hypertrophy by intracellular signalling pathways. Nat. Rev. Mol. Cell Biol. *7*: 589–600.

Hennekens, C.H. (2002). Update on aspirin in the treatment and prevention of cardiovascular disease. Am. J. Manag. Care *8*: S691-700.

Ho, J.E., Lyass, A., Lee, D.S., Vasan, R.S., Kannel, W.B., Larson, M.G., et al. (2013). Predictors of new-onset heart failure differences in preserved versus reduced ejection fraction. Circ. Hear. Fail. *6*: 279–286.

Hoidy, W.H., Jaber, F.A., and Al-Askiry, M.A. (2019). Association of CYP1A1 rs1048943 polymorphism with prostate cancer in Iraqi men patients. Asian Pacific J. Cancer Prev. *20*: 3839–3842.

Hong, C.C., Tang, B.K., Hammond, G.L., Tritchler, D., Yaffe, M., and Boyd, N.F. (2004). Cytochrome P450 1A2 (CYP1A2) activity and risk factors for breast cancer: a cross-sectional study. Breast Cancer Res. *6*: R352.

Hong, M., Park, N., and Chun, Y.J. (2014). Role of annexin A5 on mitochondria-dependent apoptosis induced by tetramethoxystilbene in human breast cancer cells. Biomol. Ther. *22*: 519–524.

Houston, J.B., Kenworthy, K.E., and Houston, J.B. (2000). IN VITRO-IN VIVO SCALING OF CYP KINETIC DATA NOT CONSISTENT WITH THE CLASSICAL MICHAELIS-MENTEN MODEL. DRUG Metab. Dispos. *28*:.

Hua, Y., Zhang, Y., Ceylan-Isik, A.F., Wold, L.E., Nunn, J.M., and Ren, J. (2011). Chronic akt activation accentuates aging-induced cardiac hypertrophy and myocardial contractile dysfunction: Role of autophagy. Basic Res. Cardiol. *106*: 1173–1191.

Huang, C.C., Chang, M.T., Leu, H.B., Yin, W.H., Tseng, W.K., Wu, Y.W., et al. (2020). Association of Arachidonic Acid-derived Lipid Mediators with Subsequent Onset of Acute Myocardial Infarction in Patients with Coronary Artery Disease. Sci. Rep. *10*:.

Huderson, A.C., Rekha Devi, P. V., Niaz, M.S., Adunyah, S.E., and Ramesh, A. (2019). Alteration of benzo(a)pyrene biotransformation by resveratrol in Apc Min/+ mouse model of colon carcinogenesis. Invest. New Drugs *37*: 238–251.

Hwang, J.T., Kwon, D.Y., Park, O.J., and Kim, M.S. (2008). Resveratrol protects ROS-induced cell death by activating AMPK in H9c2 cardiac muscle cells. Genes Nutr. *2*: 323–326.

Imaoka, S., Hashizume, T., and Funae, Y. (2005). Localization of rat cytochrome P450 in various tissues and comparison of arachidonic acid metabolism by rat P450 with that by human P450 orthologs. Drug Metab. Pharmacokinet. *20*:.

Imig, J.D. (2012). Epoxides and Soluble Epoxide Hydrolase in Cardiovascular Physiology. Physiol. Rev. *92*: 101–130.

Inamdar, A., and Inamdar, A. (2016). Heart Failure: Diagnosis, Management and Utilization. J. Clin. Med. *5*: 62.

Ingelman-Sundberg, M. (2009). Concerning Cytochromes P450: Role in the Metabolism and Toxicity of Drugs and other Xenobiotics . Edited by Costas Ioannides. ChemMedChem *4*: 473–474.

Issan, Y., Hochhauser, E., Guo, A., Gotlinger, K.H., Kornowski, R., Leshem-Lev, D., et al. (2013). Elevated level of pro-inflammatory eicosanoids and EPC dysfunction in diabetic patients with cardiac ischemia. Prostaglandins Other Lipid Mediat. *100–101*: 15–21.

Ivanov, I., Romanov, S., Ozdoba, C., Holzhütter, H.G., Myagkova, G., and Kuhn, H. (2004). Enantioselective substrate specificity of 15-lipoxygenase 1. Biochemistry *43*: 15720–8.

Jackson, G. (2000). ABC of heart failure: Pathophysiology. BMJ *320*: 167–170.

Jacob, J., Chopra, S., Cherian, D., and Verghese, P. (2013). Physiology and clinical significance of natriuretic hormones. Indian J. Endocrinol. Metab. *17*: 83.

Jennings, B.L., Estes, A.M., Anderson, L.J., Fang, X.R., Yaghini, F.A., Fan, Z., et al. (2012). Cytochrome P450 1B1 gene disruption minimizes deoxycorticosterone acetate-salt-induced hypertension and associated cardiac dysfunction and renal damage in mice. Hypertension *60*: 1510–1516.

Jennings, B.L., Montanez, D.E., May, M.E., Estes, A.M., Fang, X.R., Yaghini, F.A., et al. (2014). Cytochrome P450 1B1 contributes to increased blood pressure and cardiovascular and renal dysfunction in spontaneously hypertensive rats. Cardiovasc. Drugs Ther. *28*: 145–161.

Jennings, B.L., Sahan-Firat, S., Estes, A.M., Das, K., Farjana, N., Fang, X.R., et al. (2010). Cytochrome P450 1B1 contributes to angiotensin II-induced hypertension and associated pathophysiology. Hypertension *56*: 667–674.

Jeong, E.M., and Dudley, S.C. (2015). Diastolic dysfunction: Potential new diagnostics and therapies. Circ. J. *79*: 470–477.

Johnson, A.L., Edson, K.Z., Totah, R.A., and Rettie, A.E. (2015). Cytochrome P450 ω-

Hydroxylases in Inflammation and Cancer. Adv. Pharmacol. *74*: 223–62.

Jorge-Nebert, L.F., Jiang, Z., Chakraborty, R., Watson, J., Jin, L., McGarvey, S.T., et al. (2010). Analysis of human CYP1A1 and CYP1A2 genes and their shared bidirectional promoter in eight world populations. Hum. Mutat. *31*: 27–40.

Joseph, M., Brady, R., Attridge, R., Cota, J., Horlen, C., Lusk, K., et al. (2019). Critically Ill Recipients of Weight-Based Fluconazole Meeting Drug-Induced Liver Injury Network Criteria. Hosp. Pharm. *54*: 378–384.

Kahan, T., and Bergfeldt, L. (2005). Left ventricular hypertrophy in hypertension: Its arrhythmogenic potential. Heart *91*: 250–256.

Kaide, J.I., Wang, M.H., Wang, J.S., Zhang, F., Gopal, V.R., Falck, J.R., et al. (2003). Transfection of CYP4A1 cDNA increases vascular reactivity in renal interlobar arteries. Am. J. Physiol. - Ren. Physiol. *284*: 51–56.

Kajiwara, A., Saruwatari, J., Kita, A., Kamihashi, R., Miyagawa, H., Sakata, M., et al. (2013). Sex differences in the effect of cytochrome P450 2C19 polymorphisms on the risk of diabetic retinopathy: a retrospective longitudinal study in Japanese patients with type 2 diabetes. Pharmacogenet. Genomics *23*: 717–20.

Kang, J.-H. (2014). Protein Kinase C (PKC) Isozymes and Cancer. New J. Sci. *2014*: 1–36.

Kapelyukh, Y., Henderson, C.J., Scheer, N., Rode, A., and Wolf, C.R. (2019). Defining the contribution of CYP1A1 and CYP1A2 to drug metabolism using humanized CYP1A1/1A2 and Cyp1a1/Cyp1a2 knockout mice. Drug Metab. Dispos. *47*: 907–918.

Katare, P.B., Bagul, P.K., Dinda, A.K., and Banerjee, S.K. (2017). Toll-Like Receptor 4 Inhibition Improves Oxidative Stress and Mitochondrial Health in Isoproterenol-Induced Cardiac Hypertrophy in Rats. Front. Immunol. *8*: 719.

Kawamura, N., Kubota, T., Kawano, S., Monden, Y., Feldman, A.M., Tsutsui, H., et al. (2005). Blockade of NF-κB improves cardiac function and survival without affecting inflammation in TNF-α-induced cardiomyopathy. Cardiovasc. Res. *66*: 520–529.

Kawano, S., Kubota, T., Monden, Y., Kawamura, N., Tsutsui, H., Takeshita, A., et al. (2005). Blockade of NF-κB ameliorates myocardial hypertrophy in response to chronic infusion of angiotensin II. Cardiovasc. Res. *67*: 689–698.

Kawano, S., Kubota, T., Monden, Y., Tsutsumi, T., Inoue, T., Kawamura, N., et al. (2006). Blockade of NF-κB improves cardiac function and survival after myocardial infarction. Am. J. Physiol. - Hear. Circ. Physiol. *291*:.

Kessler-Icekson, G., Barhum, Y., Schaper, J., Schaper, W., Kaganovsky, E., and Brand, T. (2002). ANP expression in the hypertensive heart. Exp. Clin. Cardiol. *7*: 80–4.

Khouri, M.G., Peshock, R.M., Ayers, C.R., Lemos, J.A. De, and Drazner, M.H. (2010). A 4-tiered classification of left ventricular hypertrophy based on Left ventricular

geometry the dallas Heart study. Circ. Cardiovasc. Imaging *3*: 164–171.

Khoza, S., Moyo, I., and Ncube, D. (2017). Comparative Hepatotoxicity of Fluconazole, Ketoconazole, Itraconazole, Terbinafine, and Griseofulvin in Rats. J. Toxicol. *2017*:.

Kim, D., and Guengerich, F.P. (2004). Enhancement of 7-methoxyresorufin O-demethylation activity of human cytochrome P450 1A2 by molecular breeding. Arch. Biochem. Biophys. *432*: 102–108.

Kolwicz, S.C., and Tian, R. (2011). Glucose metabolism and cardiac hypertrophy. Cardiovasc. Res. *90*: 194–201.

Konhilas, J.P., and Leinwand, L.A. (2006). Partnering up for cardiac hypertrophy. Circ. Res. *98*: 985–987.

Konkel, A., and Schunck, W.H. (2011). Role of cytochrome P450 enzymes in the bioactivation of polyunsaturated fatty acids. Biochim Biophys Acta *1814*: 210–222.

Kopp, E., and Ghosh, S. (1994). Inhibition of NF-κB by sodium salicylate and aspirin. Science (80-.). *265*: 956–959.

Korashy, H., and El-Kadi, A. (2006). The role of aryl hydrocarbon receptor in the pathogenesis of cardiovascular diseases. Drug Metab. Rev. *38*: 411–450.

Krasulova, K., Holas, O., and Anzenbacher, P. (2017). Influence of amlodipine enantiomers on human microsomal cytochromes p450: Stereoselective time-dependent inhibition of CYP3A enzyme activity. Molecules *22*:.

Ku, H.C., Lee, S.Y., Wu, Y.K.A., Yang, K.C., and Su, M.J. (2016). A model of cardiac remodeling through constriction of the abdominal aorta in rats. J. Vis. Exp. *2016*: 54818.

Kumar, S., Seqqat, R., Chigurupati, S., Kumar, R., Baker, K.M., Young, D., et al. (2011). Inhibition of nuclear factor κb regresses cardiac hypertrophy by modulating the expression of extracellular matrix and adhesion molecules. Free Radic. Biol. Med. *50*: 206–215.

Kurutas, E.B. (2016). The importance of antioxidants which play the role in cellular response against oxidative/nitrosative stress: Current state. Nutr. J. *15*:.

Laethem, R.M., Balazy, M., Falck, J.R., Laethem, C.L., and Koop, D.R. (1993). Formation of 19(S)-, 19(R)-, and 18(R)-hydroxyeicosatetraenoic acids by alcohol-inducible cytochrome P450 2E1. J. Biol. Chem. *268*: 12912–8.

Lalande, S., and Johnson, B.D. (2008). Diastolic dysfunction: A link between hypertension and heart failure. Drugs of Today *44*: 503–513.

Lamon, B.D., Upmacis, R.K., Deeb, R.S., Koyuncu, H., and Hajjar, D.P. (2010). Inducible nitric oxide synthase gene deletion exaggerates MAPK-mediated

cyclooxygenase-2 induction by inflammatory stimuli. Am J Physiol Hear. Circ Physiol *299*: H613-23.

Lavandero, S., Foncea, R., Pérez, V., and Sapag-Hagar, M. (1998). Effect of inhibitors of signal transduction on IGF-1-induced protein synthesis associated with hypertrophy in cultured neonatal rat ventricular myocytes. FEBS Lett. *422*: 193–196.

Lee, D.S., Gona, P., Vasan, R.S., Larson, M.G., Benjamin, E.J., Wang, T.J., et al. (2009). Relation of disease pathogenesis and risk factors to heart failure with preserved or reduced ejection fraction: Insights from the framingham heart study of the national heart, lung, and blood institute. Circulation *119*: 3070–3077.

Lewis, D.F. V, Ito, Y., and Goldfarb, P.S. (2006). Cytochrome P450 Structures and Their Substrate Interactions. DRUG Dev. Res. Drug Dev. Res *66*: 19–2419.

Leychenko, A., Konorev, E., Jijiwa, M., and Matter, M.L. (2011). Stretch-Induced hypertrophy activates NFkB-Mediated VEGF secretion in adult cardiomyocytes. PLoS One *6*:.

Li, F., Zhu, W., and Gonzalez, F.J. (2017). Potential role of CYP1B1 in the development and treatment of metabolic diseases. Pharmacol Ther *178*: 18–30.

Li, Y., Ha, T., Gao, X., Kelley, J., Williams, D.L., Browder, I.W., et al. (2004). NF-κ activation is required for the development of cardiac hypertrophy in vivo. Am. J. Physiol. - Hear. Circ. Physiol. *287*:.

Liao, H.-H., Jia, X.-H., Liu, H.-J., Yang, Z., and Tang, Q.-Z. (2016). The Role of PPARs in Pathological Cardiac Hypertrophy and Heart Failure. Curr. Pharm. Des. *23*: 1677–1686.

Lin, J.H., and Lu, A.Y. (1997). Role of pharmacokinetics and metabolism in drug discovery and development. Pharmacol. Rev. *49*: 403–49.

Lipp, P., and Reither, G. (2011). Protein kinase C: The 'Masters' of calcium and lipid. Cold Spring Harb. Perspect. Biol. *3*: 1–17.

Liu, J., Sridhar, J., and Foroozesh, M. (2013a). Cytochrome P450 family 1 inhibitors and structure-activity relationships. Molecules *18*: 14470–14495.

Liu, J., Taylor, S.F., Dupart, P.S., Arnold, C.L., Sridhar, J., Jiang, Q., et al. (2013b). Pyranoflavones: A group of small-molecule probes for exploring the active site cavities of cytochrome P450 enzymes 1A1, 1A2, and 1B1. J. Med. Chem. *56*: 4082–4092.

Liu, M., Hurn, P.D., and Alkayed, N.J. (2004). Cytochrome P450 in neurological disease. Curr. Drug Metab. *5*: 225–34.

Liu, M., and Yokomizo, T. (2015). The role of leukotrienes in allergic diseases. Allergol. Int. *64*: 17–26.

Löfgren, S., Baldwin, R.M., Carlerös, M., Terelius, Y., Fransson-Steen, R., Mwinyi, J.,

et al. (2009). Regulation of human CYP2C18 and CYP2C19 in transgenic mice: influence of castration, testosterone, and growth hormone. Drug Metab. Dispos. *37*: 1505–12.

Lopaschuk, G.D., Karwi, Q.G., Tian, R., Wende, A.R., and Abel, E.D. (2021). Cardiac Energy Metabolism in Heart Failure. Circ. Res. 1487–1513.

Lorenzen, A., and Kennedy, S.W. (1993). A fluorescence-based protein assay for use with a microplate reader. Anal. Biochem. *214*: 346–348.

Lowry, O.H., Rosebrough, N.J., Farr, A.L., and Randall, R.J. (1951). Protein measurement with the Folin phenol reagent. J Biol Chem *193*: 265–275.

LOWRY, O.H., ROSEBROUGH, N.J., FARR, A.L., and RANDALL, R.J. (1951). Protein measurement with the Folin phenol reagent. J. Biol. Chem. *193*: 265–275.

Lu, C., Berg, C., Prakash, S.R., Lee, F.W., and Balani, S.K. (2008). Prediction of pharmacokinetic drug-drug interactions using human hepatocyte suspension in plasma and cytochrome P450 phenotypic data. III. in vitro-in vivo correlation with fluconazole. Drug Metab. Dispos. *36*: 1261–1266.

Lund, A.K., Goens, M.B., Kanagy, N.L., and Walker, M.K. (2003). Cardiac hypertrophy in aryl hydrocarbon receptor null mice is correlated with elevated angiotensin II, endothelin-1, and mean arterial blood pressure. Toxicol. Appl. Pharmacol. *193*: 177–87.

Luo, G., Zeldin, D.C., Blaisdell, J.A., Hodgson, E., and Goldstein, J.A. (1998). Cloning and expression of murine CYP2Cs and their ability to metabolize arachidonic acid. Arch. Biochem. Biophys. *357*: 45–57.

Lymperopoulos, A., Rengo, G., and Koch, W.J. (2013). Adrenergic nervous system in heart failure: Pathophysiology and therapy. Circ. Res. *113*: 739–753.

Maaten, J.M. ter, and Voors, A.A. (2016). Renal dysfunction in heart failure with a preserved ejection fraction: cause or consequence? Eur. J. Heart Fail. *18*: 113–114.

Maayah, Z.H., Abdelhamid, G., and El-Kadi, A.O.S. (2015a). Development of cellular hypertrophy by 8-hydroxyeicosatetraenoic acid in the human ventricular cardiomyocyte, RL-14 cell line, is implicated by MAPK and NF-κB. Cell Biol. Toxicol. *31*: 241–259.

Maayah, Z.H., Althurwi, H.N., Abdelhamid, G., Lesyk, G., Jurasz, P., and El-Kadi, A.O.S. (2016). CYP1B1 inhibition attenuates doxorubicin-induced cardiotoxicity through a mid-chain HETEs-dependent mechanism. Pharmacol Res *105*: 28–43.

Maayah, Z.H., Althurwi, H.N., El-Sherbeni, A.A., Abdelhamid, G., Siraki, A.G., and El-Kadi, A.O.S.S. (2017). The role of cytochrome P450 1B1 and its associated mid-chain hydroxyeicosatetraenoic acid metabolites in the development of cardiac hypertrophy induced by isoproterenol. Mol Cell Biochem *429*: 151–165.

Maayah, Z.H., and El-Kadi, A.O.S. (2016a). 5-, 12- and 15-Hydroxyeicosatetraenoic

acids induce cellular hypertrophy in the human ventricular cardiomyocyte, RL-14 cell line, through MAPK- and NF-kappaB-dependent mechanism. Arch Toxicol *90*: 359–373.

Maayah, Z.H., and El-Kadi, A.O.S. (2016b). The role of mid-chain hydroxyeicosatetraenoic acids in the pathogenesis of hypertension and cardiac hypertrophy. Arch Toxicol *90*: 119–136.

Maayah, Z.H., Elshenawy, O.H., Althurwi, H.N., Abdelhamid, G., and El-Kadi, A.O.S. (2015b). Human fetal ventricular cardiomyocyte, RL-14 cell line, is a promising model to study drug metabolizing enzymes and their associated arachidonic acid metabolites. J. Pharmacol. Toxicol. Methods *71*: 33–41.

Maayah, Z.H., Levasseur, J., Siva Piragasam, R., Abdelhamid, G., Dyck, J.R.B.B., Fahlman, R.P., et al. (2018). 2-Methoxyestradiol protects against pressure overload-induced left ventricular hypertrophy. Sci Rep *8*: 2780.

Maciejewska, D., Ossowski, P., Drozd, A., Ryterska, K., Jamioł-Milc, D., Banaszczak, M., et al. (2015). Metabolites of arachidonic acid and linoleic acid in early stages of non-alcoholic fatty liver disease--A pilot study. Prostaglandins Other Lipid Mediat. *121*: 184–9.

MacPherson, L., and Matthews, J. (2010). Inhibition of aryl hydrocarbon receptor-dependent transcription by resveratrol or kaempferol is independent of estrogen receptor α expression in human breast cancer cells. Cancer Lett. *299*: 119–129.

Maddox, T.M., Januzzi, J.L., Allen, L.A., Breathett, K., Butler, J., Davis, L.L., et al. (2021). 2021 Update to the 2017 ACC Expert Consensus Decision Pathway for Optimization of Heart Failure Treatment: Answers to 10 Pivotal Issues About Heart Failure With Reduced Ejection Fraction: A Report of the American College of Cardiology Solution Set Oversight Committee. J. Am. Coll. Cardiol. *77*: 772–810.

Magyar, K., Halmosi, R., Palfi, A., Feher, G., Czopf, L., Fulop, A., et al. (2012). Cardioprotection by resveratrol: A human clinical trial in patients with stable coronary artery disease. Clin. Hemorheol. Microcirc. *50*: 179–187.

Maillet, M., Berlo, J.H. Van, and Molkentin, J.D. (2013). Molecular basis of physiological heart growth: Fundamental concepts and new players. Nat. Rev. Mol. Cell Biol. *14*: 38–48.

Malhotra, B., Dickins, M., Alvey, C., Jumadilova, Z., Li, X., Duczynski, G., et al. (2011). Effects of the moderate CYP3A4 inhibitor, fluconazole, on the pharmacokinetics of fesoterodine in healthy subjects. Br. J. Clin. Pharmacol. *72*: 263–269.

Malik, K.U., Jennings, B.L., Yaghini, F.A., Sahan-Firat, S., Song, C.Y., Estes, A.M., et al. (2012). Contribution of cytochrome P450 1B1 to hypertension and associated pathophysiology: A novel target for antihypertensive agents. Prostaglandins Other Lipid Mediat. *98*: 69–74.

Manabe, I., Shindo, T., and Nagai, R. (2002). Gene expression in fibroblasts and fibrosis involvement in cardiac hypertrophy. Circ. Res. *91*: 1103–1113.

Mann, D.L., and Bristow, M.R. (2005). Mechanisms and models in heart failure: The biomechanical model and beyond. Circulation *111*: 2837–2849.

Manning, B.D., and Toker, A. (2017). AKT/PKB Signaling: Navigating the Network. Cell *169*: 381–405.

Mao, J.T., Smoake, J., Park, H.K., Lu, Q.Y., and Xue, B. (2016). Grape Seed Procyanidin Extract Mediates Antineoplastic Effects against Lung Cancer via Modulations of Prostacyclin and 15-HETE Eicosanoid Pathways. Cancer Prev Res *9*: 925–932.

Martínez-Jiménez, C.P., Jover, R., Donato, M.T., Castell, J. V, and Gómez-Lechón, M.J. (2007). Transcriptional regulation and expression of CYP3A4 in hepatocytes. Curr. Drug Metab. *8*: 185–94.

Martynowicz, H., Janus, A., Nowacki, D., and Mazur, G. The role of chemokines in hypertension. Adv. Clin. Exp. Med. *23*: 319–25.

Mathur, S.N., Albright, E., and Field+, F.J. (1990). 12-Hydroxyeicosatetraenoic acid is metabolized by beta-oxidation in mouse peritoneal macrophages. Identification of products and proposed pathway. J. Biol. Chem. *8*: 21048–21055.

Matsumura, N., Takahara, S., Maayah, Z.H., Parajuli, N., Byrne, N.J., Shoieb, S.M., et al. (2018). Resveratrol improves cardiac function and exercise performance in MI-induced heart failure through the inhibition of cardiotoxic HETE metabolites. J. Mol. Cell. Cardiol. *125*: 162–173.

Mayer, B., Lieb, W., Götz, A., König, I.R., Kauschen, L.F., Linsel-Nitschke, P., et al. (2006). Association of a functional polymorphism in the CYP4A11 gene with systolic blood pressure in survivors of myocardial infarction. J. Hypertens. *24*: 1965–70.

McDonald, M., Virani, S., Chan, M., Ducharme, A., Ezekowitz, J.A., Giannetti, N., et al. (2021). CCS/CHFS Heart Failure Guidelines Update: Defining a New Pharmacologic Standard of Care for Heart Failure With Reduced Ejection Fraction. Can. J. Cardiol. *37*: 531–546.

McFadyen, M.C.E., Cruickshank, M.E., Miller, I.D., McLeod, H.L., Melvin, W.T., Haites, N.E., et al. (2001). Cytochrome P450 CYP1B1 over-expression in primary and metastatic ovarian cancer. Br. J. Cancer *85*: 242–246.

McKay, J.A., Melvin, W.T., Ah-See, A.K., Ewen, S.W.B., Greenlee, W.F., Marcus, C.B., et al. (1995). Expression of cytochrome P450 CYP1B1 in breast cancer. FEBS Lett. *374*: 270–272.

McMullen, J.R., Shioi, T., Zhang, L., Tarnavski, O., Sherwood, M.C., Kang, P.M., et al. (2003). Phosphoinositide 3-kinase(p110α) plays a critical role for the induction of physiological, but not pathological, cardiac hypertrophy. Proc. Natl. Acad. Sci. U. S. A.

100: 12355–12360.

McMurray, J., Chopra, M., Abdullah, I., Smith, W.E., and Dargie, H.J. (1993). Evidence of oxidative stress in chronic heart failure in humans. Eur. Heart J. *14*: 1493–1498.

Mescher, M., and Haarmann-Stemmann, T. (2018). Modulation of CYP1A1 metabolism: From adverse health effects to chemoprevention and therapeutic options. Pharmacol. Ther. *187*: 71–87.

Metra, M., and Teerlink, J.R. (2017). Heart failure. Lancet *390*: 1981–1995.

Mikstacka, R., Baer-Dubowska, W., Wieczorek, M., and Sobiak, S. (2008). Thiomethylstilbenes as inhibitors of CYP1A1, CYP1A2 and CYP1B1 activities. Mol. Nutr. Food Res.

Mikstacka, R., Przybylska, D., Rimando, A.M., and Baer-Dubowska, W. (2007). Inhibition of human recombinant cytochromes P450 CYP1A1 and CYP1B1 by trans-resveratrol methyl ethers. Mol. Nutr. Food Res. *51*: 517–524.

Miller, G.P. (2008). Advances in the interpretation and prediction of CYP2E1 metabolism from a biochemical perspective. Expert Opin. Drug Metab. Toxicol. *4*: 1053–64.

Miller, M.S. (1994). Transplacental Lung Carcinogenesis: A Pharmacogenetic Mouse Model for the Modulatory Role of Cytochrome P450 1A1 on Lung Cancer Initiation. Chem. Res. Toxicol. *7*: 471–481.

Minamiyama, Y., Takemura, S., Akiyama, T., Imaoka, S., Inoue, M., Funae, Y., et al. (1999). Isoforms of cytochrome P450 on organic nitrate-derived nitric oxide release in human heart vessels. FEBS Lett. *452*: 165–9.

Miyajima, A., Kuroda, Y., Sakemi-Hoshikawa, K., Usami, M., Mitsunaga, K., Irie, T., et al. (2020). Inhibitory and inductive effects of 4- or 5-methyl-2-mercaptobenzimidazole, thyrotoxic and hepatotoxic rubber antioxidants, on several forms of cytochrome P450 in primary cultured rat and human hepatocytes. Toxicol. Reports *7*: 979–985.

Morgan D', C., Wolf, A., and Sacks, G.& (2003). Methods and products related to 16-HETE analogs.

Müller, A.L., and Dhalla, N.S. (2013). Differences in concentric cardiac hypertrophy and eccentric hypertrophy. In Cardiac Adaptations: Molecular Mechanisms, (Springer New York), pp 147–166.

Murdoch, C.E., Zhang, M., Cave, A.C., and Shah, A.M. (2006). NADPH oxidase-dependent redox signalling in cardiac hypertrophy, remodelling and failure. Cardiovasc. Res. *71*: 208–215.

Murray, G.I., Taylor, M.C., McFadyen, M.C.E., McKay, J.A., Greenlee, W.F., Burke,

M.D., et al. (1997). Tumor-specific Expression of Cytochrome P450 CYP1B1. Cancer Res. *57*:.

Myasoedova, K.N. (2008). New findings in studies of cytochromes P450. Biochem. *73*: 965–969.

Nakamura, M., and Sadoshima, J. (2018). Mechanisms of physiological and pathological cardiac hypertrophy. Nat. Rev. Cardiol. *15*: 387–407.

Nathan, C. (2002). Points of control in inflammation. Nature *420*: 846–52.

Nayeem, M.A. (2018a). Role of oxylipins in cardiovascular diseases. Acta Pharmacol. Sin. *39*: 1142–1154.

Nayeem, M.A. (2018b). Role of oxylipins in cardiovascular diseases. Acta Pharmacol. Sin. *39*: 1142–1154.

Nebert, D.W., Dalton, T.P., Okey, A.B., and Gonzalez, F.J. (2004). Role of aryl hydrocarbon receptor-mediated induction of the CYP1 enzymes in environmental toxicity and cancer. J. Biol. Chem. *279*: 23847–23850.

Nebert, D.W., Wikvall, K., and Miller, W.L. (2013). Human cytochromes P450 in health and disease. Philos. Trans. R. Soc. B Biol. Sci. *368*:.

Nelson, D.R., Koymans, L., Kamataki, T., Stegeman, J.J., Feyereisen, R., Waxman, D.J., et al. (1996). P450 superfamily: Update on new sequences, gene mapping, accession numbers and nomenclature. Pharmacogenetics *6*: 1–42.

Nguyen, L.A., He, H., and Pham-Huy, C. (2006). Chiral drugs: an overview. Int. J. Biomed. Sci. *2*: 85–100.

Nguyen, X., Wang, M.H., Reddy, K.M., Falck, J.R., and Schwartzman, M.L. (1999). Kinetic profile of the rat CYP4A isoforms: arachidonic acid metabolism and isoform-specific inhibitors. Am. J. Physiol. *276*: R1691-700.

Ni, L., Zhou, C., Duan, Q., Lv, J., Fu, X., Xia, Y., et al. (2011). β-AR blockers suppresses ER stress in cardiac hypertrophy and heart failure. PLoS One *6*: e27294.

Nicks, A.M., Kesteven, S.H., Li, M., Wu, J., Chan, A.Y., Naqvi, N., et al. (2020). Pressure overload by suprarenal aortic constriction in mice leads to left ventricular hypertrophy without c-Kit expression in cardiomyocytes. Sci. Rep. *10*: 1–12.

Nita, M., and Grzybowski, A. (2016). The Role of the Reactive Oxygen Species and Oxidative Stress in the Pathomechanism of the Age-Related Ocular Diseases and Other Pathologies of the Anterior and Posterior Eye Segments in Adults. Oxid. Med. Cell. Longev. *2016*:.

Nyagode, B.A., Williams, I.R., and Morgan, E.T. (2014). Altered Inflammatory Responses to Citrobacter rodentium Infection, but not Bacterial Lipopolysaccharide, in Mice Lacking the Cyp4a10 or Cyp4a14 Genes. Inflammation *37*: 893–907.

Oliw, E.H. (1990). Biosynthesis of 20-hydroxyeicosatetraenoic acid (20-HETE) and 12 (S)-HETE by renal cortical microsomes of the cynomolgus monkey. Eicosanoids *3*: 161–164.

Olson, E.N., and Molkentin, J.D. (1999). Prevention of cardiac hypertrophy by calcineurin inhibition: Hope or hype? Circ. Res. *84*: 623–632.

Ong, C.E., Pan, Y., and Mak, J.W. (2017). The roles of cytochromes P450 in vascular biology and cardiovascular homeostasis.

Ooi, M., and Allen, S.C. (2008). Heart failure with a normal ejection fraction. C. J. Geriatr. Med. *10*: 72–75.

Oparil, S., Bishop, S.P., and Clubb, F.J. (1984). Myocardial cell hypertrophy or hyperplasia. Hypertension *6*: 38–43.

Pallazola, V.A., Davis, D.M., Whelton, S.P., Cardoso, R., Latina, J.M., Michos, E.D., et al. (2019). A Clinician's Guide to Healthy Eating for Cardiovascular Disease Prevention. Mayo Clin. Proc. Innov. Qual. Outcomes *3*: 251–267.

Park, J.H., Kim, H., and Kim, S.H. (2018). Abstract 2327: Azole antifungal drugs induce cell death by suppressing mTOR through PI3K/Akt inhibition in human breast cancer. Cancer Res. *78*: 2327–2327.

Park, Y.J., Yoo, S.A., Kim, M., and Kim, W.U. (2020). The Role of Calcium–Calcineurin–NFAT Signaling Pathway in Health and Autoimmune Diseases. Front. Immunol. *11*: 195.

Pastrakuljic, A., Tang, B.K., Roberts, E.A., and Kalow, W. (1997). Distinction of CYP1A1 and CYP1A2 activity by selective inhibition using fluvoxamine and isosafrole. Biochem. Pharmacol. *53*: 531–538.

Patrick, K.S., and Straughn, A.B. (2016). Absorption Differences between Immediate-Release Dexmethylphenidate and dl-Methylphenidate. Drug Metab. Dispos. *44*: 418–21.

Patrono, C., Morais, J., Baigent, C., Collet, J.-P., Fitzgerald, D., Halvorsen, S., et al. (2017). Antiplatelet Agents for the Treatment and Prevention of Coronary Atherothrombosis. J. Am. Coll. Cardiol. *70*: 1760–1776.

Paulus, W.J., and Tschöpe, C. (2013). A novel paradigm for heart failure with preserved ejection fraction: Comorbidities drive myocardial dysfunction and remodeling through coronary microvascular endothelial inflammation. J. Am. Coll. Cardiol. *62*: 263–271.

Pavek, P., and Dvorak, Z. (2008). Xenobiotic-induced transcriptional regulation of xenobiotic metabolizing enzymes of the cytochrome P450 superfamily in human extrahepatic tissues. Curr. Drug Metab. *9*: 129–143.

Percie du Sert, N., Hurst, V., Ahluwalia, A., Alam, S., Avey, M.T., Baker, M., et al. (2020). The ARRIVE guidelines 2.0: Updated guidelines for reporting animal research.

PLOS Biol. *18*: e3000410.

Pergola, C., Dodt, G., Rossi, A., Neunhoeffer, E., Lawrenz, B., Northoff, H., et al. (2008). ERK-mediated regulation of leukotriene biosynthesis by androgens: a molecular basis for gender differences in inflammation and asthma. Proc. Natl. Acad. Sci. U. S. A. *105*: 19881–6.

Pergola, C., and Werz, O. (2010). 5-Lipoxygenase inhibitors: a review of recent developments and patents. Expert Opin Ther Pat *20*: 355–375.

Phrommintikul, A., Tran, L., Kompa, A., Wang, B., Adrahtas, A., Cantwell, D., et al. (2008). Effects of a Rho kinase inhibitor on pressure overload induced cardiac hypertrophy and associated diastolic dysfunction. Am. J. Physiol. - Hear. Circ. Physiol. *294*: 1804–1814.

Pingili, A.K., Davidge, K.N., Thirunavukkarasu, S., Khan, N.S., Katsurada, A., Majid, D.S.A., et al. (2017). 2-Methoxyestradiol Reduces Angiotensin II-Induced Hypertension and Renal Dysfunction in Ovariectomized Female and Intact Male Mice. Hypertens. (Dallas, Tex. 1979) *69*: 1104–1112.

Pitoulis, F.G., and Terracciano, C.M. (2020). Heart Plasticity in Response to Pressure- and Volume-Overload: A Review of Findings in Compensated and Decompensated Phenotypes. Front. Physiol. *11*: 92.

Plitt, G.D., Spring, J.T., Moulton, M.J., and Agrawal, D.K. (2018). Mechanisms, diagnosis, and treatment of heart failure with preserved ejection fraction and diastolic dysfunction. Expert Rev. Cardiovasc. Ther. *16*: 579–589.

Pol, A. van der, Gilst, W.H. van, Voors, A.A., and Meer, P. van der (2019). Treating oxidative stress in heart failure: past, present and future. Eur. J. Heart Fail. *21*: 425–435.

Ponikowski, P., Voors, A.A., Anker, S.D., Bueno, H., Cleland, J.G.F., Coats, A.J.S., et al. (2016). 2016 ESC Guidelines for the diagnosis and treatment of acute and chronic heart failure. Eur. J. Heart Fail. *18*: 891–975.

Porro, B., Songia, P., Squellerio, I., Tremoli, E., and Cavalca, V. (2014). Analysis, physiological and clinical significance of 12-HETE: a neglected platelet-derived 12-lipoxygenase product. J Chromatogr B Anal. Technol Biomed Life Sci *964*: 26–40.

Powell, W.S., and Rokach, J. (2015). Biosynthesis, biological effects, and receptors of hydroxyeicosatetraenoic acids (HETEs) and oxoeicosatetraenoic acids (oxo-ETEs) derived from arachidonic acid. Biochim. Biophys. Acta - Mol. Cell Biol. Lipids *1851*: 340–355.

Putney, J.W., and Tomita, T. (2012). Phospholipase C signaling and calcium influx. Adv. Biol. Regul. *52*: 152–164.

Qi, H.P., Wang, Y., Zhang, Q.H., Guo, J., Li, L., Cao, Y.G., et al. (2015). Activation of peroxisome proliferator-activated receptor γ (PPARγ) through NF-κB/brg1 and TGF-β 1 pathways attenuates cardiac remodeling in pressure-overloaded rat hearts. Cell.

Physiol. Biochem. *35*: 899–912.

Qu, W., Bradbury, J.A., Tsao, C.C., Maronpot, R., Harry, G.J., Parker, C.E., et al. (2001). Cytochrome P450 CYP2J9, a new mouse arachidonic acid omega-1 hydroxylase predominantly expressed in brain. J. Biol. Chem. *276*: 25467–79.

Radmark, O., Werz, O., Steinhilber, D., and Samuelsson, B. (2015). 5-Lipoxygenase, a key enzyme for leukotriene biosynthesis in health and disease. Biochim Biophys Acta *1851*: 331–339.

Rajaraman, G., Yang, G., Chen, J., and Chang, T.K.H. (2009). Modulation of CYP1B1 and CYP1A1 gene expression and activation of aryl hydrocarbon receptor by Ginkgo biloba extract in MCF-10A human mammary epithelial cells. Can. J. Physiol. Pharmacol. *87*: 674–683.

Ray, P.D., Huang, B.W., and Tsuji, Y. (2012). Reactive oxygen species (ROS) homeostasis and redox regulation in cellular signaling. Cell. Signal. *24*: 981–990.

Reddy, Y.K., Reddy, L.M., Capdevila, J.H., and Falck, J.R. (2003). Practical, asymmetric synthesis of 16-hydroxyeicosa-5(Z),8(Z), 11(Z),14(Z)-tetraenoic acid (16-HETE), an endogenous inhibitor of neutrophil activity. Bioorg. Med. Chem. Lett. *13*: 3719–20.

Rendic, S. (2002). Summary of information on human CYP enzymes: Human P450 metabolism data. Drug Metab. Rev. *34*: 83–448.

Revermann, M., Mieth, A., Popescu, L., Paulke, A., Wurglics, M., Pellowska, M., et al. (2011). A pirinixic acid derivative (LP105) inhibits murine 5-lipoxygenase activity and attenuates vascular remodelling in a murine model of aortic aneurysm. Br J Pharmacol *163*: 1721–1732.

Ricciotti, E., and FitzGerald, G.A. (2011). Prostaglandins and inflammation. Arterioscler. Thromb. Vasc. Biol. *31*: 986–1000.

Rocic, P., and Schwartzman, M.L. (2018). 20-HETE in the regulation of vascular and cardiac function. Pharmacol. Ther. *192*: 74–87.

Roger, V.L. (2013). Epidemiology of heart failure. Circ. Res. *113*: 646–659.

Rohini, A., Agrawal, N., Koyani, C.N., and Singh, R. (2010). Molecular targets and regulators of cardiac hypertrophy. Pharmacol. Res. *61*: 269–280.

Roman, R.J. (2002). P-450 metabolites of arachidonic acid in the control of cardiovascular function. Physiol Rev *82*: 131–185.

Rosenkranz, S., Kramer, T., Gerhardt, F., Opitz, C., Olsson, K.M., and Hoeper, M.M. (2019). Pulmonary hypertension in HFpEF and HFrEF: Pathophysiology, diagnosis, treatment approaches. Herz.

Rothermel, B.A., McKinsey, T.A., Vega, R.B., Nicol, R.L., Mammen, P., Yang, J., et

al. (2001). Myocyte-enriched calcineurin-interacting protein, MCIP1, inhibits cardiac hypertrophy in vivo. Proc. Natl. Acad. Sci. U. S. A. *98*: 3328–3333.

Roux, P.P., and Blenis, J. (2004). ERK and p38 MAPK-Activated Protein Kinases: a Family of Protein Kinases with Diverse Biological Functions. Microbiol. Mol. Biol. Rev. *68*: 320–344.

Sadoshima, J., and Izumo, S. (1995). Rapamycin selectively inhibits angiotensin II-induced increase in protein synthesis in cardiac myocytes in vitro: Potential role of 70-kD S6 kinase in angiotensin II-induced cardiac hypertrophy. Circ. Res. *77*: 1040–1052.

Saini, S., Hirata, H., Majid, S., and Dahiya, R. (2009). Functional significance of cytochrome P450 1B1 in endometrial carcinogenesis. Cancer Res. *69*: 7038–7045.

Sala, V., Gallo, S., Leo, C., Gatti, S., Gelb, B.D., and Crepaldi, T. (2012). Signaling to cardiac hypertrophy: Insights from human and mouse RASopathies. Mol. Med. *18*: 938–947.

Sawyer, D.B., Siwik, D.A., Xiao, L., Pimentel, D.R., Singh, K., and Colucci, W.S. (2002). Role of oxidative stress in myocardial hypertrophy and failure. J. Mol. Cell. Cardiol. *34*: 379–388.

Schoonbroodt, S., Ferreira, V., Best-Belpomme, M., Boelaert, J.R., Legrand-Poels, S., Korner, M., et al. (2000). Crucial Role of the Amino-Terminal Tyrosine Residue 42 and the Carboxyl-Terminal PEST Domain of IκBα in NF-κB Activation by an Oxidative Stress. J. Immunol. *164*: 4292–4300.

Schwarz, D., Kisselev, P., Ericksen, S.S., Szklarz, G.D., Chernogolov, A., Honeck, H., et al. (2004). Arachidonic and eicosapentaenoic acid metabolism by human CYP1A1: highly stereoselective formation of 17(R),18(S)-epoxyeicosatetraenoic acid. Biochem. Pharmacol. *67*: 1445–57.

Sciarretta, S., Volpe, M., and Sadoshima, J. (2014). Mammalian target of rapamycin signaling in cardiac physiology and disease. Circ. Res. *114*: 549–564.

Sello, M.M., Jafta, N., Nelson, D.R., Chen, W., Yu, J.H., Parvez, M., et al. (2015). Diversity and evolution of cytochrome P450 monooxygenases in Oomycetes. Sci. Rep. *5*:.

Sergentanis, T.N., and Economopoulos, K.P. (2010). Four polymorphisms in cytochrome P450 1A1 (CYP1A1) gene and breast cancer risk: A meta-analysis. Breast Cancer Res. Treat. *122*: 459–469.

Serrano-Mollar, A., and Closa, D. (2005). Arachidonic acid signaling in pathogenesis of allergy: therapeutic implications. Curr. Drug Targets. Inflamm. Allergy *4*: 151–5.

Sharma, K., and Kass, D.A. (2014). Heart Failure With Preserved Ejection Fraction. Circ. Res. *115*: 79–96.

Shimada, T., Gillam, E.M., Sutter, T.R., Strickland, P.T., Guengerich, F.P., and

Yamazaki, H. (1997). Oxidation of xenobiotics by recombinant human cytochrome P450 1B1. Drug Metab. Dispos. *25*: 617–22.

Shimada, T., Hayes, C.L., Yamazaki, H., Amin, S., Hecht, S.S., Guengerich, F.P., et al. (1996). Activation of Chemically Diverse Procarcinogens by Human Cytochrome P-450 1B1. Cancer Res. *56*:.

Shimizu, I., and Minamino, T. (2016). Physiological and pathological cardiac hypertrophy. J. Mol. Cell. Cardiol. *97*: 245–262.

Shiojima, I., and Walsh, K. (2006). Regulation of cardiac growth and coronary angiogenesis by the Akt/PKB signaling pathway. Genes Dev. *20*: 3347–3365.

Shoham, S., Groll, A.H., Petraitis, V., and Walsh, T.J. (2017). Systemic Antifungal Agents. In Infectious Diseases, (Elsevier), pp 1333-1344.e4.

Shoieb, S.M., and El-Kadi, A.O.S. (2018a). *S*- Enantiomer of 19-Hydroxyeicosatetraenoic Acid Preferentially Protects Against Angiotensin II-Induced Cardiac Hypertrophy. Drug Metab. Dispos. *46*: 1157–1168.

Shoieb, S.M., and El-Kadi, A.O.S. (2018b). S-enantiomer of 19-hydroxyeicosatetraenoic acid preferentially protects against angiotensin II-induced cardiac hypertrophy. Drug Metab. Dispos. *46*: 1157–1168.

Shoieb, S.M., and El-Kadi, A.O.S. (2018c). S-Enantiomer of 19-Hydroxyeicosatetraenoic Acid Preferentially Protects Against Angiotensin II-Induced Cardiac Hypertrophy. Drug Metab. Dispos. dmd.118.082073.

Shoieb, S.M., and El-Kadi, A.O.S. (2020). Resveratrol attenuates angiotensin II-induced cellular hypertrophy through the inhibition of CYP1B1 and the cardiotoxic mid-chain HETE metabolites. Mol. Cell. Biochem. *471*: 165–176.

Shoieb, S.M., El-Sherbeni, A.A., and El-Kadi, A.O.S. (2019a). Identification of 19-(*S/R*)Hydroxyeicosatetraenoic Acid as the First Endogenous Noncompetitive Inhibitor of Cytochrome P450 1B1 with Enantioselective Activity. Drug Metab. Dispos. *47*: 67–70.

Shoieb, S.M., El-Sherbeni, A.A., and El-Kadi, A.O.S. (2019b). Identification of 19-(S/R)hydroxyeicosatetraenoic acid as the first endogenous noncompetitive inhibitor of cytochrome P450 1B1 with enantioselective activity. Drug Metab. Dispos. *47*: 67–70.

Shoieb, S.M., El-Sherbeni, A.A., and El-Kadi, A.O.S. (2019c). Subterminal hydroxyeicosatetraenoic acids: Crucial lipid mediators in normal physiology and disease states. Chem. Biol. Interact. *299*: 140–150.

Siegel, M.I., McConnell, R.T., and Cuatrecasas, P. (1979). Aspirin-like drugs interfere with arachidonate metabolism by inhibition of the 12-hydroperoxy-5,8,10,14-eicosatetraenoic acid peroxidase activity of the lipoxygenase pathway. Proc. Natl. Acad. Sci. U. S. A. *76*: 3774–8.

Sim, S.C., and Ingelman-Sundberg, M. (2006). The human cytochrome P450 Allele Nomenclature Committee Web site: submission criteria, procedures, and objectives. Methods Mol. Biol. *320*: 183–191.

Simm, A., Schlüter, K.D., Diez, C., Piper, H.M., and Hoppe, J. (1998). Activation of p70(S6) kinase by β-adrenoceptor agonists on adult cardiomyocytes. J. Mol. Cell. Cardiol. *30*: 2059–2067.

Singh, H., and Schwartzman, M.L. Renal vascular cytochrome P450-derived eicosanoids in androgen-induced hypertension. Pharmacol. Rep. *60*: 29–37.

Sleire, L., Førde, H.E., Netland, I.A., Leiss, L., Skeie, B.S., and Enger, P.Ø. (2017). Drug repurposing in cancer. Pharmacol. Res. *124*: 74–91.

Smith, W.L., DeWitt, D.L., and Garavito, R.M. (2000). Cyclooxygenases: structural, cellular, and molecular biology. Annu. Rev. Biochem. *69*: 145–82.

Somchit, N., Norshahida, A.R., Hasiah, A.H., Zuraini, A., Sulaiman, M.R., and Noordin, M.M. (2004). Hepatotoxicity induced by antifungal drugs itraconazole and fluconazole in rats: A comparative in vivo study. Hum. Exp. Toxicol. *23*: 519–525.

Song, C.Y., Ghafoor, K., Ghafoor, H.U., Khan, N.S., Thirunavukkarasu, S., Jennings, B.L., et al. (2016). Cytochrome P450 1B1 Contributes to the Development of Atherosclerosis and Hypertension in Apolipoprotein E-Deficient Mice. Hypertens. (Dallas, Tex. 1979) *67*: 206–13.

Souders, C.A., Bowers, S.L.K., and Baudino, T.A. (2009). Cardiac fibroblast: The renaissance cell. Circ. Res. *105*: 1164–1176.

Sousa Abreu, R. De, Penalva, L.O., Marcotte, E.M., and Vogel, C. (2009). Global signatures of protein and mRNA expression levels. Mol. Biosyst. *5*: 1512–1526.

Stevens, D.A., Diaz, M., Negroni, R., Montero-Gei, F., Castro, L.G.M., Sampaio, S.A.P., et al. (1997). Safety evaluation of chronic fluconazole therapy. Chemotherapy *43*: 371–377.

Sugumar, H., Nanayakkara, S., Prabhu, S., Voskoboinik, A., Kaye, D.M., Ling, L.-H., et al. (2019). Pathophysiology of Atrial Fibrillation and Heart Failure. Cardiol. Clin. *37*: 131–138.

Sülo›lu, A.K., Koçkaya, E.A., Karacao›lu, E., Selmanolu, G., and Lo›o›lu, E. (2015). In vivo toxicity of a new antifungal agent 2,4-dithiophenoxy-1-iodo-4-bromo benzene: A follow up on our in vitro study. Arh. Hig. Rada Toksikol. *66*: 63–72.

Sun, C.W., Alonso-Galicia, M., Taheri, M.R., Falck, J.R., Harder, D.R., and Roman, R.J. (1998). Nitric oxide-20-hydroxyeicosatetraenoic acid interaction in the regulation of K+ channel activity and vascular tone in renal arterioles. Circ. Res. *83*: 1069–79.

Sundaresan, N.R., Pillai, V.B., and Gupta, M.P. (2011). Emerging roles of SIRT1 deacetylase in regulating cardiomyocyte survival and hypertrophy. J. Mol. Cell.

Cardiol. *51*: 614–618.

Sung, M.M., Das, S.K., Levasseur, J., Byrne, N.J., Fung, D., Kim, T.T., et al. (2015). Resveratrol Treatment of Mice With Pressure-Overload–Induced Heart Failure Improves Diastolic Function and Cardiac Energy Metabolism. Circ. Hear. Fail. *8*: 128–137.

Tacconelli, S., and Patrignani, P. (2014). Inside epoxyeicosatrienoic acids and cardiovascular disease. Front. Pharmacol. *5*: 239.

Tanaka, K., Honda, M., and Takabatake, T. (2001). Redox regulation of MAPK pathways and cardiac hypertrophy in adult rat cardiac myocyte. J. Am. Coll. Cardiol. *37*: 676–685.

Tang, Y., Scheef, E.A., Wang, S., Sorenson, C.M., Marcus, C.B., Jefcoate, C.R., et al. (2009). CYP1B1 expression promotes the proangiogenic phenotype of endothelium through decreased intracellular oxidative stress and thrombospondin-2 expression. Blood *113*: 744–754.

Thandapilly, S.J., Louis, X.L., Yang, T., Stringer, D.M., Yu, L., Zhang, S., et al. (2011). Resveratrol prevents norepinephrine induced hypertrophy in adult rat cardiomyocytes, by activating NO-AMPK pathway. Eur. J. Pharmacol. *668*: 217–224.

Theken, K.N., Deng, Y., Alison Kannon, M., Miller, T.M., Poloyac, S.M., and Lee, C.R. (2011). Activation of the acute inflammatory response alters cytochrome P450 expression and eicosanoid metabolism. Drug Metab. Dispos. *39*: 22–29.

Thum, T., and Borlak, J. (2000). Cytochrome P450 mono-oxygenase gene expression and protein activity in cultures of adult cardiomyocytes of the rat. Br. J. Pharmacol. *130*: 1745–52.

Thum, T., and Borlak, J. (2002). Testosterone, cytochrome P450, and cardiac hypertrophy. FASEB J. *16*: 1537–49.

Tokizane, T., Shiina, H., Igawa, M., Enokida, H., Urakami, S., Kawakami, T., et al. (2005a). Cytochrome P450 1B1 is overexpressed and regulated by hypomethylation in prostate cancer. Clin. Cancer Res. *11*: 5793–801.

Tokizane, T., Shiina, H., Igawa, M., Enokida, H., Urakami, S., Kawakami, T., et al. (2005b). Cytochrome P450 1B1 is overexpressed and regulated by hypomethylation in prostate cancer. Clin. Cancer Res. *11*: 5793–5801.

Tomaselli, G.F., and Zipes, D.P. (2004). What causes sudden death in heart failure? Circ. Res. *95*: 754–763.

Traenckner, E.B.M., and Baeuerle, P.A. (1995). Appearance of apparently ubiquitin-conjugated IκB-α during its phosphorylation-induced degradation in intact cells. J. Cell Sci. *108*: 79–84.

Tromp, J., Lim, S.L., Tay, W.T., Teng, T.H.K., Chandramouli, C., Ouwerkerk, W., et

al. (2019). Microvascular disease in patients with diabetes with heart failure and reduced ejection versus preserved ejection fraction. Diabetes Care *42*: 1792–1799.

Tsao, C.C., Foley, J., Coulter, S.J., Maronpot, R., Zeldin, D.C., and Goldstein, J.A. (2000a). CYP2C40, a unique arachidonic acid 16-hydroxylase, is the major CYP2C in murine intestinal tract. Mol. Pharmacol. *58*: 279–87.

Tsao, C.C., Foley, J., Coulter, S.J., Maronpot, R., Zeldin, D.C., and Goldstein, J.A. (2000b). CYP2C40, a unique arachidonic acid 16-hydroxylase, is the major CYP2C in murine intestinal tract. Mol. Pharmacol. *58*: 279–287.

Tsatsakis, A.M., Zafiropoulos, A., Tzatzarakis, M.N., Tzanakakis, G.N., and Kafatos, A. (2009). Relation of PON1 and CYP1A1 genetic polymorphisms to clinical findings in a cross-sectional study of a Greek rural population professionally exposed to pesticides. Toxicol. Lett. *186*: 66–72.

Tsuchiya, Y., Nakajima, M., Kyo, S., Kanaya, T., Inoue, M., and Yokoi, T. (2004). Human CYP1B1 Is Regulated by Estradiol via Estrogen Receptor. Cancer Res. *64*: 3119–3125.

Vakili, B.A., Okin, P.M., and Devereux, R.B. (2001). Prognostic implications of left ventricular hypertrophy. Am. Heart J. *141*: 334–341.

Valencia-Olvera, A.C., Morán, J., Camacho-Carranza, R., Prospéro-García, O., and Espinosa-Aguirre, J.J. (2014). CYP2E1 induction leads to oxidative stress and cytotoxicity in glutathione-depleted cerebellar granule neurons. Toxicol. In Vitro *28*: 1206–14.

Vazquez, B., Rios, A., and Escalante, B. (1995). Arachidonic acid metabolism modulates vasopressin-induced renal vasoconstriction. Life Sci. *56*: 1455–66.

Vila, L. (2004). Cyclooxygenase and 5-lipoxygenase pathways in the vessel wall: role in atherosclerosis. Med Res Rev *24*: 399–424.

Visser, S.P. de, Ogliaro, F., Sharma, P.K., and Shaik, S. (2002). What factors affect the regioselectivity of oxidation by cytochrome p450? A DFT study of allylic hydroxylation and double bond epoxidation in a model reaction. J. Am. Chem. Soc. *124*: 11809–26.

Walsh, A.A., Szklarz, G.D., and Scott, E.E. (2013). Human cytochrome P450 1A1 structure and utility in understanding drug and xenobiotic metabolism. J. Biol. Chem. *288*: 12932–12943.

Wang, A.-W., Song, L., Miao, J., Wang, H.-X., Tian, C., Jiang, X., et al. (2015a). Baicalein attenuates angiotensin II-induced cardiac remodeling via inhibition of AKT/mTOR, ERK1/2, NF-κB, and calcineurin signaling pathways in mice. Am. J. Hypertens. *28*: 518–26.

Wang, B., Ouyang, J., and Xia, Z. Effects of triiodo-thyronine on angiotensin-induced cardiomyocyte hypertrophy: reversal of increased beta-myosin heavy chain gene

expression. Can. J. Physiol. Pharmacol. *84*: 935–41.

Wang, B., Yang, Q., Sun, Y.Y., Xing, Y.F., Wang, Y. Bin, Lu, X.T., et al. (2014a). Resveratrol-enhanced autophagic flux ameliorates myocardial oxidative stress injury in diabetic mice. J. Cell. Mol. Med. *18*: 1599–1611.

Wang, J.S., Zhang, F., Jiang, M., Wang, M.H., Zand, B.A., Abraham, N.G., et al. (2004). Transfection and functional expression of CYP4A1 and CYP4A2 using bicistronic vectors in vascular cells and tissues. J. Pharmacol. Exp. Ther. *311*: 913–920.

Wang, L., Gao, M., Chen, J., Yang, Z., Sun, J., Wang, Z., et al. (2015b). Resveratrol ameliorates pressure overload-induced cardiac dysfunction and attenuates autophagy in rats. J. Cardiovasc. Pharmacol. *66*: 376–382.

Wang, P.-X., Li, Z.-M., Cai, S.-D., Li, J.-Y., He, P., Huang, Y., et al. (2017). C33(S), a novel PDE9A inhibitor, protects against rat cardiac hypertrophy through upregulating cGMP signaling. Nat. Publ. Gr. *38*:.

Wang, W., and Lu, M. (1995). Effect of arachidonic acid on activity of the apical K+ channel in the thick ascending limb of the rat kidney. J. Gen. Physiol. *106*: 727–43.

Wang, X., Ni, L., Yang, L., Duan, Q., Chen, C., Edin, M.L., et al. (2014b). CYP2J2-Derived epoxyeicosatrienoic acids suppress endoplasmic reticulum stress in heart failure. Mol. Pharmacol. *85*: 105–115.

Wang, Z., Chen, Y., Drbohlav, L.M., Wu, J.Q., and Wang, M.Z. (2016). Development of an in Vitro Model to Screen CYP1B1-Targeted Anticancer Prodrugs. J. Biomol. Screen. *21*: 1090–1099.

Ware, W.R. (2017). Natural Cancer Therapy and Prevention Targeted on Cancer Cells and Cancer Stem Cells Based on the Cytochrome P45O Enzyme CYP1B1: A Commentary. Altern. Ther. Health Med. *23*: 50–58.

Wei, S., Rothstein, E.C., Fliegel, L., Dell'italia, L.J., and Lucchesi, P.A. (2001). Differential MAP kinase activation and Na+/H+ exchanger phosphorylation by H2O2 in rat cardiac myocytes. Am. J. Physiol. - Cell Physiol. *281*:.

Werck-Reichhart, D., and Feyereisen, R. (2000). Cytochromes P450: a success story. Genome Biol. *1*: REVIEWS3003.

Werz, O., and Steinhilber, D. (2006). Therapeutic options for 5-lipoxygenase inhibitors. Pharmacol Ther *112*: 701–718.

Westphal, C., Konkel, A., and Schunck, W.-H.H. (2015). Cytochrome p450 enzymes in the bioactivation of polyunsaturated Fatty acids and their role in cardiovascular disease. Adv Exp Med Biol *851*: 151–187.

Wilkins, B.J., and Molkentin, J.D. (2002). Calcineurin and cardiac hypertrophy: Where have we been? Where are we going? J. Physiol. *541*: 1–8.

Williams, J.S., Hopkins, P.N., Jeunemaitre, X., and Brown, N.J. (2011). CYP4A11 T8590C polymorphism, salt-sensitive hypertension, and renal blood flow. J. Hypertens. *29*: 1913–8.

Wing, R.R., Lang, W., Wadden, T.A., Safford, M., Knowler, W.C., Bertoni, A.G., et al. (2011). Benefits of modest weight loss in improving cardiovascular risk factors in overweight and obese individuals with type 2 diabetes. Diabetes Care *34*: 1481–1486.

Wright, J.W., Krebs, L.T., Stobb, J.W., and Harding, J.W. (1995). The angiotensin IV system: Functional implications. Front. Neuroendocrinol. *16*: 23–52.

Wu, C.-C., Gupta, T., Garcia, V., Ding, Y., and Schwartzman, M.L. (2014). 20-HETE and blood pressure regulation: clinical implications. Cardiol. Rev. *22*: 1–12.

Wu, C.-C., and Schwartzman, M.L. (2011). The role of 20-HETE in androgen-mediated hypertension. Prostaglandins Other Lipid Mediat. *96*: 45–53.

Xiao, B., Li, X., Yan, J., Yu, X., Yang, G., Xiao, X., et al. (2010). Overexpression of Cytochrome P450 Epoxygenases Prevents Development of Hypertension in Spontaneously Hypertensive Rats by Enhancing Atrial Natriuretic Peptide. J. Pharmacol. Exp. Ther. *334*: 784–794.

Xie, H.G., Huang, S.L., Xu, Z.H., Xiao, Z.S., He, N., and Zhou, H.H. (1997). Evidence for the effect of gender on activity of (S)-mephenytoin 4'-hydroxylase (CYP2C19) in a Chinese population. Pharmacogenetics *7*: 115–9.

Xu, F., Falck, J.R., Ortiz de Montellano, P.R., and Kroetz, D.L. (2004). Catalytic activity and isoform-specific inhibition of rat cytochrome p450 4F enzymes. J. Pharmacol. Exp. Ther. *308*: 887–95.

Xu, X., Zhang, X.A., and Wang, D.W. (2011). The roles of CYP450 epoxygenases and metabolites, epoxyeicosatrienoic acids, in cardiovascular and malignant diseases. Adv. Drug Deliv. Rev. *63*: 597–609.

Yaghini, F.A., Song, C.Y., Lavrentyev, E.N., Ghafoor, H.U.B.B., Fang, X.R., Estes, A.M., et al. (2010). Angiotensin II-Induced Vascular Smooth Muscle Cell Migration and Growth Are Mediated by Cytochrome P450 1B1-Dependent Superoxide Generation. Hypertension *55*: 1461–1467.

Yancy, C.W., Jessup, M., Bozkurt, B., Butler, J., Casey, D.E., Colvin, M.M., et al. (2017). 2017 ACC/AHA/HFSA Focused Update of the 2013 ACCF/AHA Guideline for the Management of Heart Failure: A Report of the American College of Cardiology/American Heart Association Task Force on Clinical Practice Guidelines and the Heart Failure Society of America. J. Am. Coll. Cardiol. *70*: 776–803.

Yancy, C.W., Jessup, M., Bozkurt, B., Butler, J., Casey, D.E., Drazner, M.H., et al. (2013). 2013 ACCF/AHA Guideline for the Management of Heart Failure: A Report of the American College of Cardiology Foundation/American Heart Association Task Force on Practice Guidelines. J. Am. Coll. Cardiol. *62*: e147–e239.

Yang, X., Solomon, S., Fraser, L.R., Trombino, A.F., Liu, D., Sonenshein, G.E., et al. (2008). Constitutive regulation of CYP1B1 by the aryl hydrocarbon receptor (AhR) in pre-malignant and malignant mammary tissue. J. Cell. Biochem. *104*: 402–417.

Yin, Z., Wang, X., Zhang, L., Zhou, H., Wei, L., and Dong, X. (2016). Aspirin Attenuates Angiotensin II-induced Cardiomyocyte Hypertrophy by Inhibiting the Ca(2+)/Calcineurin-NFAT Signaling Pathway. Cardiovasc. Ther. *34*: 21–9.

Yoshida, S., Hirai, A., Tamura, Y., and Yoshida, S. (1990). Possible involvement of arachidonic acid metabolites of cytochrome P450 monooxygenase pathway in vasopressin-stimulated glycogenolysis in isolated rat hepatocytes. Arch. Biochem. Biophys. *280*: 346–51.

Yousif, M.H.M., Benter, I.F., and Roman, R.J. (2009). Cytochrome P450 metabolites of arachidonic acid play a role in the enhanced cardiac dysfunction in diabetic rats following ischaemic reperfusion injury. Auton. Autacoid Pharmacol. *29*: 33–41.

Yun, U.J., and Yang, D.K. (2020). Sinapic acid inhibits cardiac hypertrophy via activation of mitochondrial Sirt3/SOD2 signaling in neonatal rat cardiomyocytes. Antioxidants *9*: 1–17.

Yune-Fang Ueng, ‡, Takashi Kuwabara, Young-Jin Chun, § and, and Guengerich*, F.P. (1997). Cooperativity in Oxidations Catalyzed by Cytochrome P450 3A4†. Biochemistry *36*: 370–381.

Zanger, U.M., and Schwab, M. (2013). Cytochrome P450 enzymes in drug metabolism: Regulation of gene expression, enzyme activities, and impact of genetic variation. Pharmacol. Ther. *138*: 103–141.

Zechner, D., Thuerauf, D.J., Hanford, D.S., McDonough, P.M., and Glembotski, C.C. (1997). A role for the p38 mitogen-activated protein kinase pathway in myocardial cell growth, sarcomeric organization, and cardiac-specific gene expression. J. Cell Biol. *139*: 115–127.

Zehorai, E., Yao, Z., Plotnikov, A., and Seger, R. (2010). The subcellular localization of MEK and ERK-A novel nuclear translocation signal (NTS) paves a way to the nucleus. Mol. Cell. Endocrinol. *314*: 213–220.

Zhai, P., Gao, S., Holle, E., Yu, X., Yatani, A., Wagner, T., et al. (2007). Glycogen synthase kinase-3α reduces cardiac growth and pressure overload-induced cardiac hypertrophy by inhibition of extracellular signal-regulated kinases. J. Biol. Chem. *282*: 33181–33191.

Zhang, F., Deng, H., Kemp, R., Singh, H., Gopal, V.R., Falck, J.R., et al. (2005). Decreased levels of cytochrome P450 2E1-derived eicosanoids sensitize renal arteries to constrictor agonists in spontaneously hypertensive rats. Hypertens. (Dallas, Tex. 1979) *45*: 103–8.

Zhang, L., Li, Y., Chen, M., Su, X., Yi, D., Lu, P., et al. (2014a). 15-LO/15-HETE

mediated vascular adventitia fibrosis via p38 MAPK-dependent TGF-beta. J Cell Physiol *229*: 245–257.

Zhang, L., Li, Y., Chen, M., Su, X., Yi, D., Lu, P., et al. (2014b). 15-LO/15-HETE Mediated Vascular Adventitia Fibrosis via p38 MAPK-Dependent TGF-β. J. Cell. Physiol. *229*: 245–257.

Zhang, T., Bai, J., Huang, M., Li, R., Liu, Y., Liu, A., et al. (2020a). Posaconazole and fluconazole prophylaxis during induction therapy for pediatric acute lymphoblastic leukemia. J. Microbiol. Immunol. Infect.

Zhang, W., Elimban, V., Nijjar, M.S., Gupta, S.K., and Dhalla, N.S. (2003). Role of mitogen-activated protein kinase in cardiac hypertrophy and heart failure. Exp. Clin. Cardiol. *8*: 173–183.

Zhang, Y., El-Sikhry, H., Chaudhary, K.R., Batchu, S.N., Shayeganpour, A., Jukar, T.O., et al. (2009). Overexpression of CYP2J2 provides protection against doxorubicin-induced cardiotoxicity. Am. J. Physiol. - Hear. Circ. Physiol. *297*: 37–46.

Zhang, Y., Wang, S., Huang, Y., Yang, K., Liu, Y., Bi, X., et al. (2020b). Inhibition of CYP1B1 ameliorates cardiac hypertrophy induced by uremic toxin. Mol. Med. Rep. *21*: 393–404.

Zhao, X., Falck, J.R., Gopal, V.R., Inscho, E.W., and Imig, J.D. (2004). P2X receptor-stimulated calcium responses in preglomerular vascular smooth muscle cells involves 20-hydroxyeicosatetraenoic acid. J. Pharmacol. Exp. Ther. *311*: 1211–1217.

Zhou, C., Huang, J., Li, Q., Zhan, C., Xu, X., Zhang, X., et al. (2018). CYP2J2-derived EETs attenuated ethanol-induced myocardial dysfunction through inducing autophagy and reducing apoptosis. Free Radic Biol Med *117*: 168–179.

Zhu, Y., Schieber, E.B., McGiff, J.C., and Balazy, M. (1995). Identification of arachidonate P-450 metabolites in human platelet phospholipids. Hypertens. (Dallas, Tex. 1979) *25*: 854–9.

Ziaeian, B., and Fonarow, G.C. (2016). Epidemiology and aetiology of heart failure. Nat. Rev. Cardiol. *13*: 368–378.

Zile, M.R., Gottdiener, J.S., Hetzel, S.J., McMurray, J.J., Komajda, M., McKelvie, R., et al. (2011). Prevalence and significance of alterations in cardiac structure and function in patients with heart failure and a preserved ejection fraction. Circulation *124*: 2491–2501.

Zordoky, B.N., and El-Kadi, A.O. (2008). Modulation of cardiac and hepatic cytochrome P450 enzymes during heart failure. Curr Drug Metab *9*: 122–128.

Zordoky, B.N.M., Aboutabl, M.E., and El-Kadi, A.O.S. (2008). Modulation of cytochrome P450 gene expression and arachidonic acid metabolism during isoproterenol-induced cardiac hypertrophy in rats. Drug Metab. Dispos. *36*: 2277–2286.

Zordoky, B.N.M., and El-Kadi, A.O.S. (2007). H9c2 cell line is a valuable in vitro model to study the drug metabolizing enzymes in the heart. J. Pharmacol. Toxicol. Methods *56*: 317–22.

Zou, J.G., Ma, Y.T., Xie, X., Yang, Y.N., Pan, S., Adi, D., et al. (2014). The association between CYP1A1 genetic polymorphisms and coronary artery disease in the Uygur and Han of China. Lipids Health Dis. *13*:.

Zou, L.X., Chen, C., Yan, X., Lin, Q.Y., Fang, J., Li, P.B., et al. (2019). Resveratrol Attenuates Pressure Overload-Induced Cardiac Fibrosis and Diastolic Dysfunction via PTEN/AKT/Smad2/3 and NF-κB Signaling Pathways. Mol. Nutr. Food Res. *63*: e1900418.

Zu, L., Guo, G., Zhou, B., and Gao, W. (2016). Relationship between metabolites of arachidonic acid and prognosis in patients with acute coronary syndrome. Thromb Res *144*: 192–201.

(2005). Cytochrome P450 (Boston, MA: Springer US).

(2020). Drug Development and Drug Interactions: Table of Substrates, Inhibitors and Inducers | FDA.